DPhil Thesis

Effects of chronic hyperglycaemia on pancreatic β-cell metabolism and insulin biosynthesis



Matthew Lloyd
Hertford College

Hilary 2023

Abstract

Chronic hyperglycaemia severely impairs the coupling between pancreatic β-cell glucose metabolism and insulin secretion that forms an essential part of blood glucose homeostasis. This thesis focuses on two effects of hyperglycaemia-induced alterations in β-cell metabolism: a decline in insulin biosynthesis and accumulation of glycogen.

Chronic hyperglycaemia results in large reductions in insulin mRNA levels and insulin content. In this thesis, I show that the severity of the decline in insulin biosynthesis depends on the level and duration of hyperglycaemia, both in intact islets and in β-cell lines. I then explore the metabolic signals that cause this loss, using the rat β-cell line INS-1 832/13. Downregulation of insulin gene expression was prevented by glucokinase inhibition and induced by GAPDH inhibition, indicating that accumulation of glycolytic intermediates downstream of glucokinase and upstream of GAPDH was responsible. Further experiments using a non-metabolisable glucose analogue suggested that glucose-6-phosphate is the most critical of these metabolites.

Chronic hyperglycaemia also results in the formation of large glycogen deposits. Since β-cells do not normally store glycogen, the causes and consequences of β-cell glycogen accumulation are incompletely understood and contested. In this thesis, I explore how changes in glucose metabolism and the AMPK/mTOR signalling axis relate to increased glycogen storage during hyperglycaemia. Glycogen accumulation was prevented by inhibition of the gluconeogenic enzyme fructose-1,6-bisphosphatase and by inhibition of mTORC1 signalling through S6K1 but was

increased by AMPK activation. Glycogen accumulation appears to be driven both by direct effects of glucose-6-phosphate and indirect effects of the accumulation of glycolytic intermediates, including activation of mTORC1. Further work is needed to determine whether glycogen affects β-cell function, such as by interfering with metabolism-secretion coupling or impairing autophagy.

These studies help to clarify the mechanisms by which diabetes/chronic hyperglycaemia inhibits the principal function of pancreatic β-cells, the production of insulin.

Contents

Acknowledgements 9

Declaration of authorship 10

Publications arising from this work 11

List of abbreviations and glossary 12

A note on gene and protein nomenclature 14

1. INTRODUCTION 15

1.1 Overview of β-cell metabolism and the regulation of insulin biosynthesis 15
1.1.1 Overview of stimulus-secretion coupling 15
1.1.2 Regulation of insulin transcription 21
1.1.3 Post-transcriptional regulation of insulin biosynthesis 23

1.2 Changes in β-cell metabolism and insulin expression in hyperglycaemia: a vicious cycle 25
1.2.1 Metabolic impairment in hyperglycaemia 25
1.2.2 Insulin biosynthesis is diminished in chronic hyperglycaemia and type 2 diabetes 27
1.2.3 Potential pathways for downregulation of insulin biosynthesis 29
1.2.4 Is the loss of insulin reversible? 32

1.3 The role of glycogen in β-cell dysfunction: more questions than answers 33
1.3.1 Overview of glycogen metabolism and its regulation 34
1.3.2 Is excess glycogen a driver or only a symptom of β-cell dysfunction? 39

1.4 Summary of the project aims 42

2. MATERIALS AND METHODS 43

2.1 INS-1 (832/13) cell culture 43

2.2 EndoC cell culture 44
2.2.1 EndoC-βH1 44
2.2.2 EndoC-βH5 44

2.3 Animal experiments 45

2.4 Islet isolation and culture 46

2.5 siRNA experiments 46
2.5.1 INS-1 cells 46
2.5.2 EndoC cells 47

2.6 RNA extraction and RT-qPCR 47
2.6.1 INS-1 cells and islets 47
2.6.2 EndoC cells 48

2.7 Protein extraction, SDS-PAGE and western blotting 49

2.8 Insulin secretion and content assays 49
2.8.1 INS-1 cells 49
2.8.2 Islets 50
2.8.3 EndoC-βH1 50
2.8.4 EndoC-βH5 51

2.9 Data analysis and statistics 52

3. LOSS OF INSULIN BIOSYNTHESIS CORRESPONDS TO THE SEVERITY AND DURATION OF HYPERGLYCAEMIA 58

3.1 Summary 58

3.2 Introduction 58

3.3 Materials and methods 62
3.3.1 Time course experiment 62
3.3.2 Animal experiments 63

3.4 Dependence of insulin gene expression on glucose concentration and duration of hyperglycaemia 63
3.4.1 Studies in INS-1 cells 64
3.4.2 Studies in human β-cell models 72
3.4.2.1 Studies in EndoC-βH1 cells 72
3.4.2.2 Studies in EndoC-βH5 cells 76
3.4.3 Modelling impaired glucose tolerance, mild hyperglycaemia and severe hyperglycaemia in the βV59M mouse via titration of tamoxifen dosage 78

3.5 Discussion 85

4. HYPERGLYCAEMIA-INDUCED METABOLIC DYSREGULATION CAUSES THE LOSS OF INSULIN BIOSYNTHESIS 92

4.1 Summary 92

4.2 Introduction 93

4.3 Materials and methods 98

4.4 Identification of metabolic factors underlying the loss of insulin biosynthesis 100

4.4.1 Glucokinase inhibition reveals that glucose metabolites rather than glucose *per se* trigger repression of insulin gene expression 100
4.4.2 Mitochondrial fuels do not cause loss of insulin biosynthesis 103
4.4.3 Inhibition of GAPDH at low glucose causes downregulation of insulin gene expression 110
4.4.4 Effects of siRNA knockdown of the glycolytic enzymes phosphofructokinase and aldolase 114
4.4.5 The non-metabolisable glucose analogue 2-deoxyglucose causes a loss of insulin biosynthesis 120
4.4.6 Pentose phosphate pathway inhibition reduces insulin biosynthesis at low glucose but has no effect at high glucose 125
4.4.7 Polyol pathway inhibition reduces insulin biosynthesis at low glucose but has no effect at high glucose 130

4.5 Discussion 134

5. INVESTIGATING DOWNSTREAM EFFECTORS MEDIATING THE LOSS OF INSULIN BIOSYNTHESIS 139

5.1 Summary 139

5.2 Introduction 140

5.3 Materials and methods 144

5.4 Results 144
5.4.1 Chronically high intracellular calcium is not a significant cause of hyperglycaemia-induced insulin gene repression 144
5.4.2 Signalling through ChREBP and TXNIP contributes to the repression of insulin gene expression 146
5.4.3 SHP is upregulated in hyperglycaemia by a G6P-independent mechanism 160
5.4.4 Inhibiting mTORC1/S6K1 signalling does not prevent the loss of insulin expression in hyperglycaemia 162
5.4.5 Metformin increased insulin gene expression in euglycaemia but did not prevent loss in hyperglycaemia 165

5.5 Discussion 168

6. SIRNA SCREEN TO IDENTIFY KEY REGULATORS OF INSULIN BIOSYNTHESIS AND SECRETION IN HUMAN B-CELL LINES 173

6.1 Summary 173

6.2 Introduction 174

6.3 Methods 175

6.4 Results 175
6.4.1 siRNA screen in EndoC-βH1 cells 175
6.4.1 siRNA screen in EndoC-βH5 cells 181

6.5 Discussion 190

7. CAUSES AND CONSEQUENCES OF GLYCOGEN ACCUMULATION IN THE HYPERGLYCAEMIC B-CELL 195

7.1 Summary 195

7.2 Introduction 196

7.3 Materials and methods 200
7.3.1 Glycogen quantification 201
7.3.2 Autophagy detection assay 201

7.4 Results 202
7.4.1 Glycogen assay optimisation and validation 202
7.4.2 Mannoheptulose prevents glycogen accumulation in chronic hyperglycaemia 204
7.4.3 Temporal dynamics of glycogen accumulation and breakdown following onset and reversal of hyperglycaemia 205
7.4.4 Identification of metabolic factors driving glycogen accumulation in β-cells 207
7.4.4.1 GAPDH inhibition did not increase glycogen accumulation in LG-cells 207
7.4.4.2 FBPase inhibition partially prevented glycogen accumulation 208
7.4.4.3 ALDOB knockdown did not affect glycogen accumulation 210
7.4.5 Investigating the relationship between β-cell glycogen and the AMPK/mTOR signalling axis 212
7.4.5.1 Metformin prevents glycogen accumulation 212
7.4.5.2 Inhibition of mTOR signalling via S6K1 prevents glycogen accumulation 213
7.4.5.3 AMPK activators enhance glycogen accumulation 214
7.4.6 Investigating the regulation of PTG expression 216
7.4.7 Inhibition of glycogen phosphorylase increases glycogen accumulation 224
7.4.8 Impact of glycogen stores on insulin secretion 225
7.4.9 Investigating the relationship between β-cell glycogen and defective autophagy 227

7.5 Discussion 229

8. DISCUSSION AND FUTURE DIRECTIONS 236

8.1 Summary 236

8.2 Exploring the hyperglycaemia-induced downregulation of insulin biosynthesis 238
8.2.1 A privileged role for MAFA in the regulation of insulin gene expression? 240

8.3 Exploring the causes and consequences of β-cell glycogen accumulation 243

8.4 Limitations of these studies 245

8.5 Therapeutic potential of glucokinase inhibition 249

8.6 Closing remarks 251

REFERENCES 251

Acknowledgements

First and foremost, I would like to thank my primary supervisor Professor Dame Frances Ashcroft for her mentorship and direction over the last four years, as well as for her careful reading of this thesis and many suggested improvements. This work would not have been possible had I not also benefited from the help of Dr Elizabeth Haythorne, who has both provided practical assistance in the laboratory and aided my scientific development.

I very grateful to Dr Carina Ämmälä for agreeing to inherit the role of industrial supervisor when she joined the Novo Nordisk Research Centre Oxford (NNRCO).

I must also thank the Ashcroft group research assistants Dr Malgorzata (Gosia) Cyranka and Raúl Terrón-Expósito for their help, and Dr Iwona Szczerbinska, Annamaria Tessitore, and Alejandro Ragel Lopez for practical training and support at NNRCO.

I am also grateful to the BBSRC and Novo Nordisk for funding me, and to the Oxford Interdisciplinary Bioscience DTP for training.

Finally, I would like to thank my family and friends for their support, especially my partner Ella for being by my side throughout the journey.

Declaration of authorship

The work in this thesis is all my own, with the following exceptions:

The animal work described in chapter 2, section 3 was performed by Dr Elizabeth Haythorne and Dr Malgorzata Cyranka.

The steps of islet isolation (chapter 2, section 4) up to and including collagenase inflation were performed by Dr Elizabeth Haythorne. I performed the subsequent steps of islets isolation, insulin content determination, and RNA extraction and RT-qPCR in collaboration with Dr Elizabeth Haythorne, and Dr Malgorzata Cyranka.

The following data were provided by Dr Elizabeth Haythorne:

- Insulin secretion with mitochondrial substrates (figure 4.4a)
- ADP/ATP assay (figure 4.13d)
- Insulin secretion and insulin content with FBPase inhibitor (figures 7.5a and 7.5b)

Publications arising from this work

Haythorne, E., Lloyd, M., Walsby-Tickle, J., Tarasov, A. I., Sandbrink, J., Portillo, I., Exposito, R. T., Sachse, G., Cyranka, M., Rohm, M., Rorsman, P., McCullagh, J., & Ashcroft, F. M. (2022). Altered glycolysis triggers impaired mitochondrial metabolism and mTORC1 activation in diabetic β-cells. *Nature Communications 2022 13:1*, *13*(1), 1–19. https://doi.org/10.1038/s41467-022-34095-x

Ashcroft, F. M., Lloyd, M., & Haythorne, E. A. (2023). Glucokinase activity in diabetes: too much of a good thing? *Trends in Endocrinology and Metabolism*, *34*(2), 119–130. https://doi.org/10.1016/j.tem.2022.12.007

List of abbreviations and glossary

2-DG	2-deoxyglucose
3'-UTR	3'-untranslated region
6-AN	6-aminonicotinamide
6-PGD	6-phosphogluconate dehydrogenase
AICAR	5-Aminoimidazole-4-carboxamide ribonucleotide
AMPK	AMP-activated protein kinase
ANOVA	Analysis of variance
BSA	Bovine serum albumin
βV59M	Mouse model with β-cell-specific expression of a V59M amino acid substitution in the K_{ATP} channel subunit Kir6.2 (KCNJ11)
cDNA	Complementary DNA (product of reverse transcription)
CRE	Cyclic AMP response element
DMSO	Dimethyl sulfoxide
ELISA	Enzyme-linked immunosorbent assay
ER	Endoplasmic reticulum
F1,6BP	Fructose 1,6-bisphosphate
F2,6BP	Fructose 2,6-bisphosphate
FBPase	Fructose-1,6-bisphosphatase
FBPi	Fructose-1,6-bisphosphatase inhibitor (MB05032)
FBS	Foetal bovine serum
G6P	Glucose-6-phosphate
G6PD	Glucose-6-phosphate dehydrogenase
GAPDH	Glyceraldehyde 3-phosphate dehydrogenase
GKAs	Glucokinase activators
GLUT	Glucose transporter (of the SLC2A family)
GOF	Gain-of-function
GPi	Glycogen phosphorylase inhibitor (CAS 648926-15-2)
GSIS	Glucose-stimulated insulin secretion
GYS	Glycogen synthase
HFD	High fat diet
HTRF	Homogeneous Time-Resolved Fluorescence
IGT	Impaired glucose tolerance
INS-1 832/13	Rat insulinoma cell line
IPGTT	Intraperitoneal glucose tolerance test
KA	Koningic acid
LEU	Leucine
MANNO	D-mannoheptulose

MIN6	A mouse insulinoma-derived cell line
MK8722	AMPK activator MK8722
MMS	Monomethyl succinate
mTOR(C1)	Mechanistic target of rapamycin (complex 1)
ND	Non-diabetic
ns	Non-significant
OCR	Oxygen consumption rate
OXPHOS	Oxidative phosphorylation
PAS	Periodic acid-Schiff stain
PDK1	Pyruvate dehydrogenase kinase 1
PFK	Phosphofructokinase
PK	Pyruvate kinase
PKA	cAMP-dependent protein kinase A
PP1	Protein phosphatase 1
PPP	Pentose phosphate pathway
PTG	Protein targeting to glycogen (PPP1R3C)
PYG	Glycogen phosphorylase
PYR	Methyl pyruvate
SCID mice	Severe combined immunodeficient mice
SD	Standard deviation
S.E.M.	Standard error of the mean
SI	Stimulation index
S6Ki	S6K1 inhibitor (PF-4708671)
T2D	Type 2 diabetes mellitus
TXNIP	Thioredoxin-interacting protein
UPR	Unfolded protein response
Veh	Vehicle (i.e. DMSO)

A note on gene and protein nomenclature

In accordance with the HUGO Gene Nomenclature Committee (HGNC) guidelines and with the guidelines of the International Committee on Standardized Genetic Nomenclature for Mice and the Rat Genome and Nomenclature Committee, gene and protein symbols used in this thesis are formatted as follows:

Human gene symbols comprise all uppercase letters and are italicised; human proteins use all uppercase letters and are not italicised.

Mouse and rat genes comprise an uppercase first letter followed by all lowercase letters and are italicised; mouse and rat proteins use all uppercase letters and are not italicised.

1. Introduction

1.1 Overview of β-cell metabolism and the regulation of insulin biosynthesis

1.1.1 Overview of stimulus-secretion coupling

Pancreatic β-cells are endocrine cells within the islets of Langerhans which continually monitor blood glucose and secrete appropriate quantities of insulin to maintain glucose levels within a safe range. For humans, this range is approximately 4-8 mmol/l, accounting for variation between the fasting and postprandial states. Changes in blood glucose equilibrate with the β-cell cytosol thanks to the expression of a high-K_m glucose transporter. In mice, GLUT2 fulfils this role, whereas human β-cells express GLUT1 at a higher level than GLUT2 (Rorsman & Ashcroft, 2018). GLUT1 has a lower K_m than GLUT2, which is thought to account for insulin secretion being initiated at a lower threshold of 3 mM glucose in humans, versus 6 mM glucose in mice (Rorsman & Ashcroft, 2018). The expression of glucokinase, an isoform of hexokinase with a low affinity for glucose (K_m of 7-8 mM) and large V_{max}, enables the β-cell to phosphorylate all incoming glucose and thus function as a glucose sensor. Oxidation of glucose, the primary nutrient stimulus (secretagogue) for insulin secretion, through glycolysis and oxidative phosphorylation produces ATP. Elevation of the intracellular ATP/ADP ratio causes ATP-sensitive potassium channels (K_{ATP} channels) to close, resulting in plasma membrane depolarisation and opening of voltage-gated calcium channels. The resultant influx of Ca^{2+} triggers the exocytosis of insulin granules (Rorsman & Ashcroft, 2018). These steps are summarised in figure 1.1. There is some debate over the relative importance of ATP produced by pyruvate kinase (PK) versus mitochondrial

ATP production in closing K_{ATP} channels: ATP exported from the mitochondria has canonically been considered to be the key metabolic coupling factor (Prentki et al., 2013; Wiederkehr & Wollheim, 2012), but this paradigm has been challenged by more recent studies showing that membrane-associated PK can close K_{ATP} channels by locally generating ATP (Dhar-Chowdhury et al., 2005; Lewandowski et al., 2020). According to this new model, the phosphoenolpyruvate (PEP) cycle integrates signals from metabolism of glucose and other nutrients such as amino acids to stimulate local ATP production by PK at the plasma membrane. This local increase in ATP levels initiates insulin secretion, while ATP production by oxidative phosphorylation (OXPHOS) acts to sustain insulin secretion only after the initial membrane depolarisation and Ca^{2+} influx causes the ATP/ADP ratio to fall (due to the workload of exocytosis and ion transport), resulting in stimulation of OXPHOS (Foster et al., 2022; Merrins et al., 2022). It is proposed that β-cells oscillate between these two states termed $Mito_{Cat}$ and $Mito_{Ox}$, respectively.

The calcium-dependent mechanism described above is known as the triggering pathway. Less well understood is the amplifying pathway, which can further increase insulin secretion when K_{ATP} channels are already fully closed and serves to optimise the secretory response to glucose and other stimuli (Henquin, 2000). A variety of coupling factors, including NADH, citrate, and glutamate, have been proposed to mediate the amplifying pathway, yet the only consensus is that the amplifying signals are mitochondrially-derived (Panten et al., 2013; Wiederkehr & Wollheim, 2012).

In keeping with the need to maintain tight coupling of cytosolic and mitochondrial metabolic fluxes, β-cells normally display low expression of lactate dehydrogenase (LDHA) and monocarboxylate transporters (Sdao et al., 2021; Zhao et al., 2001),

ensuring that most pyruvate directly enters the TCA cycle through pyruvate dehydrogenase (and to a lesser extent through pyruvate carboxylase) rather than being diverted into lactate production (Cuozzo et al., 2022). However, it should be noted that substantial expression of LDHB has recently been reported in human islets, resulting in 6-fold higher lactate accumulation than mouse islets (Cuozzo et al., 2022). Due to the lack of monocarboxylate transporters for lactate export, this lactate will accumulate until it inhibits its own production.

Underscoring the importance of appropriate K_{ATP} channel activity for glucose homeostasis, activating mutations in either of the K_{ATP} channel subunits (the pore-forming Kir6.2 and the regulatory SUR1) cause several rare forms of monogenic diabetes. These include a valine to methionine amino acid substitution (V59M) in Kir6.2 (KCNJ11), which causes permanent neonatal diabetes (Gloyn et al., 2004). This mutation is often associated with developmental delay, a condition known as intermediate DEND (iDEND) syndrome[1] (Flanagan et al., 2006; Hattersley & Ashcroft, 2005). β-cell-selective expression of this mutation in transgenic mice (termed βV59M mice) leads to rapid β-cell hyperpolarisation and resultant hypoinsulinaemia and hyperglycaemia, with blood glucose reaching >20 mM within 2 days of induction (Brereton et al., 2014). These mice provide an ideal model for studying the effects of chronic hyperglycaemia specifically, without the confounding factors of insulin resistance or dyslipidaemia. An added advantage is that the phenotype is both inducible (with tamoxifen injection) and reversible (with sulphonylureas). In this thesis, studies of native islets from the βV59M mouse complement experiments using INS-1 cells, a radiation-induced stable rat insulinoma line with relatively high insulin content

[1] DEND is a triad of Developmental delay, Epilepsy, and Neonatal Diabetes

(~20% of native β-cell content) and robust stimulation of insulin secretion by physiological glucose concentrations (Asfari et al., 1992). Specifically, these cells are the 832/13 clone, which exhibits particularly robust glucose-stimulated insulin secretion (GSIS) (Hohmeier et al., 2000), but I will refer to them as simply INS-1 cells for convenience. INS-1 cells provide a largely pure β-cell population, notwithstanding that some glucagon production is detectable from the cells (Bollheimer et al., 2005), in which quantity of material is not a limiting factor and hyperglycaemia can be modelled with a high-glucose culture medium. The limitations of the model are discussed in chapter 8.

When β-cells are challenged with an (unphysiologically) abrupt increase in blood glucose, as occurs in a glucose tolerance test, GSIS follows a biphasic profile (figure 1.2), with a rapid transient peak lasting less than 10 minutes giving way to a period of sustained release (Rorsman & Ashcroft, 2018). Insulin secretion is switched off when the stimulus is removed, although when glucose is given orally the second phase can be extended and potentiated by the incretin effect. The incretins glucagon-like peptide-1 (GLP-1) and gastric inhibitory peptide (GIP) are hormones produced in the gut (by L and K cells, respectively). By binding and activating their specific G protein-coupled receptors on the β-cell, incretins increase insulin secretion through stimulation of adenylyl cyclase, leading to elevated levels of cyclic AMP and intracellular calcium, the latter being increased via a combination of L-type Ca^{2+} channel opening and release from the ER (Jones et al., 2018; Kim & Egan, 2008). The incretin effect describes the phenomenon whereby, for an equivalent level of glycaemia, oral glucose elicits a higher insulin secretory response than does intravenous glucose (Nauck & Meier, 2016). This effect is diminished or lost in T2D, largely due to downregulation of the GIP receptor (Kim & Egan, 2008). The readily releasable pool of secretory

granules near the plasma membrane, which comprises only 1-2% of the total granules in the β-cell (Rorsman & Ashcroft, 2018), is thought to be responsible for the first phase of insulin secretion, while the second phase depends on trafficking and exocytosis of granules from deeper within the cell. Newly-synthesised insulin contributes to the late phase, starting to be released after 30 minutes, and is released preferentially over existing stores (Jainandunsing et al., 2016; Rhodes & Halban, 1987).

Figure 1.1: Overview of stimulus-secretion coupling and the role of K_{ATP} channels

Figure created with BioRender.com

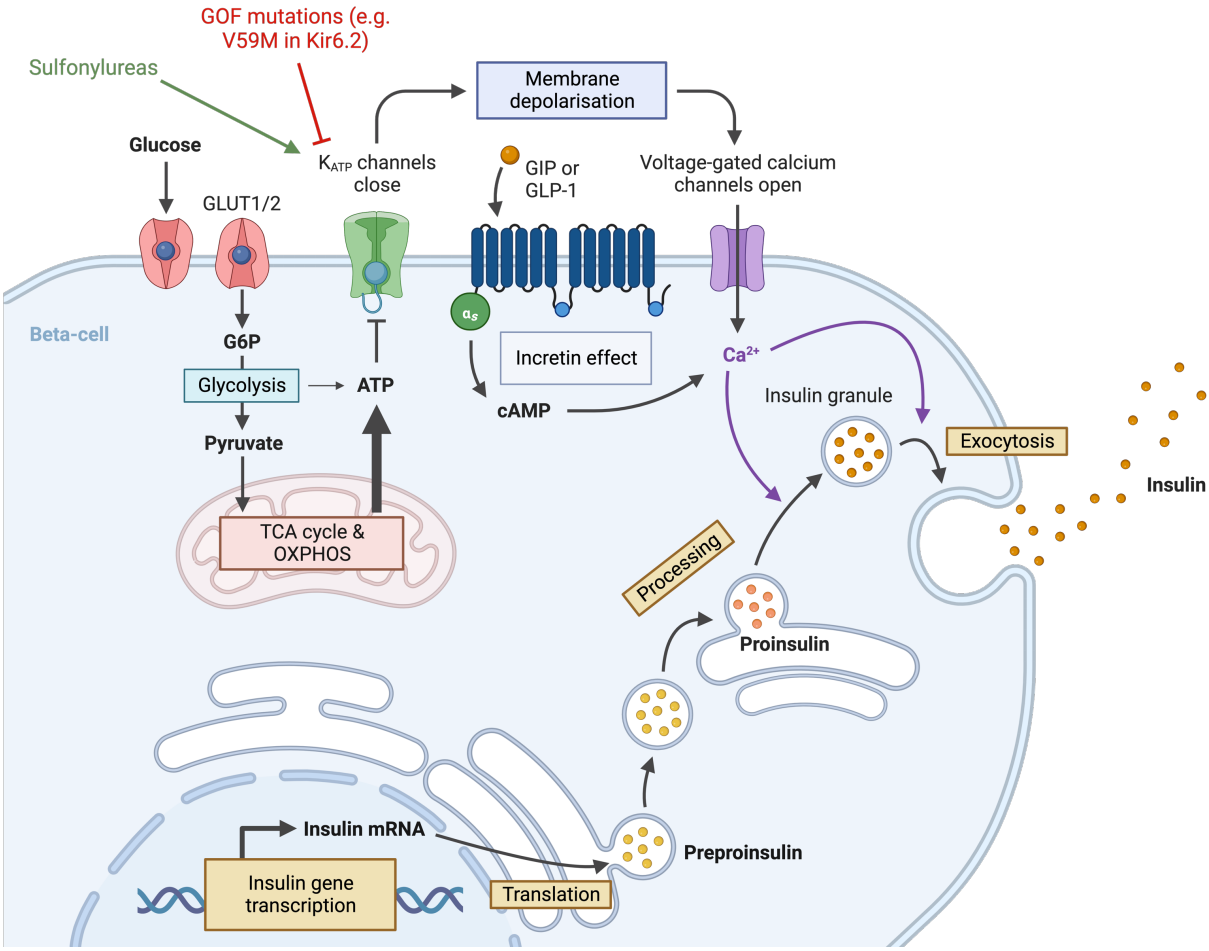

Figure 1.2: Schematic diagram of biphasic insulin secretion following a glucose tolerance test in non-diabetic and type 2 diabetic subjects

Representative of a diabetic subject with severe insulin deficiency.

Figure created with BioRender.com

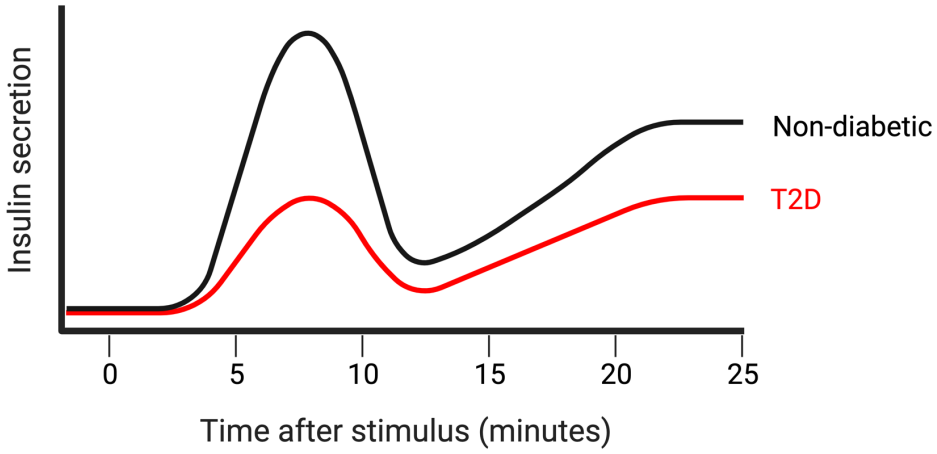

1.1.2 Regulation of insulin transcription

Transcriptional initiation is the first and arguably the most important control point in the process of insulin biosynthesis. Insulin biosynthesis begins with transcription of the single gene, *INS,* in humans, or the two insulin genes, *Ins1* and *Ins2*, in mice and rats. *Ins2* is directly orthologous to human *INS* and *Ins1* is the product of a gene duplication-transposition event (Shiao et al., 2008). Although the human and rodent insulin promoters differ significantly in structure (Hay & Docherty, 2006), both are regulated by the same array of transcription factors. In this thesis, I will focus on a set of five transcription factors known collectively as β-cell identity genes due to their importance in differentiation and maintenance of the β-cell fate. Indeed, it is the expression of the correct specific combination of transcriptional regulators that defines the β-cell lineage and (mostly) restricts insulin expression to this cell type (Sander & German, 1997). The five transcription factors are MAFA, NEUROD1 (also known as BETA2), NKX6-1, PAX6, and PDX1. Among these, PDX1 appears to have a more dominant role in primates than in other mammals (Bernardo et al., 2008), although all of the components of the transcriptional network are interdependent.

Rising glucose promotes the nuclear translocation of the β-cell identity genes, which then act synergistically to induce insulin transcription by binding to a highly conserved arrangement of *cis*-acting elements found in a ~400bp sequence upstream of the transcriptional start site. The A, C1, C2, and E elements of the promoter bind, respectively, PDX1, MAFA, PAX6, and the E47/NEUROD1 heterodimer (Hay & Docherty, 2006). MAFA, E47/NEUROD1 and PDX1 bind to the mouse *Ins2* promoter cyclically with a periodicity of 10-15 min; PDX1 binding and cycling is abolished at low (1 mM) glucose, whereas the other factors are unaffected (Barrow et al., 2006). Of all

the β-cell identity genes, MAFA is the most specific to β-cells (Matsuoka et al., 2004). MAFA acts downstream of NKX6-1, which is required for its expression and differentiates insulin$^+$ from glucagon$^+$ MAFB-expressing cells (Cerf, 2006; Nishimura et al., 2006). The human insulin promoter additionally contains a unique Z element, the deletion of which markedly reduces promoter activity (Pino et al., 2005). Finally, most mammalian insulin promoters contain 1 cyclic AMP response element (CRE), although the human promoter has 4 CREs (Hay & Docherty, 2006). When glucose is chronically elevated, the insulin promoter is inhibited. The potential underlying mechanisms will be discussed in section 1.2.

Figure 1.3: Simplified architecture of the rat insulin II gene showing key *cis*-acting elements in the promoter bound by their associated transcription factors

Figure created with BioRender.com

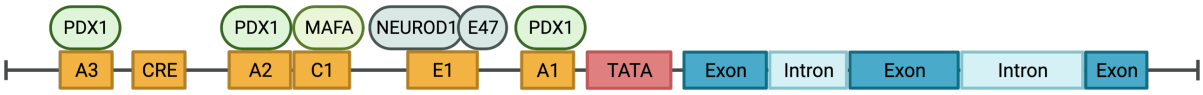

As outlined above, the same transcription factor network underlying insulin biosynthesis and secretion is also essential for β-cell differentiation. Over the course of development, from multipotent precursors to the mature β-cell, this network becomes increasingly complex (Servitja & Ferrer, 2004, fig. 4). One example of the non-linearity of the mature β-cell transcriptional network is that MAFA and PAX6 each activate insulin transcription directly and indirectly, through upregulation of *PDX1* (Servitja & Ferrer, 2004). Such an organisation enables modulation of insulin transcription on both short-term and long-term timescales in response to transient and sustained metabolic signals.

Disruption of this transcriptional network occurs in T2D and is a hallmark of dedifferentiation, a phenotypic alteration (beyond the range of normal heterogeneity) that involves the loss of critical β-cell machinery. The precise definition of dedifferentiation is contested by those who believe that β-cells regress to a precursor state and those who believe that dedifferentiated β-cells represent a novel state distinct from immature β-cells or their precursor (Weir et al., 2013). In support of the first definition, severe diabetes in *db/db* mice (resulting in only 10-15% of islet cells being insulin-positive) was associated with loss of MAFA and PDX1 and marked increases in staining for Neurog3, Oct4, and L-Myc (Talchai et al., 2012). This was attributed to loss of FoxO1, as ablation of FoxO1 had similar results. Correlative evidence from T2D islets suggests FoxO1 is similarly important in human β-cell differentiation (Cinti et al., 2016). The study by Cinti et al. found signs of possible transdifferentiation into other islet cell types as well as reversion to a precursor-like state characterised by expression of ALDH1A3, a key marker and apparent driver of dedifferentiation (Son et al., 2023). Reversal of dedifferentiation is possible through restoration of glucose homeostasis or through direct pharmacological intervention, such as ALDH1A3 inhibition (Son et al., 2023; Son & Accili, 2023). The β-cell transcriptional network can also display plasticity to guard against dedifferentiation. For instance, MAFB plays an essential role in β-cell differentiation during embryonic development but is usually restricted to α-cells in adult mice, although it is maintained in human adults. However, there is evidence that MAFB can maintain β-cell identity under pathological conditions in which MAFA is deficient (Z. Deng et al., 2022).

1.1.3 Post-transcriptional regulation of insulin biosynthesis

By far the most abundant transcripts in the β-cell are those encoding insulin, which comprise ~20% of all mRNA (100,000 to 200,000 molecules) in a mature β-cell (Van Lommel et al., 2006). Maintaining a large reserve of mRNA enables the rapid synthesis of new insulin when required to replenish the pool of insulin granules. Consequently, mRNA stability, which is positively regulated via binding of polypyrimidine tract-binding protein (PTB) to the 3'-untranslated region (3'-UTR) (Fred & Welsh, 2005), represents another control point in insulin biosynthesis. Experiments using actinomycin D at a concentration that inhibits RNA synthesis by ~90% showed that the enhancement of insulin biosynthesis by high (15.3 mM) glucose relative to 2.8 mM glucose over a 2-hour incubation was reduced from 8-fold to 2-fold (Alan Permutt & Kipnis, 1972). This demonstrates that insulin biosynthesis is driven predominantly by transcription, but that translation and proinsulin processing also make a significant contribution to the overall rate of biosynthesis. The effect of actinomycin D only became apparent after 45 minutes, showing that the early glucose-stimulated increase in insulin biosynthesis was attributable to the pre-existing mRNA pool.

Due to the aforementioned relative preference for the secretion of newly synthesised insulin, the rate of translation and processing may impact the rate of secretion in spite of the large storage pool – a murine β-cell typically contains ~13,000 insulin granules, occupying >10% of the cell volume (Dean, 1973). Short-term regulation of insulin biosynthesis by glucose (over the first 2 hours of stimulation) is predominantly mediated at the translational level (Itoh & Okamoto, 1980; Skelly et al., 1996). Not only does glucose stimulate global protein synthesis through mTOR-mediated phosphorylation of S6K1 and 4E-BP1 (Liu & Sabatini, 2020), but acute [glucose] elevation selectively further stimulates translation of preproinsulin mRNA, and probably enhances the efficiency of mRNA localisation to the endoplasmic reticulum

(ER) and nascent preproinsulin translocation across the ER membrane (M. Welsh et al., 1986; N. Welsh et al., 1991).

1.2 Changes in β-cell metabolism and insulin expression in hyperglycaemia: a vicious cycle

While β-cells initially respond to insulin resistance by increasing insulin secretion in a compensatory manner, this eventually becomes unsustainable. Both phases of glucose-stimulated secretion are impaired in type 2 diabetes (T2D), with first-phase secretion being particularly blunted (Hosker et al., 1989), while basal secretion in the fasted state is (inappropriately) increased. Progressive impairment of insulin secretion in T2D contributes to worsening hyperglycaemia, which in turn adversely affects β-cell function, constituting a vicious cycle. Moreover, as will be reviewed in detail below, diabetic β-cells contain less insulin. It is therefore of paramount importance to understand how hyperglycaemia impacts β-cell metabolism and impairs biosynthesis and secretion of insulin.

1.2.1 Metabolic impairment in hyperglycaemia

Major changes in β-cell metabolism occur during chronic hyperglycaemia, resulting in impairment of both glycolytic and oxidative glucose metabolism, with glucose-induced increases in ATP, NADH and oxygen consumption rate (OCR) all being reduced in islets isolated from βV59M mice (Haythorne et al., 2019). A lower ATP/ADP ratio in response to glucose stimulation is likewise apparent in human islets isolated from T2D

subjects relative to non-diabetic control islets (Anello et al., 2005). Multi-omics approaches have revealed some of the alterations underlying this impairment (Haythorne et al., 2019, 2022; Hou et al., 2017; Segerstolpe et al., 2016). Several glycolytic intermediates are substantially increased in hyperglycaemia, while most TCA cycle intermediates are less abundant. Metabolic gene and protein expression is similarly affected, with those involved in glycolysis/gluconeogenesis being generally upregulated (table 4.1), whereas those involved in the TCA cycle and oxidative phosphorylation are generally downregulated (table 4.2). Strikingly, high (25 mM) glucose culture of human islets caused downregulation of 11 of the 13 mitochondrially-encoded respiratory chain subunits (Brun et al., 2015). Changes in gene expression observed following 4 weeks of hyperglycaemia in a 90% pancreatectomy rat model include upregulation of mitochondrial uncoupling protein 2 (*Ucp2*) and upregulation of *Ldha* and monocarboxylate transporter isoforms *Mct1*, *Mct2*, and *Mct4* (Ross Laybutt et al., 2002), although these findings could partly reflect changes in non-β-cells, and experiments using INS-1 cells found that increases in the proton leak and lactate export during hyperglycaemia were quite modest (Göhring et al., 2013). These changes are nonetheless signs that the β-cell is struggling to cope with a nutrient overload whether by dissipating the mitochondrial membrane potential or diverting metabolites into alternative pathways. Increased expression of components of mitochondrial shuttles, such as *AGC2* (involved in the malate-aspartate shuttle), in chronic high glucose-cultured human islets suggests an increased need to regenerate cytosolic NAD^+ (Brun et al., 2015). Major bottlenecks at glyceraldehyde 3-phosphate dehydrogenase (GAPDH), which has dramatically reduced activity (likely due to a shortage of the cofactor NAD^+), and pyruvate dehydrogenase, which is inhibited by pyruvate dehydrogenase kinase 1 (PDK1), may explain the severely impaired flux

through glycolysis and into the TCA cycle in hyperglycaemia (Davis et al., 2020; Haythorne et al., 2022).

Experiments using selective inhibitors and siRNA knockdowns of key glycolytic enzymes suggest that accumulation of a glycolytic metabolite between phosphofructokinase (PFK) and GAPDH – one or more of F1,6BP, DHAP or GA3P – is a key mediator of many of the effects of chronic hyperglycaemia on β-cell metabolism, including the marked upregulation of mTORC1 (Haythorne et al., 2022). However, insulin biosynthesis appears to be regulated by a different mechanism as inhibition of the downstream mediator of mTOR signalling S6K1, while correcting many of the metabolic defects, neither prevented nor restored (in INS-1 cells and islets, respectively) the loss of insulin content observed in hyperglycaemia/diabetes (Haythorne et al., 2022). A core aim of this thesis is therefore to ascertain how hyperglycaemia-induced metabolic dysregulation is linked to the downregulation of insulin biosynthesis.

1.2.2 Insulin biosynthesis is diminished in chronic hyperglycaemia and type 2 diabetes

It is well-established that insulin content is diminished in hyperglycaemic and T2D islets, though there is some debate over whether this signifies β-cell dedifferentiation (possibly to a progenitor-like state), loss of β-cells (by apoptosis), or simply that the β-cells are emptied of insulin.

In the βV59M mouse model, insulin content falls precipitously following the induction of hyperglycaemia, with a ~70% reduction after 4 weeks; insulin mRNA is also

reduced, by >40% (Brereton et al., 2014). Ultrastructural analysis showed that the β-cells are still present but contain very few insulin granules (Brereton et al., 2014). In another K_{ATP}-GOF mouse model with a different Kir6.2 mutation, pancreas insulin content was reduced by ~80% 30 days after hyperglycaemia was induced (Z. Wang et al., 2014). In the latter model, expression of Ngn3 (a marker of islet progenitor cells) was induced in diabetic β-cells, indicating dedifferentiation, and could be reversed by blood glucose normalisation by insulin therapy; upregulation of Ngn3 (*Neurog3*) was found at the mRNA but not the protein level in βV59M islets (Brereton et al., 2014).

Several studies have assessed insulin content in *ex vivo* human islets cultured at high glucose. Islets cultured for 4 days or longer at a severely hyperglycaemic concentration of 33 mM glucose show reduced insulin content, mRNA levels, insulin promoter activity and PDX1 binding activity (Marshak et al., 1999). Looking at more physiological glucose levels, long-term culture of ND islets at 8, 10, and 20 mM glucose reduces insulin content relative to that at 5 mM glucose in a dose-dependent manner (Tariq et al., 2022). Single cell transcriptomic profiling of human islets revealed a median decline in *INS* mRNA levels of 8% in T2D β-cells relative to non-diabetic β-cells (Segerstolpe et al., 2016). In addition to studies using islets taken directly from donors, studies of human pseudoislets[2] show that 2 weeks of high-glucose culture severely reduces insulin content (Mir-Coll et al., 2021). Strikingly, the decline at 8 mM glucose was comparable to that at higher glucose concentrations (11 and 16.7 mM), indicating that even blood glucose levels within the target range for patients with T2D are sufficient to drive a significant decline in insulin biosynthesis.

[2] Standardised human islet microtissues are produced by dissociation of donor islets and reaggregation of constituent cells into pseudoislets of uniform size and composition.

In T2D patients, insulin content is approximately one third lower than in non-diabetic subjects (Henquin et al., 2017). Losses of some 40% of β-cell volume have been reported in T2D islets and attributed to increased apoptosis (Butler et al., 2003). However, studies such as this may overestimate β-cell loss by quantifying β-cell volume using immunostaining for insulin. Careful studies using both immunohistochemistry and electron microscopy to identify cells by morphology and ultrastructure as well as quantifying insulin have concluded that marked degranulation of β-cells, rather than loss of β-cells, mostly accounts for the low insulin content of T2D islets (Cinti et al., 2016; Marselli et al., 2014). Nevertheless, some argue that only 1-3% of β-cells are "empty" and that β-cell mass really is reduced as islets are reduced in size in T2D (Weir et al., 2020).

1.2.3 Potential pathways for downregulation of insulin biosynthesis

Paradoxically, glucose stimulates insulin biosynthesis in the short term but has an inhibitory effect in the longer term (Alan Permutt & Kipnis, 1972; Lawrence et al., 2005; Olson et al., 1993). Many different mechanisms for the downregulation of insulin biosynthesis have been proposed, impacting each step of the process from transcriptional initiation to proteolytic processing. However, the relative importance of each of these pathways, and how they become dysregulated in chronic hyperglycaemia, remains uncertain. In this thesis, I aim to elucidate the initial steps by which metabolic alterations trigger the downregulation of insulin biosynthesis.

In the early 1990s, studies using the hamster cell line HIT-T15 established that insulin promoter complex formation is impaired by chronic high glucose culture (Olson et al., 1993), though more work would be needed to discover the underlying mechanisms.

As the intricacies of the transcriptional regulation of insulin have subsequently been teased out, it has emerged that the β-cell identity genes are also downregulated by chronic hyperglycaemia. In a 90% pancreatectomy model, rats had 13 mM mean blood glucose at 10 weeks post-pancreatectomy and RNAseq revealed that expression of *Ins1*, *Ins2*, *Mafa*, *Pax6* and *Pdx1* had halved compared to the control group; *Neurod1* and *Nkx6-1* were reduced by 40% and 70% respectively (Ebrahimi et al., 2020). When expression at 4 weeks was analysed, hyperglycaemia-induced downregulation of the identity genes had begun, but expression of the insulin genes had not yet changed. This suggests that downregulation of the identity genes causes transcriptional repression of *Ins1* and *Ins2*. In support of this idea is the observation that *MAFA* and *PDX1* are among the most downregulated genes in T2D islets (Marselli et al., 2020). *Mafa*, *Nkx6-1* and *Pdx1* were also downregulated in diabetes induced by acute insulin resistance (Blum et al., 2014). The changes in expression of insulin, associated transcription factors, and selected markers of (de)differentiation that occur in diabetic βV59M islets are summarised in table 1.1.

Table 1.1: Changes in mRNA and protein expression of key transcription factors regulating insulin expression and selected markers of β-cells (de)differentiation in control and diabetic βV59M islets

RNAseq data from 4 control and 3 diabetic mice; protein mass spectrometry data from 4 control and 4 diabetic mice. FC = fold change (diabetic vs control): red = up, blue = down in diabetes. The most upregulated or downregulated transcripts/proteins have the strongest intensity of colour. Some proteins were not detected by mass spectrometry (empty boxes). P-values: red = $p \geq 0.05$ (non-significant), green = $p < 0.05$ (significant). Data taken from RNAseq and proteomics experiments described by Haythorne et al. (2019): transcriptomics data are available in the European Nucleotide Archive (https://www.ebi.ac.uk/ena) under the accession number ERP114395 and mass spectrometric proteomics data are deposited to the ProteomeXchange

Consortium via the PRIDE partner repository with the data set identifier PXD012979 and 10.6019/PXD012979.

Gene	Full name	RNAseq islet		Protein MS islet	
		FC (Db vs C)	p-value	FC (Db vs C)	p-value
Chga	Chromogranin A	0.41	2.03E-26	0.12	2.40E-05
Gcg	Glucagon	2.46	3.40E-10	0.85	5.35E-01
Ins1	Insulin-1	0.58	4.67E-05	0.24	1.02E-03
Ins2	Insulin-2	0.66	4.88E-07	0.51	1.53E-01
Mafa	MAF BZIP transcription factor A	1.33	2.14E-01		
Mafb	MAF BZIP transcription factor B	1.26	3.15E-02		
Mlxip	Mlx interacting protein (MondoA)	0.85	4.27E-02		
Mlxipl	Mlx interacting protein like (ChREBP)	0.78	4.27E-02	0.21	2.34E-05
Neurod1	Neuronal differentiation 1	0.97	6.95E-01		
Neurog3	Neurogenin 3	0.67	3.39E-02		
Nkx6-1	NK6 homeobox 1	0.64	1.06E-04		
Pax6	Paired box 8	0.90	1.48E-01		
Pdx1	Pancreatic and duodenal homeobox 1	0.83	6.63E-02	0.58	8.62E-03
Stat3	Signal transducer and activator of transcription 3	1.87	1.01E-11	1.45	4.27E-02
Txnip	Thioredoxin interacting protein	8.74	2.72E-39	44.52	5.40E-03
Ucn3	Urocortin 3	0.12	1.24E-33	0.33	6.99E-02

Thus, transcriptional repression of the insulin gene(s) occurs through inhibition of complex formation at the promoter and downregulation of the expression of key transcription factors. In chapter 5, I will address three potential pathways for this. Firstly, sustained elevation of cytosolic calcium has been postulated to result in ERK1/2 switching, through its (calcineurin-dependent) phosphorylation status, from activating the insulin promoter when glucose increases acutely to inhibiting promoter activity during chronic hyperglycaemia (Lawrence et al., 2005). Based on immunoprecipitation experiments, this was attributed to the binding partner for NFAT switching from MAFA to CCAAT enhancer-binding protein β (C/EBP-β), which is upregulated in some models of diabetes (Seufert et al., 1998). Secondly, small heterodimer partner (SHP, also known as NR0B2), which is upregulated significantly

in chronic hyperglycaemia in INS-1 cells (figure 5.8a), is reported to block p300-mediated MAFA/PDX1 complex formation (Park et al., 2007). Thirdly, thioredoxin-interacting protein (TXNIP), one of the most highly upregulated proteins in hyperglycaemia, downregulates MAFA by inhibiting STAT3, thereby inducing miR-204 (a largely β-cell-specific microRNA), which in turn targets the 3'-UTR of *Mafa* (Xu et al., 2013). These three pathways are summarised schematically in figure 5.1.

Once transcription is completed, mature preproinsulin mRNA is stabilised by PTB. However, chronic hyperglycaemia upregulates miR-133a, which reduces PTB protein levels (Fred et al., 2010). The final step of insulin biosynthesis, following cleavage of the signal peptide, is the processing of proinsulin to insulin. Translation of proprotein convertase 1 (PCSK1) is acutely stimulated by glucose (Zakaria et al., 2021), but PCSK1 protein levels decrease in chronic hyperglycaemia (βV59M proteomics data), which could reduce processing efficiency. Moreover, impaired proinsulin processing and induction of the adaptive unfolded protein response (UPR), leading in time to excessive ER stress, has been associated with progression from normal to impaired glucose tolerance (IGT) and the subsequent transition to T2D (Brusco et al., 2022). Under chronic ER stress, the effects of the UPR switch from beneficial to harmful, and include reduced expression of *Mafa*, *Neurod1*, *Nkx6-1*, and *Pdx1*, and in turn reduced insulin gene expression (Sharma et al., 2021; Son & Accili, 2023).

1.2.4 Is the loss of insulin reversible?

T2D remission is possible through bariatric surgery or very-low-calorie diets, with a restoration of insulin biosynthesis likely attributable to a combination of lower blood

glucose and enhanced incretin action (Karra et al., 2010; Lean et al., 2018). This knowledge raises the question of how readily β-cell function, including insulin biosynthesis, is recoverable through restoration of normoglycaemia. Reversal of diabetes (after 4 weeks) in βV59M mice by 4 weeks of glibenclamide treatment restored normal insulin content (Brereton et al., 2014). Human islets cultured at very high (33 mM) glucose and restored to normoglycaemia on day 6 showed a partial recovery of insulin content 3 days after reversal, while the insulin content of those maintained at high glucose continued to decline between days 4 and 9 (Marshak et al., 1999). Thus, it is apparent that the loss of insulin is reversible given enough time, with greater duration of hyperglycaemia leading to more severe insulin loss and a correspondingly slower recovery. Does there come a point, however, when recovery is no longer possible? Can therapeutic interventions slow or prevent the decline and maintain sufficient β-cell function to avoid diabetes progression? Determining the mechanism by which hyperglycaemia causes downregulation of insulin biosynthesis is a crucial step towards answering these questions and identifying potential targets for drug discovery.

1.3 The role of glycogen in β-cell dysfunction: more questions than answers

Although euglycaemic islets contain very low or undetectable levels of glycogen, glycogen accumulation in the β-cells of diabetic patients was discovered as early as 1951 and has subsequently been observed in many animal models of diabetes or hyperglycaemia (Ashcroft et al., 2017). In addition, a number of ultrastructural studies have mistakenly described “empty” or “vacuolated” β-cells, both in animal models

(Jung et al., 2008) and in human T2D and T1D donor islets (Masini et al., 2009; Poudel et al., 2015), as glycogen is washed out and lost unless certain fixation methods, for instance using lead tetraacetate or lead citrate (Brereton et al., 2016; Graf & Klessen, 1981), are used to preserve it. In T2D, substantial glycogen deposits are present in donor islets even when the disease is successfully diet-controlled, with HbA1c at 6.6% (Ashcroft et al., 2017). Glycogen synthesis is initiated rapidly in response to increased glucose availability and is proportional to the severity of hyperglycaemia. There is a linear relationship between the extracellular glucose concentration and glycogen content of INS-1 cells exposed to high (10, 15, 20, or 25 mM) glucose for 1 hour (Mugabo et al., 2017). Healthy β-cells are highly sensitive to changes in blood glucose; if β-cells metabolise glucose released from stored glycogen, this will disrupt proper stimulus-secretion coupling, and could drive elevated basal insulin secretion in T2D. However, the functional significance of increased β-cell glycogen storage remains contentious: is it protective or deleterious? Is it a cause as well as a consequence of metabolic dysregulation?

1.3.1 Overview of glycogen metabolism and its regulation

Glycogen is the cellular storage form of glucose, and is mostly found in skeletal muscle, where it facilitates muscle contraction, and in liver, where it supports blood glucose homeostasis. Much smaller quantities are stored in other tissues, including neurons and glial cells in the brain, kidney, and erythrocytes, as well as pancreatic β-cells. Each glycogen particle is centred on a molecule of the protein glycogenin (GYG), which synthesises a priming oligosaccharide. Glycogen synthase (GYS) then elongates the incipient glucose polymer by adding uridine diphosphate glucose (UDP-glucose) units through α-1,4 glycosidic linkages. When a chain reaches around 12

glucose units long, glycogen branching enzyme (GBE) transfers a chain of 7 units to a non-terminal residue, forming an α-1,6 glycosidic bond. This process continues to produce a large, dynamic, multibranched structure with many terminal residues, enabling rapid mobilisation while also increasing the solubility of the molecule and reducing osmotic pressure. GYS is the rate-limiting enzyme in glycogenesis, while glycogen phosphorylase (PYG) catalyses the rate-limiting step in glycogenolysis, which is the cleavage of α-1,4 linkages to release glucose 1-phosphate. Glycogen breakdown also requires the action of glycogen debranching enzyme, which removes the branch points and thereby releases around 10% of the molecule as free glucose. Some of the enzymes involved in glycogen metabolism have multiple isoforms; the isoforms expressed in β-cells are listed in table 1.2.

Figure 1.4: Overview of glycogen metabolism

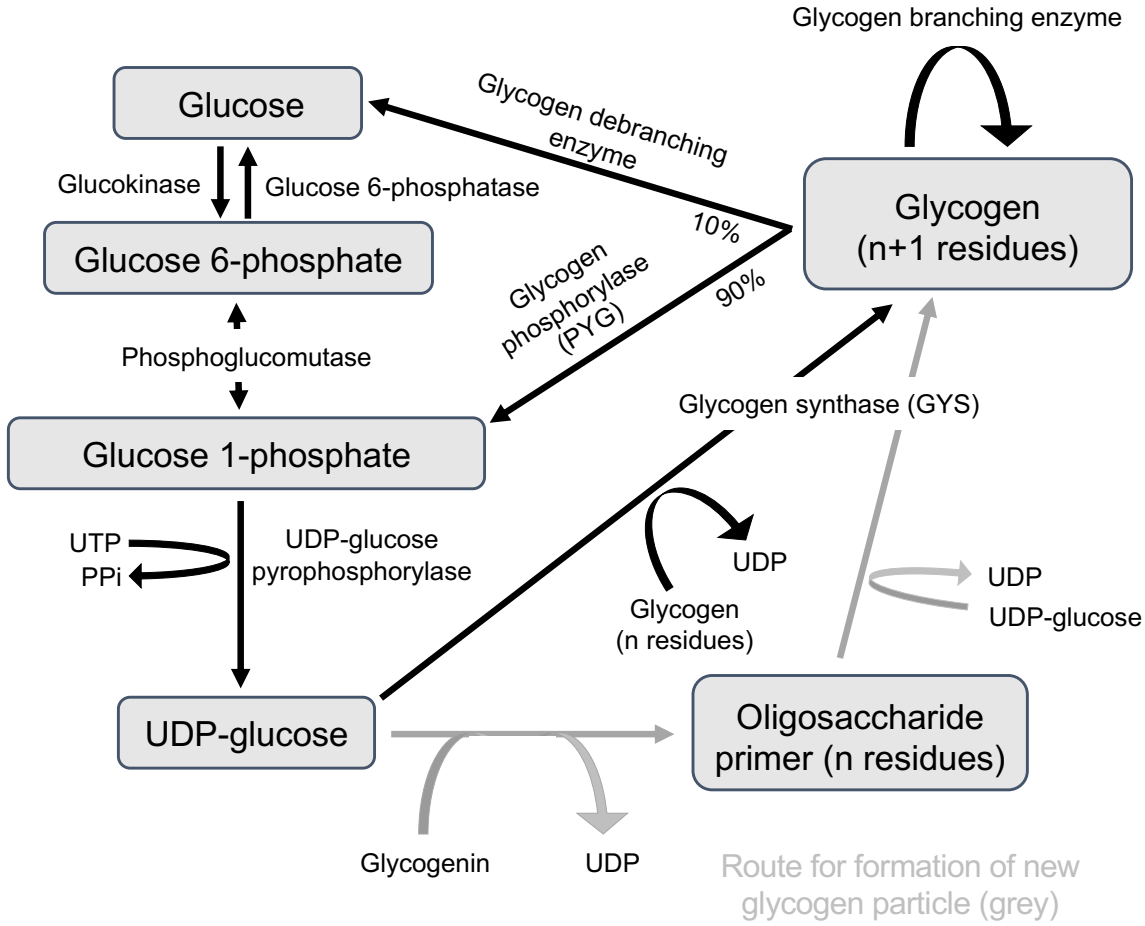

Table 1.2: Isoforms expressed in human and rat β-cell lines of the key enzymes of glycogen metabolism

Enzyme	Gene(s) expressed in human (EndoC) β-cells	Gene(s) expressed in INS-1 cells
Glycogenin	*Gyg1*, *Gyg2*	*Gyg1*
Glycogen synthase	*Gys1*	*Gys1*
Glycogen phosphorylase	*Pygb*, *Pygl, Pygm**	*Pygb*, *Pygl*

*Very low expression level

Unfortunately, little is known about the regulation of glycogen metabolism in β-cells specifically, so much must be inferred by reference to studies in other tissues, even though this may not be valid. Glycogen metabolism in β-cells is regulated via protein

phosphorylation, allostery, and control of the expression of some proteins (see table 1.3). GYS is inactivated by phosphorylation, while PYG is activated by phosphorylation. 9 phosphorylation sites have been characterised for GYS1 (Zois & Harris, 2016); those considered most important are the AMPK site at Ser8 (site 2) and GSK3 sites at Ser641 and Ser645 (sites 3a and 3b). Phosphorylation at these sites may hold GYS in the tense state[3] by strengthening inter-subunit electrostatic interactions (Marr et al., 2022). GYS is activated through dephosphorylation by protein phosphatase 1 (PP1) and allosterically by G6P. PYG is activated by phosphorylase kinase (PhK) at a single site (Ser14); PhK is in turn activated by cAMP-dependent protein kinase A (PKA). PYG also binds multiple allosteric effectors: signals of low cellular energy status (AMP and inorganic phosphate) and glucose 1-phosphate stabilise the relaxed I state, helping to mobilise glucose when needed, while glucose, ATP, purine nucleosides and G6P stabilise the tense (T) state. GYS expression does not change significantly with glycaemia, but PYGL and GBE1 (glycogen branching enzyme) are upregulated at the mRNA and protein level in chronic hyperglycaemia (table 1.3).

The PP1 regulatory subunit PPP1R3C (or PPP1R5), also known as protein targeting to glycogen (PTG), is strongly and rapidly induced by glucose, being upregulated approximately 5-fold in diabetic βV59M islets (Brereton et al., 2016). In hepatocytes, PTG is induced by fructose 2,6-bisphosphate-mediated recruitment of the G6P-activated transcription factor MondoA to its promoter (Petrie et al., 2013) and in neurons it is regulated at the protein level by proteasome-dependent degradation

[3] The glycogen synthase tetramer can exist in a ‘tense’ state (a tight conformation) or a ‘relaxed’ (more active) state

(Vilchez et al., 2007). PTG recruits PP1 to glycogen particles and dramatically reduces the phosphorylation status of GYS. Control of PTG expression is critically important, since overexpression studies have shown that its powerful capacity to stimulate glycogenesis is independent of both glycogen and G6P levels, at least in skeletal muscle (Lerín et al., 2000; Montori-Grau et al., 2011). PTG is in fact one of at least 7 glycogen-targeting subunits, each with a different pattern of tissue specificity (Zois & Harris, 2016); it is known that glycogen-targeting subunits affect the size and subcellular distribution of glycogen particles (Montori-Grau et al., 2011), yet the significance of expressing different combinations of these subunits for glycogen regulation under different metabolic stresses is unclear.

Table 1.3: Changes in mRNA and protein expression of key genes involved in glycogen metabolism in control and diabetic βV59M islets

FC = fold change (diabetic vs control): red = up, blue = down in diabetes. The most upregulated or downregulated transcripts/proteins have the strongest intensity of colour. Some proteins were not detected by mass spectrometry (empty boxes). P-values: red = p≥0.05 (non-significant), green = p<0.05 (significant). Data taken from RNAseq and proteomics experiments described by Haythorne et al. (2019): transcriptomics data are available in the European Nucleotide Archive (https://www.ebi.ac.uk/ena) under the accession number ERP114395 and mass spectrometric proteomics data are deposited to the ProteomeXchange Consortium via the PRIDE partner repository with the data set identifier PXD012979 and 10.6019/PXD012979.

Gene	Full name	RNAseq islet		Protein MS islet	
		FC (Db vs C)	p-value	FC (Db vs C)	p-value
Gbe1	Glycogen branching enzyme	2.28	1.59E-10	4.29	2.08E-04
Gyg1	Glycogenin	0.88	1.33E-01	3.93	2.33E-06
Gys1	Glycogen synthase 1	1.10	4.34E-01		
Ppp1r1a	PP1 regulatory subunit 1a	0.68	1.31E-03	0.71	2.20E-01
Ppp1r3c	PP1 regulatory subunit 3c (PTG)	6.08	2.07E-09		
Ppp1r3d	PP1 regulatory subunit 3d	0.44	2.15E-06		

Pygb	Glycogen phosphorylase, brain form	1.16	1.19E-01	1.76	1.13E-03
Pygl	Glycogen phosphorylase, liver form	2.96	3.93E-16	2.55	2.35E-03
Ugp2	UDP-glucose pyrophosphorylase	0.87	1.24E-01	1.64	8.34E-03

Despite the considerable knowledge outlined here of mechanisms for regulating glycogen metabolism, how altered β-cell metabolism drives its accumulation in hyperglycaemic conditions is not fully understood (Ashcroft et al., 2017). Gaining a better understanding of this link is therefore one of the aims of this thesis.

1.3.2 Is excess glycogen a driver or only a symptom of β-cell dysfunction?

As diabetic β-cells have impaired glucose metabolism, lack the outlet of lactate export, and have reduced expression of glucose-6-phosphatase, glycogen synthesis is likely to be (in the short term) a safe outlet for excess fuel that cannot be oxidised during episodes of hyperglycaemia, alongside glycerol release (Cantley et al., 2009; Mugabo et al., 2017). However, excess glycogen accumulation has been postulated to be deleterious for β-cell function. Outstanding questions include whether glycogen accumulation exacerbates the dysregulation of metabolism and metabolism-secretion coupling and/or impairs autophagy and causes cell death.

Mobilising glycogen when glucose levels fall could disrupt the tight stimulus-secretion coupling normally exhibited by β-cells, thereby disrupting whole-body glucose homeostasis (Malaisse, 2016). Indeed, in islets pre-incubated for 20h at high-glucose and transferred to a glucose-free medium, rapid glycogenolysis when cAMP/PKA signalling was stimulated by theophylline evoked a dramatic transient burst of insulin release. (Malaisse et al., 1977). A similar enhancement of glycogenolysis and insulin

secretion via cAMP elevation has been reported with IBMX and forskolin (Andersson et al., 2016). Thus β-cell glycogen storage has the potential to contribute to hyperinsulinaemia in T2D.

Autophagy, the recycling of cellular components through the lysosomes, provides an alternative mechanism for glycogen breakdown to glycogenolysis by PYG. Intriguingly, glycogen accumulation at high glucose proceeds at around twice the rate of glycogen mobilisation when glucose is subsequently lowered (Andersson et al., 2016), suggesting that β-cells may be unable to clear glycogen stores during sustained hyperglycaemia without sufficient windows of euglycaemia. This would put pressure on the autophagic system, which is known to be impaired in T2D (Masini et al., 2009), at a time when autophagy is inhibited by the hyperglycaemia-induced upregulation of mTORC1 (Ardestani et al., 2018). 4-week diabetic βV59M islets display markers of impaired autophagic flux, including increased ubiquitin aggregates and p62 protein, both of which co-localised with glycogen deposits (Brereton et al., 2016). Meanwhile, restoration of normoglycaemia dramatically increased the number of autophagosomes, which (along with the lysosomes) were found to contain glycogen particles (Brereton et al., 2016). Glycogen accumulation *per se* has been shown to cause autophagic impairment in neurons (Duran et al., 2014), another cell type that stores very little glycogen under physiological conditions, so it is reasonable to propose that this also applies to β-cells. In summary, the autophagic-lysosomal system appears unable to degrade β-cell glycogen quickly enough while hyperglycaemia persists.

Glycogen accumulation is also implicated in increased β-cell apoptosis in hyperglycaemia and diabetes. 2-week diabetic βV59M islets were found to contain cleaved caspase-3 and apoptotic bodies; the latter, like the autophagosomes, contained glycogen (Brereton et al., 2016). Moreover, increased glycogen accumulation following siRNA knockdown of UGP2 was associated with increased caspase-3 activation (Brereton et al., 2016). Glycogen is known to be pro-apoptotic in neuronal cells and contributes to neurodegeneration (Duran et al., 2012; Vilchez et al., 2007).

Some, however, have argued against glycogen being a contributor to β-cell dysfunction. A pancreas-specific knockout of GYS1 did not affect β-cell function, demonstrating that glycogen metabolism is non-essential under non-diabetic conditions (Mir-Coll et al., 2016). However, this is unsurprising considering that glycogen accumulation does not occur in euglycaemia. The same study also generated a PTG overexpression (PTG^{OE}) mouse model, which forced significantly increased glycogen accumulation at high glucose in *ex vivo* islets, but found that glucose tolerance was normal, even on an HFD, and there was no increase in β-cell death (Mir-Coll et al., 2016). However, the authors observed that glycogen in PTG^{OE} islets was mobilised during an overnight fast; such mobilisation of glycogen stores at times of low extracellular glucose likely explains the lower glycaemia and increased insulinaemia of PTG^{OE} islets and is consistent with the hypothesis that glycogen breakdown can trigger inappropriate insulin secretion. Surprisingly, one study of glycogen phosphorylase inhibitors (GPi) in MIN6 cells, a mouse insulinoma-derived cell lines, reported that PYG inhibition (which increased cellular glycogen content) improved β-cell function and survival, including enhanced GSIS and increased mRNA

and protein expression of PDX1 and insulin (Nagy et al., 2018). To explain this, the authors hypothesised that glycogen particles serve as a hub for protein-protein interactions, especially mTOR (which was activated by GPi treatment, as indicated by enhanced phosphorylation of S6K1) and members of the InsR signalling pathway. It should be noted, however, that these conclusions were based on quite moderate increases in glycogen under euglycaemic conditions (5.5 mM glucose), which may limit their relevance to hyperglycaemia. Unfortunately, the proposed interaction with mTOR (arising from an *in silico* screen) was not validated experimentally, but it would be of considerable interest to know if glycogen can bind mTOR and thereby regulate β-cell metabolism, since, in hyperglycaemic β-cells, hyperactivated mTOR impairs mitochondrial metabolism and GSIS (Haythorne et al., 2022).

1.4 Summary of the project aims

As outlined above, chronic hyperglycaemia in pancreatic β-cells causes both a metabolic impairment and a loss of insulin mRNA and protein. Hyperglycaemic β-cells accumulate glycogen, the consequences of which for β-cell function remains uncertain. I therefore aimed:

1. To establish whether the metabolic impairment is responsible for the decline in insulin biosynthesis, and, if so, to identify the metabolic signal that initiates this decline.
2. To determine whether changes in β-cell metabolism lead to increased glycogen storage during hyperglycaemia, whether glycogen exacerbates the dysregulation of metabolism and metabolism-secretion coupling, and whether glycogen can impair autophagy and induce β-cell death.

2. Materials and Methods

2.1 INS-1 (832/13) cell culture

INS-1 cells were originally developed by Claes Wollheim (Geneva) and supplied by Patrik Rorsman (Oxford). INS-1 832/13 cells were cultured in a humidified atmosphere of 5% CO_2/95% air at 37°C in RPMI 1640 medium supplemented with 10% foetal bovine serum (FBS), 1% Penicillin/Streptomycin, 50 μM β-mercaptoethanol, 1 mM sodium pyruvate, 10 mM HEPES and 1% GlutaMAX (standard culture medium; all Sigma). For maintenance, cells were cultured at 11 mM glucose in T75 flasks. Cells were passaged using a 3 mins incubation with TrypLE Express Enzyme (Life Technologies), which was subsequently quenched with standard culture medium; cells were then pelleted and re-suspended in fresh media. Cells were passaged twice weekly, and cells used in experiments were from passage 25 up to a maximum of passage 40. For experiments, cells were seeded into TC-treated plates (6-well, 12-well, 24-well, or 96-well, as required for the experiment) and cultured at 5 mM (low glucose: LG) or 25 mM (high glucose: HG) to reproduce normoglycaemia (control) or hyperglycaemia (diabetes), respectively. For some experiments, cells were cultured at other glucose concentrations and/or in the presence of other metabolic substrates (methyl pyruvate, methyl succinate, leucine) as indicated in the relevant chapter. When small molecules in solution in DMSO were added to the medium, an equivalent volume of DMSO (dependent on the stock concentration, but typically a 1:1000 dilution was used) was added to control cells, labelled as vehicle (veh) in figure legends.

2.2 EndoC cell culture

2.2.1 EndoC-βH1

For maintenance, EndoC-βH1 cells (Human Cell Design) were propagated in OPTIβ1 medium (Human Cell design). Cells were cultured in 10cm or 15cm tissue culture dishes (Helena Biosciences, 93100T) pre-coated for at least 1h with 1% ECM gel (Sigma, E1270), 1% Penicillin/Streptomycin (Gibco, 15140122), and 2 µg/ml Fibronectin (Sigma, F1141) in high-glucose DMEM (Gibco, 41965-039). Cells were split every 7–10 days and seeded at a density of 70,000–75,000 cells/cm^2. For experiments, cells were seeded into pre-coated 96-well plates (Helena Biosciences, 92696T). Automated cell counting was performed using the NucleoCounter NC-250 (chemometec).

2.2.2 EndoC-βH5

EndoC-βH5 cells (Human Cell Design) were cultured according to the manufacturer's protocol. Briefly, cells were rapidly thawed and seeded at a density of 60,000 cells/well into pre-coated 96-well plates. Cells were cultured in a humidified atmosphere of 5% CO_2/95% air at 37°C in ULTIβ1 medium (Human Cell Design). Where relevant, reverse transfection was performed as described in Section 2.5. Media was replaced after 24h with fresh ULTIβ1 (5.5 mM glucose) or ULTIβ1 supplemented with glucose to different concentrations. Immediately after this, cells that were previously transfected were re-transfected with fresh siRNA/RNAiMAX as described in Section 2.5.2. GSIS was performed 5 days after the media change as described in Section 2.8.

2.3 Animal experiments

This work was performed collaboratively, as explained in the declaration of authorship.

The MGI ID for floxed Kir6.2-V59M mice is 3832575.

This work was carried out under the PPL no. P6C1A2A98.

All experiments on mice were conducted in accordance with the UK Animals (Scientific Procedures) Act (1986) and approved by the Department of Physiology, Anatomy and Genetics ethical review committee. βV59M mice, which hemizygously express the Kir6.2-V59M transgene specifically in their β-cells, were generated using Cre-lox technology. First, the mouse strain R26StopKir6.2-V59M*lox/*+ (ROSA) was generated: the Kir6.2-V59M transgene, preceded by a loxP-flanked STOP sequence and followed by a flippase (FLP) recombinase target (FRT)-flanked internal ribosome entry site (IRES) GFP cassette, was targeted to the ROSA26 locus by homologous recombination in ES cells (Girard et al., 2009). Heterozygous ROSA mice were then crossed with RIPII-Cre-ER mice (in which Cre recombinase is expressed under the control of the rat insulin promoter II). For further details, see figure 1 from Girard et al. (2009) and chapter 3 (section 3.4.3). The background strain was C57BL6/J (Jackson Labs, USA). Both male and female mice were used. Transgene expression was induced at 12 weeks of age by subcutaneous injection of tamoxifen (Sigma) in corn oil. Tamoxifen-injected wild-type, RIPII-Cre-ER, and floxed STOP Kir6.2-V59M littermates were used as controls. All mice were bred from established stocks in the facility. Mice had unrestricted access to water and a regular chow diet (63% carbohydrate, 23% protein, 4% fat; Special Diet Services, RM3). Mice were maintained on a 12-hour light-dark cycle at 21°C and 45-55% relative humidity. Body weight and blood glucose levels were monitored routinely. Blood glucose levels were

measured from the tail vein using the Freestyle Lite device and Freestyle Lite test strips (both Abbott).

2.4 Islet isolation and culture

Mice were humanely culled by cervical dislocation. Pancreata were inflated with collagenase solution at 1 mg/ml (Collagenase NB 8 Broad Range, Nordmark, S1745602), resected and placed in a water bath at 37°C for 10min. After washing, islets were purified on a Histopaque-1119 (Merck, #11191) / Histopaque-1083 (Merck, #10831) gradient. Before sample collection, islets were cultured in RPMI-1640 medium containing 11 mM glucose (control) or 25 mM glucose (diabetic), plus 10% FBS, penicillin (100 U/ml) and streptomycin (0.1 mg/ml) solution (all Thermo Fisher Scientific) at 37°C, in a humidified atmosphere of 5% CO_2/95% air. For determination of insulin content, 10 size-matched islets were collected in acid ethanol. For RNA extraction, all remaining islets were washed with PBS and pelleted before addition of lysis buffer.

2.5 siRNA experiments

2.5.1 INS-1 cells

All siRNAs were resuspended in siRNA buffer (Dharmacon, B-002000-UB-100) and aliquots were stored at -20°C. Cells were reverse transfected at a final concentration of 25 nM siRNA with 1.5 µl/well RNAiMAX (Invitrogen, 13778100) in OptiMEM (Gibco, 11058021). 100,000-150,000 INS-1 cells/well (split as described in section 2.1) in 450 µl media were seeded directly onto 50 µl siRNA/RNAiMAX/OptiMEM mix in a 24-well

plate after 15-20 minutes room-temperature incubation of the mix. Catalogue numbers of siRNAs used (all Dharmacon ON-TARGETplus SMARTPool) are listed in Table 2.1.

2.5.2 EndoC cells

All siRNAs were resuspended in siRNA buffer (Dharmacon, B-002000-UB-100) and aliquots were stored at -20°C. Cells were reverse transfected at a final concentration of 25 nM siRNA with 0.2 µl/well RNAiMAX (Invitrogen, 13778-150) in OptiMEM (Gibco, 13778-150). 40,000 EndoC-βH1 or 60,000 EndoC-βH5 cells/well (split or thawed, respectively, as described in section 2.2) in 90 µl media were seeded directly onto 10 µl siRNA/RNAiMAX/OptiMEM mix after 15-20 minutes room-temperature incubation of the mix. For (forward) re-transfection, the siRNA/RNAiMAX/OptiMEM mix was prepared in the same way and dispensed onto the culture medium. Catalogue numbers of siRNAs used (all Dharmacon ON-TARGETplus SMARTPool) are listed in Table 2.2.

2.6 RNA extraction and RT-qPCR

2.6.1 INS-1 cells and islets

Total RNA was isolated using the ReliaPrep RNA Miniprep System (Promega, Z6012) or Qiazol lysis reagent (Qiagen) or the RNeasy Mini Kit (Qiagen) per the relevant manufacturer's instructions. RNA concentration was determined using a NanoDrop ND-1000 spectrophotometer (Thermo Scientific). 500 ng samples of RNA were reverse transcribed using the High-Capacity cDNA Reverse Transcription Kit (Applied Biosystems). qPCR was performed using the StepOne Plus Real-Time PCR system

with MicroAmp Optical 96-Well Reaction Plates (both Applied Biosystems). Each reaction consisted of 5 µl amplified cDNA sample, 1 µl TaqMan gene expression probe, 10 µl TaqMan Fast Universal Master Mix, and nuclease-free water (to a final volume of 20 µl). Using the Fast ramp speed, the reaction cycle comprised an initial denaturation for 20 s at 95 °C, followed by 40 cycles of 95°C/1 s and 60°C/20 s, with data collection on the 60°C hold. The StepOne Plus Real-Time PCR software (Applied Biosystems) was used to measure threshold cycle (Ct) values. Gene expression was quantified using the delta-delta Ct method (Livak & Schmittgen, 2001) with normalisation to the housekeeping genes *Hspa8* or *Hprt1* (both for INS-1) or *Actb* (for islets). Housekeeping genes were selected for the stability of their expression with changes in glycaemia. TaqMan gene expression probes used are listed in Table 2.3 for INS-1 cells and Table 2.4 for islets.

2.6.2 EndoC cells

RNA was extracted using the Dynabeads mRNA DIRECT Purification Kit (Invitrogen, 10563755) according to the manufacturer's protocol but with the volumes scaled as follows: cells were lysed in 90 µl lysis buffer and mixed with 10 µl of beads in lysis buffer, washes were performed in 100 µl of buffers A and B, and RNA was eluted in 8 µl elution buffer. DNase treatment and reverse transcription were performed using SuperScript IV VILO Master Mix with ezDNase Enzyme (Invitrogen, 11766500) per the manufacturer's protocol. qPCR was performed using TaqMan Fast Advanced Master Mix (Invitrogen, 4444557) in 10 µl reaction volume containing 2 µl of cDNA (diluted 1:5) in 384-well plates on the Biorad CFX384. Gene expression was quantified using the delta-delta Ct method with normalisation to the housekeeping gene *TBP*. TaqMan gene expression probes used are listed in Table 2.5.

2.7 Protein extraction, SDS-PAGE and western blotting

INS-1 cells were lysed in Pierce RIPA buffer (Thermo Scientific) containing cOmplete EDTA-free protease inhibitor cocktail and, when appropriate, PhosSTOP phosphatase inhibitor cocktail (both Roche) for 5 min on ice. Samples were centrifuged at 14,000 rcf for 15 min to pellet cellular debris. Protein concentration was determined using the Pierce BCA Protein Assay Kit (Thermo Scientific) following the manufacturer's instructions. Proteins were separated on 4-12% SDS-polyacrylamide gels under reducing conditions (20 µg total protein per lane), blotted onto nitrocellulose membranes, and incubated with specific primary antibodies overnight at 4°C. The antibodies and dilutions used are listed in Table 2.6. Blocking buffer was 0.1% TBS-T with 5% milk. HRP-conjugated secondary antibodies were detected using SuperSignal West Pico PLUS Chemiluminescent Substrate (Thermo Scientific). Band intensities were quantified using LI-COR Image Studio software.

2.8 Insulin secretion and content assays

2.8.1 INS-1 cells

Cells were washed twice in Krebs-Ringer-bicarbonate buffer containing 140 mM NaCl, 3 mM KCl, 0.5 mM NaH_2PO_4, 2 mM $NaHCO_3$ [saturated with CO2], 1.5 mM $CaCl_2$, 0.5 mM $MgSO_4$, 10 mM HEPES (pH 7.4) and 0.1% (w/v) fatty acid-free BSA. Cells were washed twice and pre-stimulated with Krebs-BSA buffer containing 2 mM glucose for 60 min before being incubated with Krebs-BSA buffer containing 2 or 20 mM glucose for 30 min. Both pre-stimulation and stimulation incubations were performed in a

shaking water bath at 37°C. The supernatant (secreted insulin) was collected and cells harvested either in acid ethanol (total insulin content) or in RIPA lysis buffer (protein content). Insulin concentrations in the supernatant and cell lysates were quantified by insulin ELISA (Mercodia, 10-1247-10) and protein content by BCA assay. Secreted and total insulin were normalised to protein content as a proxy for cell number to account for differences in growth rates[4].

2.8.2 Islets

Insulin secretion was assayed in triplicate using groups of 10 size-matched islets, isolated from control and diabetic βV59M mice 2 weeks after tamoxifen injection. Islets (10/well) were pre-stimulated at 2G for 1h as described for INS-1 cells, then incubated at 2 or 20 mM glucose for 1h. Secreted and total insulin were measured as described for INS-1 cells and data were expressed per islet.

2.8.3 EndoC-βH1

GSIS: Cells were incubated in OPTIβ2 starvation medium (Human Cell design) for 2h prior to the assay. Cells were washed twice with βKrebs (Human Cell Design) to which was added 0.1% BSA (Fraction V, fatty acid free, Roche, 10775835001) on the day of the assay. Cells were then starved in βKrebs-BSA (no glucose) for 1 h at 37°C in 5% CO_2. Cells were stimulated in βKrebs-BSA containing either no glucose, 20 mM glucose (Sigma, G8644-100 ml), or 20 mM glucose + 45 μM IBMX (Sigma, I5879-100 mg) for 1 h at 37°C. Supernatants were collected for secreted insulin quantification.

[4] DNA content may also be used but is more difficult to reliably measure.

Cells were then lysed in TETG lysis buffer (20 mM Tris-HCl pH 8.0, 2 mM EGTA, 137 mM NaCl, 1% Triton X-100, 10% glycerol) for quantification of insulin content; some wells were reserved instead for automated cell counting.

Homogeneous Time-Resolved Fluorescence (HTRF): Insulin was quantified using the Insulin High Range HTRF kit (CisBio, 61IN1PEG). For secreted insulin, supernatant was used directly; for insulin content, lysates were first diluted 1:10 in β-Krebs-BSA. Anti-insulin XL655 and Eu3+ were mixed in a 2:1 ratio: 25 µl of antibody mix and 5 µl of sample were dispensed into a 384-well assay plate (Perkin Elmer OptiPlate-384, 6007290). After overnight incubation, protected from light, time-resolved fluorescence was measured in a CLARIOstar Plus plate reader (BMG LABTECH) using the manufacturer's recommended settings. Insulin concentration was calculated using the MARS data analysis software (BMG LABTECH).

2.8.4 EndoC-βH5

GSIS: Cells were incubated in ULTIβ2 starvation medium (Human Cell design) for 2h prior to the assay. GSIS was performed as described for βH1 cells, except that cells were stimulated for 40 min.

HTRF: Insulin was quantified as described for βH1 cells, except that dilutions of 1:2 and 1:20 were used for supernatant (secreted) and lysate (content) samples, respectively.

2.9 Data analysis and statistics

Unless otherwise stated, data are presented as mean ± the standard error of the mean (S.E.M.). For islet studies, n indicates the number of mice, and for INS-1 and EndoC cells, n indicates the number of independent experiments. For each experiment on INS-1 cells, at least 2 technical replicates were performed, and the mean of these replicates was taken as n = 1. Where individual data points are plotted, these each represent one experiment (the mean of the technical replicates) unless otherwise stated in the figure legend. For experiments on EndoC cells, 3-6 technical replicates were performed in most instances. A different passage of cells was used for each experiment. GraphPad Prism 9 was used for statistical analysis. Since data passed normality testing (D'Agostino-Pearson omnibus K2 test) where n was sufficiently large for the test to be performed, normality was generally assumed and statistical tests chosen accordingly. Two-tailed Student's t-test was used for comparison of two groups, and one-way ANOVA with Bonferroni's multiple comparisons test for comparison of multiple groups. The tests and post-test corrections used are indicated in the figure legends. Non-significant (ns) p-value > 0.05, * p-value < 0.05, ** p-value < 0.01, *** p-value < 0.001, **** p-value < 10^{-4}.

2.12 Tables

Table 2.1: siRNAs used in INS-1 cells

siRNA	**Catalogue number (Dharmacon)**
Aldoa	L-098770-02-0005
Aldob	L-099911-02-0005

Mlxipl	L-092970-02-0005
Non-targeting control	D-001810-10-05
Pfkl	L-089868-02-0005
Pfkm	L-091957-02-0005
Txnip	L-089121-02-0005

Table 2.2: siRNAs used in EndoC cells

siRNA	**Catalogue number (Dharmacon)**
FBP1	L-008725-00-0005
GAPDH	L-004253-00-0005
GPI	L-004900-00-0005
INS	L-011058-00-0005
PDK1	L-005019-00-0005
PFKL	L-006822-00-0005
PPP1R3C	L-017077-00-0005
PYGL	L-009569-00-0005
TXNIP	L-010814-00-0005

Table 2.3: TaqMan gene expression assays used in INS-1 cells

Gene	Catalogue number (Applied Biosystems)
Aldoa	Rn00820577_g1
Aldob	Rn01768292_m1
Eno1	Rn01518942_gH
Hprt1	Rn01527840_m1
Hspa8	Rn00821191_g1
Idh2	Rn01478119_m1
Ins1	Rn02121433_g1
Ins2	Mm00731595_gH
Mafa	Rn00845206_s1
Mdh2	Mm00725890_s1
Mlxip	Mm01202115_m1
Mlxipl	Mm02342723_m1
Ndufa4	Mm00809672_s1
Ndufs8	Mm00523063_m1
Neurod1	Rn01280117_m1
Nkx6-1	Rn01450076_m1
Nr0b2	Rn00589173_m1
Pax6	Rn00689608_m1
Pdk1	Rn00587598_m1
Pdx1	Rn00755591_m1
Pfkfb2	Mm00435575_m1

Pfkfb3	Rn00678825_m1
Pfkl	Mm00435587_m1
Pfkm	Mm01309576_m1
Ppp1r3c	Mm01204084_m1
Pygl	Rn00573974_m1
Sdha	Rn00590475_m1
Txnip	Mm00452393_m1

Table 2.4: TaqMan gene expression assays used in islets

Gene	**Catalogue number (Applied Biosystems)**
Actb	Mm02619580_g1
Aldob	Mm00523293_m1
Ins1	Mm01950294_s1
Ins2	Mm00731595_gH
Mafa	Mm00845206_s1
Nkx6-1	Mm00454961_m1
Pax6	Mm00443081_m1
Pdx1	Mm00435565_m1
Ppp1r3c	Mm01204084_m1
Txnip	Mm00452393_m1

Table 2.5: TaqMan gene expression assays used in EndoC cells

Gene	Catalogue number (Applied Biosystems)
FBP1	Hs00983323_m1
GAPDH	Hs02758991_g1
GPI	Hs00976715_m1
INS	Hs00355773_m1
MAFA	Hs04419852_s1
MLXIPL	Hs00975714_m1
NEUROD1	Hs01922995_s1
NKX6-1	Hs00232355_m1
PAX6	Hs01088114_m1
PDK1	Hs01561847_m1
PDX1	Hs00236830_m1
PFKL	Hs01036347_m1
PPP1R3C	Hs00193642_m1
PYGL	Hs00958087_m1
TBP	Hs00427620_m1
TXNIP	Hs01006897_g1

Table 2.6: Antibodies used for Western blot

Antibody	Concentration	Source
Rabbit anti-Alpha-tubulin	1:1000	Cell Signaling Technology (2144)
Rabbit anti-TXNIP	1:1000	Cell Signaling Technology (14715)

ECL anti-rabbit IgG, HRP linked (from donkey)	1:5000	GE Healthcare NA934

3. Loss of insulin biosynthesis corresponds to the severity and duration of hyperglycaemia

3.1 Summary

1. Insulin gene expression in INS-1 cells showed a bell-shaped relationship with [glucose], being highest at 5 mM, moderately reduced at 0 and 2 mM, and severely impaired by higher glucose concentrations (8, 11, 16.7 and 25 mM). The β-cell identity genes *Mafa* and *Pdx1* showed a similar relationship, whereas *Neurod1*, *Nkx6-1* and *Pax6* were downregulated at high glucose but not at low glucose.
2. Insulin gene expression in INS-1 cells declined rapidly at the onset of hyperglycaemia and recovered slowly when hyperglycaemia was reversed. The β-cell identity genes also declined rapidly with hyperglycaemia onset but mostly recovered within 48 hours of reversal.
3. Insulin biosynthesis was less susceptible to hyperglycaemia in the human β-cell lines EndoC-βH1 and EndoC-βH5, although a modest impairment by high glucose was observed in the more phenotypically mature βH5 cells.
4. The insulin content of islets from diabetic βV59M mice correlated negatively with increasing blood glucose, appearing to decline progressively with impaired glucose tolerance, mild hyperglycaemia, and severe hyperglycaemia.

3.2 Introduction

While it is well-established that chronic hyperglycaemia impairs insulin biosynthesis, it is less clear what the threshold blood glucose level is above which this impairment starts to occur. In this thesis, and in previous studies (Haythorne et al., 2022), we have

mainly modelled hyperglycaemia *in vitro* mostly using a glucose concentration of 25 mM in the culture medium. However, while such severe hyperglycaemia can be sustained in βV59M mice, blood glucose very rarely reaches these levels in patients with T2D (table 3.1). It is therefore important to establish the extent to which insulin biosynthesis is impaired at more clinically relevant levels of hyperglycaemia. Moreover, different β-cell models vary in their sensitivity to glucose, so it is important in the first instance to characterise the relationship between glucose concentration and insulin gene expression for a given model. Previous studies have found that quite mild hyperglycaemia (13 mM blood glucose) is sufficient to substantially reduce insulin mRNA levels *in vivo* in rats (Ebrahimi et al., 2020), while *ex vivo* culture of human islets (1 week) or human pseudoislets (2 weeks) at 8 mM glucose significantly reduced insulin content, suggesting that the threshold is quite low (Mir-Coll et al., 2021; Tariq et al., 2022).

Table 3.1: Fasting and postprandial blood glucose ranges in non-diabetic, pre-diabetic, and diabetic subjects

	Non-diabetic	Pre-diabetic	T2D	GCK-MODY[5]
Fasting blood glucose (mM)	4.0-5.8	5.5-6.9	6.2-10.4	5.5-8
2-hour postprandial blood glucose (mM)	≤7.8	7.8-11	>11 (typically 13-17)	6.6-11.2
HbA1c (%)	5.5-5.9	5.7-6.4	≥6.5	5.5-7.5

Table compiled from: (Steele et al., 2014; Stride et al., 2002); www.diabetes.org.uk, www.diabetesgenes.org.uk

[5] Glucokinase Maturity Onset Diabetes of the Young (GCK-MODY) is caused by inactivating mutations in *GCK* and characterised by lifelong fasting hyperglycaemia with minimal prevalence of diabetic complications.

The second outstanding question this chapter addresses is how readily the impairment of insulin biosynthesis by chronic hyperglycaemia can be reversed. Previous studies using the βV59M mouse model have shown the loss of insulin content (as measured by insulin-positive area in islet immunostaining) to be fully reversible within 4 weeks (Brereton et al., 2014), but did not investigate how quickly insulin stores are replenished following restoration of euglycaemia. To do so at high temporal resolution would be very laborious, requiring either the culling of a great number of mice or the frequent collection of blood samples for quantification of c-peptide as an indirect measure by which to interpolate changes in insulin production. However, INS-1 cells represent a highly tractable model for such an investigation since samples can easily be collected at regular intervals.

A review of the literature gives a rough indication of how long reversal of the loss of insulin may take, though it likely depends on the severity and duration of hyperglycaemia before restoration of normoglycaemia as well as the model used. In islets isolated from streptozotocin-treated rats (which had ~7 mM fasting blood glucose), the loss of insulin content and insulin mRNA and the impairments in the (pro)insulin biosynthesis rate and glucose-stimulated insulin secretion (GSIS) were all reversed after 7 days of culture at 5.6 mM glucose (N. Welsh & Hellerström, 1990). Two days were insufficient to reduce those deficits, but the progress of β-cell recovery between days 2 and 7 was not monitored. Meanwhile, partial recovery of insulin content (from ~10% to ~35% of baseline) and mRNA levels (from ~60% to ~85% of baseline) was apparent 3 days after human islets in *ex vivo* culture were restored from 33 to 5 mM glucose (Marshak et al., 1999).

Unfortunately, cadaveric human donor islets are difficult to reliably obtain, vary in quality and are prone to necrosis at the islet core, and have heterogeneous patient histories with respect to various physiological parameters and to medication, which can complicate interpretation of results. For a pure and readily available source of human β-cells, I used EndoC cells. EndoC cells are now produced by Human Cell Design, but EndoC-βH1 (abbreviated to βH1) were originally developed by Raphael Scharfmann and colleagues using targeted oncogenesis in human foetal pancreatic buds (Ravassard et al., 2011). Briefly, pancreases were transduced with lentiviral vectors expressing the immortalising SV40 Large T-antigen (SV40LT) under the control of the rat insulin promoter (RIP) and transplanted under the kidney capsule in severe combined immunodeficient (SCID) mice; insulinomas developed as the pancreatic tissue matured, and the resulting β-cells were transduced with human telomerase reverse transcriptase (hTERT), also under RIP control, regrafted into other SCID mice, and finally expanded *in vitro* (Scharfmann et al., 2016). EndoC-βH5 (βH5) cells differ from βH1 cells in that they have undergone Cre-mediated excision of the SV40LT and hTERT transgenes to make them mature and non-proliferative (Brawerman et al., 2022).

In this chapter, I investigate whether mild hyperglycaemia impairs insulin biosynthesis, as well as how quickly the loss of insulin occurs during hyperglycaemia and to what extent it is reversible. Although this thesis is focused primarily on chronic hyperglycaemia, I am also interested in the change in insulin gene expression in the first few hours of hyperglycaemia onset, as this could shed light on how β-cells respond to postprandial blood glucose elevation. As previous studies have not systematically examined how expression of the β-cell identity genes changes with [glucose], I tracked the expression of *Mafa*, *Neurod1*, *Nkx6-1*, *Pax6* and *Pdx1*

alongside the insulin genes. In this way, I aimed to establish whether all of these genes change in the same way or whether there are any differences that point to a key role for certain transcription factor(s) in mediating the hyperglycaemia-induced repression of insulin transcription. Much of this work was done using INS-1 cells, but I also sought to translate findings from that cell line into EndoC human β-cell models, and to show impairment of insulin biosynthesis by mild hyperglycaemia following induction of diabetes in βV59M mice. Thus, I hoped to demonstrate that the processes described are common across species and occur *in vivo* as well as in a pure β-cell population.

3.3 Materials and methods

INS-1 cells were cultured as described in chapter 2 (section 2.1). RNA extraction and qPCR was conducted as described in section 2.6.1. Insulin secretion and content were assayed as described in sections 2.8.2.

EndoC cells were cultured as described in chapter 2 (section 2.2). RNA extraction and qPCR was conducted as described in section 2.6.1. Insulin secretion and content were assayed as described in sections 2.8.3 and 2.8.4.

3.3.1 Time course experiment

INS-1 cells were maintained (at 11 mM glucose) as described in section 2.1 until being seeded into 6-well plates: in each plate there were 3 wells cultured at 5 mM glucose and 3 wells at 25 mM glucose and there was one plate per time point. After 48 hrs, the media was replaced in all wells such that those cells previously cultured at 5 mM glucose were moved to 25 mM glucose, and vice versa. This media change marked

the start of the time course (0 hrs); samples were collected at the indicated times thereafter by adding lysis buffer and immediately freezing the plate for subsequent RNA extraction. I refreshed the media at 48 hrs for cells cultured for 72 hrs after the onset or reversal of hyperglycaemia to ensure glucose was not depleted. Data (RQ values) are expressed relative to 5 mM glucose at 0 hrs.

3.3.2 Animal experiments

This work was performed collaboratively, as explained in the declaration of authorship.

Mice were weighed immediately prior to injection to calculate the dose of tamoxifen in micrograms per gram of body weight. Control and βV59M mice were injected at 12 weeks of age and were culled 3 weeks after being injected. Free-fed blood glucose was measured prior to tamoxifen injection (starting blood glucose) and on the day of islet isolation (week 3 blood glucose). An intraperitoneal glucose tolerance test (IPGTT) was performed 2 weeks after tamoxifen injection (1 week before mice were culled). Islet isolation was performed as described in section 2.4. Measurement of insulin content was performed as described in section 2.8 and RNA extraction and RT-qPCR were performed as described in section 2.6.

3.4 Dependence of insulin gene expression on glucose concentration and duration of hyperglycaemia

3.4.1 Studies in INS-1 cells

Note: in this and subsequent chapters, LG-cells refer to INS-1 cells cultured for 48 hrs at 5 mM glucose, and HG-cells to INS-1 cells cultured for 48 hrs at 25 mM glucose.

Figure 3.1a demonstrates the severe impairment of GSIS by chronic hyperglycaemia. There was a 2-fold stimulation of insulin secretion when glucose was elevated from 2 mM to 20 mM glucose in LG-cells. By contrast, in HG-cells basal secretion at 2 mM glucose was reduced to <25% of the level in LG-cells and there was no longer any significant stimulation of secretion by 20 mM glucose. I also calculated the stimulation index (SI) for secretion from LG-cells and HG-cells (figure 3.1b), since this is frequently reported. The SI is the ratio of secretion at 20 mM to 2 mM glucose. However, it is apparent that this is a flawed measure. Because of the reduction in insulin secretion at 2 mM glucose in HG-cells, there is no significant difference in SI between LG-cells and HG-cells, despite there being a large difference in the actual magnitude of secretion stimulated by 20 mM glucose.

The total insulin content of HG-cells was <20% of that of LG-cells (figure 3.1c). Steady state insulin content depends on the rates of preproinsulin mRNA translation and proteolytic processing into mature insulin as well as the rates of secretion and degradation, so I next looked at mRNA levels. There is a good correspondence between insulin mRNA levels, which fell by ~90% in HG-cells (figure 3.2), and insulin content. This suggests that the primary cause of the reduction in insulin content is downregulation of gene expression.

To determine how quickly insulin gene expression declines following the onset of hyperglycaemia, and to what extent the decline is reversible, I characterised the

temporal dynamics over a 72-hour time course. Plated cells were cultured at LG or HG for 48 hours before being transferred to HG (onset) or LG (reversal) respectively for 1, 3, 6, 12, 24, 48, or 72 hours. Expression of *Ins1* and *Ins2* mRNA in INS-1 cells was very sensitive to the extracellular glucose concentration, falling sharply by ~50% in the first 6 hours and ~75% in the first 12 hours following the onset of hyperglycaemia (figure 3.2). Remarkably, even after just 3 hours there was a ~25% decline in insulin mRNA, suggesting that postprandial glucose spikes seen in pre-diabetic or diabetic individuals (see table 3.1) have the potential to significantly impair insulin biosynthesis. Whereas blood glucose returns to baseline within 3 hours following a mixed meal in nondiabetic subjects, subjects with T2D have elevated blood glucose for up to 6 hours afterwards (Basu et al., 2009): there is scope for considerable loss of insulin mRNA during this time. Ideally, in future I would explore whether insulin mRNA levels fall after 2-3 hours at 11 mM glucose, as this is the diagnostic postprandial blood glucose threshold for T2D (table 3.1). After 12 hours, the decline continued at a slower rate for the remaining 60 hours of the experiment. Both genes followed a very similar time course, indicating that they are regulated in the same way.

I next examined the relationship between extracellular glucose concentration and insulin gene expression. For this experiment, I used a 48-hour incubation as this was sufficient to stabilise the reduction in expression at 25 mM glucose (figure 3.2). Insulin gene expression displayed a bell-shaped dependence on [glucose], increasing between 0 mM and 5 mM glucose, reaching a maximum around 5 mM glucose (the control condition, to which all data are normalised), and then dropping sharply from 8 mM through progressively higher concentrations (figure 3.3). Expression was only 10% of baseline at 25 mM glucose, as in figure 3.2. While 0 mM glucose represents an extreme case that will not occur physiologically, it is interesting to note how mRNA

levels differ between 0 and 2 mM glucose for some genes, including *Ins1*, *Mafa*, and *Pdx1*, but not others, such as *Ins2*.

As part of this experiment, I also quantified the expression of the β-cell identity genes *Mafa*, *Neurod1*, *Nkx6-1*, *Pax6*, and *Pdx1* (figure 3.3). These transcription factors displayed a similar pattern of expression to the insulin genes that they regulate in their response to elevated glucose, but can be divided into two groups based on their expression at low (2 mM) and zero glucose. *Mafa* and *Pdx1* showed significantly lower expression at 0 mM than at 5 mM glucose, conforming to the bell-shaped dependence on [glucose] shown by the insulin genes. They were also particularly strongly downregulated at high glucose, complementing findings from T2D human islets (Marselli et al., 2020). In contrast, expression of *Neurod1*, *Nkx6-1*, and *Pax6* was similar at 0, 2, and 5 mM glucose, and only decreased at higher glucose concentrations. A striking finding is that all of the genes examined were significantly downregulated at 11 mM glucose (the concentration normally used for routine culture of INS-1 cells), and all except *Pax6* ($p = 0.08$) were significantly downregulated at 8 mM glucose. Thus, mild hyperglycaemia clearly impairs insulin biosynthesis in INS-1 cells.

Figure 3.4a compares the changes in gene expression over time following the restoration of euglycaemia with those following the onset of hyperglycaemia, shown in figure 3.2. As already described, *Ins1* and *Ins2* mRNA levels declined rapidly following the onset of hyperglycaemia: each had fallen by ~50% at 6 hrs and ~75% at 12 hrs. By contrast, recovery of *Ins1* and *Ins2* expression following restoration of normoglycaemia was very slow, reaching only ~50% and ~25%, respectively, of normal levels after 72 hours. All five of the transcription factors examined were

downregulated following the onset of hyperglycaemia, generally stabilising at a new steady state within 24 hours. *Neurod1* and *Nkx6-1* reached their nadir at 12 hrs before rebounding slightly during the following 12 hours. *Mafa* appeared to be slightly upregulated during the first three hours of hyperglycaemia, consistent with reports that it is acutely induced by high glucose but downregulated by chronically high glucose levels (Hang & Stein, 2011). Expression of the identity genes was mostly restored following a return to low glucose, but *Mafa* expression did not substantially recover within 72 hours and instead showed a time course similar to insulin. It could be argued that the slow recovery of insulin gene expression is partly a result of increasing cell density (diluting the increase in mRNA levels through cell division) and a relative scarcity of nutrients (although the media was refreshed every 24 hours). However, in a single exploratory experiment where cells were transferred from 11 mM to 5 mM glucose, expression of *Ins1*, *Ins2*, and *Mafa* increased sharply after just 24 hours (figure 3.4b), indicating that the recovery from chronic culture at 25 mM glucose is not an artefact and is truly very slow.

Figure 3.1: Chronic hyperglycaemia impairs GSIS and reduces insulin content

(a) Basal and glucose-stimulated insulin secretion (ng/ml/µg protein) from INS-1 cells incubated with 5 or 25 mM glucose for 48 hrs. n=5. ****$p < 10^{-4}$, ns (non-significant); 2-way ANOVA with Bonferroni's correction.

(b) Stimulation index values calculated from data in (a) for LG-cells and HG-cells. ns (non-significant); two-tailed unpaired Student's t-test.

(c) Total insulin content (ng/µg protein) of INS-1 cells incubated with 5 or 25 mM glucose for 48 hrs. n=6. ****$p < 10^{-4}$; two-tailed unpaired Student's t-test.

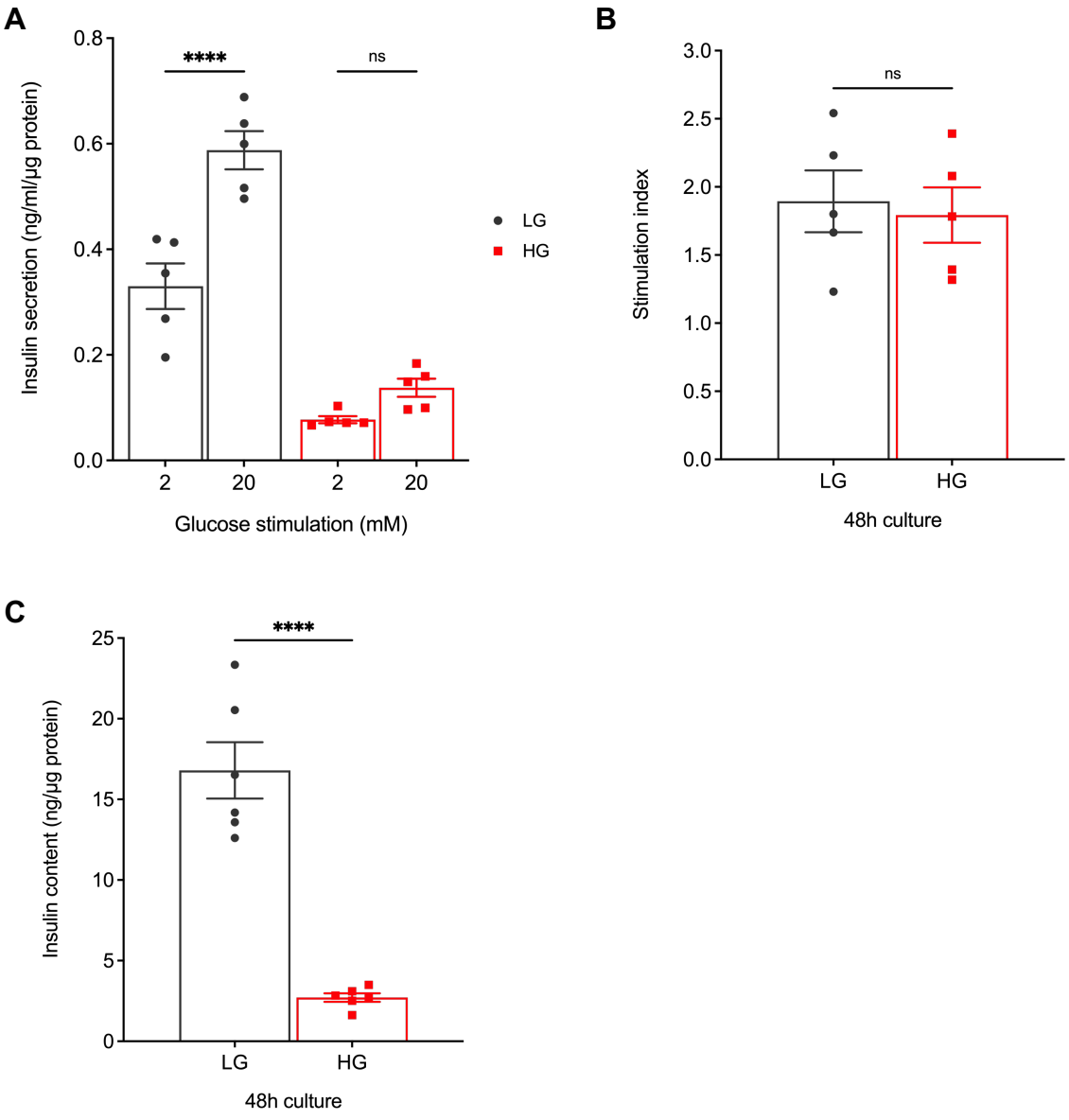

Figure 3.2: mRNA levels of the insulin genes decline rapidly following the onset of hyperglycaemia

qPCR analysis of the expression of the insulin genes in INS-1 cells at time points of 1, 3, 6, 12, 24, 48 and 72 hrs following onset of hyperglycaemia. Cells were pre-cultured at 5 mM glucose for 48 hrs before being transferred to 25 mM glucose at the time point 0. n=3, with 3 technical replicates per experiment.

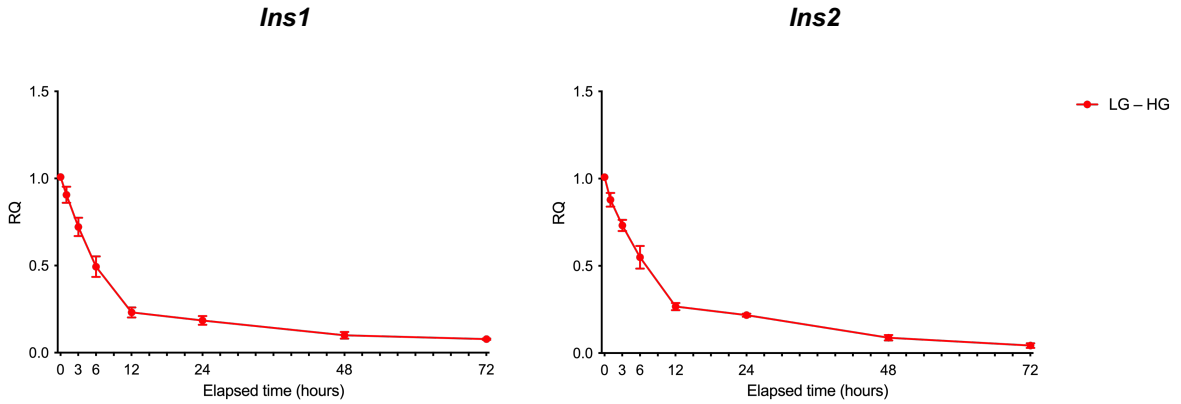

Figure 3.3: Reduced expression of the insulin genes and β-cell identity genes in chronic hyperglycaemia

qPCR analysis of the expression of the insulin genes and selected β-cell identity genes in INS-1 cells incubated with 0, 2, 5, 8, 11, 16.7 and 25 mM glucose for 48 hrs. n=2-5. *p < 0.05, **p < 0.01, ***p < 0.001, ****p < 10^{-4}; 1-way ANOVA with Bonferroni's correction.

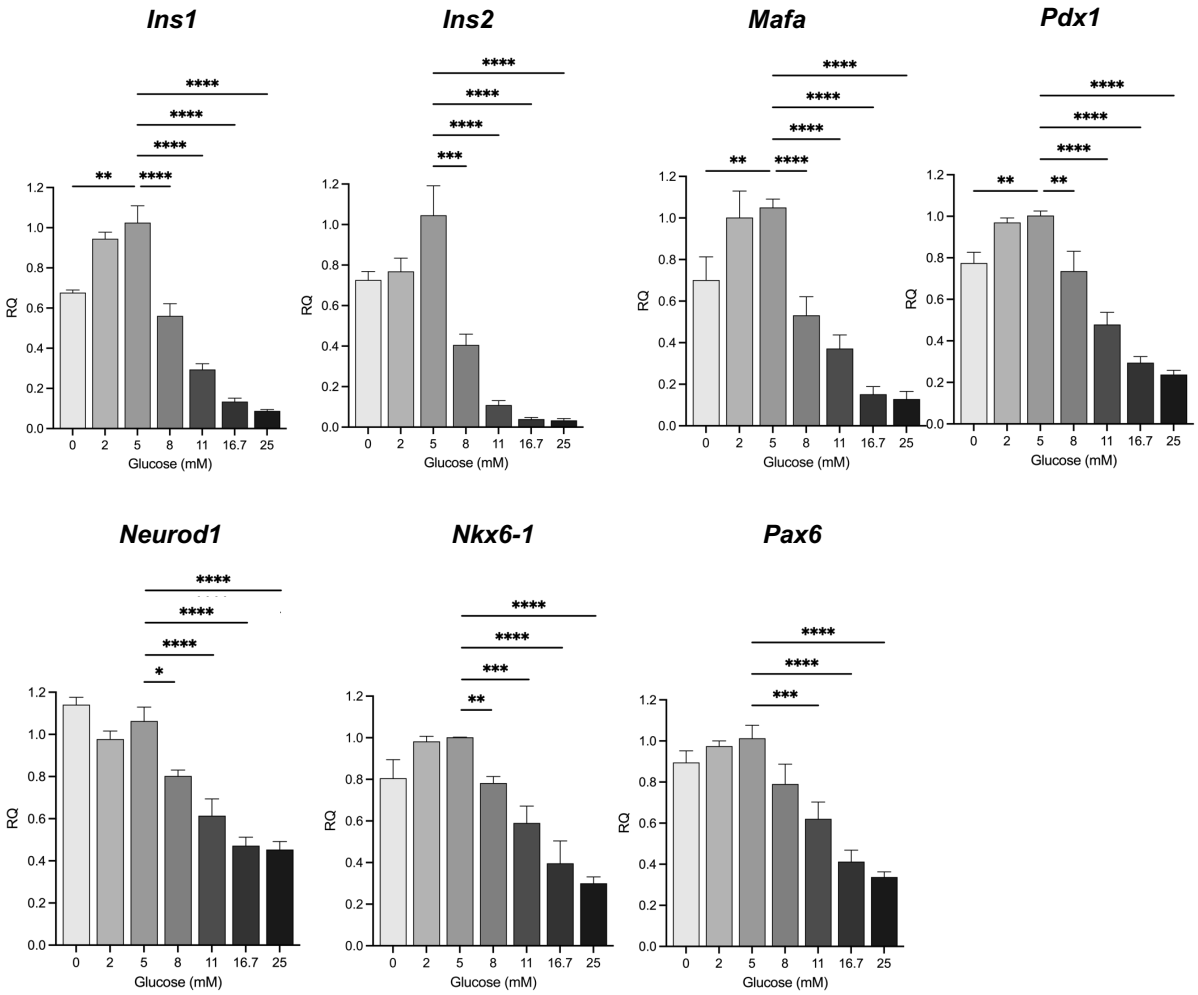

Figure 3.4: Time course of mRNA levels of the insulin genes and β-cell identity genes up to 72 hrs following the onset or reversal of hyperglycaemia

(a) qPCR analysis of the expression of the insulin genes and selected β-cell identity genes in INS-1 cells at time points of 1, 3, 6, 12, 24, 48 and 72 hrs following onset or reversal of hyperglycaemia. Cells were pre-cultured at 5 or 25 mM glucose for 48 hrs before being transferred to the opposite condition (25 or 5 mM to simulate onset or reversal, respectively) at the time point 0. n=2-3, with 3 technical replicates per experiment.

(b) qPCR analysis of the expression of the insulin genes and *Mafa* in INS-1 cells at time points of 12, 24, 48 and 72 hrs following transfer from 11 mM glucose to LG or HG at the time point 0. n=1; mean of technical replicates ± SD shown.

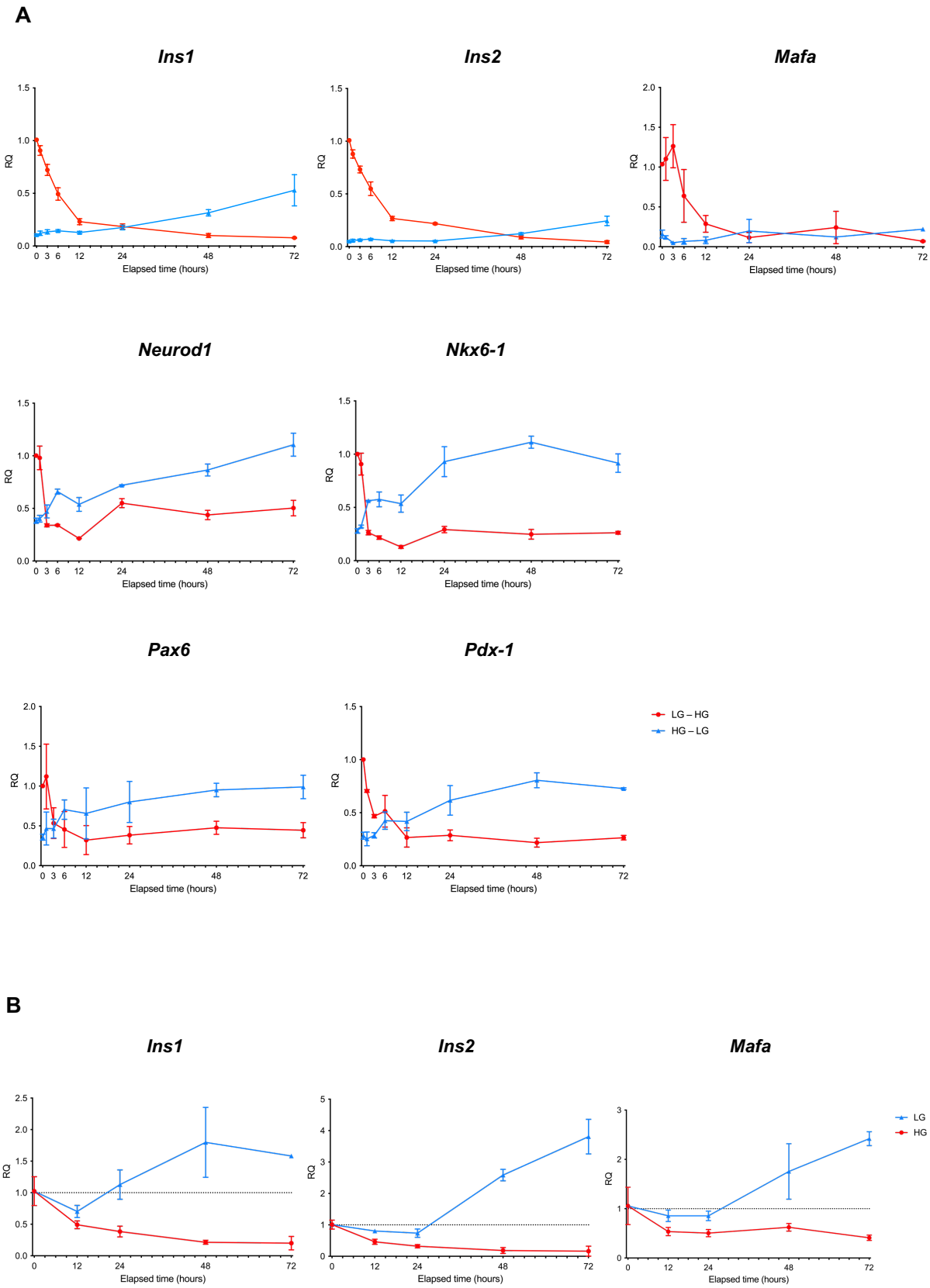
A
Ins1
Ins2
Mafa
Neurod1
Nkx6-1
Pax6
Pdx-1
RQ
Elapsed time (hours)
LG – HG
HG – LG
B
Ins1
Ins2
Mafa
RQ
Elapsed time (hours)
LG
HG

3.4.2 Studies in human β-cell models

I assessed the response to chronic hyperglycaemia in two human β-cell models: the immortalised EndoC-βH1 cell line and the recently available EndoC-βH5 cells, which display a closer-to-native phenotype. These experiments were carried out at the Novo Nordisk Research Institute Oxford (NNRCO) as part of my 4-month industrial placement.

3.4.2.1 Studies in EndoC-βH1 cells

Since EndoC-βH1 cells have a population doubling time more than twice that of INS-1 cells, I used incubations of at least 96 hours to model chronic hyperglycaemia. Even after 8 days of hyperglycaemia, the cells maintained reasonably robust GSIS, showing slightly increased basal secretion and a moderate decline in the stimulation index[6], and appearing to show only a modest decline in insulin content (figure 3.5). According to standard protocol for EndoC cells, insulin secretion was measured at 0 mM glucose, 20 mM glucose, and at 20 mM glucose with IBMX (which potentiates secretion through elevation of cAMP levels, leading to activation of protein kinase A). Insulin secretion and content were consistent with typical values reported for monolayer cultures in previous studies (Tsonkova et al., 2018), but the low resolution of insulin secretion and the low insulin content (about 10% of native human β-cells) remain major limitations of this model. It has subsequently been found that a decline in GSIS (stimulated by 20 mM glucose) in hyperglycaemic βH1 cells becomes more apparent if the starvation step, which I reduced to 2 hours from the 24 hours used in standard protocols in an attempt to prevent this decline being masked, is skipped completely (Karen Arevad

[6] SI was calculated to enable comparison with existing literature.

Cappelen, unpublished observations). Perhaps hyperglycaemia-induced impairment of GSIS would be also more apparent in EndoC-βH1 cells cultured in pseudoislets, which exhibit a greater stimulatory index when cultured under euglycaemic conditions (Tsonkova et al., 2018).

My initial investigations found that chronic hyperglycaemia had inconsistent effects on mRNA levels of insulin and the β-cell identity genes (figure 3.6). Whereas *PDX1* expression was much higher at 5.5 mM glucose than any other glucose concentration after 96 hrs incubation, there was no consistent relationship between [glucose] and expression of the other genes (figure 3.6a). That *INS* was not markedly downregulated by high glucose is surprising considering the observed downregulation of *PDX1*, as this transcription factor is particularly important for controlling insulin gene expression in human β-cells (Bernardo et al., 2008). However, given that *INS* and *MAFA* showed very low expression at zero glucose, as did *PDX1* at 2 mM glucose, it is possible that the glucose dose-response curve for insulin gene expression in βH1 cells peaks at a concentration between 2 and 5.5 mM. If so, this would likely be due to the expression of GLUT1 in human β-cells. As this shifts the threshold glucose concentration for insulin secretion, it would make sense for the glucose dose-response curve for insulin gene expression to also be shifted to a lower concentration.

A long duration of hyperglycaemia appears to be required for a substantial reduction in insulin mRNA to occur in βH1 cells, as 8 days of high glucose culture led to a ~65% reduction in *INS* expression at 25 mM glucose and a ~55% reduction at 35 mM glucose (figure 3.6b). Intriguingly, *MAFA* expression was again lower in cells cultured at 25 mM glucose (reduced by ~75%) than those cultured at 35 mM glucose (reduced by ~35%). Unfortunately, I ran out of time to measure the expression of the other β-cell

identity genes in these samples, but I would expect them to also be more downregulated after 8 days than after 96 hrs.

Figure 3.5: Modestly impaired GSIS and insulin content after 8 days of hyperglycaemia in EndoC-βH1 cells

(a) Basal and glucose-stimulated insulin secretion (ng/10^6 cells/hr) from EndoC-βH1 cells incubated with 5.5, 25 or 35 mM glucose for 8 days and stimulated with 0 mM glucose (G), 20G or 20G + 45 μM IBMX for 1 hr. n=1; mean of technical replicates ± SD shown.

(b) 20G data in (a) represented as stimulation index.

(c) Total insulin content (ng/10^6 cells) of EndoC-βH1 cells incubated with 5.5, 25 or 35 mM glucose for 8 days. n=1; mean of technical replicates ± SD shown.

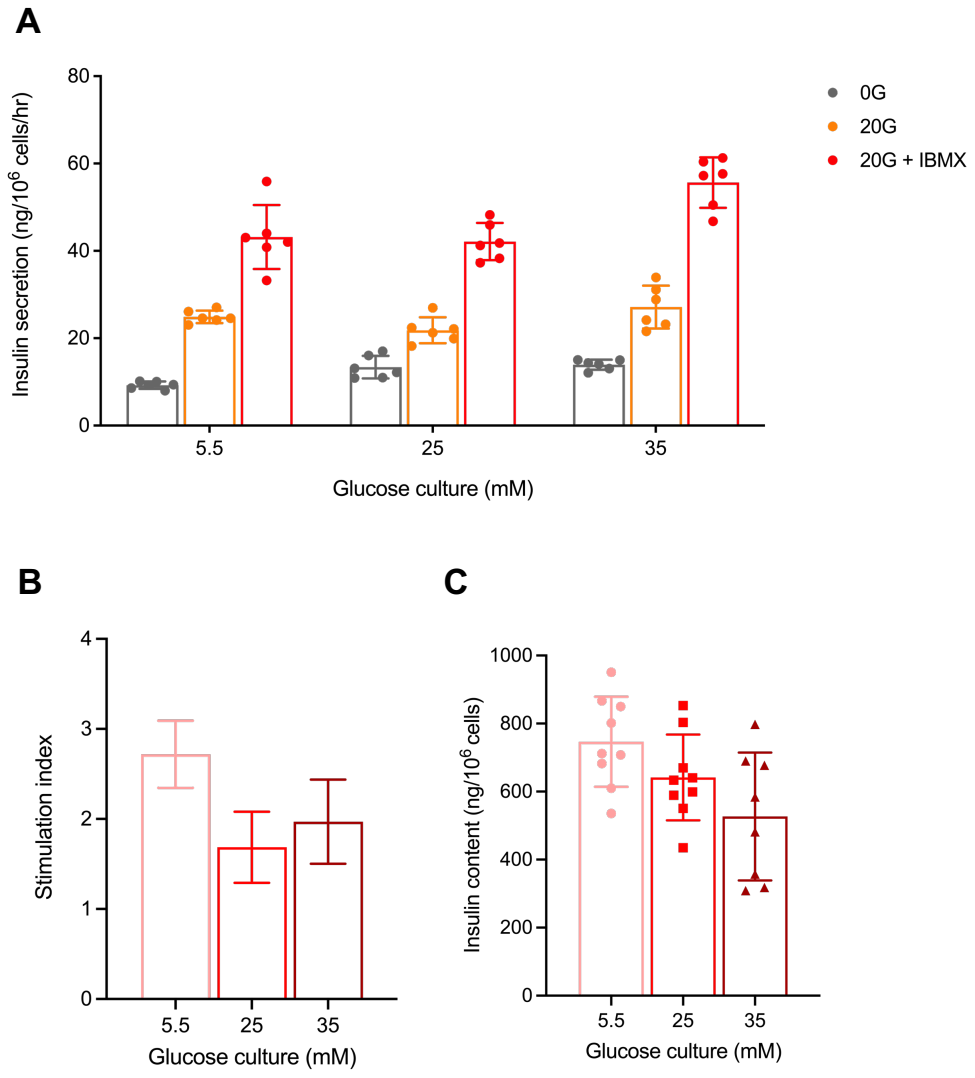

Figure 3.6: Reduced expression of the insulin genes and β-cell identity genes with longer duration of hyperglycaemia in EndoC-βH1 cells

(a) qPCR analysis of the expression of the insulin genes and selected β-cell identity genes in EndoC-βH1 cells incubated with 0, 2, 5.5, 8, 11, 16.7, 25 and 35 mM glucose for 4 days. n=1 for 2 and 35 mM glucose and n=2 for 0, 5.5, 8, 11, 16.7 and 25 mM glucose; mean of technical replicates ± SD shown.

(b) qPCR analysis of the expression of the insulin genes and selected β-cell identity genes in EndoC-βH1 cells incubated with 5.5, 25 and 35 mM glucose for 8 days. n=1; mean of technical replicates ± SD shown.

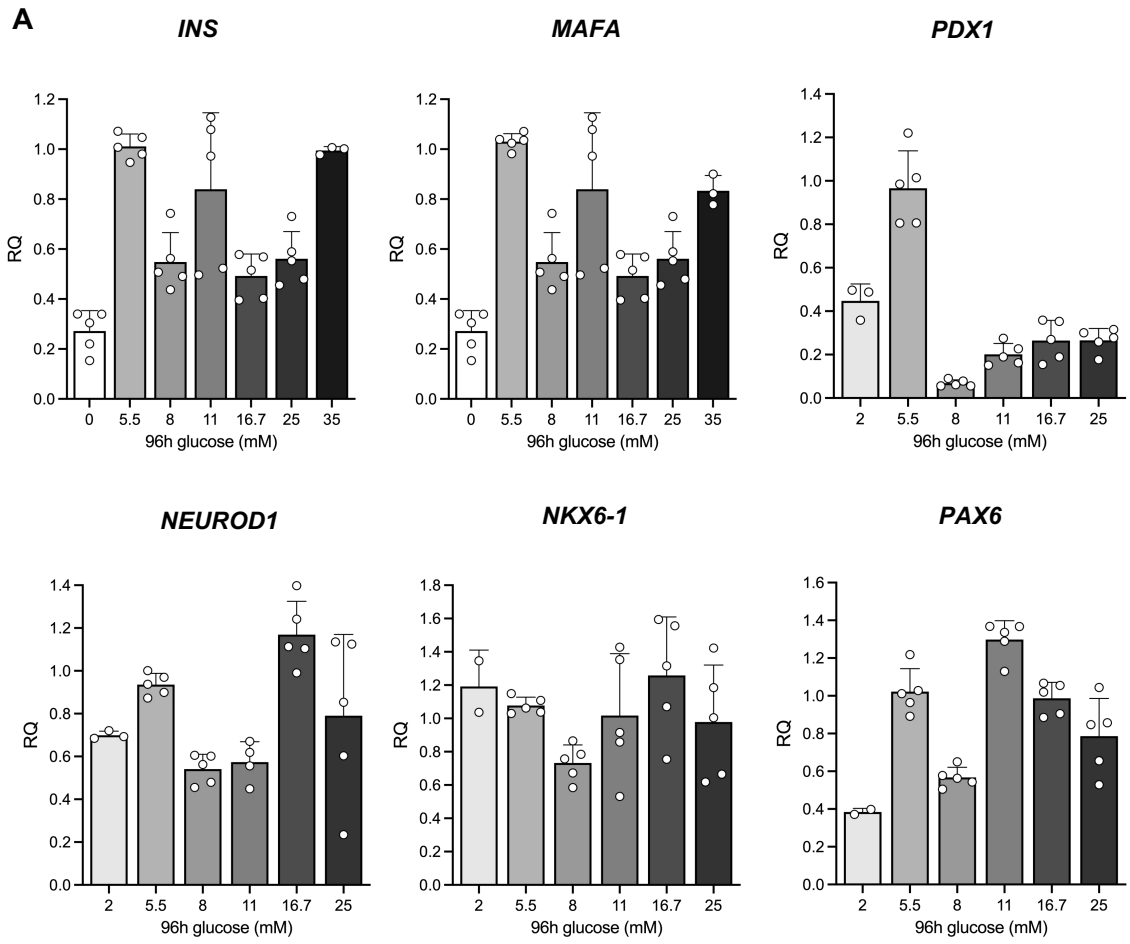

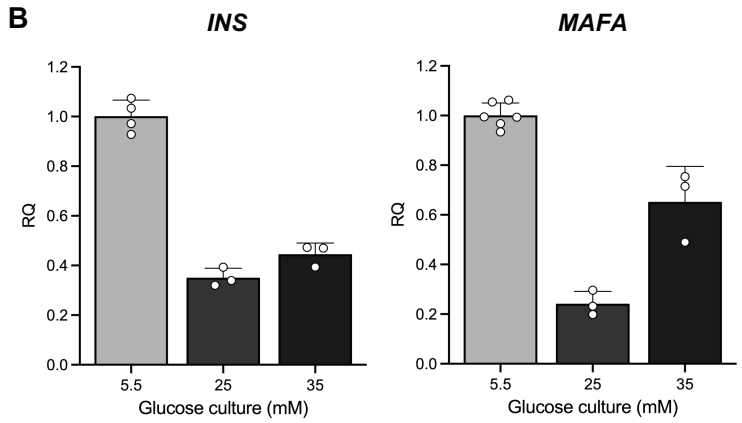

3.4.2.2 Studies in EndoC-βH5 cells

Due to the limitations of βH1 cells, I switched to the novel EndoC-βH5 cells. Comparing figures 3.5 and 3.7, we can see that βH5 cells secrete insulin at a much higher rate than βH1 cells. Because of this, a shorter incubation (40 mins) is used to measure secretion from βH5 cells. βH5 cells also have 10-fold higher insulin content than βH1 cells, consistent with their reported phenotypic maturity. They also appear slightly more susceptible to glucotoxicity than βH1 cells, although still much less so than INS-1 cells (figure 3.1). 5 days of culture at 35 mM glucose resulted in a >20% loss of insulin content ($p<0.0001$), and there was a trend towards impaired GSIS, though more experiments are required to confirm this (figure 3.7). Basal secretion was unaffected by hyperglycaemia. Again, insulin secretion from cells cultured at 5.5 mM glucose was consistent with typical values reported in previous studies (Szczerbinska et al., 2022).

After 5 days high glucose culture, *INS* mRNA levels were ~20% lower at 25 mM than at 5.5 mM glucose. However, *MAFA* was paradoxically upregulated by chronic hyperglycaemia, perhaps in an unsuccessful effort to increase *INS* expression, and, with the possible exception of *NKX6-1*, none of the identity genes were substantially

downregulated (figure 3.8). This suggests that other modes of transcriptional repression or post-transcriptional mechanisms mediate the modest decline in *INS* mRNA.

Figure 3.7: GSIS and insulin content after 5 days of hyperglycaemia in EndoC-βH5 cells

(a) Basal and glucose-stimulated insulin secretion (ng/10^6 cells/hr) from EndoC-βH5 cells incubated with 5.5, 25 or 35 mM glucose for 5 days and stimulated with 0 or 20 mM glucose for 40 mins. n=1; with mean of technical replicates ± SD shown.
(b) Means in (a) represented as stimulation index.
(c) Total insulin content (µg/10^6 cells) of EndoC-βH5 cells incubated with 5.5, 25 or 35 mM glucose for 5 days. n=5 for 5.5G and 35G; n=3 for 25G. ****$p < 10^{-4}$, 1-way ANOVA with Bonferroni's correction.

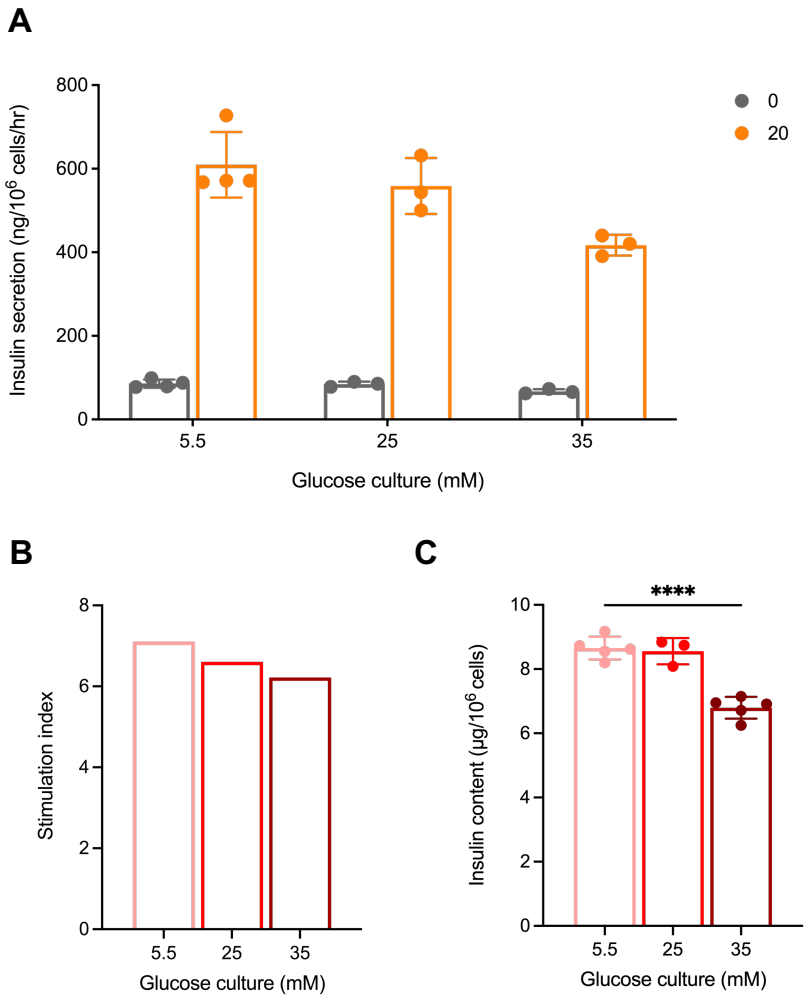

Figure 3.8: Expression of the insulin genes and β-cell identity genes is inconsistently affected by chronic hyperglycaemia in EndoC-βH5 cells

qPCR analysis of the expression of the insulin genes and selected β-cell identity genes in EndoC-βH5 cells incubated with 5.5, 25 and 35 mM glucose for 5 days. n=2; individual values with error bars showing mean of technical replicates ± SD.

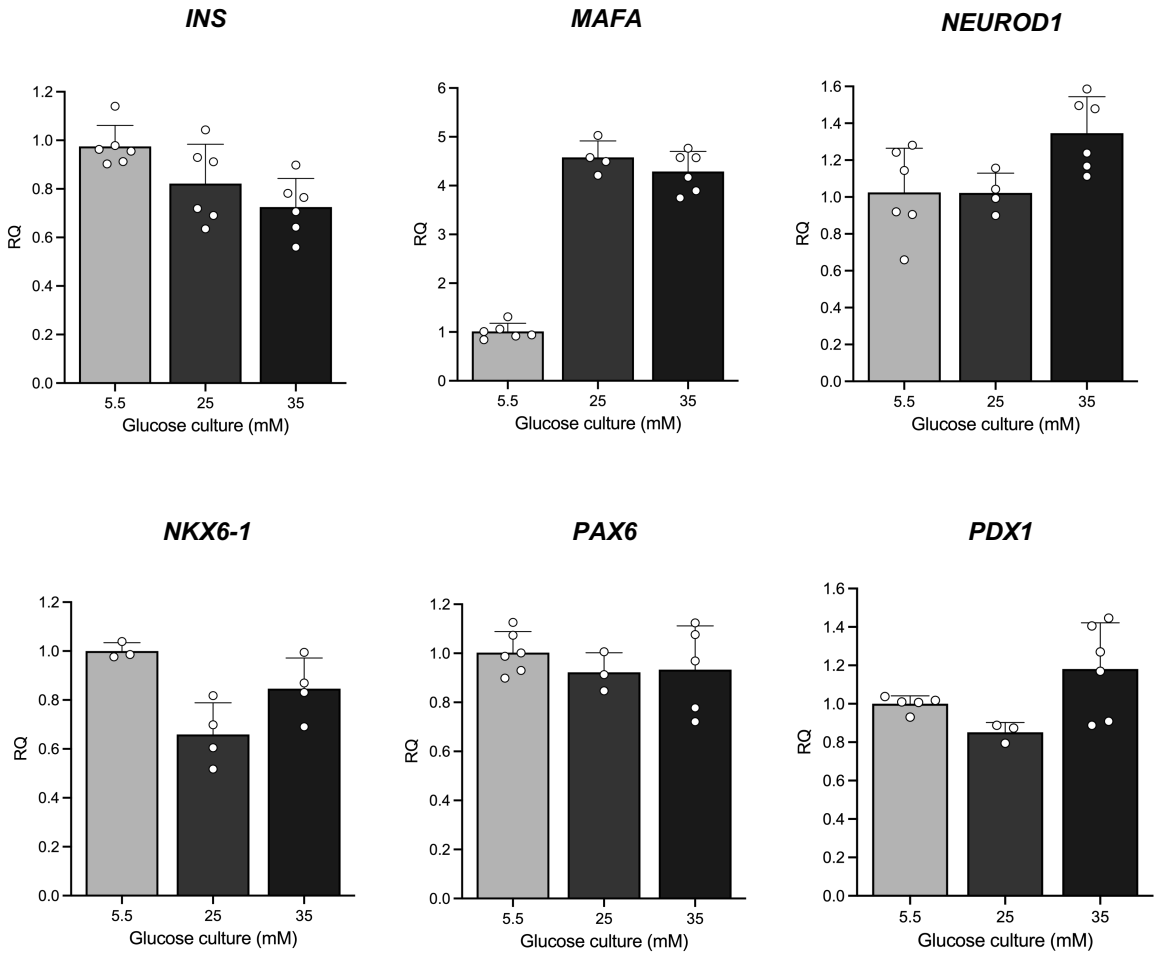

3.4.3 Modelling impaired glucose tolerance, mild hyperglycaemia and severe hyperglycaemia in the βV59M mouse via titration of tamoxifen dosage

In order to study the relationship between the severity of hyperglycaemia and the loss of insulin biosynthesis *in vivo*, we leveraged the inducible nature of diabetes in the

βV59M mouse. To breed these mice, we crossed floxed Kir6.2-V59M mice with RIP-CreER mice. The former carry the V59M activating mutation in Kir6.2, which is found in patients with neonatal diabetes, downstream of a floxed STOP codon. RIP-CreER mice (which have normal glucose tolerance) express Cre-recombinase under control of the rat insulin promoter, enabling its β-cell specific expression in response to tamoxifen injection. In offspring co-expressing both the Kir6.2-V59M transgene and Cre-recombinase (βV59M mice) the Kir6.2-V59M transgene is activated upon tamoxifen injection. Wild-type and single transgenic Kir6.2-V59M and RIP-CreER mice were also injected with tamoxifen and used as controls.

When the gain-of-function K_{ATP} channel mutation is activated in the βV59M mice, insulin secretion is abolished and hyperglycaemia swiftly ensues. We sought to produce different severities of hyperglycaemia by adjusting the dose of tamoxifen used to induce expression of transgenic Kir6.2, taking advantage of the property of the model that the transgene is not switched on in every β-cell. Tamoxifen doses ranging from 20 to 25 μg per gram body weight were used to induce mild hyperglycaemia, while 200 μg per gram body weight was used to induce severe hyperglycaemia (table 3.2). Although increasing the dose of tamoxifen increases the proportion of β-cells expressing the transgene, there is some variation in the phenotype produced by a given dose since this is not a perfect relationship. Moreover, each islet effectively contains a different mosaic of hyperpolarised and excitable β-cells which will vary in their electrical connectivity. Some βV59M mice injected with a low tamoxifen dose did not become diabetic but did show impaired glucose tolerance in the IPGTT and were accordingly categorised as IGT. Transgenic mice were categorised into three groups according to their final blood glucose before being humanely culled: IGT (normal blood

glucose, i.e. <12 mM), mild hyperglycaemic (12-16 mM), and severe hyperglycaemic (>16 mM). Control mice had 6-12 mM blood glucose.

Table 3.2: Genotypes and phenotypes of the mice used in this study

Mouse	Sex	Genotype	Tamoxifen dose (µg/g body weight)	Days diabetic	Initial blood glucose (mM)	Week 3 blood glucose (mM)	Category assigned
1	Male	Control	25	19	10.6	9.5	Control
2	Male	βV59M	25	19	10.2	15.2	Mild
3	Male	Control	25	19	11.6	8.9	Control
4	Male	Control	25	19	11.5	9.8	Control
5	Male	βV59M	25	19	12.2	11.4	IGT
6	Male	Control	200	19	12.3	7.8	Control
7	Male	βV59M	200	19	8.9	27.8	Severe
8	Male	Control	200	19	11.7	10.1	Control
9	Male	βV59M	200	19	7.9	27.2	Severe
10	Female	Control	20	21	8.3	9.0	Control
11	Female	βV59M	20	21	8.4	15.3	Mild
12	Female	βV59M	20	21	7.3	15.6	Mild
13	Female	βV59M	20	21	8.6	14.8	Mild
14	Female	Control	20	21	5.2	6.1	Control
15	Female	Control	20	21	7.2	8.4	Control
16	Male	βV59M	22.5	18	12.6	10.3	IGT
17	Male	βV59M	22.5	18	10.2	11.2	IGT
18	Male	Control	22.5	18	6.0	9.6	Control
19	Male	βV59M	22.5	18	12.3	10.0	IGT
20	Male	Control	22.5	18	10.7	6.5	Control
21	Male	Control	22.5	18	8.4	12.1	Control
22	Female	Control	20	22	8.1	8.9	Control
23	Female	βV59M	20	22	6.9	13.7	Mild
24	Female	βV59M	20	22	8.3	15.1	Mild

25	Female	βV59M	20	22	7.9	17.6	Severe
26	Female	Control	20	22	7.7	9.0	Control
27	Male	βV59M	200	21	7.8	26.8	Severe
28	Male	βV59M	200	21	6.7	>27.8	Severe
29	Male	Control	200	21	8.1	11.0	Control
30	Male	Control	200	21	8.1	7.1	Control
31	Female	Control	200	21	7.9	10.1	Control
32	Female	Control	200	21	8.3	6.0	Control
33	Female	βV59M	200	21	8.0	>27.8	Severe
34	Female	βV59M	200	21	7.6	>27.8	Severe
35	Male	βV59M	20	23	6.8	14.7	Mild
36	Male	Control	20	23	7.3	9.5	Control
37	Male	Control	20	23	7.5	8.4	Control
38	Male	βV59M	20	23	8.1	15.0	Mild
39	Female	Control	20	23	7.4	8.3	Control
40	Female	βV59M	20	23	7.4	13.7	Mild
41	Male	Control	20	23	8.3	8.2	Control
42	Male	βV59M	20	23	7.8	14.1	Mild
43	Female	Control	12.5	26	7.8	7.8	Control
44	Female	Control	12.5	26	7.9	10.7	Control
45	Female	βV59M	12.5	26	7.9	11.3	IGT
46	Female	βV59M	12.5	26	8.3	9.2	IGT
47	Male	βV59M	12.5	26	8.8	9.6	IGT
48	Male	Control	12.5	26	8.4	11.5	Control
49	Male	βV59M	12.5	26	9.1	10.3	IGT
50	Male	Control	12.5	26	9.4	7.7	Control

Figure 3.9: Loss of insulin content in βV59M islets corresponds to the severity of hyperglycaemia

Insulin content (ng/islet) of isolated islets from IGT, mild, and severe hyperglycaemic βV59M mice. Each data point represents one mouse (average insulin content of 10

size-matched islets): control n=23; IGT n=11; mild HG n=9; severe HG n=7. Control and severe HG groups compared by two-tailed unpaired Student's t-test.

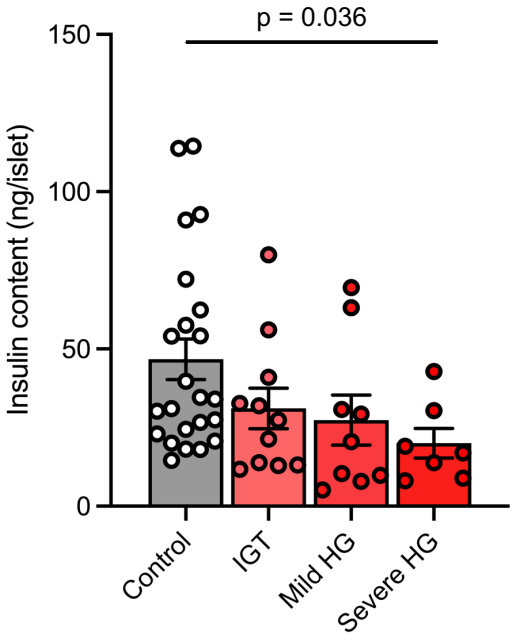

Although quite variable between individual mice, islet insulin content appears to decline with increasing blood glucose concentration, being progressively less in mice with IGT, mild hyperglycaemia, and severe hyperglycaemia compared to control mice (figure 3.9). In the severely hyperglycaemic mice, insulin content declined by almost 60% (p=0.036), compared to ~70% when mice had similarly elevated blood glucose for 4 weeks (Brereton et al., 2014). We would therefore expect the decline in insulin content in IGT and mild HG mice to continue over a fourth week of their respective phenotypes, and indeed IGT might progress to mild hyperglycaemia through progressive impairment of β-cell function. These results provide valuable *in vivo* corroboration of my findings in INS-1 cells, arguing that our models are valid for advancing our understanding of how β-cell dysfunction progresses as glycaemic control deteriorates.

Figure 3.10: Relationship between degree of hyperglycaemia and expression of the insulin genes and β-cell identity genes in βV59M mice

qPCR analysis of the expression of the insulin genes and selected β-cell identity genes in islets from IGT, mild, and severe hyperglycaemic βV59M mice. Each data point represents one mouse.

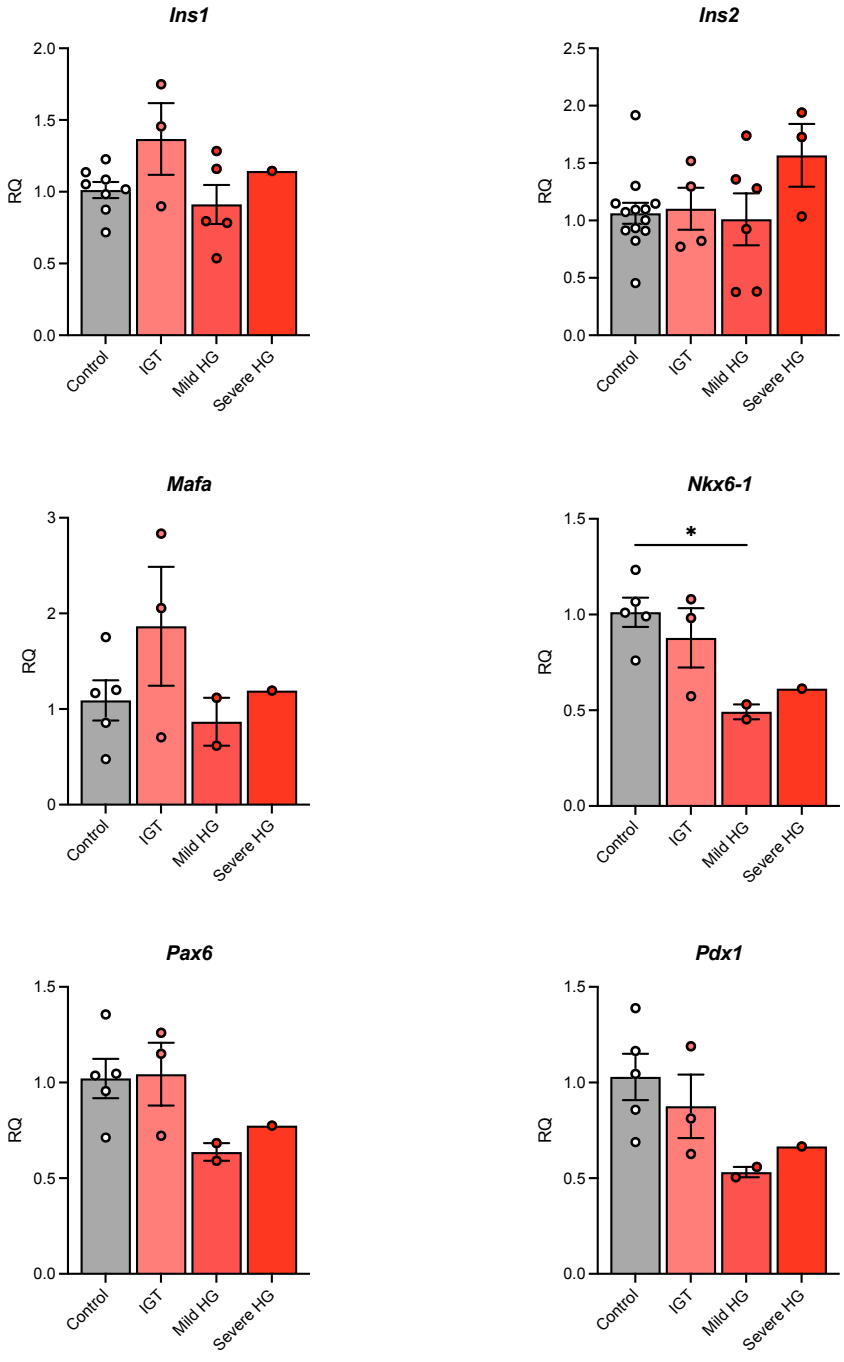

Trends in expression of the insulin genes and β-cell identity genes in IGT, mild HG, and severe HG mice were less clear (figure 3.10), and interpretation of these results is confounded by the small numbers of mice sampled. Transdifferentiation of α-cells to β-cells or vice versa caused by prolonged hyperglycaemia could perhaps also confound results. *Gcg* is upregulated 2.46 fold in islets isolated from diabetic βV59M mice (table 1.1), but α-cell markers were not otherwise investigated. Surprisingly, there appeared to be no downregulation of the insulin genes in diabetic mice, and *Ins2* expression even appeared to increase in severely hyperglycaemic mice, although there were only 3 of these animals. These results are not supported by previous RNAseq data, which showed downregulation of insulin gene expression in severely hyperglycaemic mice (figure 3.11). Impaired glucose tolerance does not appear sufficient to cause downregulation of the β-cell identity genes, but (with the exception of *Mafa*) these do appear to be downregulated in mild and severe hyperglycaemia. It would be interesting if, in a well-powered study, *Ins1* proves to be more susceptible to downregulation in hyperglycaemia than *Ins2*, as this would be the opposite of what I observed in INS-1 cells.

Figure 3.11: Glibenclamide reverses the downregulation of insulin gene expression in the islets of diabetic βV59M mice

Ins1 and *Ins2* transcripts per million (tpm) counts in isolated islets from βV59M mice (from RNAseq). Each data point represents one mouse: control (black) n=4; 2 weeks diabetic (red) n=3; 2 weeks diabetic + 2 weeks glibenclamide (orange) n=4. **p < 0.01; 1-way ANOVA with Bonferroni's correction. Data taken from RNAseq experiments described by Haythorne et al. (2019): transcriptomics data are available in the European Nucleotide Archive (https://www.ebi.ac.uk/ena) under the accession number ERP114395.

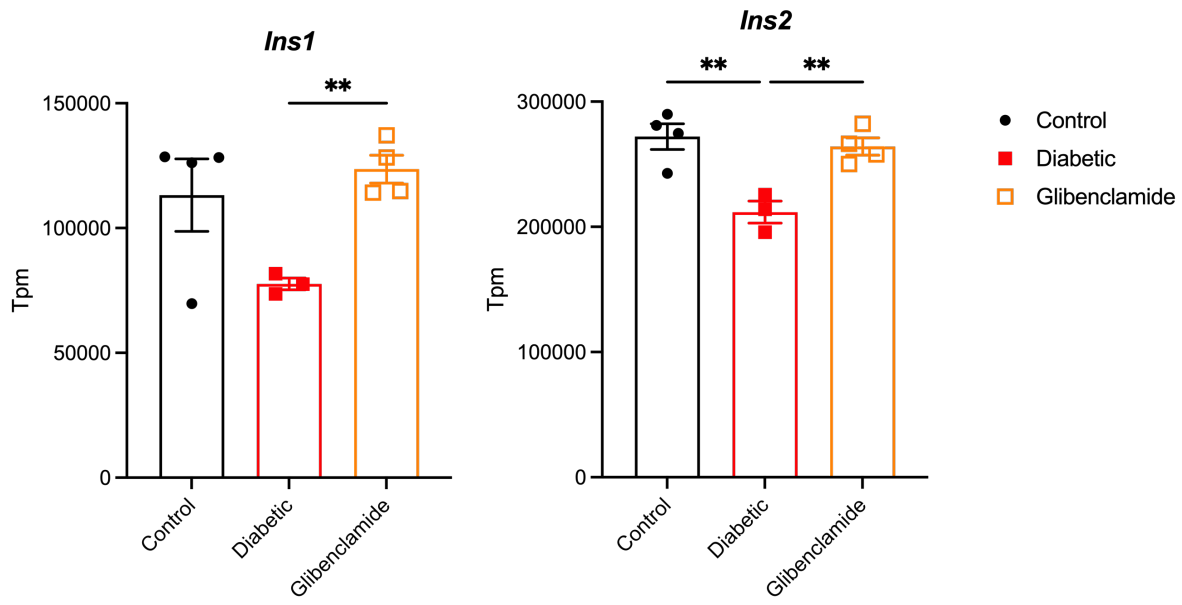

3.5 Discussion

Since chronic hyperglycaemia is believed to drive the decline in β-cell function in T2D, it is important to know at what level of hyperglycaemia this decline begins. Although insulin biosynthesis is known to be impaired in chronic hyperglycaemia, it was striking how much insulin mRNA levels in INS-1 cells were reduced at glucose concentrations as low as 8 mM (figure 3.3). Standard medium containing 11 mM glucose is used for INS-1 cell line maintenance to optimise cell growth, yet it is apparent that these conditions are not optimal for insulin gene expression. Loss of insulin biosynthesis in response to mild hyperglycaemia was also apparent *in vivo* (figure 3.9). This reduction in insulin content might be more robust to experimental variation and islet heterogeneity if the total insulin content of the pancreas were measured, but I used isolated islets since other islets from the same pancreata were required for RNA samples. Cellular insulin content depends on the balance between production and loss

via secretion or intracellular breakdown of insulin granules via crinophagy. High glucose, at least initially, may be expected to lead to an increased rate of exocytosis, but this cannot explain the dramatic loss of insulin content seen in chronic hyperglycaemia, which occurred in βV59M islets (which are unable to secrete insulin) as well as *in vitro*. Instead, the steep decline in insulin mRNA expression seen in INS-1 cells suggests that it is largely due to impaired production. In future investigations, pulse-chase analysis could help to track changes in the insulin mRNA pool and determine the balance between transcription and translation or degradation as insulin biosynthesis responds to changes in glycaemia. This approach could also be used to investigate changes in (pro)insulin processing, although the observation that insulin content closely tracks mRNA levels argues against a processing defect being a major factor in the loss of insulin content.

A salient feature of the glucose dose-response curves (figure 3.3) was the lower relative expression of *Mafa* and *Pdx1* at zero glucose compared to the other insulin genes. Since PDX-1 binding to the insulin promoter is abolished at 1 mM glucose (Barrow et al., 2006), it is perhaps unsurprising that *Pdx1* gene expression is diminished at very low glucose levels. Maintaining relatively high expression of the other identity genes at zero or very low glucose may enable insulin transcription to be rapidly induced when glucose enters the cell; in contrast, their downregulation at high glucose indicates that the capacity for insulin transcription is reduced. The close correspondence of the bell-shaped curves for *Ins1* and *Ins2* with those for *Mafa* and *Pdx1* invites the conclusion, consistent with previous studies (Bernardo et al., 2008), that these two are the most important transcription factors in determining the level of insulin transcription. Moreover, the observation that *Ins2* is more severely repressed than *Ins1* in INS-1 cells may be attributed to *Mafa* being more downregulated than

Pdx1. According to chromatin immunoprecipitation experiments, PDX-1 increases the association of acetylated histones H3 and H4 with the *Ins1* gene, while MAFA increases the association of acetylated histone H3 with the *Ins2* gene (Docherty et al., 2005).

Neurod1 is the least downregulated of the β-cell identity genes analysed in INS-1 cells, with only a ~60% reduction in expression at 25 mM glucose. Interestingly, a recent study mapping chromatin accessibility has identified NEUROD1 as one of the transcription factors responsible for maintaining a β-cell subtype that is enriched in T2D donor islets (G. Wang et al., 2023). The abundance of those “beta-2” cells positively correlates with HbA1c, and, although beta-2 cells display higher insulin exocytosis than beta-1 cells, the subtype shift towards beta-2 (from 33% of ND β-cells to 72% of T2D β-cells) fails to prevent an overall decline in exocytosis in T2D (G. Wang et al., 2023). The relative enrichment (by declining less than other β-cell identity genes) of NEUROD1 in INS-1 cells during hyperglycaemia could thus be interpreted as representing at least some aspects of a T2D-like phenotype.

Time course experiments in INS-1 cells revealed that insulin gene expression was very slow to recover after reversal of hyperglycaemia, with *Ins2* being particularly unresponsive (figure 3.4a). A considerable lag is apparent between the recovery in expression of the identity genes, which are largely restored to normal levels by 48 hrs post-reversal, and the insulin genes, which still have low expression at 72 hrs. Such a lag is much too long to be simply explained by the time required to translate the mRNA encoding the transcription factors and for the newly synthesised proteins to enter the nucleus and activate transcription, so its cause is unclear. Repression of insulin gene expression thus appears not to be rapidly reversible following reversal of

hyperglycaemia, although a full recovery does occur in βV59M mice within 2 weeks of the restoration of euglycaemia by glibenclamide therapy (figure 3.11), providing an upper bound for the recovery time.

Recurrent episodes of hyperglycaemia could contribute to a progressive impairment of β-cell function, with implications for the aetiology of T2D. Such unfavourable temporal dynamics could also be at play in βV59M mice injected with low doses of tamoxifen. Those animals with impaired glucose tolerance still have a sufficient number of β-cells able to depolarise in order to secrete some insulin and maintain euglycaemia, yet are unable to secrete sufficient quantities of insulin when undergoing a glucose challenge. This results in these mice experiencing a prolonged (~2 hours) postprandial elevation of blood glucose, which is akin to individuals with prediabetes (table 3.1). Prolonged spikes in postprandial blood glucose could initiate downregulation of insulin biosynthesis followed by partial recovery; if iterated, we would expect that process to drive a gradual decline in insulin biosynthesis over the long term. Although greater statistical power would be required to confirm it, there may indeed be a small decline in insulin content in IGT mice, which could be both a cause and a consequence of their impaired glucose tolerance. Taken together with the more substantial loss of insulin in mildly hyperglycaemic mice, these results indicate that loss of insulin occurs even with small elevations in blood glucose, and could begin in the early stages of T2D development. It has been suggested that insulin biosynthesis becomes rate limiting for secretion as insulin mRNA levels and content fall with worsening hyperglycaemia, so even a relatively modest loss of insulin could play a role in β-cell decompensation (Weir & Bonner-Weir, 2004).

Unfortunately, EndoC cells proved to be a poor model for investigating glucotoxicity in human β-cells. Unlike INS-1 cells, they did not display the substantial loss of insulin content that characterises the response to chronic hyperglycaemia in human islets (Mir-Coll et al., 2021; Tariq et al., 2022), although it was possible to demonstrate some loss of insulin content in βH5 cells chronically exposed to an extremely high concentration of 35 mM glucose (figure 3.7c). EndoC-βH1 cells in particular are markedly resistant to many stresses, including hyperglycaemia. To take one example, 72 hrs culture at 20 mM did not cause any significant increase in apoptosis (Tsonkova et al., 2018). In part, this may be attributable to high expression of heat shock proteins, and reflects their immature status. While transcriptionally immature β-cells defined by low expression of MAFA and PDX1 contribute to adult islet function (Nasteska et al., 2021), a population composed only of immature β-cells is not ideal for modelling chronic hyperglycaemia. In future, I aim to use InSphero islets as a human model with greater clinical relevance in which to translate my findings.

The problem of small effect sizes in EndoC cells, in contrast to the very clear changes produced by HG-culture of INS-1 cells, was compounded by the comparatively large variability in the data (both gene expression and insulin concentration data), which may have masked some changes. This variability is likely in part due to intrinsic properties of the cells, in particular their low total insulin content and correspondingly low (in absolute terms) insulin secretion, as well as being due to each sample corresponding to a relatively small number of cells (40,000 to 60,000 cells in a well of a 96-well plate). The 96-well format has the advantage that it permits high throughput for large-scale automated or semi-automated screens, but may be less well suited to this study than the 24-well plates we use for most INS-1 cell experiments. Compiling Ct values for the housekeeper gene *TBP* from multiple qPCR experiments in both

EndoC cell lines reveals that *TBP* levels are more variable in βH1 than in βH5 cells (figure 3.12), which must at least partially explain the greater variability in the normalised data seen with βH1 cells. The Ct values in βH5 cells are slightly lower on average at 35 mM glucose than at 5.5 mM glucose, suggesting that very high glucose levels cause increased *TBP* expression, potentially resulting in increased global transcription activity. Finally, limited time during my industrial placement prevented the replication of many of the experiments using EndoC cells, making it impossible to draw any firm conclusions from this work.

Figure 3.12: Expression of the housekeeper gene *TBP* shows greater variability βH1 cells than in βH5 cells

Cq values for *TBP* in (a) EndoC-βH1 cells and (b) EndoC-βH5 cells incubated chronically with 5.5, 25, or 35 mM glucose. Each data point represents the cells from one well of a 96-well plate; Ct values are collated from 3 independent experiments. Error bars show SD. *p < 0.05; 1-way ANOVA with Bonferroni's correction.

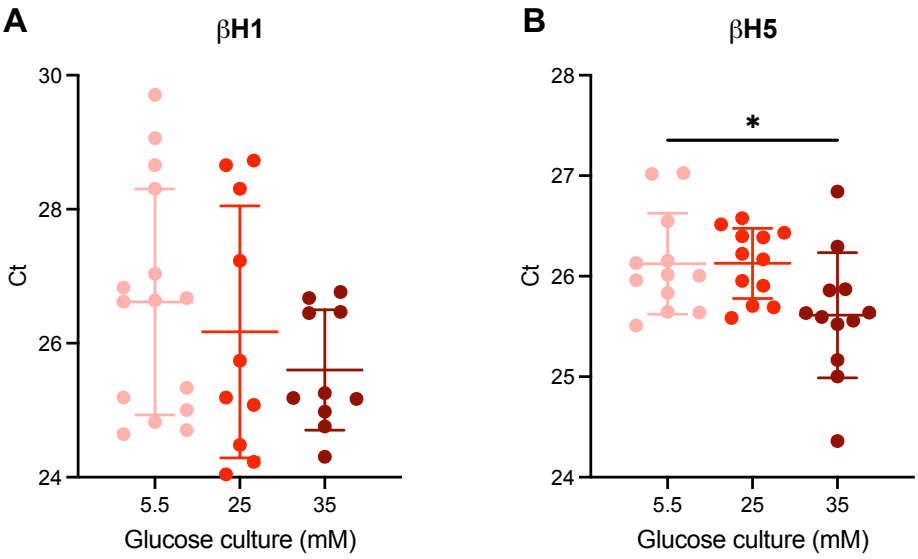

While more work is required to successfully translate findings from rodent models into human tissue, these studies have revealed two key features of the β-cell response to hyperglycaemia. Firstly, insulin biosynthesis is progressively impaired by increasing ambient glucose concentrations, starting as low as 8 mM in INS-1 cells and at a level around 12 mM or below in βV59M mice. Secondly, insulin biosynthesis is rapidly downregulated at the onset of hyperglycaemia but recovers slowly upon subsequent restoration of euglycaemia. Thus, even hyperglycaemia of mild degree and short duration can impair β-cell function and may thereby contribute to the development of T2D.

4. Hyperglycaemia-induced metabolic dysregulation causes the loss of insulin biosynthesis

4.1 Summary

1. Culturing INS-1 cells in the presence of the glucokinase inhibitor mannoheptulose prevented the detrimental effects of chronic hyperglycaemia (25 mM glucose) on insulin mRNA expression. The downregulation of insulin biosynthesis must therefore be mediated not by glucose *per se* but by a downstream glucose metabolite.
2. Culturing INS-1 cells with high concentrations (20 mM) of the mitochondrial substrates methyl pyruvate or monomethyl succinate did not impair insulin mRNA expression, indicating that the loss of insulin in chronic hyperglycaemia is not triggered by mitochondrial metabolites.
3. The GAPDH inhibitor koningic acid caused significant downregulation of insulin mRNA expression in cells cultured at 5 mM glucose (LG-cells), indicating that this is triggered by one or more glycolytic metabolites upstream of GAPDH.
4. siRNA knockdown of phosphofructokinase in LG-cells reduced expression of the insulin genes and *Mafa*, suggesting that the key metabolite(s) driving loss of insulin lie upstream of phosphofructokinase.
5. The glucose analogue 2-deoxyglucose, which is metabolised only as far as 2-deoxyglucose-6-phosphate, caused reductions in insulin mRNA and insulin content comparable to those caused by 25 mM glucose, indicating that glucose-6-phosphate (G6P) is a key metabolite that triggers downregulation of insulin gene expression and biosynthesis.

6. The pentose phosphate pathway inhibitor 6-aminonicotinamide and the polyol pathway inhibitors EBPC and tolrestat partially downregulated insulin gene expression in LG-cells but had no effect on HG-cells (cultured at 25 mM glucose). These results suggest that blocking alternative pathways of glucose metabolism causes accumulation of glycolytic intermediates akin to the effects of hyperglycaemia. Because glycolysis is already blocked at GAPDH in HG-cells, blocking these alternative pathways has no additional effect on insulin biosynthesis.

4.2 Introduction

In chapter 3, I characterised the loss of insulin mRNA and protein content during chronic hyperglycaemia. Here, I investigate the underlying causes of that loss. Previous work has shown that hyperglycaemic β-cells have impaired metabolism. Changes include an accumulation of glycolytic metabolites between phosphofructokinase and GAPDH that leads to hyperactivation of mTORC1 (Haythorne et al., 2022). However, if the same alterations in β-cell metabolism also cause the loss of insulin biosynthesis, they must do so through mechanisms other than mTOR signalling, since S6K1 inhibition did not prevent the loss of insulin content (Haythorne et al., 2022). A systematic assessment of how insulin gene expression is regulated by glucose metabolism in euglycaemia and hyperglycaemia has so far been lacking. Starting with the working hypothesis that hyperglycaemia-induced metabolic dysregulation drives the downregulation of insulin biosynthesis, I aimed to identify the metabolic signals that couple the latter process to the former.

Through the series of experiments discussed in this chapter, I narrowed down the list of candidate metabolites, first by excluding glucose itself and mitochondrial metabolites, and then by dissecting glycolysis by means of pharmacological inhibition and siRNA knockdown of selected enzymes. To monitor the effects of the various inhibitors, siRNAs, and alternative fuels used to manipulate β-cell metabolism, I measured the expression of a set of metabolic genes that are known to be upregulated or downregulated in chronic hyperglycaemia (tables 4.1 and 4.2). These include key glycolytic genes that are upregulated (*Pfkl*, *Pfkfb3*, *Aldob*, *Eno1*) or downregulated (*Pfkfb2*) in HG-cells. Switching between 6-phosphofructo-2-kinase/fructose-2,6-biphosphatase (PFK-2/FBPase-2) isoforms (from PFKFB2 to PFKFB3) favours F2,6BP production, which should enhance glycolytic flux through allosteric activation of phosphofructokinase. The fact that glycolysis is impaired in spite of these adaptations to hyperglycaemia is likely due to the bottleneck at GAPDH (Haythorne et al., 2022). The mitochondrial enzymes monitored include *Pdk1*, which inhibits PDH activity and hence pyruvate flux into the TCA cycle by phosphorylating the E1 subunit of the pyruvate dehydrogenase complex; the TCA cycle enzymes *Idh2*, *Sdha*, and *Mdh2*; and two subunits of the electron transport chain complexes I (*Ndufs8*) and IV (*Ndufa4*[7]). Figure 4.1 provides an overview of these enzymes and how their expression is altered during chronic hyperglycaemia in βV59M mouse islets.

Table 4.1: Changes in mRNA and protein expression of key genes involved in glycolysis and gluconeogenesis in control and diabetic βV59M islets

FC = fold change (diabetic vs control): red = up, blue = down in diabetes. The most upregulated or downregulated transcripts/proteins have the strongest intensity of

[7] Despite its name, NDUFA4 is actually part of complex IV rather than complex I, as originally assumed (Balsa *et al*., 2012).

colour. Some proteins were not detected by mass spectrometry (empty boxes). P-values: red = p≥0.05 (non-significant), green = p<0.05 (significant). Data taken from RNAseq and proteomics experiments described by Haythorne et al. (2019): transcriptomics data are available in the European Nucleotide Archive (https://www.ebi.ac.uk/ena) under the accession number ERP114395 and mass spectrometric proteomics data are deposited to the ProteomeXchange Consortium via the PRIDE partner repository with the data set identifier PXD012979 and 10.6019/PXD012979.

Gene	**Full name**	**RNAseq islet**		**Protein MS islet**	
		FC (Db vs C)	p-value	FC (Db vs C)	p-value
Aldoa	Aldolase A	0.63	9.29E-08	1.94	1.19E-04
Aldob	Aldolase B	315.78	6.57E-90	64.54	7.80E-08
Aldoc	Aldolase C	1.99	3.79E-08	3.54	1.80E-05
Eno1	Alpha-enolase	5.86	9.97E-27	2.17	2.47E-05
Eno2	Gamma-enolase	0.31	1.13E-09	0.27	9.10E-04
Eno3	Beta-enolase	0.31	3.37E-08	1.92	2.83E-03
Fbp1	Fructose-1,6-bisphosphatase 1	7.73	3.67E-31	9.47	3.27E-02
Fbp2	Fructose-1,6-bisphosphatase 2	232.32	1.13E-42	5.58	1.29E-03
G6pc2	Glucose-6-phosphatase 2	0.24	5.52E-19	0.50	5.95E-03
Gapdh	Glyceraldehyde 3-phosphate dehydrogenase	1.52	1.57E-06	3.31	2.11E-07
Gck	Glucokinase	0.85	2.37E-01		
Gpi1	Glucose-6-phosphate isomerase	3.48	3.86E-74		
Pfkfb1	6-phosphofructo-2-kinase/fructose-2,6-biphosphatase 1	1.71	1.52E-02		
Pfkfb2	6-phosphofructo-2-kinase/fructose-2,6-biphosphatase 2	0.62	3.46E-05	0.45	1.16E-03
Pfkfb3	6-phosphofructo-2-kinase/fructose-2,6-biphosphatase 3	8.20	3.61E-55		
Pfkl	6-phosphofructokinase, liver type	2.44	4.97E-36	3.30	7.23E-04
Pfkm	6-phosphofructokinase, muscle type	0.97	6.53E-01	1.08	5.42E-01
Pfkp	6-phosphofructokinase, platelet type	1.67	1.37E-07	1.15	4.23E-02
Pgam1	Phosphoglycerate mutase 1	0.86	1.06E-01	1.22	1.22E+00
Pgk1	Phosphoglycerate kinase 1	0.90	2.05E-01	1.23	3.69E-02
Pklr	Pyruvate kinase isozymes R/L	4.39	3.21E-51	2.87	3.88E-03
Pkm	Pyruvate kinase muscle isozyme	1.71	4.95E-12	1.41	2.14E-01
Tpi1	Triose phosphate isomerase	0.85	3.19E-02	1.45	3.75E-03

Table 4.2: Changes in mRNA and protein expression of key genes involved in mitochondrial metabolism in control and diabetic βV59M islets

FC = fold change (diabetic vs control): red = up, blue = down in diabetes. The most upregulated or downregulated transcripts/proteins have the strongest intensity of colour. Some proteins were not detected by mass spectrometry (empty boxes). P-values: red = p≥0.05 (non-significant), green = p<0.05 (significant). Data taken from RNAseq and proteomics experiments described by Haythorne et al. (2019): transcriptomics data are available in the European Nucleotide Archive (https://www.ebi.ac.uk/ena) under the accession number ERP114395 and mass spectrometric proteomics data are deposited to the ProteomeXchange Consortium via the PRIDE partner repository with the data set identifier PXD012979 and 10.6019/PXD012979.

Gene	**Full name**	**RNAseq islet**		**Protein MS islet**	
		FC (Db vs C)	p-value	FC (Db vs C)	p-value
Acly	ATP citrate lyase	3.13	8.20E-25	4.60	6.29E-05
Aco1	Aconitase (cytosolic)	1.30	1.58E-04	1.59	1.00E-03
Aco2	Aconitase (mitochondrial)	0.92	2.42E-01	0.63	2.73E-02
Aldh2	Aldehyde dehydrogenase, mitochondrial	0.47	1.28E-15	0.73	1.21E-02
Atp5g2	Subunit c of ATP synthase FO	1.12	1.81E-01		
Atpif1	ATPase inhibitor, mitochondrial (IF1)	1.26	3.36E-03	0.90	4.24E-01
Coa5	Cytochrome c oxidase assembly factor 5	1.27	2.19E-03		
Cox14	Cytochrome c oxidase assembly factor 14	1.04	5.76E-01		
Cox6a2	Cytochrome c oxidase subunit VIa polypeptide 2	0.01	4.31E-99		
Cs	Citrate synthase	1.08	2.87E-01	0.40	2.04E-02
Dlat	Dihydrolipoyl transacetylase	1.08	3.00E-01	1.48	1.85E-02
Dld	Dihydrolipoamide dehydrogenase	0.85	2.77E-02	0.34	5.98E-03
Dlst	Dihydrolipoyllysine-residue succinyltransferase component of 2-oxoglutarate dehydrogenase complex, mitochondrial	0.93	3.28E-01	0.81	5.96E-02
Fh1	Fumarase	0.66	5.58E-03		
Gpd1	Glycerol-3-phosphate dehydrogenase 1	2.59	5.91E-22	4.53	7.90E-06
Gpd2	Glycerol-3-phosphate dehydrogenase 2	3.84	9.29E-18	1.77	9.01E-02
Idh1	Isocitrate dehydrogenase 1 (NADP+-dependent), soluble	3.24	7.29E-35	3.25	9.99E-05
Idh2	Isocitrate dehydrogenase (NADP+-dependent), mitochondrial	0.58	4.05E-12	0.43	5.26E-05
Mdh1	Malate dehydrogenase, cytosolic	0.71	8.58E-07	1.06	8.21E-01
Mdh2	Malate dehydrogenase, mitochondrial	0.79	1.22E-03	0.52	3.91E-04

Ndufa1	NADH dehydrogenase [ubiquinone] 1 alpha subcomplex subunit 1	1.06	4.61E-01	0.46	5.31E-02
Ndufa4	Cytochrome c oxidase subunit Ndufa4	0.74	7.36E-05	0.35	1.18E-03
Ndufs2	NADH dehydrogenase [ubiquinone] iron-sulphur protein 2, mitochondrial	0.63	2.40E-10	0.61	9.99E-03
Ndufs8	NADH dehydrogenase [ubiquinone] iron-sulphur protein 8, mitochondrial	0.75	1.31E-03	0.36	3.34E-04
Ogdh	2-oxoglutarate dehydrogenase, mitochondrial	0.93	2.89E-01	1.17	1.48E-01
Ogdhl	2-oxoglutarate dehydrogenase-like, mitochondrial	0.65	4.93E-08	0.67	7.35E-02
Pdha1	Pyruvate dehydrogenase (lipoamide) alpha 1	1.40	5.25E-06	1.22	9.69E-02
Pdhb	Pyruvate dehydrogenase (lipoamide) beta	1.50	6.07E-09	0.98	7.53E-01
Pdk1	Pyruvate dehydrogenase kinase 1	7.55	2.08E-93	5.52	2.30E-05
Pdk4	Pyruvate dehydrogenase kinase 4	2.29	3.56E-06		
Pdp1	Pyruvate dehydrogenase phosphatase catalytic subunit 1	0.47	9.41E-09		
Ppid	Cyclophilin D	0.72	1.51E-05	0.57	4.19E-04
Prkcd	Protein kinase C delta	1.22	3.52E-02		
S100a1	S100 calcium binding protein A1	0.42	8.89E-06	0.58	5.14E-02
Sdha	Succinate dehydrogenase [ubiquinone] flavoprotein subunit, mitochondrial	0.84	2.18E-02	0.42	3.44E-03
Sdhb	Succinate dehydrogenase [ubiquinone] iron-sulphur subunit, mitochondrial	0.89	8.83E-02	0.82	2.17E-01
Sdhc	Succinate dehydrogenase cytochrome b560 subunit, mitochondrial	0.77	2.35E-04	1.11	5.61E-01
Sdhd	Succinate dehydrogenase [ubiquinone] cytochrome b small subunit, mitochondrial	1.50	7.76E-08		

Figure 4.1: Overview of the principal pathways of glucose metabolism and the effect of chronic hyperglycaemia on the abundance of thee enzymes involved

Proteins upregulated in the islets of diabetic βV59M mice are red; proteins downregulated in the islets of diabetic βV59M mice are blue; proteins not significantly altered in diabetes are black. Pathways shown in detail are upper glycolysis (glucokinase to GAPDH), lower glycolysis (GAPDH to pyruvate kinase), the pentose phosphate pathway, and the sorbitol pathway. A summary of mitochondrial metabolism is included. Based on data published by Haythorne *et al.* (2019).

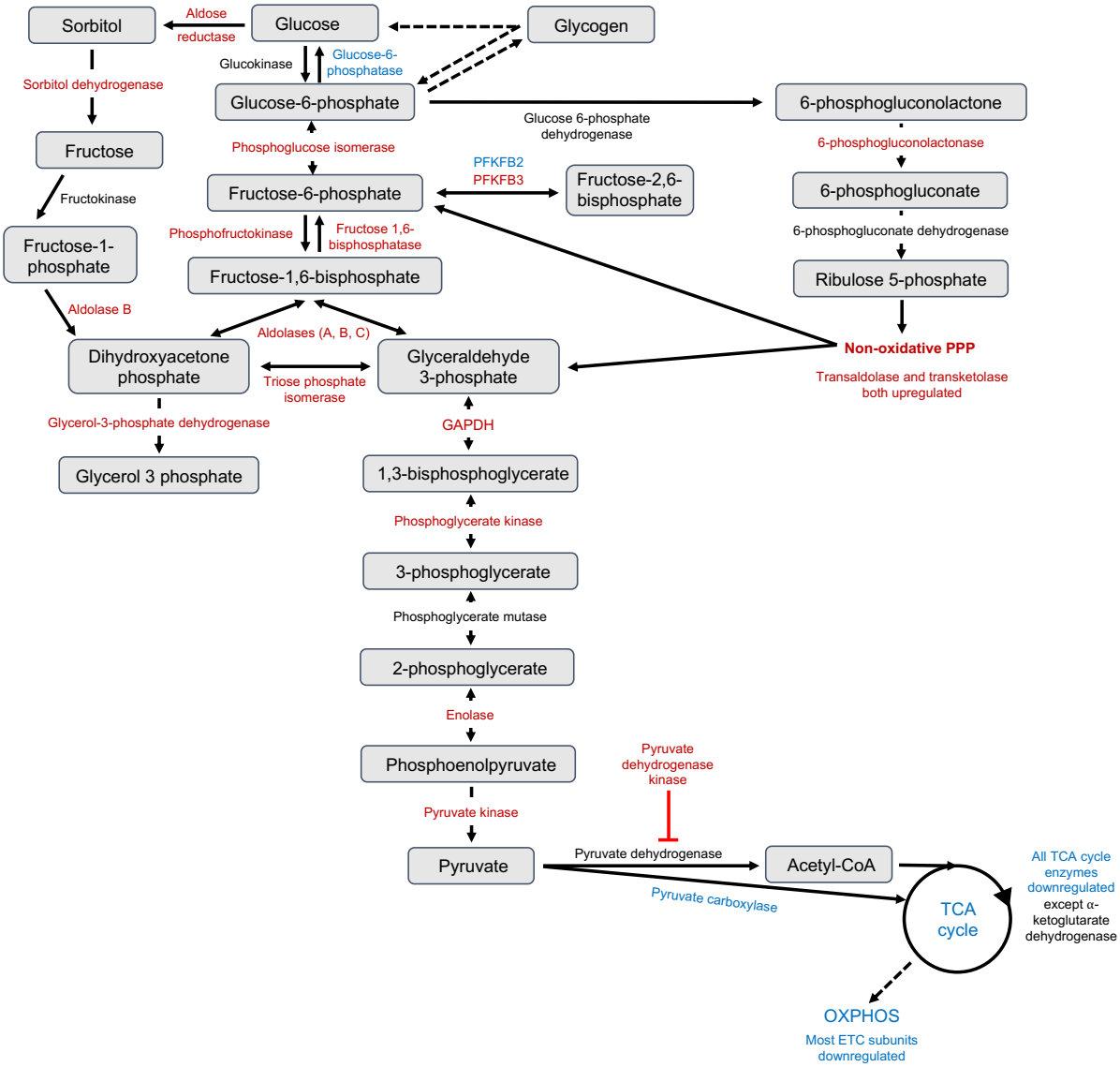

4.3 Materials and methods

Methods were as described in chapter 2, with the following additions.

4.3.1 ADP/ATP assay

The whole-cell ATP/ADP ratio was determined using a bioluminescent ADP/ATP Ratio Assay kit (Abcam, ab65313) according to the manufacturer's instructions. INS-1 cells were grown in 96-well plates, to a density of ~30,000 cells per well at the time

of harvesting. Luminescence was read on a CLARIOstar plate reader (BMG LABTECH).

4.3.2 6-phosphogluconate dehydrogenase activity assay

Enzymatic activity of 6-PGD was determined using a 6-phosphogluconate dehydrogenase assay kit (Abcam, ab241016) according to the manufacturer's instructions. INS-1 cells were grown in 6-well plates, to a density of ~10^6 cells per well at the time of harvesting. The assay was read on a CLARIOstar plate reader (BMG LABTECH) in kinetic mode: absorbance at 460 nm was read at 5 min intervals for 60 mins at 37°C. Two time points in the linear range of the reaction curve were chosen and the difference used to calculate 6-PGD activity.

4.3.3 NADP/NADPH assay

The whole-cell NADPH/$NADP^+$ ratio was determined using a colorimetric NADP/NADPH assay kit (Abcam, ab65349), and 10 kD spin columns (Abcam, ab93349) for deproteinisation (to remove enzymes that might rapidly consume NAPDH). INS-1 cells were grown in 6-well plates, to a density of ~10^6 cells per well at the time of harvesting. Cells were washed in PBS, then scraped and collected in extraction buffer; samples were then homogenised by sonication, vortexed, and centrifuged to pellet debris. The supernatants were transferred to 10 kD spin columns and centrifuged at maximum speed for 45 minutes; the flow-through was used for the assay. An aliquot of each sample was heated at 60°C for 30 minutes to decompose $NADP^+$. The assay was read on a CLARIOstar plate reader (BMG LABTECH) in kinetic mode: absorbance at 450 nm was read at 15-minute intervals for at least 60 minutes,

until the highest standard exceeded an OD of 2.0. [NADPt] (total $NADP^+$ and NADPH) and [NADPH] values were interpolated from the standard curve, and [$NADP^+$] was calculated as the difference between them.

4.4 Identification of metabolic factors underlying the loss of insulin biosynthesis

4.4.1 Glucokinase inhibition reveals that glucose metabolites rather than glucose *per se* trigger repression of insulin gene expression

To determine whether it is glucose itself or a downstream metabolite that causes the decline in insulin biosynthesis, I used mannoheptulose to inhibit glucokinase and assessed how this affected insulin gene expression after 48 hrs of culture at 5 or 25 mM glucose. Since this 7-carbon sugar is a competitive inhibitor of glucokinase, I used a relatively high concentration (10mM) of mannoheptulose to ensure adequate suppression of glucose metabolism in HG-cells.

Figure 4.2 shows the effect of mannoheptulose on expression of the insulin genes and β-cell identity genes in LG-cells and HG-cells. With the exception of *Ins2* and *Nkx6-1*, mannoheptulose did not significantly affect expression of these genes in LG-cells. It is not surprising to see some downregulation of *Ins2* expression considering the bell-shaped dependence on glucose seen in figure 3.3, as mannoheptulose-treated cells are metabolically equivalent to cells experiencing a lower glucose concentration. Importantly, mannoheptulose prevented the downregulation of almost all of the insulin and β-cell identity genes in HG-cells. The exception was *Ins2*, which only declined by

25% (as opposed to 90% in HG-cells without mannoheptulose), consistent with the particularly high sensitivity to glucose displayed by this gene in figure 3.3. Mannoheptulose also prevented the hyperglycaemia-induced declines in insulin content and secretion (Haythorne et al., 2022). These data demonstrate that glucose must not drive the loss of insulin directly: rather, downstream metabolites of glucose must be responsible.

Figure 4.2: Glucokinase inhibition prevents downregulation of the insulin genes and β-cell identity genes in chronic hyperglycaemia

qPCR analysis of the expression of the insulin genes and selected β-cell identity genes in INS-1 cells cultured for 48 hrs at 5 or 25 mM glucose ± 10 mM mannoheptulose (MANNO). n=3-6, with 2-3 technical replicates per experiment. *p < 0.05, **p < 0.01, ***p < 0.001; 1-way ANOVA with Bonferroni's correction.

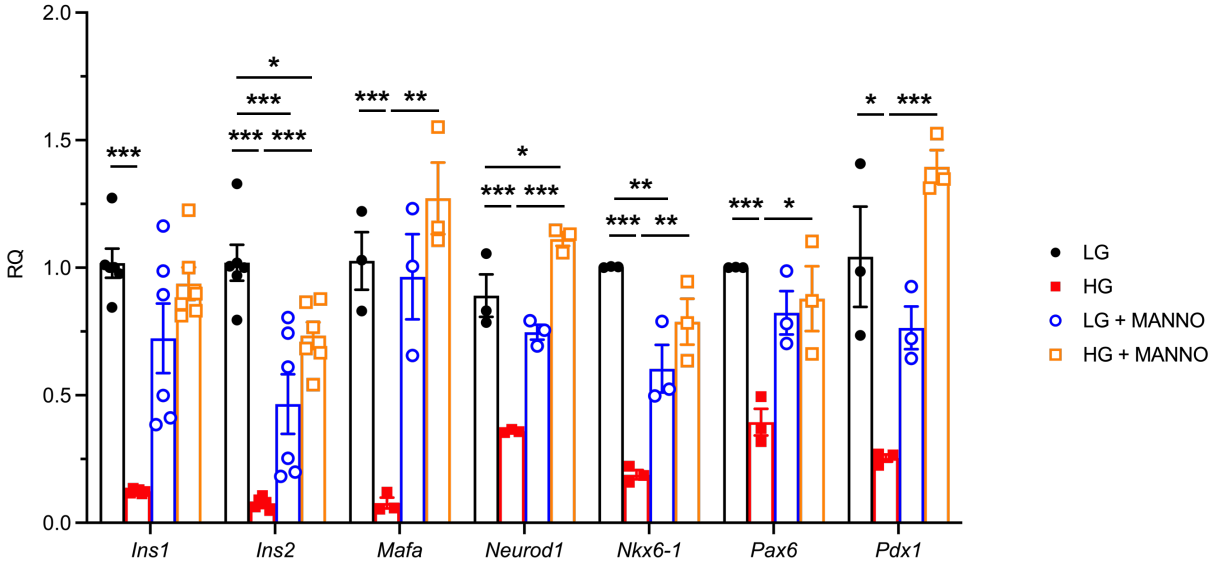

Mannoheptulose also prevented the changes in expression of glycolytic and mitochondrial (TCA cycle and OXPHOS) genes induced by hyperglycaemia (figure 4.3). Note that ALDOB is expressed at low levels in LG-cells, so small changes in *Aldob* transcript levels compared to the housekeeper gene can result in large changes

in relative expression, accounting for the wide range of RQ values seen between replicates for HG-cells. Thus, phosphorylation of glucose by glucokinase is necessary for both the metabolic dysregulation and the loss of insulin biosynthesis caused by chronic hyperglycaemia.

Figure 4.3: Glucokinase inhibition prevents the hyperglycaemia-induced changes in expression of metabolic genes

qPCR analysis of the expression of selected genes involved in **(a)** glycolytic metabolism and **(b)** mitochondrial metabolism in INS-1 cells cultured for 48 hrs at 5 or 25 mM glucose ± 10 mM mannoheptulose. n=3-6, with 2-3 technical replicates per experiment. *p < 0.05, **p < 0.01, ***p < 0.001; 1-way ANOVA with Bonferroni's correction.

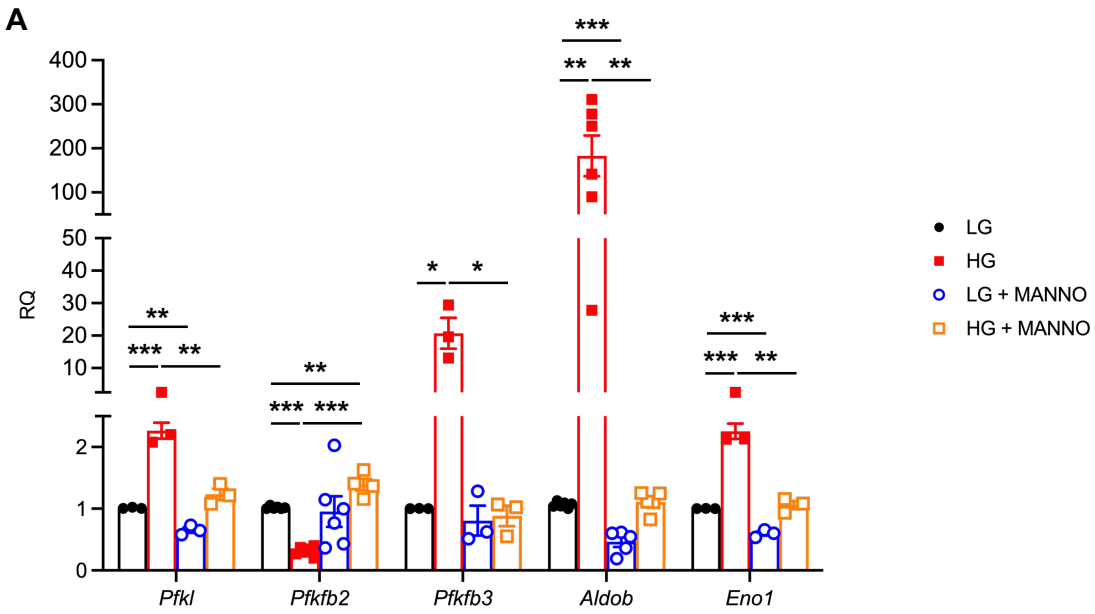

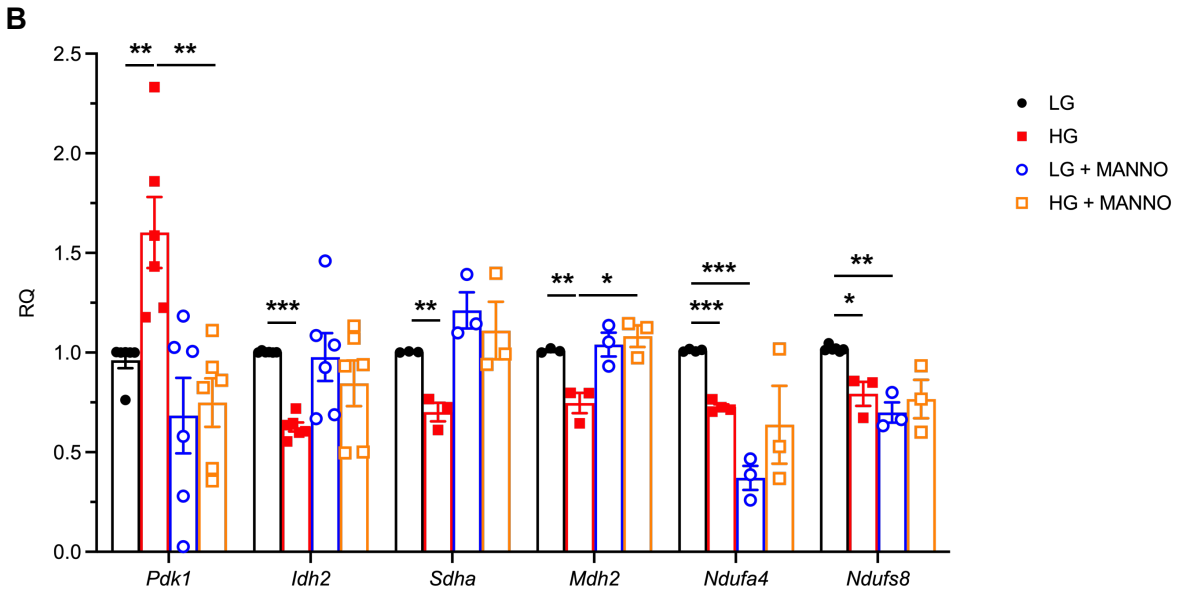

4.4.2 Mitochondrial fuels do not cause loss of insulin biosynthesis

Mitochondrial metabolism is impaired in hyperglycaemic β-cells, raising the question of whether an excess of mitochondrial metabolites might contribute to the loss of insulin biosynthesis. To investigate this possibility, I cultured cells for 48 h with metabolic substrates that bypass glycolysis and enter mitochondrial metabolism directly. The methyl ester forms of these substrates were used to ensure they would be readily taken up and utilised by the cells, since β-cells lack the monocarboxylate transporters needed for pyruvate import (Zhao et al., 2001). Concentrations of methyl pyruvate (PYR) and monomethyl succinate (MMS) that maximally stimulate insulin secretion were chosen (each 20 mM), there being no additional stimulation with 40 mM (figure 4.4a). 20 mM pyruvate is equivalent to 10 mM glucose in terms of moles of 3C units.

Expression of the insulin and β-cell identity genes was generally similar in cells cultured with 5 mM glucose (control) or 20mM of the mitochondrial substrate (figure 4.4). There was no significant difference in expression of *Nkx6-1*, *Pax6*, and *Pdx1*

between these two conditions. *Ins1*, *Ins2*, *Mafa*, and *Neurod1* all showed some reduction in expression in cells cultured with 20 mM methyl pyruvate (figure 4.4b), but this was much less than that seen with 25 mM glucose. These reductions were not large enough to significantly alter insulin content, which was not reduced in cells cultured with 20 mM PYR relative to LG-cells (Haythorne et al., 2022). This was consistent with a previous study in which chronic high pyruvate did not cause a reduction in insulin content (Göhring et al., 2013). *Neurod1* and *Pdx1* showed modest declines in cells cultured with 20 mM methyl succinate, but *Ins2* expression was slightly increased (figure 4.4c). However, a large decline in expression of all the genes measured was observed in cells cultured at 20 mM methyl pyruvate in combination with 5 mM glucose (LG + PYR). This could be due to an accumulation of upstream glycolytic intermediates caused by saturation of the mitochondria with exogenous pyruvate, preventing utilisation of glucose-derived pyruvate. The impact of LG + PYR culture on the expression of some metabolic genes, particularly *Aldob* (increased 12-fold – see figure 4.5a) and *Ppp1r3c* (increased 2-fold – see figure 7.10d), appears to support this hypothesis.

Culture with PYR or MMS had little effect on the expression of most of the glycolytic genes studied (figure 4.5), although *Pfkfb2* was downregulated by both PYR and MMS, and *Aldob* was upregulated by MMS. However, *Aldob* was highly upregulated by LG + PYR culture. Expression of the TCA cycle and OXPHOS genes studied was either unchanged or changed in the opposite direction to hyperglycaemia in cells cultured with PYR or LG + PYR (figure 4.6a). The same was true for *Pdk1*, *Idh2*, and *Mdh2* in cells cultured with MMS (figure 4.6b), but genes involved in the electron

transport chain (*Sdha*[8], *Ndufa4*, *Ndufs8*), were downregulated in these cells for reasons that are unclear.

Collectively, these findings argue that impairment of mitochondrial metabolism by chronic hyperglycaemia is a consequence of upstream metabolic bottlenecks and is not a cause of impaired insulin biosynthesis. As many genes are actively upregulated during chronic hyperglycaemia, downregulation of insulin biosynthesis cannot be due to insufficient ATP for transcription and translation. Rather, accumulation of upstream metabolite(s), likely glycolytic intermediates, must be responsible for the defects in both mitochondrial metabolism and insulin biosynthesis.

Figure 4.4: Effect of mitochondrial fuels on the expression of the insulin genes and β-cell identity genes

(a) Insulin secretion (ng/ml/μg protein) from INS-1 cells incubated with 5 mM glucose for 48 hrs and subsequently stimulated with 2 mM glucose (G), 20 mM G, 20 mM methyl pyruvate (PYR), or 40 mM PYR. n=1; mean of technical replicates ± SD shown.

(b) qPCR analysis of the expression of the insulin genes and selected β-cell identity genes in INS-1 cells cultured for 48 hrs at 5 or 25 mM glucose or with 20 mM methyl pyruvate (PYR) or at 5 mM glucose with 20 mM methyl pyruvate. n=3-5 (except *Pax6*, for which n=1), with 2-3 technical replicates per experiment. *$p < 0.05$, **$p < 0.01$, ***$p < 0.001$; 1-way ANOVA with Bonferroni's correction.

(c) qPCR analysis of the expression of the insulin genes and selected β-cell identity genes in INS-1 cells cultured for 48 hrs at 5 or 25 mM glucose or with 20 mM methyl

[8] Succinate dehydrogenase functions in both the TCA cycle and electron transport. The subunit encoded by *Sdha* catalyses the conversion of succinate to fumarate and transfers electrons to FAD.

succinate (MMS). n=3, with 2-3 technical replicates per experiment. *p < 0.05, **p < 0.01, ***p < 0.001; 1-way ANOVA with Bonferroni's correction.

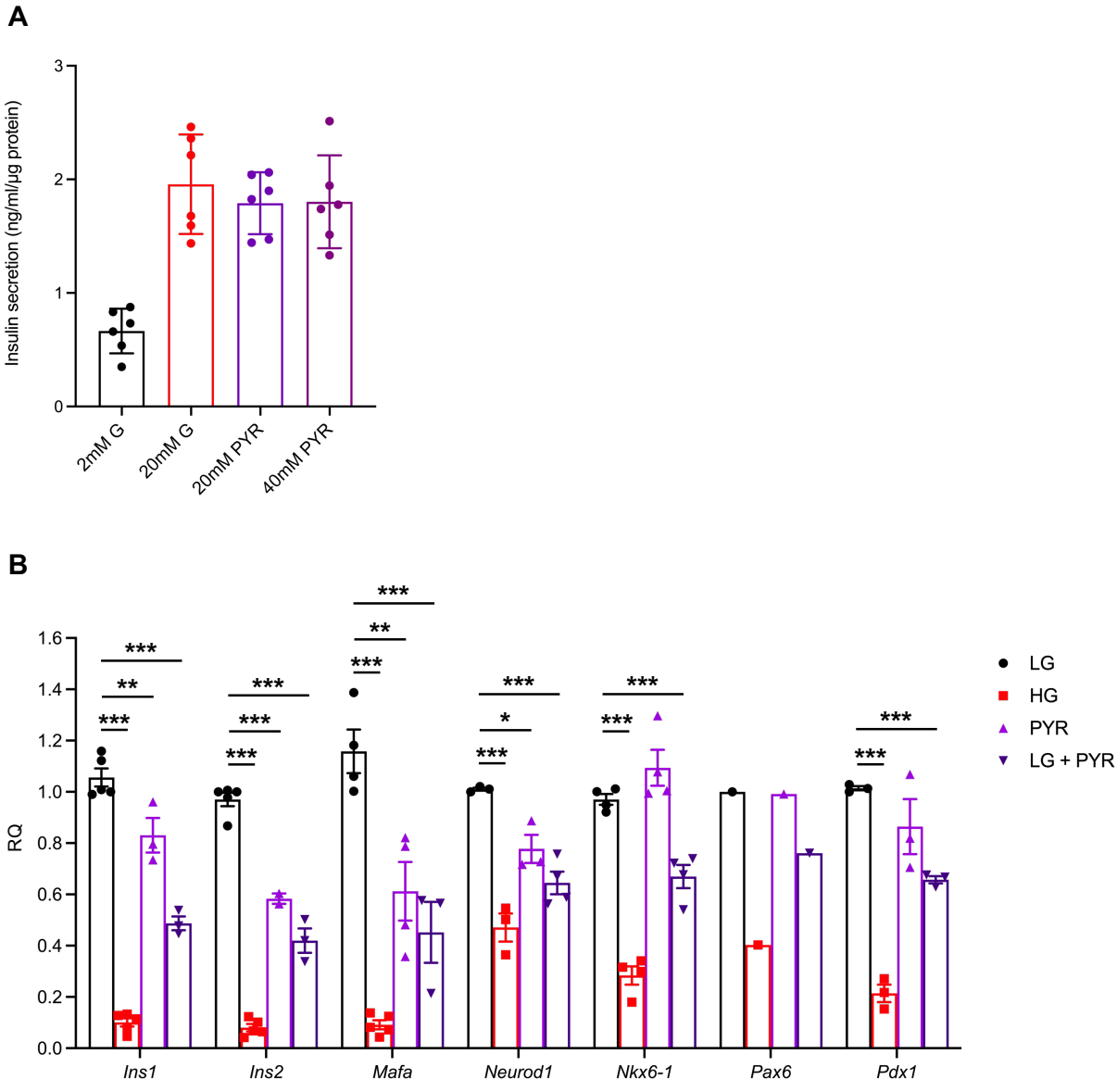

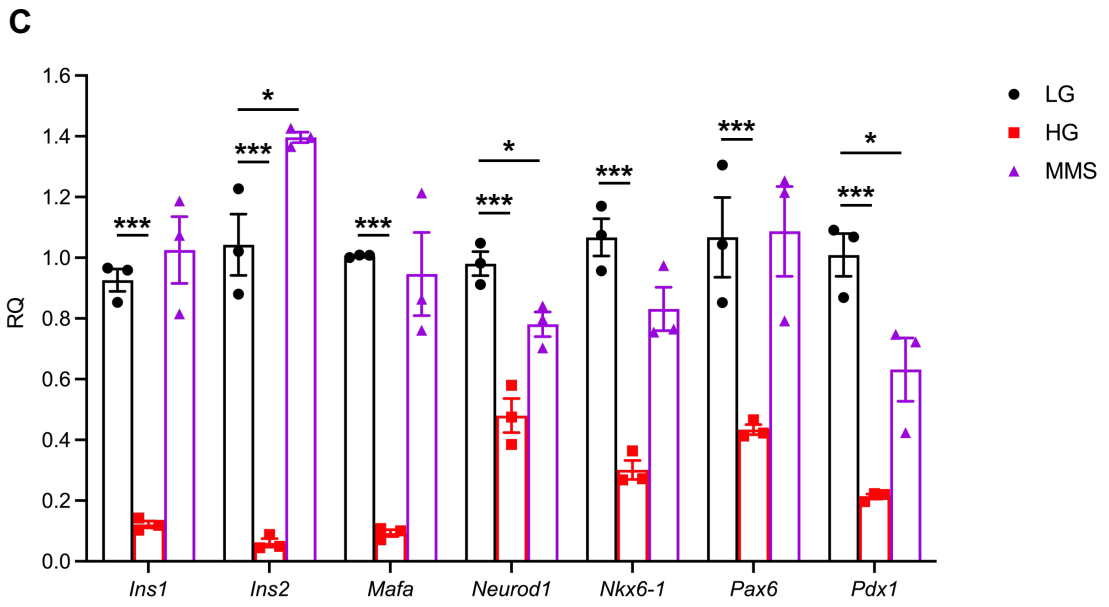

Figure 4.5: Effect of mitochondrial fuels on glycolytic gene expression

qPCR analysis of the expression of selected genes involved in glycolytic metabolism in INS-1 cells cultured for 48 hrs **(a)** at 5 or 25 mM glucose or with 20 mM methyl pyruvate or at 5 mM glucose with 20 mM methyl pyruvate and **(b)** at 5 or 25 mM glucose or with 20 mM methyl succinate. n=3-4, with 2-3 technical replicates per experiment. *p < 0.05, **p < 0.01, ***p < 0.001; 1-way ANOVA with Bonferroni's correction.

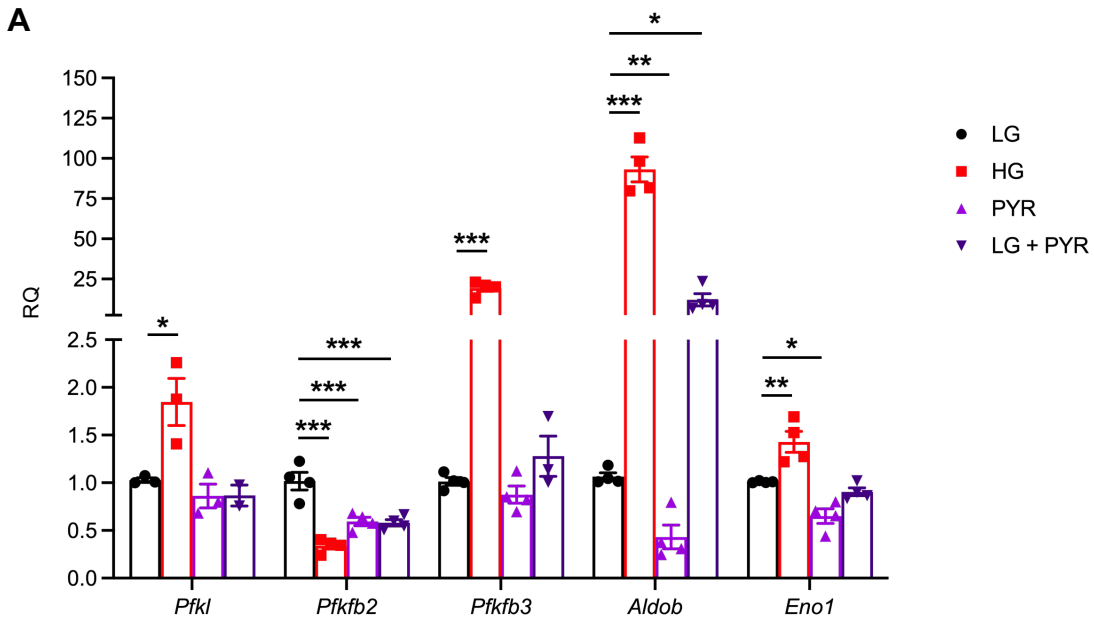

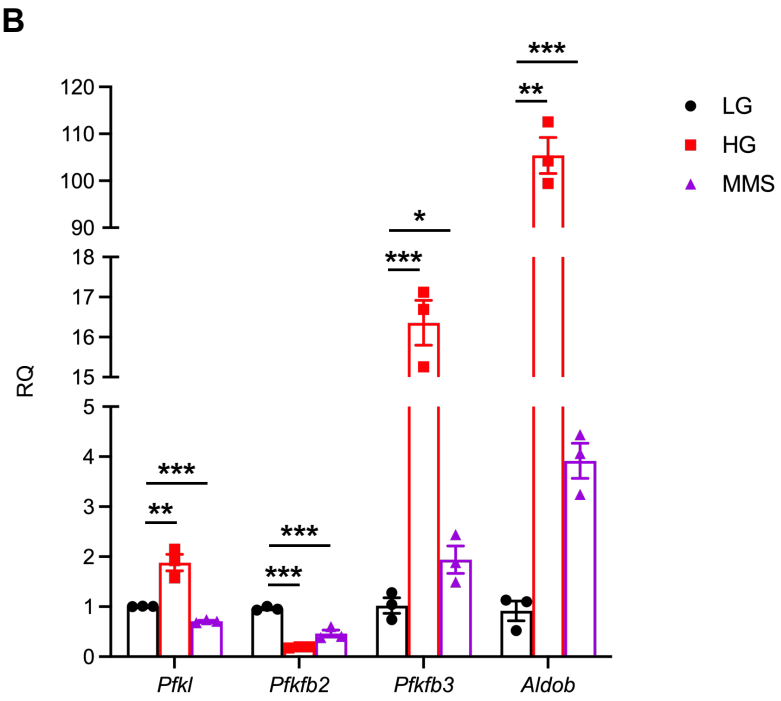

Figure 4.6: Effect of mitochondrial fuels on mitochondrial gene expression

qPCR analysis of the expression of selected genes involved in mitochondrial metabolism in INS-1 cells cultured for 48 hrs **(a)** at 5 or 25 mM glucose or with 20 mM methyl pyruvate or at 5 mM glucose with 20 mM methyl pyruvate and **(b)** at 5 or 25 mM glucose or with 20 mM methyl succinate. n=3-4, with 2-3 technical replicates per experiment. *p < 0.05, **p < 0.01, ***p < 0.001; 1-way ANOVA with Bonferroni's correction.

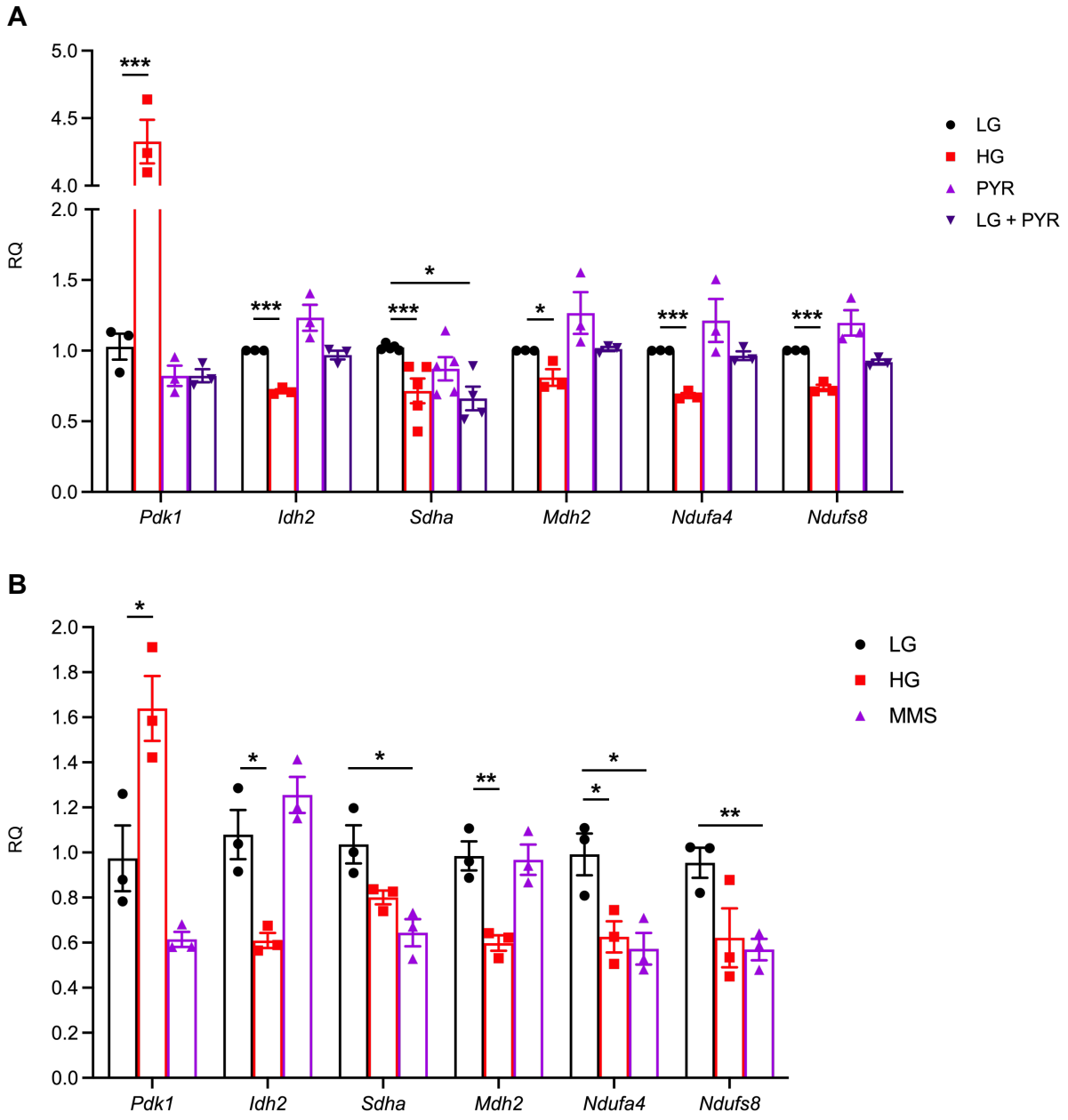

Figure 4.7: Leucine causes a partial downregulation of the insulin genes and β-cell identity genes

qPCR analysis of the expression of the insulin genes and selected β-cell identity genes in INS-1 cells cultured for 48 hrs at 5 or 25 mM glucose or with 20 mM leucine (LEU). n=3, with 2-3 technical replicates per experiment. *p < 0.05, **p < 0.01, ***p < 0.001; 1-way ANOVA with Bonferroni's correction.

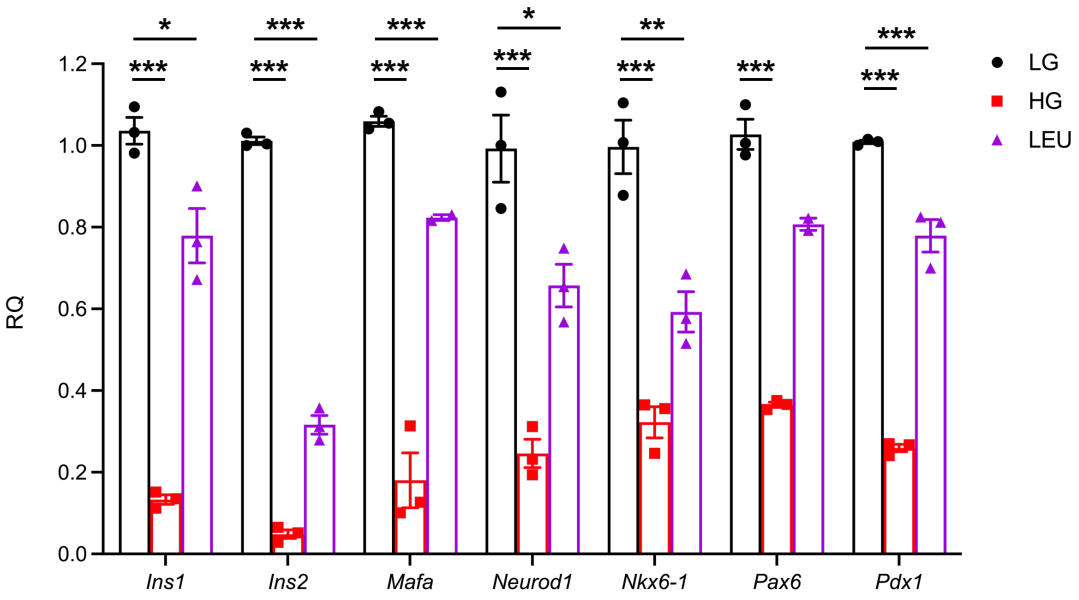

We also cultured INS-1 cells for 48 hrs with 20 mM leucine (LEU), which is catabolised in the mitochondria through a series of reactions to yield acetoacetate and acetyl-CoA. 20 mM leucine acutely stimulates insulin secretion to the same degree as 20 mM glucose (Haythorne et al., 2022). Unexpectedly, LEU caused significant downregulation of both insulin genes, especially *Ins2* (down by 70%), and all the identity genes, albeit this was less severe than in HG-cells (figure 4.7). Since the other mitochondrial fuels did not have such an effect, this is unlikely to be due to the nutrient load on the mitochondria. Instead, this effect may be due to signalling arising from high levels of leucine.

4.4.3 Inhibition of GAPDH at low glucose causes downregulation of insulin gene expression

To narrow down which glycolytic metabolite(s) might trigger inhibition of insulin gene expression, I cultured cells at 5 mM glucose with 5 μM koningic acid (KA), an irreversible inhibitor of GAPDH, in order to recapitulate the bottleneck in glycolysis

observed in hyperglycaemic β-cells. Inhibiting GAPDH in this manner caused large increases in upstream metabolites: in basal conditions (2 mM acute glucose), the DHAP/GA3P pool was increased 65-fold, F1,6BP more than 900-fold, and F6P 45-fold (Haythorne et al., 2022). I reasoned that if the key metabolites lie upstream of GAPDH, then inhibiting GAPDH would cause downregulation of insulin gene expression. This proved to be the case, with reductions of >50% and >80% in expression of *Ins1* and *Ins2*, respectively, in LG-cells treated with KA (figure 4.8). A similar ~75% decrease in insulin content also occurs in these conditions (Haythorne et al., 2022). In addition, mRNA levels of each β-cell identity gene were significantly downregulated. *Mafa* was the most severely repressed (70% decrease), but all were downregulated by at least 30%. These changes occurred in spite of increases in overall RNA content per sample[9] (the fold change in RNA yield for LG + KA relative to LG-cells was 1.33 ± 0.08 on average) and protein content, potentially resulting from stimulation of mTORC1 activity (Haythorne et al., 2022), indicating that insulin biosynthesis is actively downregulated.

Figure 4.8: Inhibition of GAPDH causes downregulation of the insulin genes and β-cell identity genes in LG-cells

qPCR analysis of the expression of the insulin genes and selected β-cell identity genes in INS-1 cells cultured for 48 hrs at 5 mM glucose ± 5 μM koningic acid (KA). n=3-6, with 2-3 technical replicates per experiment. **p < 0.01, ***p < 0.001; two-tailed unpaired Student's t-test.

[9] A sample here is the lysate from one well of a cell culture plate.

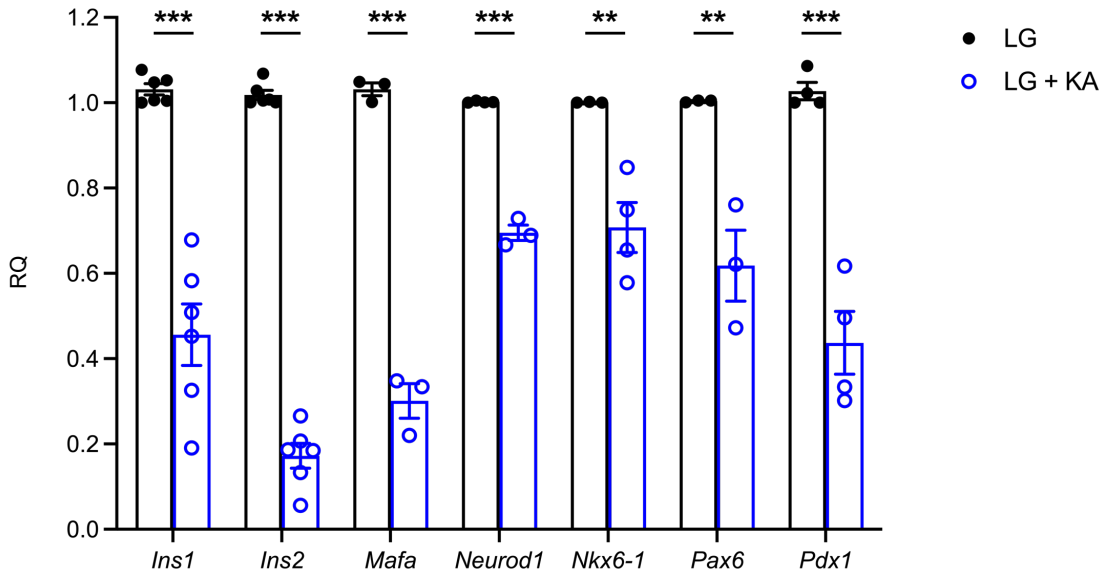

Inhibition of GAPDH also affected expression of many metabolic genes in the same way as chronic hyperglycaemia. *Pfkl*, *Pfkfb3* and *Aldob*, all of which are active in upper glycolysis, were significantly upregulated by KA in LG-cells, and all of the TCA cycle and ETC genes except *Mdh2* were downregulated (figure 4.9). However, *Eno1* and *Pdk1* were unchanged. Perhaps the latter two genes are induced by metabolites in lower glycolysis that are elevated in hyperglycaemia, such as 2-phosphoglycerate (the substrate for enolase) and pyruvate (the substrate for the target of PDK1) (Haythorne et al., 2022). The increase in expression of some glycolytic genes in the presence of KA is further evidence that reduced expression of the insulin and β-cell identity genes is not simply due to a failure to generate sufficient ATP for mRNA synthesis. A future possibility is to culture cells with KA in combination with methyl pyruvate or succinate to rule out mitochondrial starvation downstream of the glycolytic bottleneck as a cause of the changes in gene expression observed with KA. This approach would address the limitation that KA causes a more complete block in glycolysis than occurs during chronic hyperglycaemia.

Figure 4.9: Inhibition of GAPDH causes dysregulation of metabolic genes in LG-cells

qPCR analysis of the expression of selected genes involved in **(a)** glycolytic metabolism and **(b)** mitochondrial metabolism in INS-1 cells cultured for 48 hrs at 5 mM glucose ± 5 μM KA. n=3-6, with 2-3 technical replicates per experiment. **p < 0.01, ***p < 0.001; two-tailed unpaired Student's t-test.

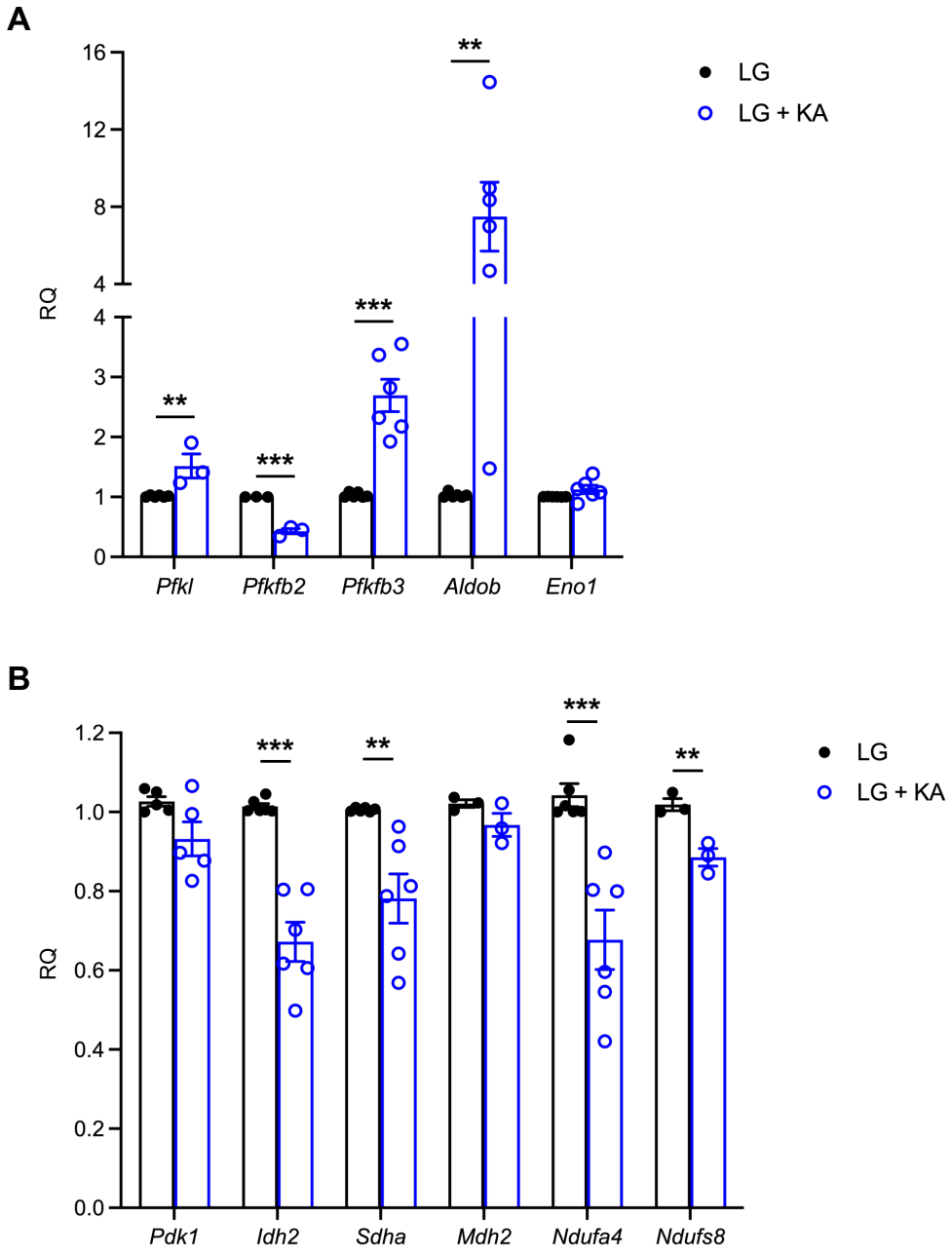

4.4.4 Effects of siRNA knockdown of the glycolytic enzymes phosphofructokinase and aldolase

Having established that the metabolites triggering the reduction in insulin gene expression lie upstream of GAPDH, I focused more closely on upper glycolysis. I considered F1,6BP and F2,6BP to be particularly attractive candidates as they are among the metabolites most dramatically increased in abundance in diabetic islets (Haythorne et al., 2022). Moreover, F2,6BP, the production of which is favoured by the isoform switch from PFKFB2 to PFKFB3 that occurs with chronic hyperglycaemia, may be a critical activator of ChREBP (Arden et al., 2012). The importance of ChREBP is discussed in chapter 5. Levels of DHAP also significantly increase in diabetes (Haythorne et al., 2022). Both F1,6BP and DHAP lie between phosphofructokinase and GAPDH, while F2,6BP is generated from F6P (figure 4.1).

To differentiate between F1,6BP (and DHAP + GA3P) and F2,6BP (and G6P + F6P), I knocked down PFK and aldolase in INS-1 cells using a cocktail of siRNAs targeting both of the isoforms of each gene that are most highly expressed in β-cells (*Pfkl* + *Pfkm* and *Aldoa* + *Aldob*, respectively)[10]. I was particularly keen to achieve robust knockdowns of Pfkl and AldoB, as these genes are upregulated in HG-cells, whereas Pfkm and Aldoa are downregulated in HG-cells.

Table 4.3: Efficiencies of PFK and aldolase knockdowns (% decrease in mRNA expression relative to control) with 50 nM and 100 nM siRNA

[10] PFKP and ALDOC are much less abundant at the protein level than the other isoforms of phosphofructokinase and aldolase.

		Gene							
		Pfkl		***Pfkm***		***Aldoa***		***Aldob***	
siRNA concentration (nM)		**50**	**100**	**50**	**100**	**50**	**100**	**50**	**100**
Glucose culture (mM)	**5**	81	80	83	83	83	77	91	76
	25	85	86	84	86	72	71	80	81

Figure 4.10: Effects of phosphofructokinase knockdown on expression of the insulin genes and β-cell identity genes

qPCR analysis of the expression of **(a)** *Pfkl* and *Pfkm* and **(b)** the insulin genes and selected β-cell identity genes in INS-1 cells cultured for 48 hrs at 5 or 25 mM glucose following siRNA knockdown of phosphofructokinase isoforms L and M. Cells were transfected with either 100 nM non-targeting control siRNA (siNT) or 50 nM siPFKL + 50 nM siPFKM. n=3, with 2-3 technical replicates per experiment. **p < 0.01, ***p < 0.001; 1-way ANOVA with Bonferroni's correction.

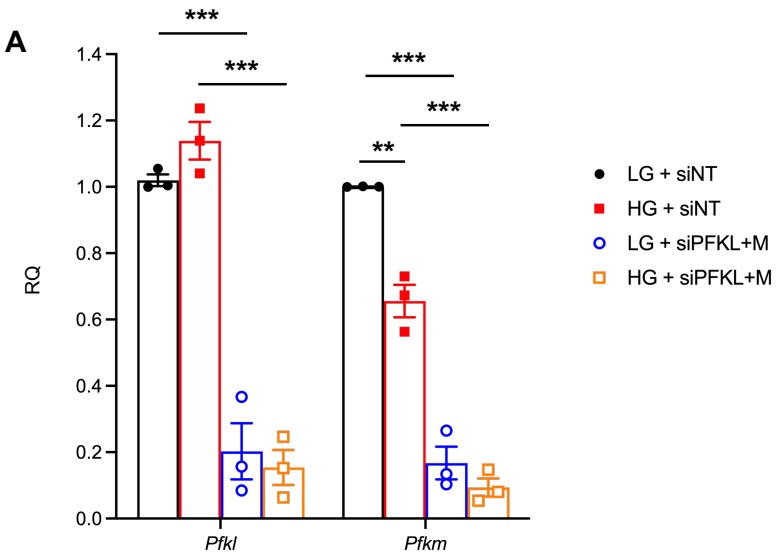

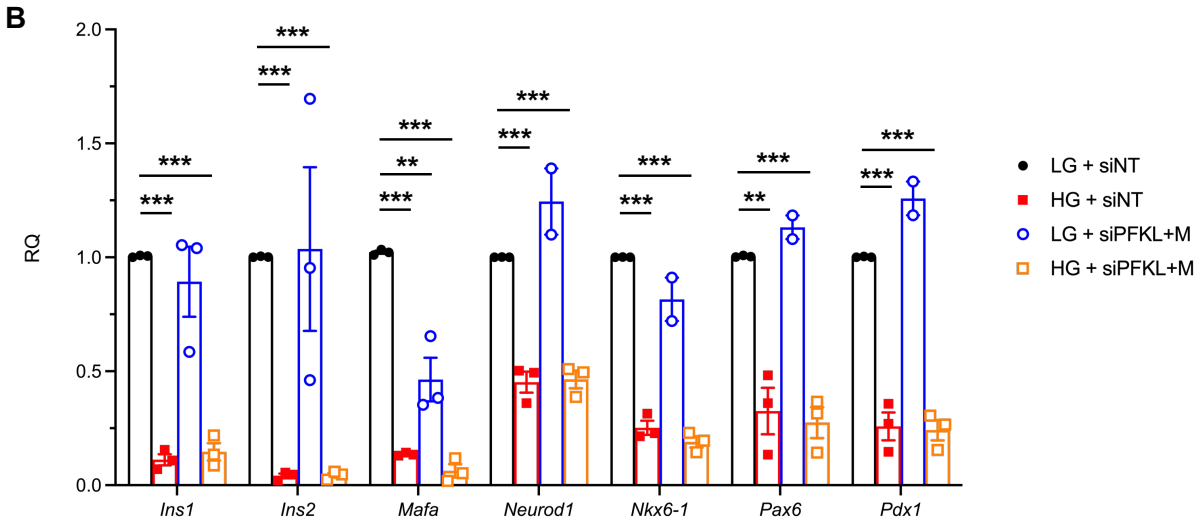

Knockdown efficiency was similar for *Pfkl* and *Pfkm*, being 80-85% (i.e. mRNA levels were reduced to 15-20% of the level in control cells transfected with non-targeting siRNA) in both LG-cells and HG-cells (figure 4.10a), and did not vary substantially between 50 nM (25 nM siPFKL + 25 nM siPFKM) and 100 nM siRNA (table 4.3). Unfortunately, expression of the insulin genes in LG-cells in which PFK was knocked down was very variable between experiments, so it is unclear whether the knockdown had an effect (figure 4.10b). The β-cell identity genes, meanwhile, present a mixed picture. Strikingly, PFK knockdown led to a ~50% decrease in *Mafa* expression in LG-cells, yet there was no significant change in the expression of the other four genes. Some of these, particularly *Pdx1*, even show a tendency towards upregulation following PFK knockdown, which could account for a lack of change in insulin mRNA levels in spite of *Mafa* being downregulated. This may indicate that *Mafa* is regulated differently from the other transcription factors or is particularly sensitive to accumulation of metabolites upstream of PFK. Knocking down PFK had no effect on expression of the insulin genes or β-cell identity genes in HG-cells, perhaps because PFK activity was already low. It is interesting to note that PFKM contributes most of

the catalytic activity of PFK, which can exist as a homo- or heterotetramer (Yaney et al., 1995), implying that the concomitant downregulation of PFKM and upregulation of PFKL in chronic hyperglycaemia leads to a fall in overall PFK activity.

Table 4.4: mRNA and protein expression of aldolase isoforms in control and diabetic βV59M islets

Data taken from RNAseq and proteomics experiments described by Haythorne et al. (2019): transcriptomics data are available in the European Nucleotide Archive (https://www.ebi.ac.uk/ena) under the accession number ERP114395 and mass spectrometric proteomics data are deposited to the ProteomeXchange Consortium via the PRIDE partner repository with the data set identifier PXD012979 and 10.6019/PXD012979.

	Transcripts per million		**Normalised protein abundance**	
	Control	Diabetic	Control	Diabetic
Aldolase A	301	221	5,087,497	9,863,928
Aldolase B	1.83	671	122,046	7,876,452
Aldolase C	7.80	18.1	26,682	94,387

Figure 4.11: Effects of aldolase knockdown on expression of the insulin genes and β-cell identity genes

qPCR analysis of the expression of **(a)** *Aldoa* and *Aldob* and **(b)** the insulin genes and selected β-cell identity genes in INS-1 cells cultured for 48 hrs at 5 or 25 mM glucose following siRNA knockdown of aldolase isoforms A and B. Cells were transfected with either 50 nM non-targeting control siRNA (siNT) or 25 nM siALDOA + 25 nM siALDOB. n=1; individual values with error bars showing mean of technical replicates ± SD.

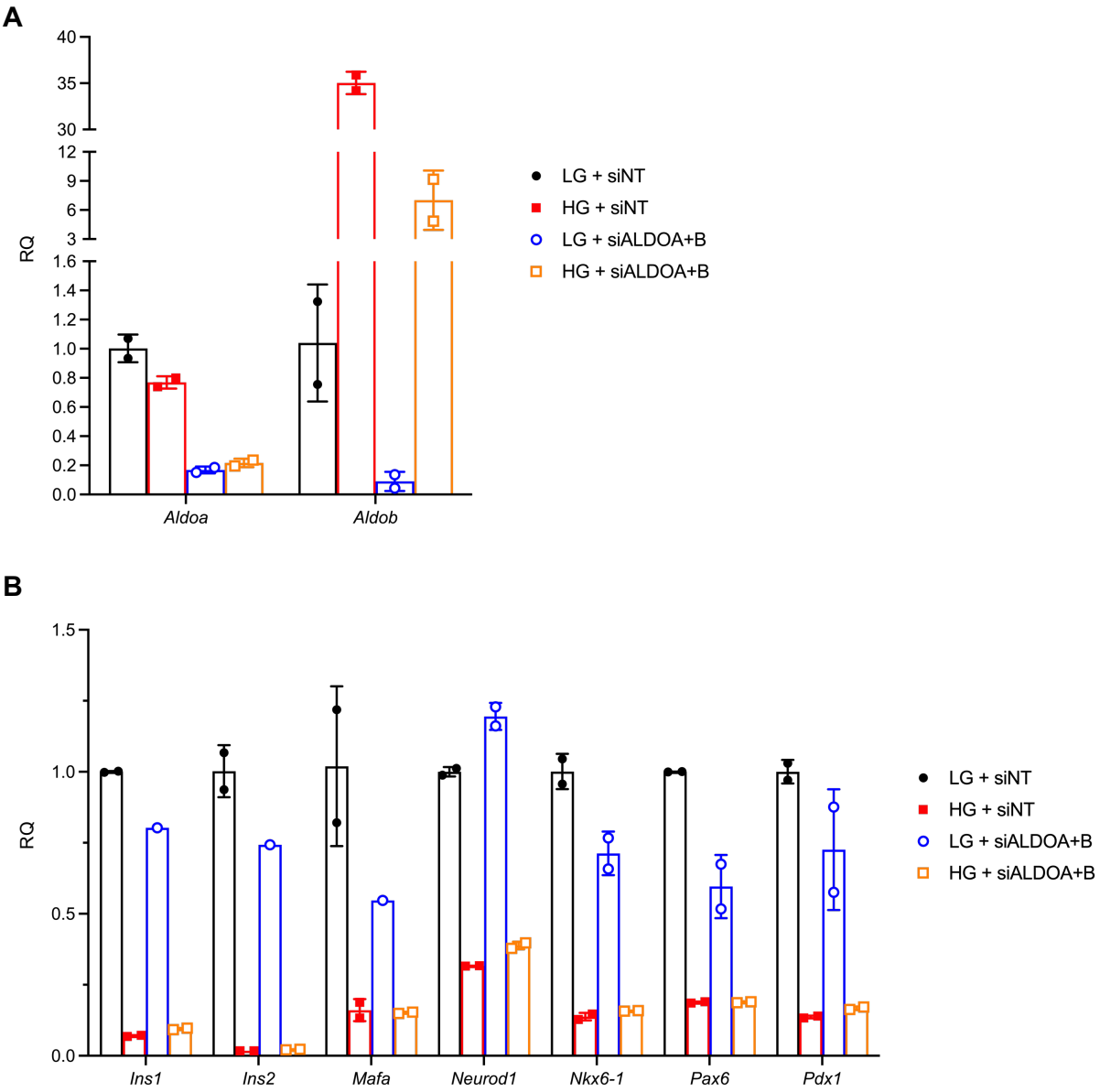

In figure 4.11, preliminary results are presented for the aldolase knockdowns. KD efficiencies were generally slightly greater with 50 nM than with 100 nM siRNA (table 4.3). Aldolase knockdown did not affect expression of the insulin genes or β-cell identity genes in HG-cells (figure 4.11b). However, in LG-cells, expression of *Ins1* was reduced by 20%, *Ins2* by 25%, *Mafa* by 45%, *Pax6* by 40%, and *Nkx6-1* and *Pdx1* by ~30%. These changes can be attributed to reduced expression of ALDOA, since this is the dominant isoenzyme and ALDOB expression is very low in LG-cells (table 4.4). Even though KD efficiencies are similar in LG-cells and HG-cells, total aldolase

expression after transfection is much higher in HG-cells due to the dramatic upregulation of ALDOB, so it is perhaps unsurprising to see no effect of knockdown in HG-cells. *Aldob* expression in HG-cells appears to stabilise by 48 hours after the onset of hyperglycaemia at a level somewhat lower than its initial peak (figure 4.12). If replicated, these results could suggest that accumulation of metabolites immediately upstream of aldolase (as well as metabolites upstream of PFK) may contribute to hyperglycaemia-induced downregulation of insulin gene expression. Of these, F1,6BP and F2,6BP are likely to be particularly critical as they are so greatly increased in abundance.

Figure 4.12: Time course of *Aldob* expression up to 72 hrs following the onset or reversal of hyperglycaemia

qPCR analysis of the expression of *Aldob* in INS-1 cells at time points of 1, 3, 6, 12, 24, 48 and 72 hrs following onset or reversal of hyperglycaemia. Cells were pre-cultured at 5 or 25 mM glucose for 48 hrs before being transferred to the opposite condition (25 or 5 mM to simulate onset or reversal, respectively) at the time point 0. n=2 up to 24 hrs and n=1 at 48 and 72 hrs, with 3 technical replicates per experiment.

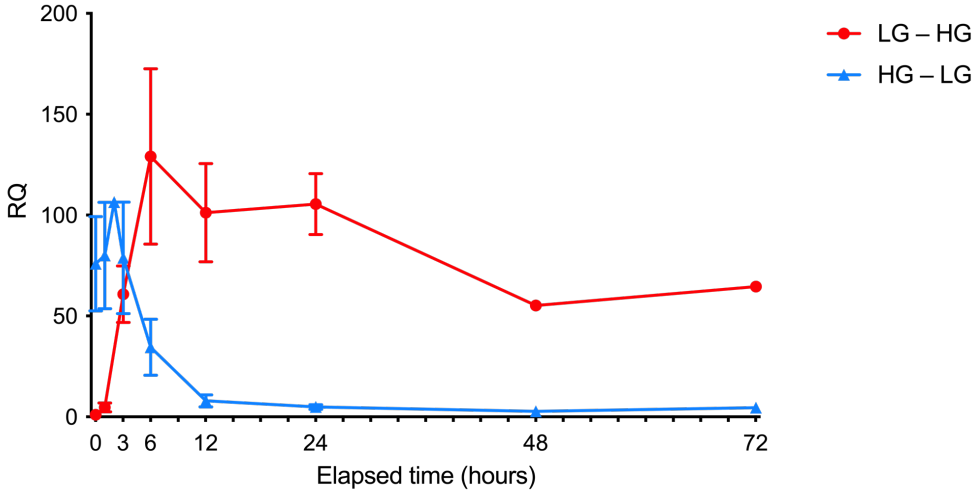

4.4.5 The non-metabolisable glucose analogue 2-deoxyglucose causes a loss of insulin biosynthesis

I next considered whether accumulation of G6P plays a role in the loss of insulin. G6P is thought to be essential for the activation of ChREBP (Dentin et al., 2012; Li et al., 2010). Elevation of G6P could thus lead to ChREBP-mediated induction of *Txnip*, and thereby downregulate insulin gene transcription (Shalev, 2014). To determine whether this is the case, I cultured INS-1 cells with 25 mM 2-deoxy-D-glucose (2-DG) for 24 hours. This glucose analogue is phosphorylated by glucokinase, producing 2-deoxyglucose-6-phosphate, but 2-DG-6-P cannot undergo further glycolysis and therefore accumulates, mimicking a build-up of G6P. A 24-hour culture was necessary as there was excessive toxicity and cell death after a 48-hour culture. However, as figure 3.2 shows, insulin mRNA levels fall by ~80% within the first 24 hours of hyperglycaemia, so this was a reasonable length of incubation for investigating changes in insulin gene expression. Total RNA and protein yields per well fell by 29% and 27%, respectively, after 24 hrs culture with 25 mM 2-DG (table 4.5), which I judged to be acceptable.

Table 4.5: Total RNA and protein yields per well for cells cultured for 24 hrs with 25 mM glucose (HG) or 25 mM 2-deoxyglucose (2-DG), normalised to LG-cells
[RNA] was determined by NanoDrop and [protein] was determined by BCA assay.

	RNA yield vs LG		**Protein yield vs LG**	
	Mean	S.E.M.	Mean	S.E.M.
LG	1		1	
HG	1.35	0.100	1.14	0.040
2-DG	0.71	0.005	0.63	0.031

Figure 4.13: 2-deoxyglucose causes loss of insulin content and downregulation of the insulin genes and β-cell identity genes comparable to hyperglycaemia

(a) Total insulin content (ng/μg protein) of INS-1 cells incubated with 5 or 25 mM glucose or with 25 mM 2-deoxyglucose (2-DG) for 24 hrs. n=3, with 3-4 technical replicates per experiment. *p < 0.05, **p < 0.01; 1-way ANOVA with Bonferroni's correction.

(b) qPCR analysis of the expression of the insulin genes and selected β-cell identity genes in INS-1 cells incubated with 5 or 25 mM glucose or with 25 mM 2-DG for 24 hrs. n=4-6, with 2-3 technical replicates per experiment. ***p < 0.001; 1-way ANOVA with Bonferroni's correction.

(c) Data in (b) with additional data from cells incubated with 5 mM glucose + 20 mM 2-DG or with 0 mM glucose for 24 hrs (n=2). ***p < 0.001; 1-way ANOVA with Bonferroni's correction.

(d) Whole-cell ATP/ADP ratio in INS-1 cells incubated with 0, 5, or 25 mM glucose or with 25 mM 2-DG for 24 hrs and subsequently stimulated with 2 or 20 mM glucose for 30 mins. n=1; mean of technical replicates ± SD shown.

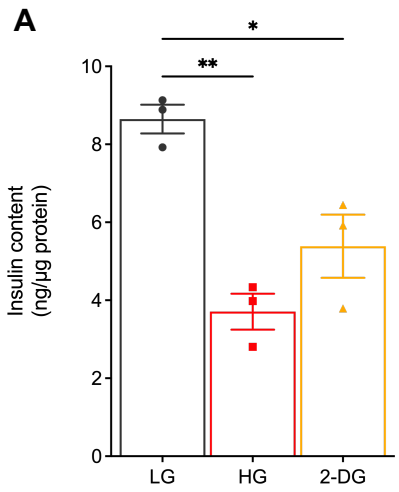

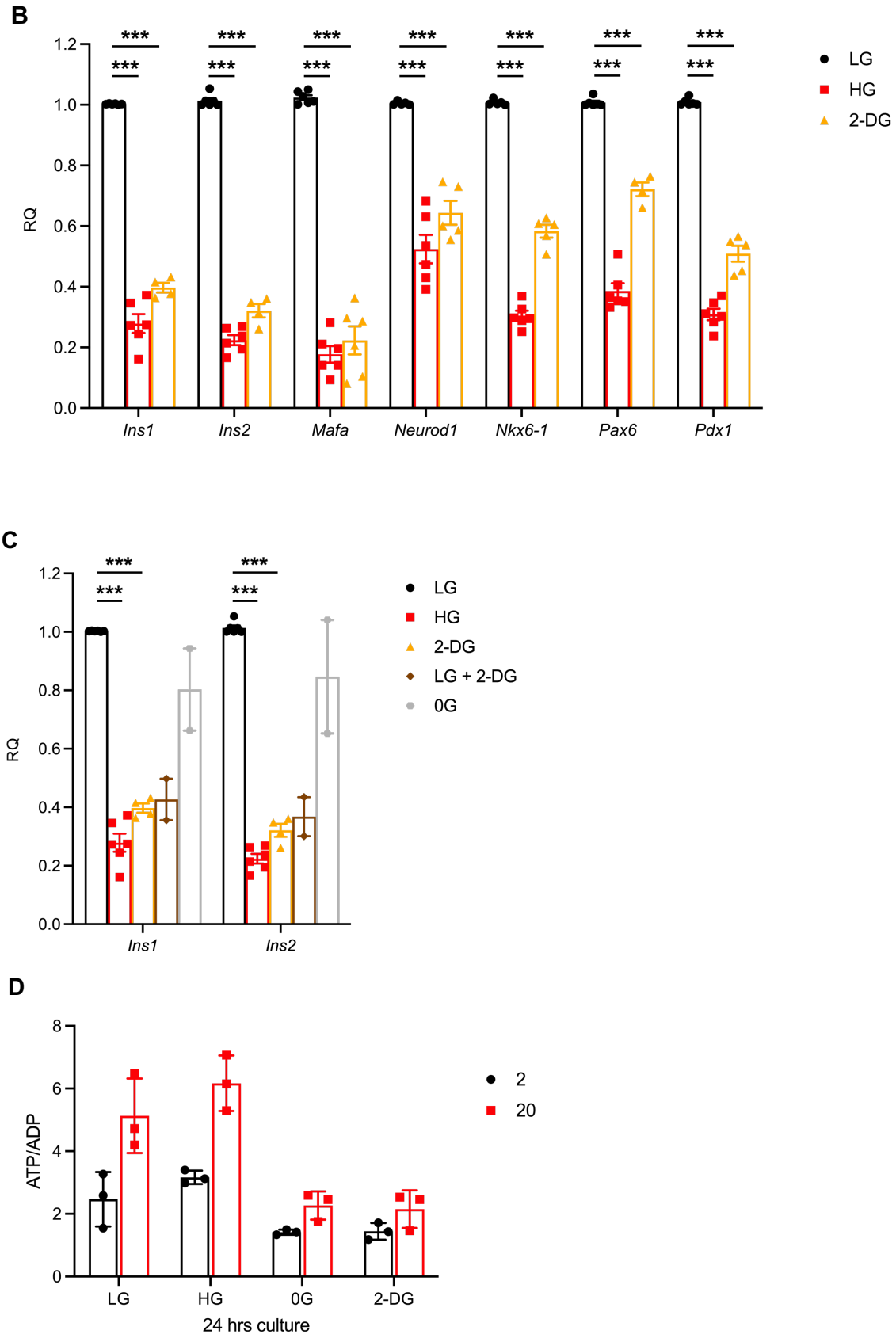
B
RQ
1.2
1.0
0.8
0.6
0.4
0.2
0.0
***
Ins1
Ins2
Mafa
Neurod1
Nkx6-1
Pax6
Pdx1
LG
HG
2-DG
C
RQ
LG
HG
2-DG
LG + 2-DG
0G
Ins1
Ins2
D
ATP/ADP
8
6
4
2
0
LG
HG
0G
2-DG
24 hrs culture
2
20

The insulin content of cells incubated with 2-DG fell by ~40% (figure 4.13a), while expression of *Ins1* was reduced by ~60% and expression of *Ins2* by ~70% (figure 4.13b). These declines were comparable to those observed in HG-cells cultured on the same plate. All 5 β-cell identity genes analysed were also significantly downregulated by 2-DG culture, accounting for the loss of insulin mRNA. These changes were not simply an effect of starvation: insulin gene expression was only modestly reduced at 0 mM glucose relative to 5 mM glucose after 48 hrs (figure 3.3), and was not significantly reduced at 0 mM glucose after 24 hrs (figure 4.13c). Moreover, the insulin genes were equally downregulated in cells cultured at 5 mM glucose + 20 mM 2-DG compared to cells cultured with 25 mM 2-DG alone (figure 4.13c). Admittedly, competition between glucose and the more abundant 2-DG for phosphorylation by glucokinase will limit the cell's ability to utilise glucose in these conditions, but accumulation of 2-DG-6-P does not block glucose metabolism altogether. Cells pre-cultured for 24 hrs with 25 mM 2-DG have a low basal ATP/ADP ratio (after 30 mins at 2 mM glucose) but appear able to increase this ratio approximately 1.5-fold when stimulated with 20 mM glucose (figure 4.13d). Basal and stimulated ATP/ADP ratios in cells cultured at 0 mM glucose or with 25 mM 2-DG are the same (figure 4.13d), suggesting that metabolism is sustained by the pyruvate and L-glutamine present in the culture medium in either case. Any pre-existing glycogen stores would be quickly run down. Multiple lines of evidence thus indicate that the changes in gene expression observed in cells incubated with 2-DG are driven by 2-DG-6-P accumulation.

2-DG caused similar changes in the expression of most metabolic genes to those seen in HG-cells (figure 4.14). Oddly, though, *Pfkl* was unchanged with 2-DG culture, while *Eno1* was downregulated. In summary, these results indicate that an increased pool

of G6P plays a critical role in mediating the hyperglycaemia-induced declines in insulin gene expression and insulin content.

Figure 4.14: 2-deoxyglucose partially mimics the effects of hyperglycaemia on the expression of metabolic genes

qPCR analysis of the expression of selected genes involved in **(a)** glycolytic metabolism and **(b)** mitochondrial metabolism in INS-1 cells incubated with 5 or 25 mM glucose or with 25 mM 2-deoxyglucose for 24 hrs. n=3-6, with 2-3 technical replicates per experiment. *p < 0.05, **p < 0.01, ***p < 0.001; 1-way ANOVA with Bonferroni's correction.

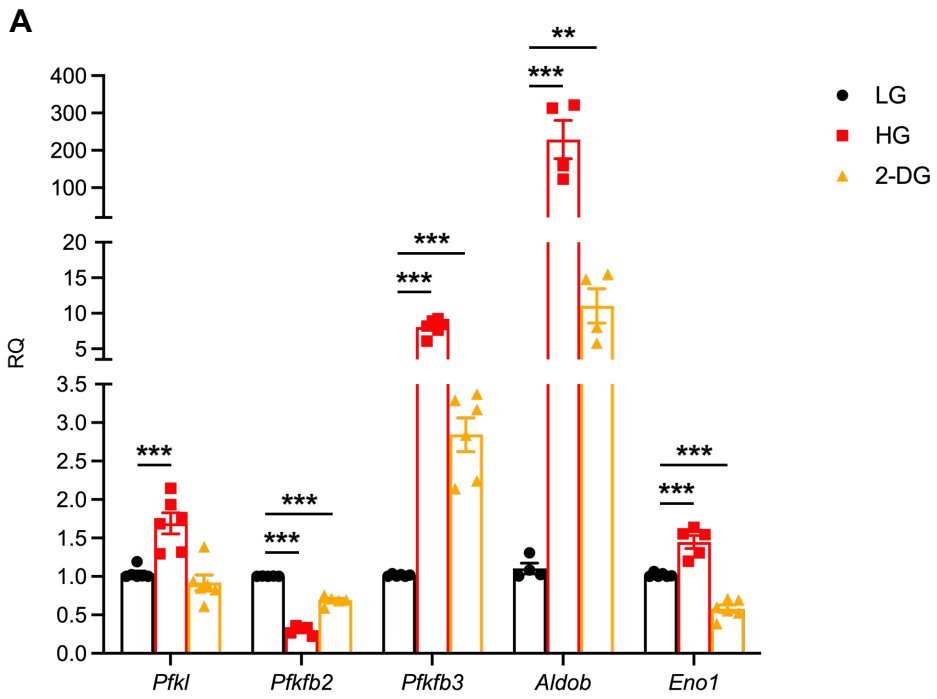

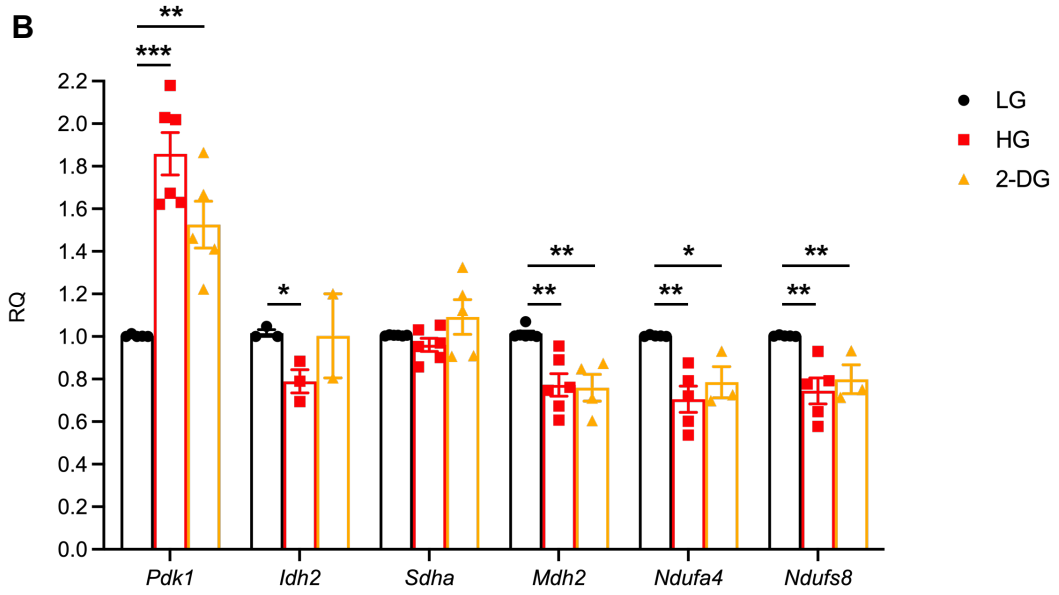

4.4.6 Pentose phosphate pathway inhibition reduces insulin biosynthesis at low glucose but has no effect at high glucose

Flux through the pentose phosphate pathway (PPP) rapidly increases upon acute stimulation of β-cells by glucose, causing elevation of the NADPH/$NADP^+$ ratio (Spégel et al., 2013). Metabolomics analysis showed large increases in PPP intermediates including 6-phosphogluconate and sedoheptulose 7-phosphate in diabetic islets (but not control islets) stimulated with 20 mM glucose (Haythorne et al., 2022). In addition, some genes encoding PPP enzymes were upregulated in diabetic islets (Haythorne et al., 2019). However, ribulose 5-phosphate, the product of 6-phosphogluconate dehydrogenase (6-PGD), was downregulated in diabetes, which could indicate that 6-PGD is affected by a shortage of $NADP^+$ much as GAPDH is throttled by a lack of NAD^+. To investigate whether chronic activation of the PPP by high glucose is involved in the impairment of insulin biosynthesis, I used 6-aminonicotinamide (6-AN) to inhibit 6-PGD, the enzyme that catalyses the third

reaction of the pathway (see figure 4.1). 6-AN will block the pathway but only partially prevent NADPH synthesis, which likely explains why it does not acutely inhibit GSIS whereas glucose-6-phosphate dehydrogenase (G6PD) inhibition does (Spégel et al., 2013). I used 100 μM 6-AN, a concentration which has previously been used to investigate the PPP in INS-1 cells and shown to induce accumulation of PPP metabolites when applied chronically (Goehring et al., 2011; Spégel et al., 2013).

To confirm inhibition of 6-PGD, I performed an enzymatic activity assay. 6-PGD was inhibited in HG-cells by both concentrations of 6-AN tested (figure 4.15a), with 100 μM appearing slightly more effective than 200 μM 6-AN (59% versus 47% inhibition, respectively). I therefore used 100 μM 6-AN for all further experiments. 6-PGD inhibition by 6-AN appeared to cause a small increase in the NADPH/$NADP^+$ ratio in LG-cells but had no clear effect in HG-cells, in which the ratio was already raised 1.6-fold relative to LG-cells (figure 4.15b). The elevated ratios of both NADPH/$NADP^+$ and NADH/NAD^+ in hyperglycaemic β-cells are indicative of an altered redox state (Haythorne et al., 2019).

The insulin genes and β-cell identity genes displayed significantly lower expression in LG-cells cultured with 6-AN relative to control cells: *Ins1* was reduced by ~65%, *Ins2* by ~80%, and the identity genes by 30-60% (figure 4.15d). Insulin content appears to be reduced too (figure 4.15c), although the difference is not quite significant ($p = 0.08$). In HG-cells, 6-AN had no effect on insulin gene expression or content. This could mean either that PPP intermediates are not involved in the impairment of insulin biosynthesis by chronic hyperglycaemia or that they are maximally elevated at 25 mM glucose such that PPP inhibition by 6-AN cannot exacerbate their effect. Results with

LG + 6-AN clearly show that maintaining normal flux through the pathway is important, though it is unclear whether it is accumulation of PPP intermediates or G6P that underlies the reduction in insulin biosynthesis in those cells.

Figure 4.15: Inhibition of the pentose phosphate pathway causes loss of insulin content and downregulation of the insulin genes and β-cell identity genes in LG- cells

(a) 6-PGD enzymatic activity (mU/ml) in cell lysates from INS-1 cells incubated with 5 or 25 mM glucose ± 100 μM or 200 μM 6-aminonicotinamide (6-AN) for 48 hrs. Control samples were treated with an equivalent volume of DMSO (veh). n=3, with 2-3 technical replicates per experiment. *p < 0.05, **p < 0.01; 1-way ANOVA with Bonferroni's correction.

(b) $NADPH/NADP^+$ ratio in cell lysates from INS-1 cells incubated with 5 or 25 mM glucose ± 100 μM or 200 μM 6-AN for 48 hrs. Control samples were treated with an equivalent volume of DMSO (veh). n=2, with 2-3 technical replicates per experiment.

(c) Total insulin content (ng/μg protein) of INS-1 cells incubated with 5 or 25 mM glucose ± 100 μM 6-AN for 48 hrs. Control samples were treated with an equivalent volume of DMSO (veh). n=3, with 4 technical replicates per experiment. LG + veh and LG + 6-AN compared by two-tailed unpaired Student's t-test.

(d) qPCR analysis of the expression of the insulin genes and selected β-cell identity genes in INS-1 cells incubated with 5 or 25 mM glucose ± 100 μM 6-AN for 48 hrs. Control samples were treated with an equivalent volume of DMSO (veh). n=3-4, with 2-3 technical replicates per experiment. **p < 0.01, ***p < 0.001; 1-way ANOVA with Bonferroni's correction.

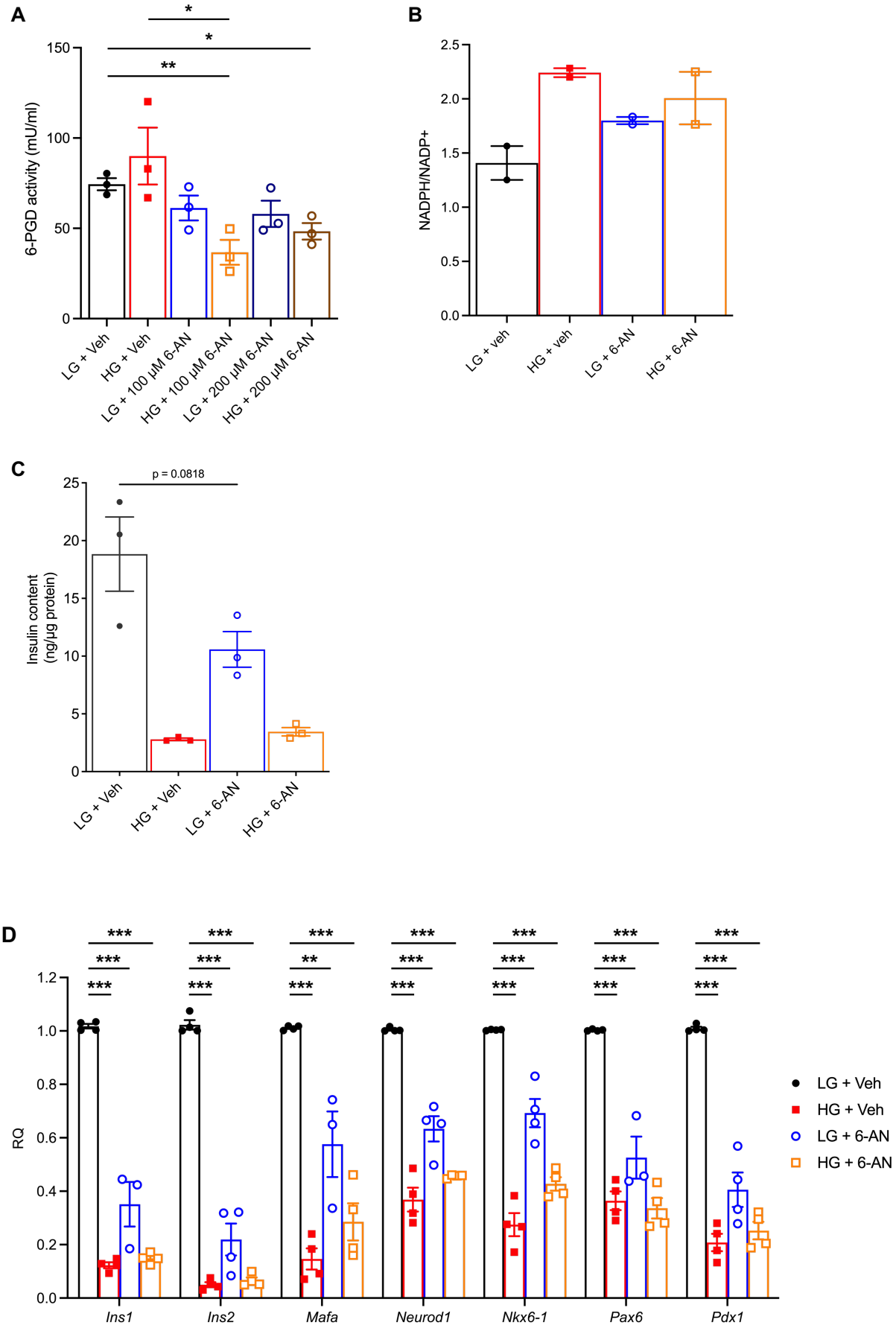
A
6-PGD activity (mU/ml)
150
100
50
0
*
*
**
LG + Veh
HG + Veh
LG + 100 µM 6-AN
HG + 100 µM 6-AN
LG + 200 µM 6-AN
HG + 200 µM 6-AN
B
NADPH/NADP+
2.5
2.0
1.5
1.0
0.5
0.0
LG + veh
HG + veh
LG + 6-AN
HG + 6-AN
C
Insulin content (ng/µg protein)
25
20
15
10
5
0
p = 0.0818
LG + Veh
HG + Veh
LG + 6-AN
HG + 6-AN
D
RQ
1.2
1.0
0.8
0.6
0.4
0.2
0.0
***
**
Ins1
Ins2
Mafa
Neurod1
Nkx6-1
Pax6
Pdx1
LG + Veh
HG + Veh
LG + 6-AN
HG + 6-AN

The impact of PPP inhibition on the expression of metabolic genes was less consistent (figure 4.16). None of the glycolytic genes were altered by 6-AN treatment in HG-cells. However, in LG-cells, 6-AN induced changes in the glycolytic regulators *Pfkfb2* and *Pfkfb3* similar to those induced by hyperglycaemia, whereas *Pfkl* and *Eno1* were downregulated by 6-AN (the opposite effect to high glucose). The effect of 6-AN on *Pfkl* and *Eno1* is similar to that of 2-DG, suggesting that G6P may be responsible. Meanwhile, three genes encoding mitochondrial proteins were restored to baseline (*Idh2* and *Ndufa4*) or even increased above control levels (*Sdha*) in HG-cells cultured with 6-AN. However, 6-AN did not significantly perturb expression of any of the mitochondrial genes tested in LG-cells.

In summary, although it is not obvious how to attribute the effects of 6-AN, it is possible that a combined effect of G6P accumulation and accumulation of PPP intermediates underlies the loss of insulin biosynthesis in chronic hyperglycaemia.

Figure 4.16: Effects of pentose phosphate pathway inhibition on the expression of metabolic genes

qPCR analysis of the expression of selected genes involved in **(a)** glycolytic metabolism and **(b)** mitochondrial metabolism in INS-1 cells incubated with 5 or 25 mM glucose ± 100 μM 6-aminonicotinamide (6-AN) for 48 hrs. Control samples were treated with an equivalent volume of DMSO. n=3-4, with 2-3 technical replicates per experiment. *p < 0.05, **p < 0.01, ***p < 0.001; 1-way ANOVA with Bonferroni's correction.

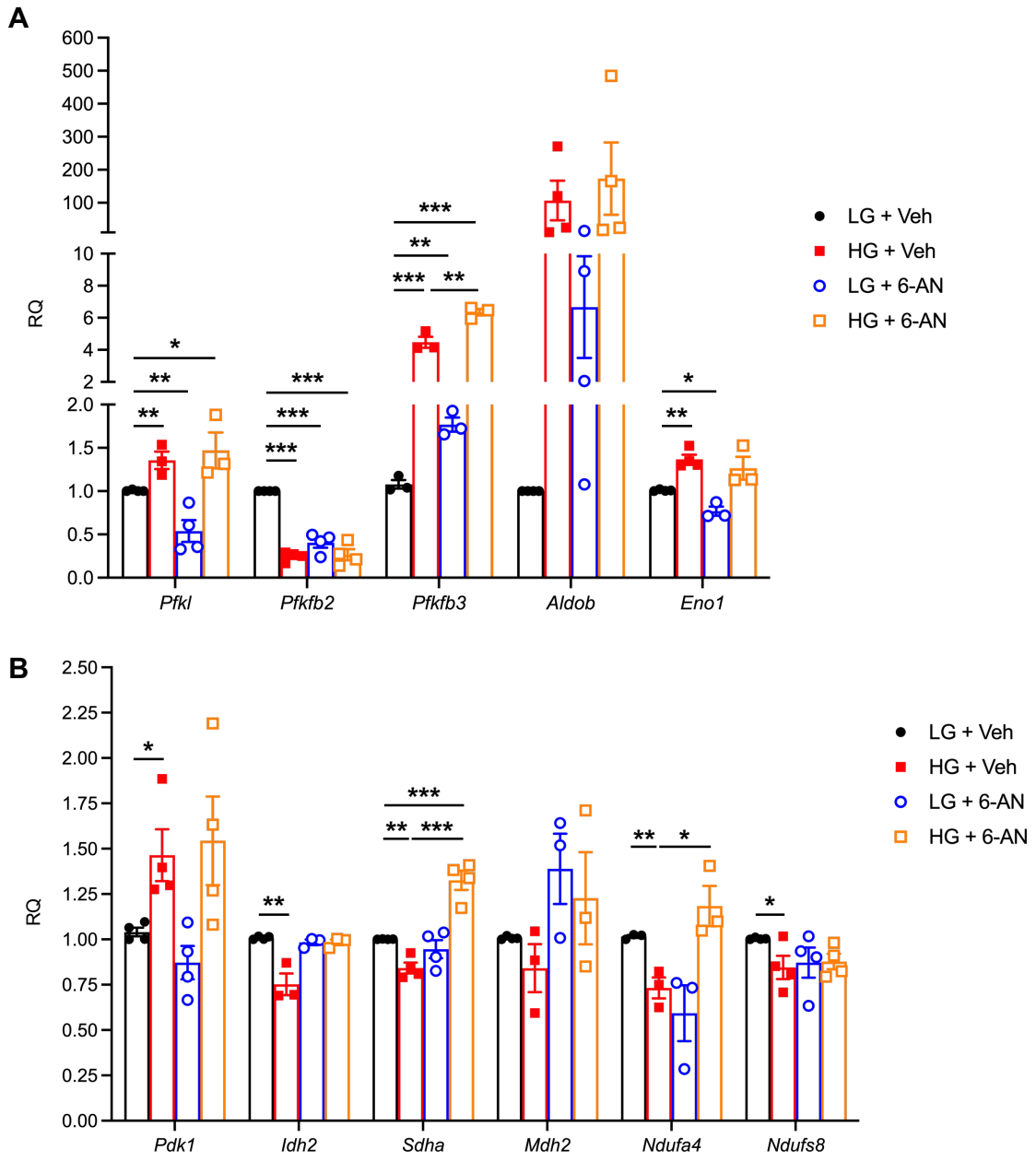

4.4.7 Polyol pathway inhibition reduces insulin biosynthesis at low glucose but has no effect at high glucose

Fructose production is increased in diabetic β-cells, as evidenced by increased ^{13}C label incorporation from glucose and increased total abundance of fructose (Haythorne et al., 2019, 2022), indicating that flux through the polyol pathway is

increased. Furthermore, the polyol pathway is one of the pathways that could deplete NAD^+ (since NAD^+ is a cofactor for sorbitol dehydrogenase), contributing to the bottleneck at GAPDH. To investigate whether chronic activation of the polyol pathway by high glucose is involved in the impairment of insulin biosynthesis, I inhibited aldose reductase using the small molecules EBPC and tolrestat, both at a working concentration of 100 μM. It is preferable to inhibit aldose reductase, blocking glucose entry into the pathway, rather than inhibiting sorbitol dehydrogenase, as excess sorbitol causes osmotic stress[11].

Aldose reductase inhibition did not affect expression of the insulin genes or β-cell identity genes in HG-cells but caused partial downregulation of most of these genes in LG-cells, with EBPC having a greater impact on insulin gene expression than tolrestat (figure 4.17). *Ins1* was down ~20% with EBPC and ~10% with tolrestat; *Ins2* was down by ~30% with EBPC and ~10% with tolrestat. This appears to be driven largely by downregulation of *Mafa* and *Nkx6-1*, which declined by ~40% and ~30% respectively with EBPC and ~30% and ~40% respectively with tolrestat. *Neurod1* and *Pax6* were the only genes that did not decrease with both inhibitors. These results are intriguing as aldose reductase has an extremely high Km for glucose (Hamada et al., 1991), meaning that its activity is very low at low glucose concentrations.

Figure 4.17: Inhibition of the polyol pathway causes partial downregulation of the insulin genes and β-cell identity genes in LG-cells

qPCR analysis of the expression of the insulin genes and selected β-cell identity genes in INS-1 cells incubated with **(a)** 5 or 25 mM glucose ± 100 μM EBPC for 48 hrs or **(b)**

[11] Increased osmotic pressure due to sorbitol accumulation is a contributing factor in diabetic complications including retinopathy and nephropathy.

5 or 25 mM glucose ± 100 μM tolrestat for 48 hrs. Control samples were treated with an equivalent volume of DMSO (veh). n=3, with 2-3 technical replicates per experiment. *p < 0.05, **p < 0.01, ***p < 0.001; 1-way ANOVA with Bonferroni's correction.

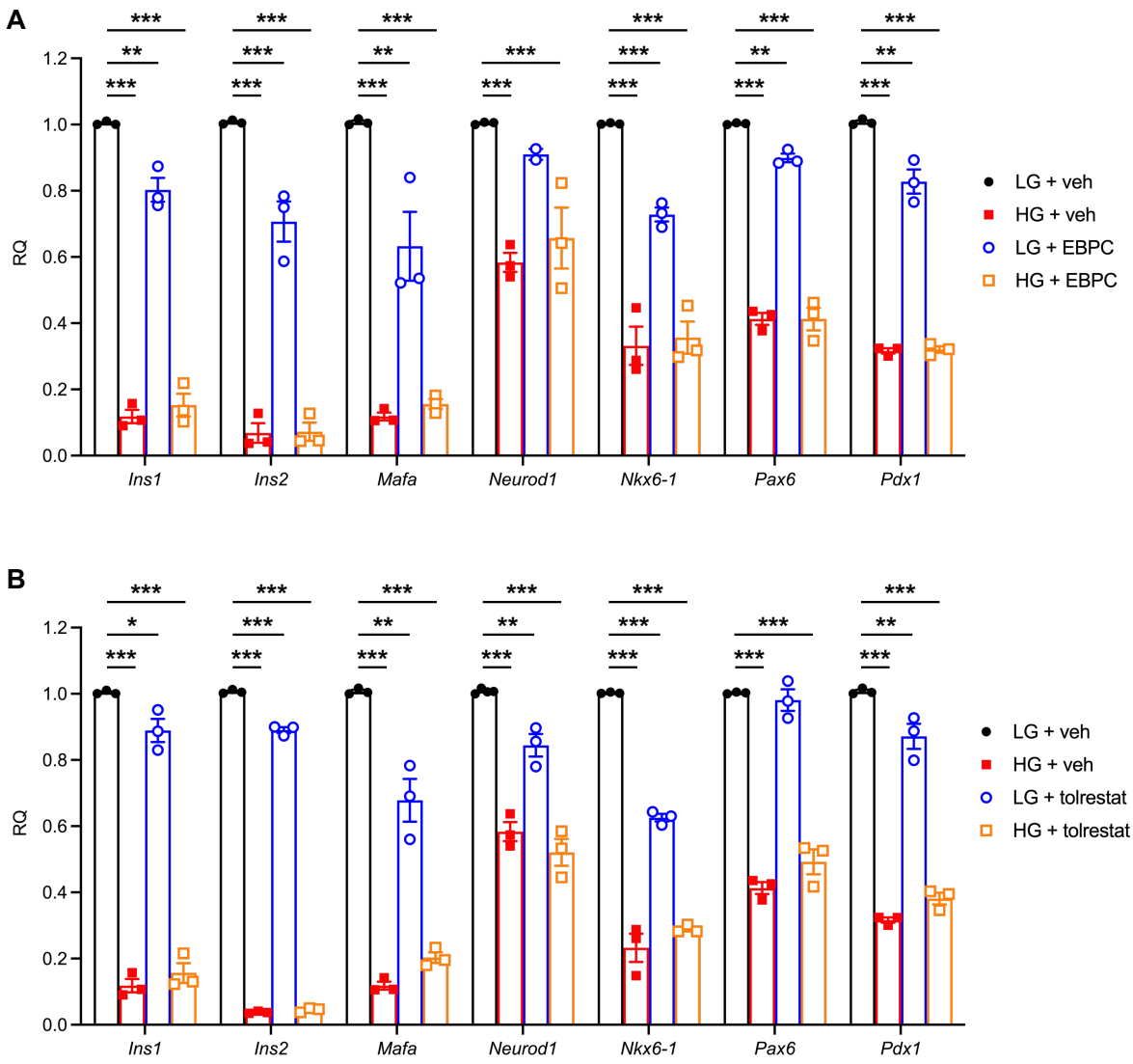

I also investigated the effects of chronic EBPC or tolrestat on selected metabolic genes. Of particular interest was Aldolase B, which catalyses the last step of the polyol pathway, converting fructose-1-phosphate to DHAP. *Aldob* expression in HG-cells was significantly reduced by aldose reductase inhibition (figure 4.18; note break in y-axis), indicating that the dramatic upregulation of this gene during hyperglycaemia is partly a response to increased flux through the pathway. Evidence from

hummingbirds, which display high *ALDOB* expression in the liver and are able to metabolise dietary fructose as efficiently as glucose, as well as from metastatic cancer cells, suggests that upregulating this enzyme helps with metabolism of large quantities of fructose (Bu et al., 2018; Osipova et al., 2023); ALDOB may be upregulated in β-cells in diabetes for the same reason.

Figure 4.18: Inhibition of the polyol pathway reduces the upregulation of AldoB in HG-cells

qPCR analysis of the expression of *Aldob* in INS-1 cells incubated with 5 or 25 mM glucose ± 100 μM EBPC or tolrestat for 48 hrs. Control samples were treated with an equivalent volume of DMSO (veh). n=3, with 2-3 technical replicates per experiment. ***p < 0.001; 1-way ANOVA with Bonferroni's correction.

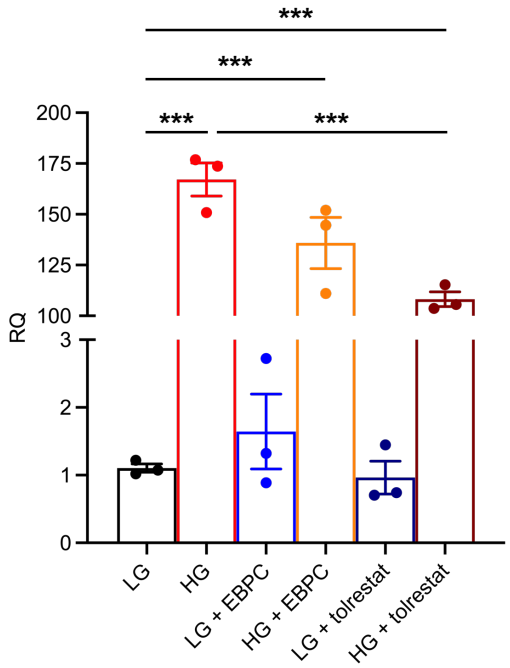

4.5 Discussion

The experiments discussed in this chapter have revealed that pooling of metabolites upstream of GAPDH largely explains the loss of insulin in chronic hyperglycaemia. Figure 4.19 provides an overview of glucose metabolism annotated with the interventions used in these experiments to probe the regulation of insulin biosynthesis.

Figure 4.19: Overview of glucose metabolism annotated with the experimental manipulations discussed in this chapter

Inhibitors indicated in red; mitochondrial substrates (PYR and MMS) in **bold**.

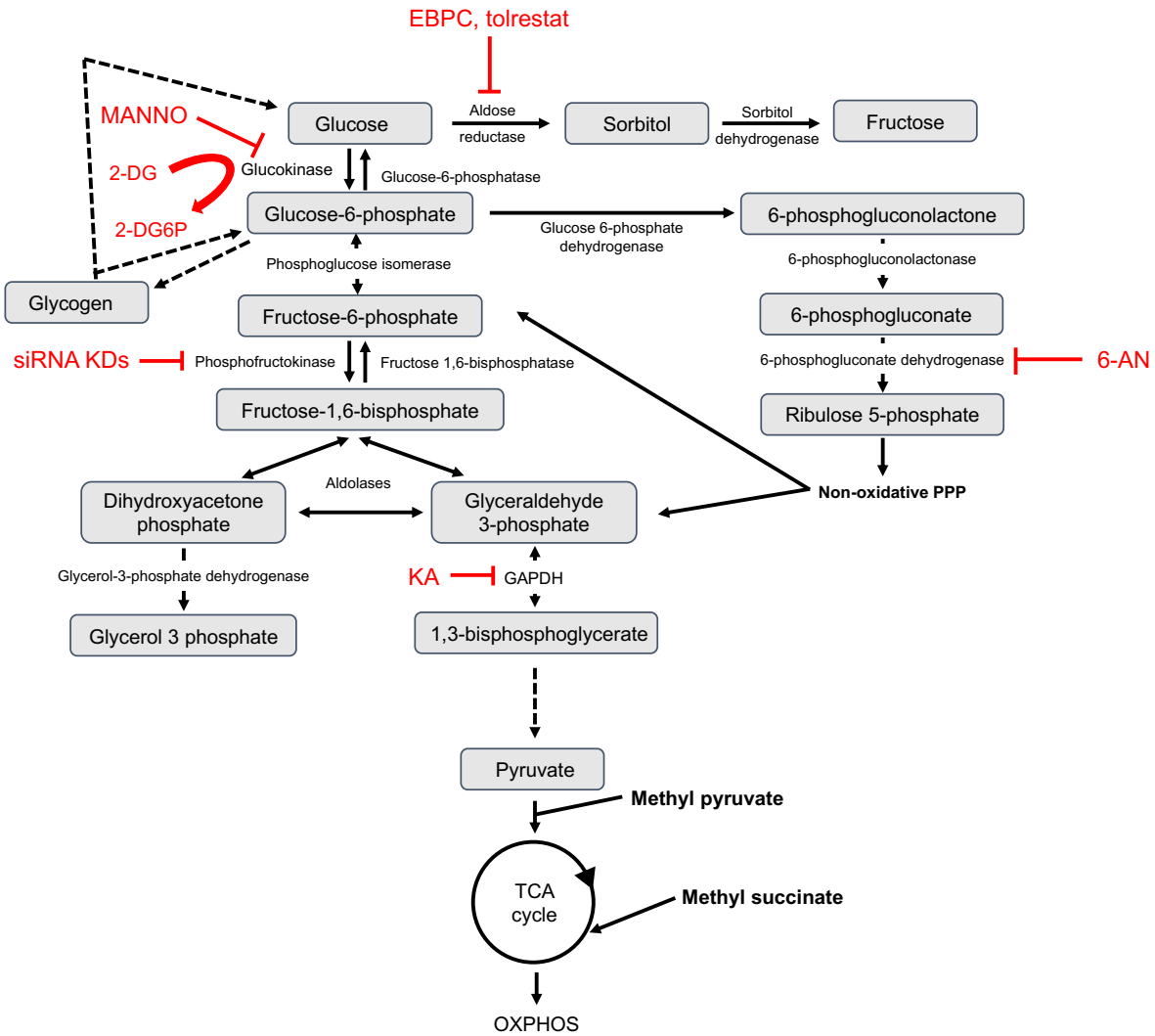

Considering the effects of 2-deoxyglucose, G6P appears to be the most important metabolite responsible for the downregulation of insulin biosynthesis. Blocking glycolysis or alternative pathways of glucose metabolism caused downregulation of insulin gene expression in euglycaemia, which I argue is primarily due to accumulation of G6P. Exactly how much G6P levels increase in hyperglycaemic β-cells is somewhat uncertain as it is a difficult metabolite to detect reliably in metabolomics experiments and reported values vary. However, G6P levels appear to be increased 2-fold in HG-cells (Haythorne et al., 2019), suggesting that cells may be sensitive to quite small changes in abundance. In another study, G6P was undetectable at 2.8 mM glucose but abundant at 16.7 mM glucose (Fernandez et al., 2008). Overexpression of G6PD dose-dependently decreases the glucose response of ChREBP in INS-1 cells (Li et al., 2010), suggesting that the PPP acts as a G6P-consuming shunt, and that, conversely, PPP inhibition increases activation of ChREBP by G6P. Glycogen synthesis is also a G6P-consuming pathway, and may help to limit the increase in G6P levels during chronic hyperglycaemia (so long as capacity to store further glycogen remains). However, accumulation of F1,6BP and/or F2,6BP may (to a lesser extent) also contribute to the downregulation of insulin biosynthesis. A recently developed fluorescent biosensor for F1,6BP promises to be a valuable tool for tracking changes in levels of this metabolite, which can be used as a proxy for glycolytic flux (Koberstein et al., 2022). Pooling of metabolites in upper glycolysis due to a bottleneck at GAPDH may adversely affect many other aspects of β-cell function. For instance, accumulation of metabolites between PFK and GAPDH is responsible for the hyperactivation of mTORC1 in chronic hyperglycaemia (Haythorne et al., 2022).

Some results were surprising and not easily explained. These include the significant downregulation of the insulin genes and all the β-cell identity genes by leucine (figure

4.7), in contrast to the other mitochondrial substrates. This is noteworthy as increased levels of circulating leucine and other BCAAs are positively associated with T2D risk (Sun et al., 2020). Leucine has some signalling roles that distinguish it from PYR and MMS, including mTORC1 activation, for which leucine is the most important amino acid in signalling amino acid availability (Melnik, 2012), and which has been suggested to contribute to β-cell exhaustion (Lynch & Adams, 2014). However, while leucine acutely stimulates mTORC1 activity, chronic incubation with leucine does not produce sustained activation of mTORC1 (Haythorne et al., 2022). Moreover, the loss of insulin biosynthesis does not appear to be mTOR-mediated, as it has different metabolic triggers to mTORC1 hyperactivation. Another possible result of chronic incubation with high levels of leucine is accumulation of a toxic metabolite due to saturation of branched-chain amino acid metabolism (Lynch & Adams, 2014). Low RNA yields (relative to LG-cells) and an unhealthy morphological appearance under the microscope of cells incubated for 48 hrs with 20 mM leucine suggests there is a degree of toxicity.

The results of pentose phosphate pathway inhibition by 6-AN were not straightforward to interpret either. Does accumulation of PPP intermediates (6-phosphogluconate and 6-phoshogluconolactone), an increased NADPH/$NADP^+$ ratio, or elevated G6P levels explain the reduction in insulin biosynthesis in LG-cells cultured with 6-AN? Aldose reductase inhibition also caused a reduction in insulin gene expression in LG-cells, albeit that decline was much smaller. This appears to suggest that an increase in G6P is part of the explanation, although it is also interesting to note that the PPP is an NADPH-producing pathway and aldose reductase is an NAPDH-consuming enzyme. Inhibiting either 6-PGD or aldose reductase should therefore elevate the NADPH/$NADP^+$ ratio, which is also elevated in chronic hyperglycaemia (figure 4.15b),

so perhaps the impacts of 6-AN and the aldose reductase inhibitors EBPC and tolrestat on insulin gene expression indicate that an increased NADPH/$NADP^+$ ratio contributes to the loss of insulin. This would presumably be an indirect effect, comparable to the high NADH/NAD^+ ratio in chronic hyperglycaemia leading to low GAPDH activity and thereby in turn to elevated levels of upstream metabolites that trigger changes in the expression of metabolic genes and the insulin genes.

The effects of 6-AN are consistent with a previous study showing that culturing INS-1 cells at 16 mM glucose or at 3 mM glucose with 100 µM 6-AN for 48 hours resulted in equivalent losses of insulin mRNA with respect to control cells cultured at 3 mM glucose (Goehring et al., 2011). Chronic activation of ERK1/2 appears to mediate the inhibition of insulin transcription by PPP metabolites, and the ERK inhibitor PD98059 partially prevented the loss of GSIS in chronic hyperglycaemia (Goehring et al., 2011). It thus appears that inadequate PPP flux does indeed cause impairment of insulin biosynthesis. That 6-AN did not cause any further impairment in HG-cells suggests that the effect is already maximal at 25 mM glucose. In future, it would be informative to test the effect of 6-AN on insulin gene expression and content in mild hyperglycaemia.

In conclusion, my investigations indicate that a combination of G6P, other upper glycolytic intermediates, and PPP intermediates accumulate during chronic hyperglycaemia and cause a severe downregulation of insulin gene expression. *Mafa* likely plays a particularly critical role, since it is the most potently downregulated of the insulin genes by high glucose, by KA, and by 2-DG. In chapter 5, I will attempt to explain why *Mafa* expression is particularly susceptible to glucotoxicity.

Some outstanding questions remain. As with the insulin genes and β-cell identity genes, the expression of metabolic genes such as *Aldob* is altered even at mildly elevated glucose concentrations and changes rapidly following the onset of hyperglycaemia. However, unlike the insulin genes, expression of most metabolic genes analysed is quickly normalised following subsequent restoration of euglycaemia (generally within 24 hours). The example of *Aldob* illustrates this (figure 4.12). Furthermore, studies by former lab members have shown similarly rapid reversal of the changes in *Pfkfb2*, *Pfkfb3*, and *Pdk1* (Maria Rohm, unpublished observations). Why then is there such a lag in recovery of insulin gene expression? Presumably some agents that negatively regulate expression of insulin and its transcription factors must persist for many hours after hyperglycaemia ends.

5. Investigating downstream effectors mediating the loss of insulin biosynthesis

5.1 Summary

1. The L-type calcium channel blocker isradipine failed to prevent the downregulation of insulin gene expression in HG-cells, indicating that elevated cytosolic Ca^{2+} does not cause the loss of insulin expression.
2. Txnip is strongly upregulated by accumulation of G6P, which is thought to be mediated by ChREBP, and signalling downstream of ChREBP is likely an important contributor to the loss of insulin mRNA during chronic hyperglycaemia. However, loss of Txnip had no effect on insulin gene expression in HG-cells but appeared to negatively affect insulin transcription in euglycaemia.
3. SHP, which has also been postulated to drive downregulation of insulin gene expression, was upregulated by koningic acid but unaffected by 2-deoxyglucose. Thus, its upregulation appears to be triggered by a metabolite upstream of GAPDH but downstream of G6P.
4. An inhibitor of S6K1 reduced insulin gene expression in LG-cells but did not affect expression in HG-cells, indicating that mTORC1 hyperactivation is not responsible for the loss of insulin expression in hyperglycaemia and that normal levels of S6K1 promote insulin expression.
5. The widely used anti-diabetic drug metformin increased insulin gene expression in LG-cells but did not affect expression in HG-cells or expression of the β-cell identity genes (with the exception of *Mafa*, which was downregulated in LG-cells).

5.2 Introduction

Through the series of experiments discussed in chapter 4, I narrowed down the list of candidate metabolites which might, by accumulating in chronic hyperglycaemia, cause the loss of insulin biosynthesis. I first excluded glucose itself, then mitochondrial metabolites, and then, by blocking glycolysis at different points, I identified G6P as the strongest candidate. Finally, I investigated the role of alternative pathways for the metabolism of G6P by inhibiting the pentose phosphate and polyol pathways. Following a review of the literature, I decided to investigate three potential pathways that might link hyperglycaemia-induced changes in metabolite abundance and intracellular signalling to reduced insulin promoter activity and transcription. These are summarised in figure 5.1.

Figure 5.1: Summary of three pathways for repression of insulin transcription discussed in this chapter

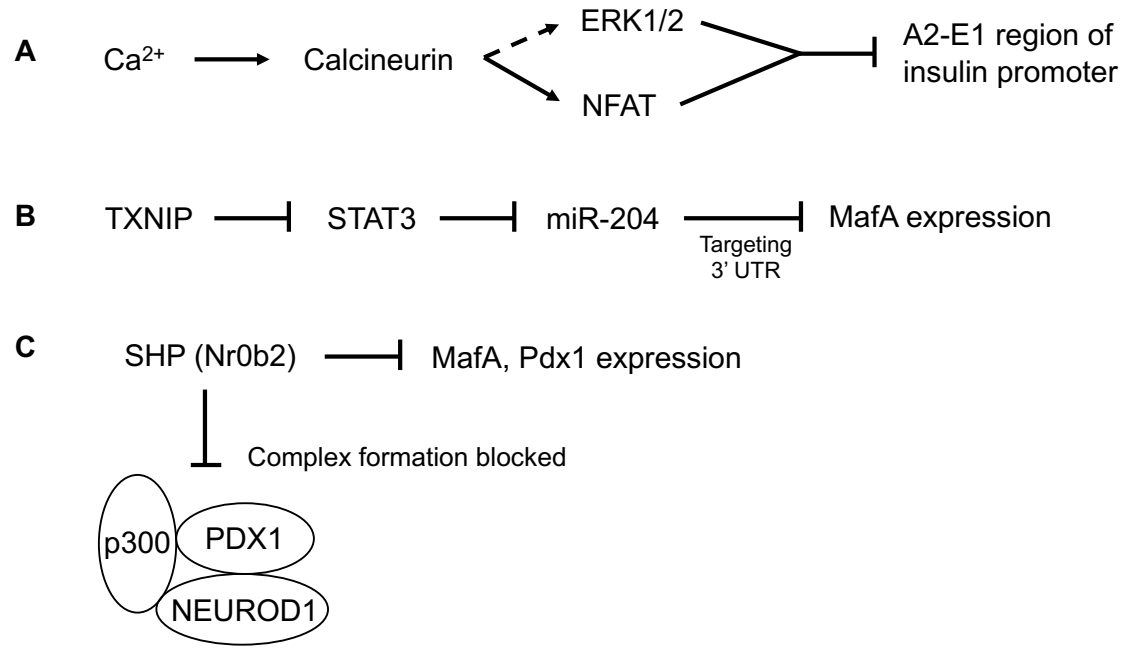

Firstly, I wanted to rule out chronic elevation of intracellular calcium as one of the changes that cause repression of insulin transcription. Chronic ERK1/2 activation downstream of the calcium-dependent phosphatase calcineurin has been proposed to cause inhibition of insulin promoter activity during chronic hyperglycaemia (Lawrence et al., 2005). Moreover, chronic β-cell depolarisation and elevation of $[Ca^{2+}]_{in}$, as induced by knockout of the K_{ATP} channel component *Abcc8*, induces dedifferentiation of a small proportion of β-cells, marked by elevated pancreatic polypeptide (*Ppy*) gene expression and reduced *Ins1* expression (Stancill et al., 2017). In support of their model, Lawrence et al. showed that calcineurin inhibitors reversed hyperglycaemia-induced repression of basal insulin promoter activity at 48 hrs (Lawrence et al., 2005). However, the authors did not show that this was linked to calcium levels. Chronic activation of ERK1/2 has also been attributed to accumulation of PPP intermediates, as inhibition of 6-PGD by 6-AN promoted ERK1/2 phosphorylation (Goehring et al., 2011). Both Goehring *et al*. and Lawrence *et al*. found that a transient peak in ERK1/2 phosphorylation was stimulated by acute high glucose but chronic hyperglycaemia then re-activated this phosphorylation. Perhaps the strongest argument *against* a significant role for chronically elevated calcium in the loss of insulin biosynthesis is that insulin mRNA levels and insulin content are significantly reduced in islets from diabetic βV59M mice despite their β-cells being (mostly) hyperpolarised (Brereton et al., 2014). Nevertheless, it is important to confirm this in β-cells that can depolarise, so I cultured INS-1 cells chronically with a calcium channel blocker.

Next, I considered to what extent the carbohydrate-responsive element-binding protein (ChREBP) and thioredoxin-interacting protein (Txnip) mediate repression of insulin expression. ChREBP is a key glucose-responsive transcription factor, active as a heterodimer with its partner MLX, which is implicated in many changes in gene

expression associated with β-cell glucotoxicity (Poungvarin et al., 2012). ChREBP is necessary and sufficient for the expression of a suite of glycolytic and lipogenic genes in INS-1 cells including alpha-enolase (*Eno1*), L-type pyruvate kinase (*Pklr*), acetyl-CoA carboxylase alpha (*Acaca*), ATP citrate lyase (*Acly*), and fatty acid synthase (*Fasn*) (Sae-Lee et al., 2016). All five of these genes are upregulated in diabetic βV59M mice (Haythorne et al., 2019). TXNIP is one of the most strongly glucose-upregulated proteins in the diabetic β-cell (table 1.1; Shalev et al., 2002). Among its myriad reported activities, including induction of oxidative stress and apoptosis, one is particularly pertinent to this thesis: it has been linked to transcriptional repression of insulin through negative regulation of Mafa (Xu et al., 2013). This transcriptional repression appears to translate into reduced insulin biosynthesis, as TXNIP-deficient mice display elevated whole-pancreas insulin content (J. Chen et al., 2008).

Transcription of *Txnip* is generally considered to be activated by ChREBP, but there are some discrepancies over the role of ChREBP versus MondoA in the regulation of *Txnip* expression. According to the model originally proposed, glucose induces the binding of ChREBP to a carbohydrate response element within the *Txnip* promoter, and ChREBP in turn recruits p300 to the promoter to stimulate acetylation of histone H4 and promote promoter occupancy by RNA polymerase II (Cha-Molstad et al., 2009). Phosphometabolite(s) responsible for ChREBP recruitment to its target promoters may be G6P (Li et al., 2010) and/or a downstream metabolite, likely F2,6BP if ChREBP is regulated in β-cells as in liver (Petrie et al., 2013). However, in EndoC-βH1 cells, *TXNIP* expression was unaffected by ChREBP knockdown but severely blunted by siRNA knockdown of MondoA, suggesting that MondoA is the glucose-responsive transcription factor that activates the *TXNIP* promoter (Richards et al., 2018). This is unlikely to reflect a genuine species difference, as Cha-Molstad et al.

(2009) demonstrated that ChREBP mediated glucose-induced *TXNIP* expression both in INS-1 cells and human islets, but it could be a peculiarity of the EndoC-βH1 model. A possible scenario is that MondoA and ChREBP both induce *Txnip* expression in β-cells, perhaps in different metabolic states, even though they are generally considered to regulate different sets of genes (Singh & Irwin, 2016). Curiously, mRNA levels of the two genes change in the opposite direction to *Txnip* during chronic hyperglycaemia: in βV59M mice, the fold change in *Mlxip* (MondoA) expression in diabetic relative to control islets is 0.85 ($p = 0.04$) and the fold change in *Mlxipl* (ChREBP) expression is 0.78 ($p = 0.04$) (Haythorne et al., 2019). However, ChREBPβ can upregulate TXNIP in an isoform-specific manner (Katz et al., 2022), so it is possible that the constitutively active β-isoform drives high expression of *Txnip* in chronic hyperglycaemia despite a decrease in total *Mlxipl* expression. To better understand the roles of ChREBP and TXNIP in regulating insulin gene expression, I investigated the metabolic regulation of *Txnip* and the effects of knocking down ChREBP or TXNIP on expression of insulin and the β-cell identity genes.

Lastly, I studied small heterodimer partner (SHP). Experiments in which SHP (*Nr0b2*) was knocked down using siRNA or overexpressed using an adenoviral vector have shown it is capable of attenuating insulin transcription by reducing expression of MAFA and PDX1 (Park et al., 2007). However, the mechanism by which SHP is upregulated in hyperglycaemic β-cells was not identified. I therefore used samples from some of the experiments described in chapter 4 to work out which metabolites are responsible for induction of this gene.

All three of the pathways shown in figure 5.1 are thought to affect MAFA expression and/or activity, with TXNIP and SHP both downregulating MAFA expression, and

ERK1/2 reducing promoter occupancy by MAFA. Notably, *MafA* is the β-cell identity gene most strongly downregulated by hyperglycaemia (figure 3.3), so the regulation of this transcription factor is of particular interest.

In addition to investigating these three pathways, I examined whether downregulation of insulin gene expression could be prevented by inhibition of mTORC1 signalling through S6K1. Chronic mTORC1 activation is deleterious to β-cell function, and S6K1 inhibition prevented much of the metabolic impairment seen in chronic hyperglycaemia (Haythorne et al., 2022). Insulin gene expression appears, however, to be sensitive to different glycolytic intermediates than those that drive mTORC1 activation. Nevertheless, I wanted to verify that chronic mTOR activation does not contribute to the hyperglycaemia-induced decline in insulin biosynthesis. I also tested whether metformin, the most widely prescribed first-line therapy for T2D, could prevent the loss of insulin biosynthesis in chronic hyperglycaemia.

5.3 Materials and methods

Methods were as described in chapter 2.

5.4 Results

5.4.1 Chronically high intracellular calcium is not a significant cause of hyperglycaemia-induced insulin gene repression

To investigate whether sustained elevation of $[Ca^{2+}]_{in}$ contributes to the decline in insulin gene expression during chronic hyperglycaemia, I used the L-type calcium

channel blocker isradipine to reduce calcium entry into INS-1 cells. I chose to block L-type channels as they account for some 50% of whole-cell calcium currents in rodent β-cells (whereas P/Q-type channels contribute 70% and L-type only 20% in human β-cells) and they play a key role in insulin secretion (Rorsman et al., 2012). 2 μM isradipine was found to suppress GSIS by 77% (Jing et al., 2005), so I tested a range of isradipine concentrations (1, 2, 5, 10 and 20 μM) and chose to continue with 5 μM as this was the highest concentration that did not adversely affect growth of the cells.

Figure 5.2: Effect of chronic calcium channel blockage by isradipine on expression of the insulin genes and β-cell identity genes

qPCR analysis of the expression of the insulin genes and selected β-cell identity genes in INS-1 cells incubated with 5 or 25 mM glucose ± 5 μM isradipine for 48 hrs. Control samples were treated with an equivalent volume of DMSO (veh). n=3, with 2-3 technical replicates per experiment. *p < 0.05, **p < 0.01, ***p < 0.001; 1-way ANOVA with Bonferroni's correction.

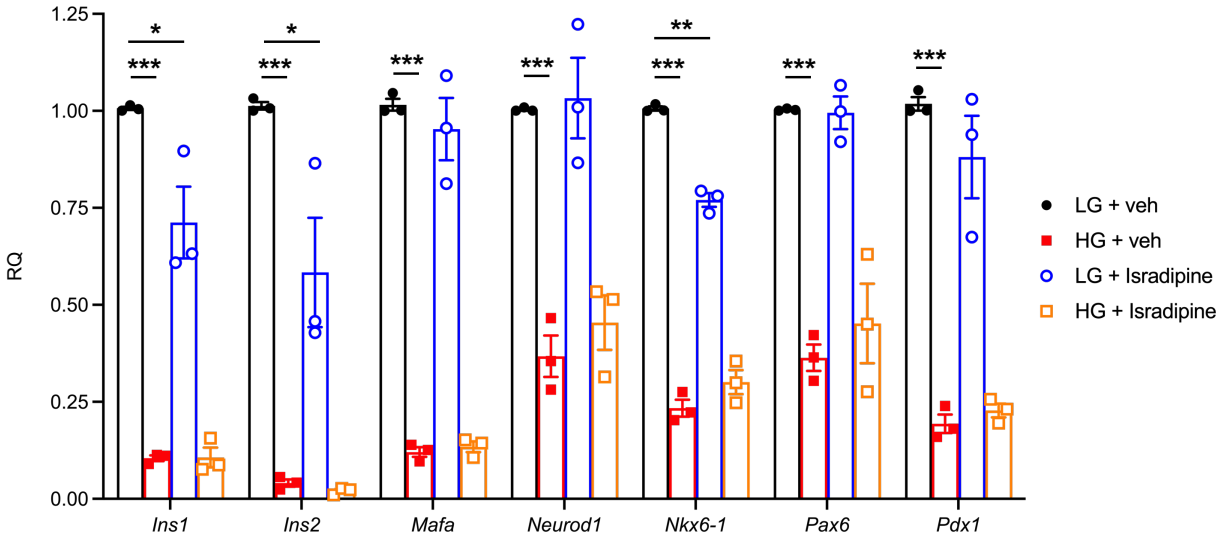

Isradipine had no effect on expression of the insulin genes or β-cell identity genes in HG-cells (figure 5.2): lowering intracellular calcium thus failed to prevent the hyperglycaemia-induced repression of insulin gene expression. In LG-cells, isradipine

reduced expression of *Ins1* and *Ins2* by ~30% and ~40%, respectively. This may be because some calcium is required for insulin transcription to occur. However, we would expect L-type channels to be mostly closed at the resting potential, as they normally open in response to membrane depolarisation at stimulatory glucose concentrations, so this result is somewhat surprising. Perhaps, since 5 mM glucose is not too far below the threshold for GSIS, we can expect enough channels to be open to explain this result. Of the five transcription factors, only *Nkx6-1* expression was affected by isradipine, being downregulated by ~25% in LG-cells. These results are broadly consistent with findings from the (euglycaemic) *Abcc8*$^{-/-}$ mouse model, in which *Ins1* and *Neurod1* were downregulated but *Mafa*, *Nkx6-1*, and *Pdx1* were unchanged (Stancill et al., 2017).

In conclusion, $[Ca^{2+}]_{in}$ does not appear to significantly affect insulin gene expression above a threshold enabling level. Excess calcium is therefore unlikely to be a major factor coupling chronic hyperglycaemia to downregulation of insulin transcription, and ERK1/2-dependent repression of insulin transcription probably occurs as a result of impaired flux through the PPP rather than elevated calcium.

5.4.2 Signalling through ChREBP and TXNIP contributes to the repression of insulin gene expression

Although TXNIP is controlled at the levels of mRNA stability and protein stability in addition to transcriptional control, there is generally good concordance between mRNA and protein levels (Shalev, 2014). In the results presented here, I mostly use mRNA levels as the measure of TXNIP expression. I also use mRNA levels as the

measure of ChREBP expression, although, somewhat curiously considering the observed upregulation of many of its target genes, *Mlxipl* (ChREBP) expression was downregulated ~65% in chronic hyperglycaemia (figure 5.3). Meanwhile, *Mlxip* (MondoA) was downregulated ~50% in HG-cells (figure 5.3).

Figure 5.3: Downregulation of MondoA and ChREBP mRNA expression in chronic hyperglycaemia

qPCR analysis of the expression of *Mlxip* (MondoA) and *Mlxipl* (ChREBP) in INS-1 cells incubated with 5 or 25 mM glucose for 48 hrs. n=7, with 2-3 technical replicates per experiment. ****$p < 10^{-4}$; two-tailed unpaired Student's t-test.

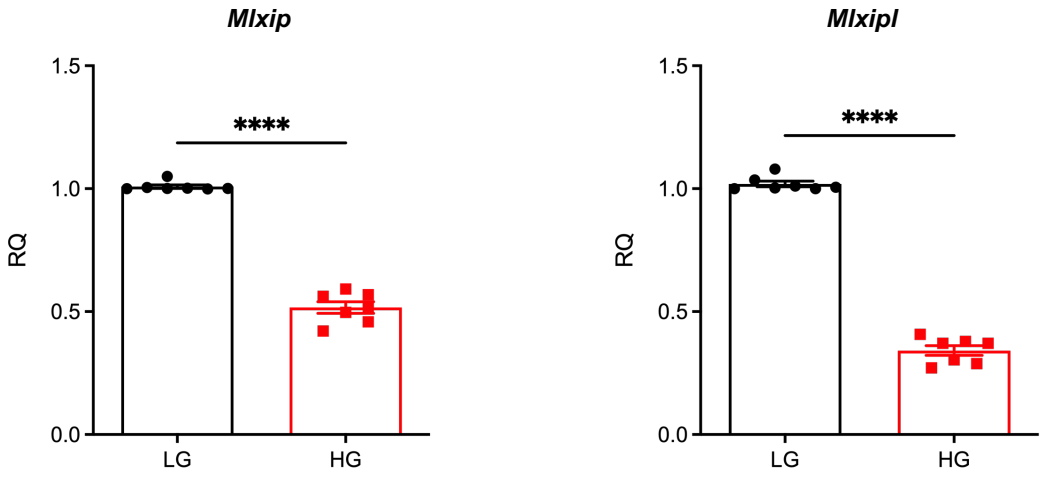

Figure 5.4: Investigating the metabolic regulation of *Txnip* expression

(a) qPCR analysis of the expression of *Txnip* in INS-1 cells incubated with 0, 2, 5, 8, 11, 16.7 and 25 mM glucose for 48 hrs. n=2-3. *p < 0.05, **p < 0.01, ***p < 0.001; 1-way ANOVA with Bonferroni's correction.

(b) Effect of varying tamoxifen dosage in βV59M mouse islets (as described in chapter 3) on *Txnip* mRNA expression. Each data point represents one mouse: n=13 for control, n=4 for IGT, n=6 for mild, n=3 for severe. *p < 0.05, ***p < 0.001; 1-way ANOVA with Bonferroni's correction.

(c) qPCR analysis of the expression of *Txnip* in INS-1 cells at time points of 1, 3, 6, 12, 24, 48 and 72 hrs following onset or reversal of hyperglycaemia. Cells were pre-cultured at 5 or 25 mM glucose for 48 hrs before being transferred to the opposite condition (25 or 5 mM to simulate onset or reversal, respectively) at the time point 0. n=3.

(d) qPCR analysis of the expression of *Txnip* in INS-1 cells cultured for 48 hrs at 5 or 25 mM glucose ± 10 mM mannoheptulose (MANNO). n=6, with 2-3 technical replicates per experiment. *p < 0.05, ***p < 0.001; 1-way ANOVA with Bonferroni's correction.

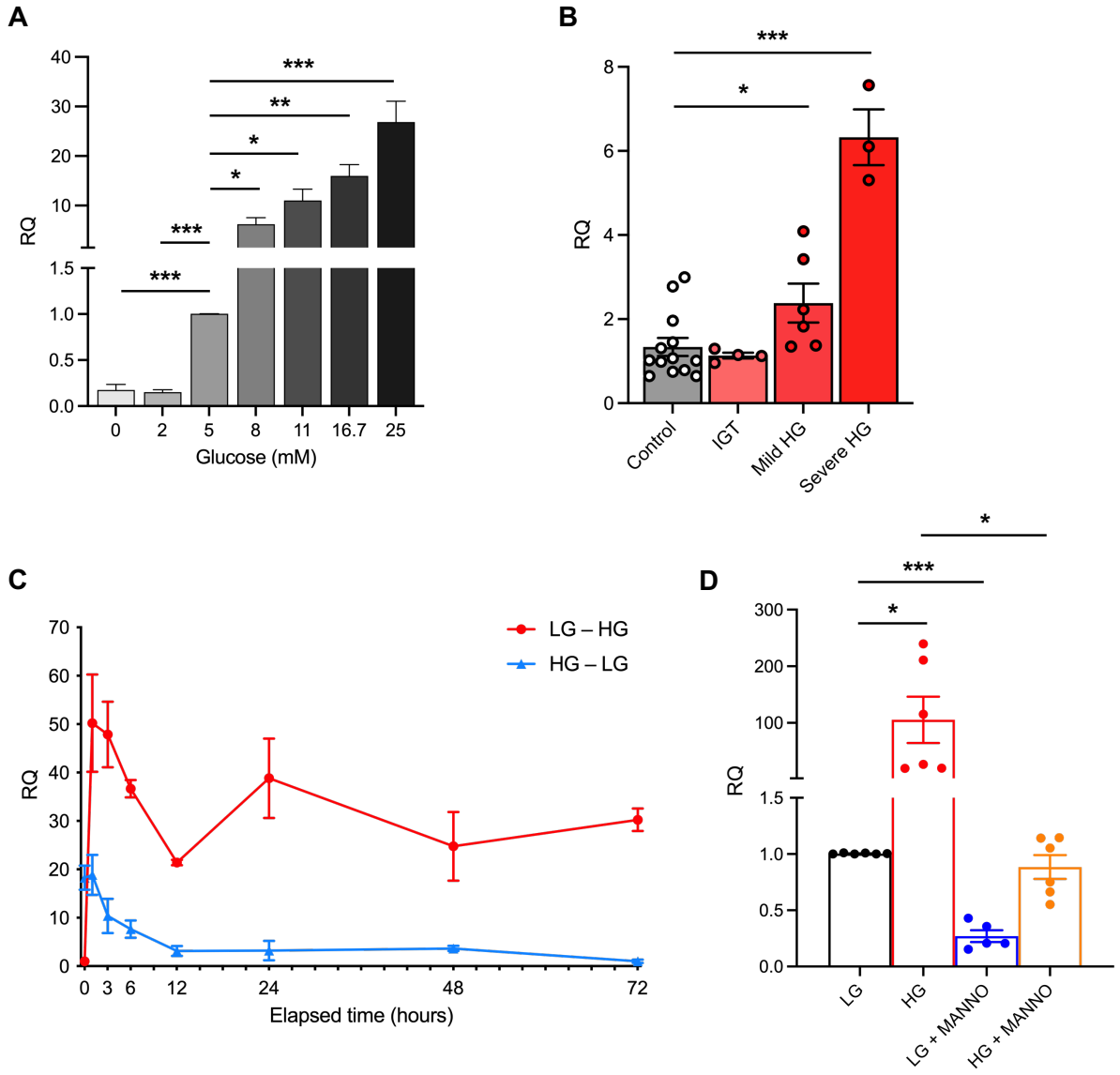

(e) qPCR analysis of the expression of *Txnip* in INS-1 cells cultured for 48 hrs at 5 or 25 mM glucose or with 20 mM methyl pyruvate (PYR) or at 5 mM glucose with 20 mM methyl pyruvate. n=4, with 2-3 technical replicates per experiment. *p < 0.05, **p < 0.01, ***p < 0.001; 1-way ANOVA with Bonferroni's correction.

(f) qPCR analysis of the expression of *Txnip* in INS-1 cells cultured for 48 hrs at 5 or 25 mM glucose or with 20 mM methyl succinate (MMS). n=3, with 2-3 technical replicates per experiment. ***p < 0.001; 1-way ANOVA with Bonferroni's correction.

(g) qPCR analysis of the expression of *Txnip* in INS-1 cells cultured for 48 hrs at 5 or 25 mM glucose or with 20 mM leucine (LEU). n=3, with 2-3 technical replicates per experiment. **p < 0.01, ***p < 0.001; 1-way ANOVA with Bonferroni's correction.

(h) qPCR analysis of the expression of *Txnip* in INS-1 cells cultured for 48 hrs at 5 mM glucose ± 5 μM koningic acid (KA). n=4, with 2-3 technical replicates per experiment. ***p < 0.001; two-tailed unpaired Student's t-test.

(i) qPCR analysis of the expression of *Txnip* in INS-1 cells incubated with 5 or 25 mM glucose or with 25 mM 2-DG for 24 hrs. n=5, with 2-3 technical replicates per experiment. *p < 0.05, ***p < 0.001; 1-way ANOVA with Bonferroni's correction.

(j) qPCR analysis of the expression of *Txnip* in INS-1 cells incubated with 5 or 25 mM glucose ± 100 μM 6-AN for 48 hrs. Control samples were treated with an equivalent volume of DMSO (veh). n=3, with 2-3 technical replicates per experiment. *p < 0.05, **p < 0.01; 1-way ANOVA with Bonferroni's correction.

(k) qPCR analysis of the expression of *Txnip* in INS-1 cells incubated with 5 or 25 mM glucose ± 100 μM EBPC or tolrestat for 48 hrs. Control samples were treated with an equivalent volume of DMSO (veh). n=3, with 2-3 technical replicates per experiment. *p < 0.05, **p < 0.01; 1-way ANOVA with Bonferroni's correction.

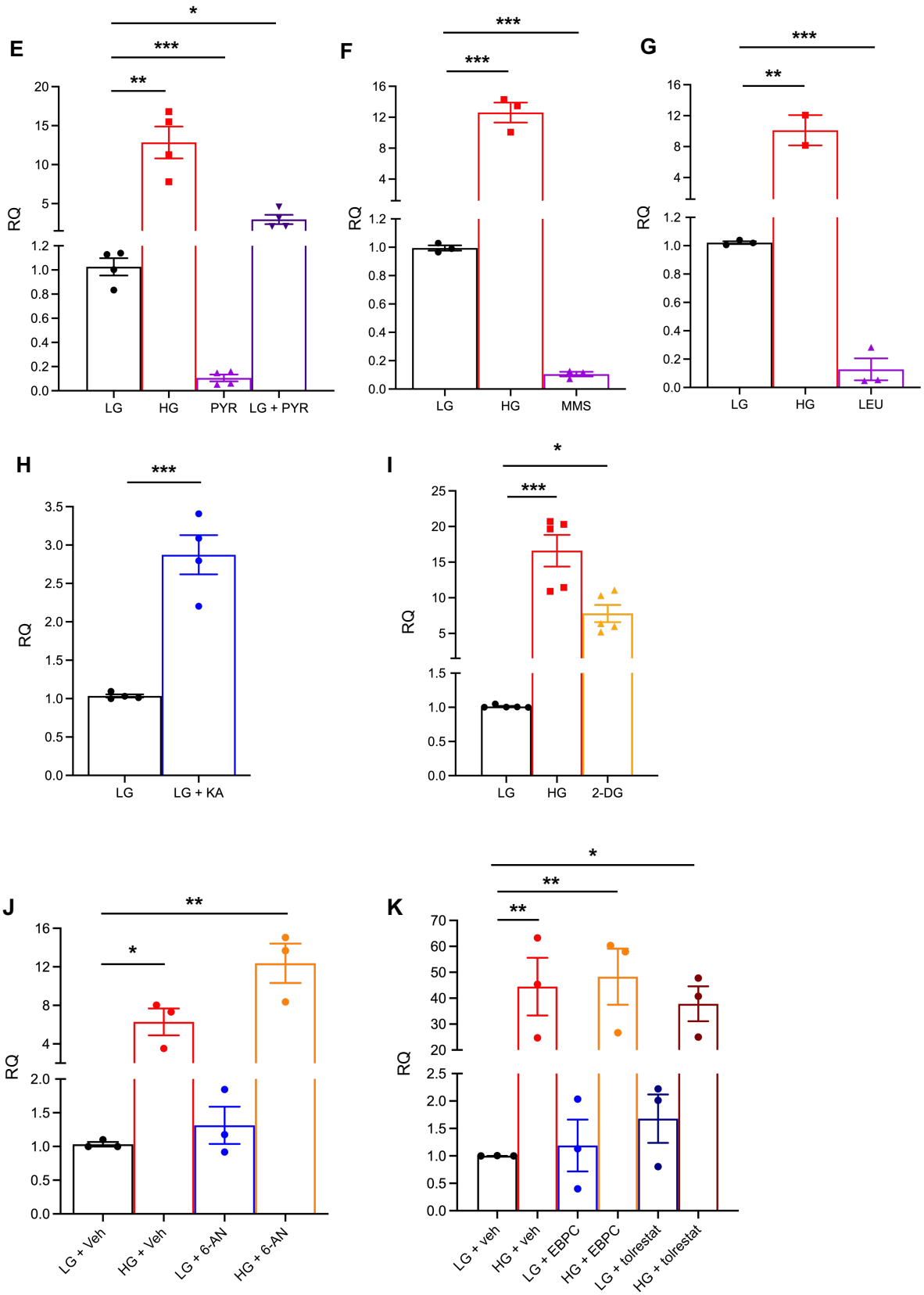
E
F
G
H
I
J
K
RQ
LG
HG
PYR
LG + PYR
MMS
LEU
LG + KA
2-DG
LG + Veh
HG + Veh
LG + 6-AN
HG + 6-AN
LG + veh
HG + veh
LG + EBPC
HG + EBPC
LG + tolrestat
HG + tolrestat

A glucose dose-response (figure 5.4a) shows how strongly *Txnip* expression in INS-1 cells depends on the glucose concentration: at 5 mM glucose, expression was already 6-fold higher than at 0 mM or 2 mM glucose, while at 8 mM glucose it was 6-fold higher than at 5 mM glucose (note the break in the y-axis). *Txnip* mRNA levels progressively increased with each higher glucose concentration tested, up to 25 mM. *Txnip* expression in islets from βV59M mice showed a similar pattern, being increased nearly 2-fold in mild HG mice and ~5-fold in severe HG mice relative to control mice (figure 5.4b). The latter value compares with a 9-fold upregulation previously recorded (table 1.1). There was no change in expression in IGT mice, which had free fed blood glucose levels within the same range as control, consistent with the absolute glucose-dependence of *Txnip* induction.

Txnip induction in response to high glucose was extremely rapid: time course experiments in INS-1 cells (figure 5.4c) revealed a 50-fold upregulation within 1 hour of hyperglycaemia onset, after which expression fell before stabilising around 30-fold above control levels during chronic hyperglycaemia. The decline in *Txnip* expression following restoration of euglycaemia was somewhat slower. There was no change in the first hour, but there was then a steady decline until the 12 hrs time point, when *Txnip* levels were 3-fold higher than baseline. Finally, by 72 hrs the upregulation of *Txnip* had been fully reversed. These temporal dynamics roughly mirror those of insulin gene expression, which has an inverse relationship with glycaemia (figure 3.4a), lending credence to the hypothesis that TXNIP makes an important contribution to the repression of insulin gene expression.

As with most hyperglycaemia-induced changes in gene expression, the upregulation of *Txnip* in HG-cells was blocked by 10 mM mannoheptulose (figure 5.4d), indicating

that it is dependent on phosphorylation of glucose by glucokinase. This suggests that mannoheptulose reduces glycolytic flux in HG-cells to a level similar to that in LG-cells. The mannoheptulose-induced decline in *Txnip* expression in LG-cells reflects the extreme sensitivity of *Txnip* to glucose seen in figure 5.4a.

In cells cultured in media supplemented only with 20 mM methyl pyruvate, *Txnip* expression was 90% below levels in LG-cells (figure 5.4e), demonstrating that glucose metabolism is essential for induction of this gene. Interestingly, *Txnip* was upregulated 3-fold in cells cultured at 5 mM glucose with 20 mM methyl pyruvate (note break in y-axis), suggesting that metabolism of methyl pyruvate suppresses glycolysis, leading to accumulation of glycolytic intermediates upstream of pyruvate, and thereby to induction of Txnip. This is the inverse effect to that of LG + PYR culture on the insulin genes and *Mafa* (figure 4.4b).

Chronic culture with methyl succinate (figure 5.4f) or leucine (figure 5.4g) had identical effects on *Txnip* expression to methyl pyruvate, producing a profound reduction in expression. GAPDH inhibition with koningic acid led to a ~3-fold upregulation of *Txnip* in LG-cells (figure 5.4h), confirming that metabolite(s) in upper glycolysis trigger expression of this gene. 24 hrs incubation with 2-DG upregulated *Txnip* expression 8-fold (figure 5.4i). Such effective stimulation by 2-DG suggests that *Txnip* expression is largely driven by G6P. A similar magnitude of *Txnip* induction by 2-DG has been reported previously following 6 hrs incubation (Minn et al., 2006).

Pentose phosphate pathway inhibition by 6-AN had no effect on *Txnip* expression in either LG-cells or HG-cells (figure 5.4j). This may suggest that G6P levels were not much affected, and that the downregulation of insulin gene expression by 6-AN in LG-cells described in chapter 4 was due to accumulation of PPP intermediates rather than

G6P. Aldose reductase inhibition by EBPC or tolrestat (figure 5.4k) had no effect on HG-cells, but tolrestat may increase *Txnip* mRNA levels in LG-cells. There was no significant difference with n=3, so further experiments would be needed to confirm if this is the case. If so, it would probably be because shutting off alternative pathways for glucose metabolism forces greater accumulation of G6P, which surely accounts at least in part for the downregulation of insulin gene expression by these inhibitors (figures 4.15 and 4.17). In chronic hyperglycaemia, each possible pathway of glucose metabolism must become overloaded, leading to the accumulation of metabolites, such as G6P, that trigger the loss of insulin.

In an effort to better understand the roles of ChREBP and TXNIP in the regulation of insulin biosynthesis, I performed siRNA knockdowns of both genes and analysed the effects on insulin gene expression. I optimised the KD conditions by testing different siRNA concentrations (25 and 50 nM) and found 25 nM to be the most effective concentration for both genes (table 5.1), although the KD efficiency for ChREBP was poor at either concentration.

Table 5.1: Efficiencies (% decrease in mRNA expression relative to control) of ChREBP and *Txnip* knockdowns with 25 and 50 nM siRNA in INS-1 cells cultured at 11 mM glucose for 48 hrs following transfection

Gene	siRNA concentration (nM)	
	25	**50**
Mlxipl	16	10
Txnip	68	65

Figure 5.5 shows the results of ChREBP knockdown. ChREBP is already significantly downregulated (~70%) in HG-cells, and siRNA against *Mlxipl* caused no further

reduction in mRNA levels (nominally 4% on average, but this is not significant). Despite this, the knockdown led to small but significant increases in expression of *Neurod1*, *Nkx6-1*, *Pax6*, and *Pdx1* in HG-cells. In LG-cells, a significant reduction in ChREBP expression was achieved, with 31% KD efficiency. In spite of this poor efficiency, knockdown of ChREBP resulted in some enhancement of expression of insulin and the β-cell identity genes: in particular, *Ins2* was upregulated 1.36-fold in LG-cells ($p = 0.002$). This finding supports the hypothesis that activation of ChREBP can, at least partially, cause a loss of insulin biosynthesis. The hypothesis that ChREBP downregulates insulin gene expression in chronic hyperglycaemia appears difficult to reconcile with the hyperglycaemia-induced reduction in *Mlxipl* expression unless the proportion of ChREBP that is constitutively active is increased in HG-cells. Unfortunately, as I measured only total *Mlxipl* expression, without distinguishing between the alpha and beta isoforms, I cannot tell whether this is the case.

Figure 5.5: Effects of siRNA knockdown of ChREBP on expression of the insulin genes and β-cell identity genes

qPCR analysis of the expression of **(a)** *Mlxipl* and **(b)** the insulin genes and selected β-cell identity genes in INS-1 cells cultured for 48 hrs at 5 or 25 mM glucose following siRNA knockdown of ChREBP (MLXIPL). Cells were transfected with either 25 nM non-targeting control siRNA (siNT) or 25 nM siMLXIPL. n=3, with 2-3 technical replicates per experiment. *p < 0.05, **p < 0.01, ***p<0.001; 1-way ANOVA with Bonferroni's correction.

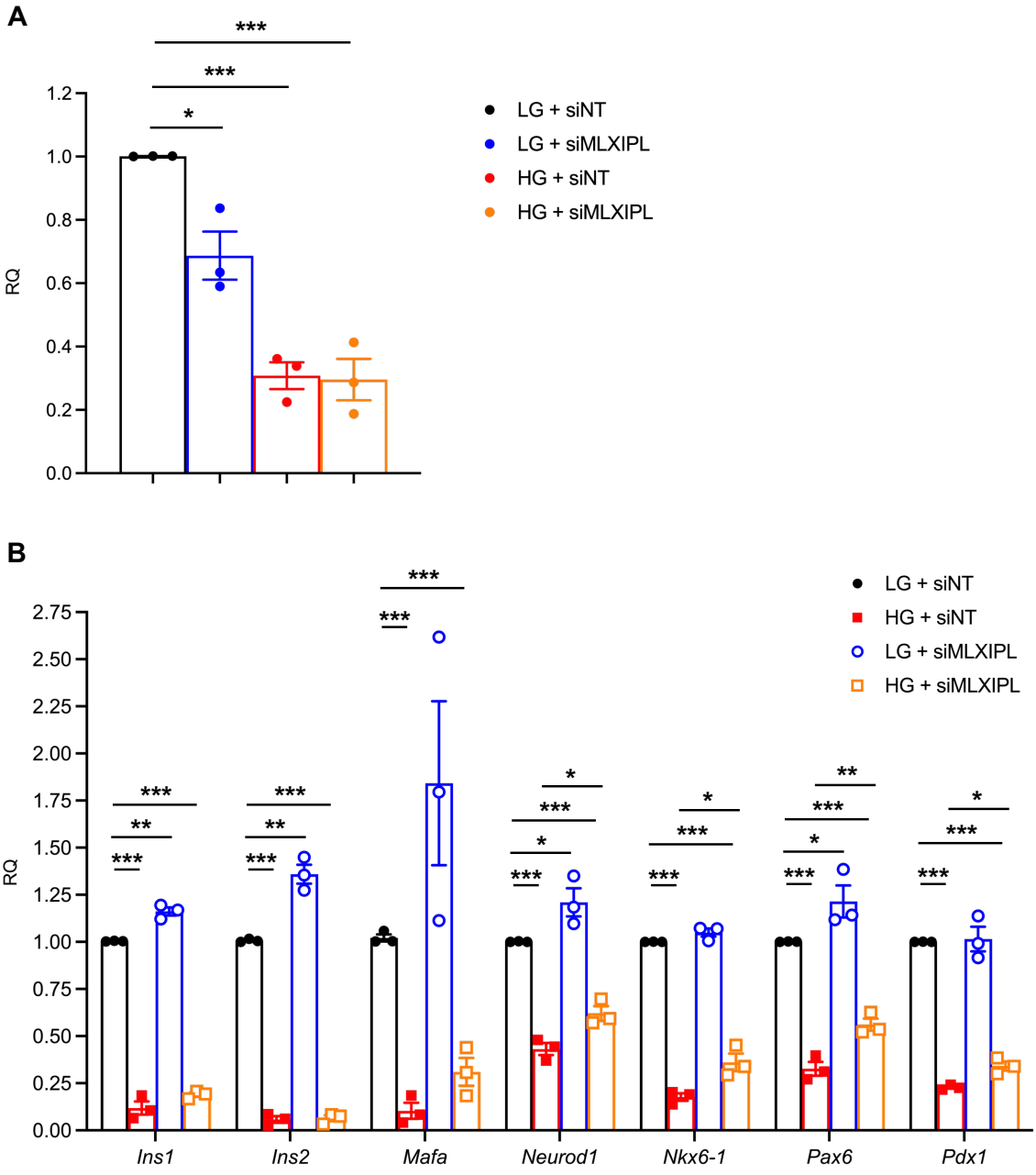

Figure 5.6: Effects of siRNA knockdown of Txnip on expression of the insulin genes and β-cell identity genes

(a) qPCR analysis of the expression of *Txnip* in INS-1 cells cultured for 48 hrs at 5 or 25 mM glucose following siRNA knockdown of TXNIP. Cells were transfected with either 25 nM non-targeting control siRNA (siNT) or 25 nM siTXNIP. n=3, with 2-3 technical replicates per experiment. *p < 0.05, **p < 0.01; 1-way ANOVA with Bonferroni's correction.

(b) Western blot analysis of TXNIP protein levels in INS-1 cells cultured for 48 hrs at 5 mM glucose (samples 1-6) or 25 mM glucose (samples 7-12) following siRNA knockdown of TXNIP. Cells were transfected with either 50 nM non-targeting control siRNA (siNT, samples 3, 4, 9, and 10) or 25 nM siTXNIP (samples 5, 6, 11, and 12) or were treated with lipofectamine only and not transfected (samples 1, 2, 7, and 8). n=2. **(i)** Membrane probed with anti-TXNIP antibody (TXNIP bands are close to 50 kDa marker). **(ii)** Membrane probed with anti-alpha-tubulin antibody after stripping. **(iii)** TXNIP band intensity normalised to alpha-tubulin loading control band intensity (HG-cells only, as TXNIP was undetectable in LG-cells). n=1, with 2 technical replicates.

(c) qPCR analysis of the expression of the insulin genes and selected β-cell identity genes in INS-1 cells cultured for 48 hrs at 5 or 25 mM glucose following siRNA knockdown of TXNIP. Cells were transfected with either 25 nM non-targeting control siRNA (siNT) or 25 nM siTXNIP. n=3, with 2-3 technical replicates per experiment. *p < 0.05, **p < 0.01, ***p<0.001; 1-way ANOVA with Bonferroni's correction.

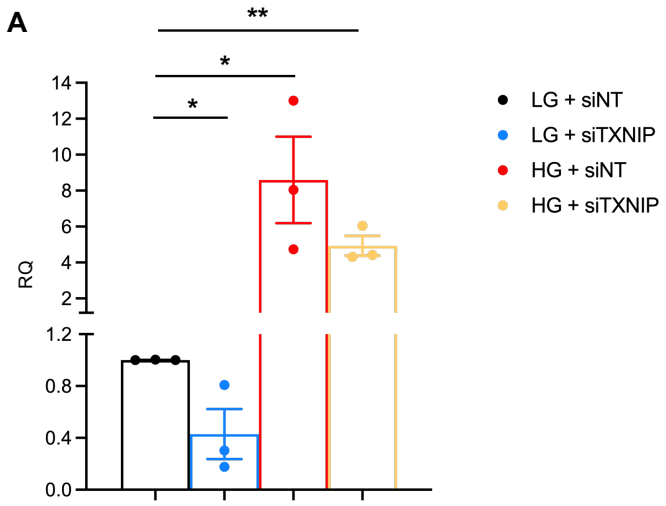

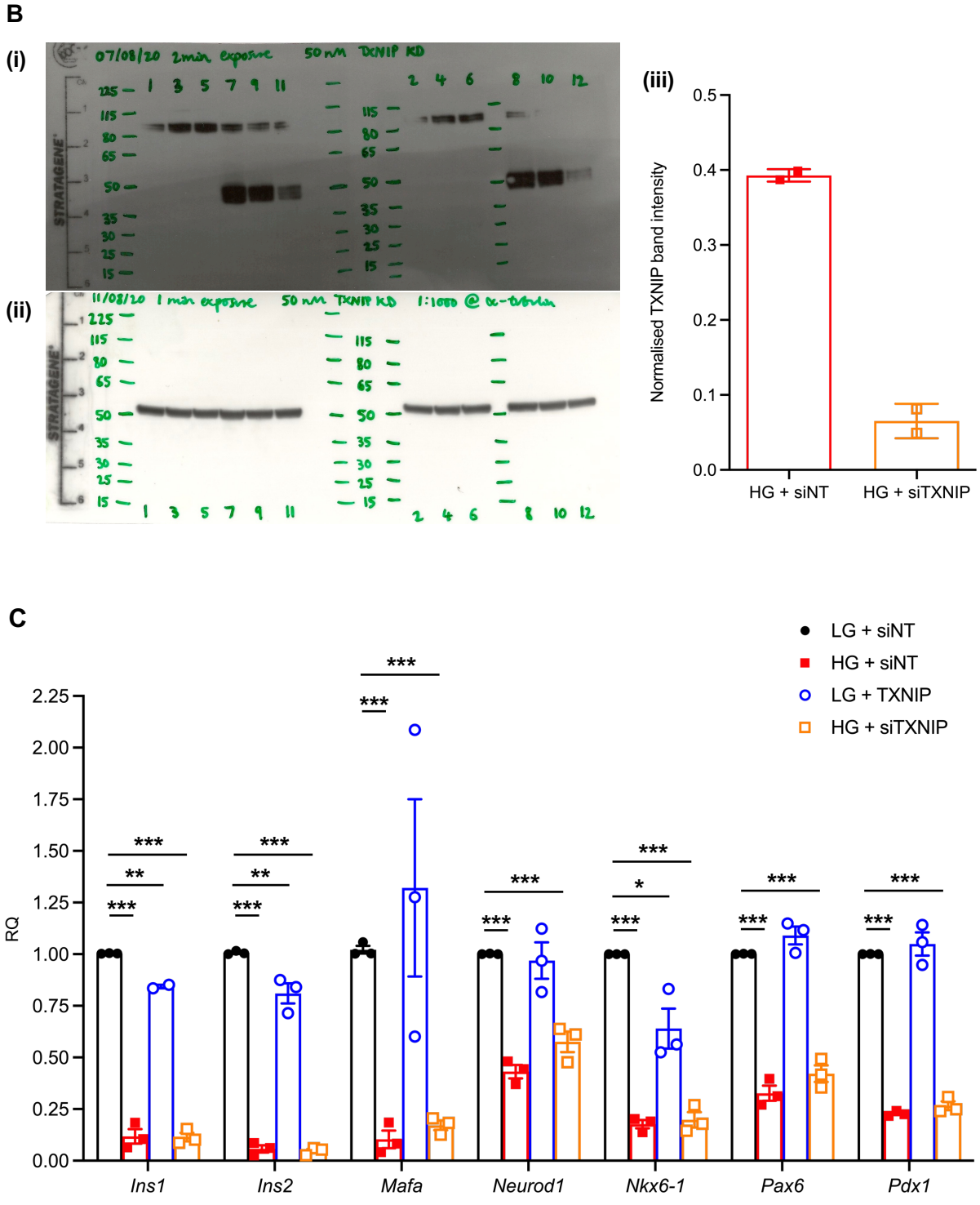

Figure 5.6 shows the results of *Txnip* knockdown. KD efficiency, as determined by transcript levels, was 57% in LG-cells but only 43% in HG-cells (figure 5.6a; note break in y-axis). However, when TXNIP protein levels were quantified following a separate knockdown experiment (using a higher siRNA concentration of 50 nM), there was an

83% average reduction in expression in HG-cells (figure 5.6b), suggesting that TXNIP knockdowns were more effective at the protein level. Knocking down TXNIP had no discernible effect on expression of the insulin genes or β-cell identity genes in HG-cells (figure 5.6c). However, as *Txnip* remained more than 4-fold upregulated at the mRNA level after being knocked down, a deleterious role for TXNIP cannot be ruled out on the basis of this experiment. Surprisingly, TXNIP KD in LG-cells had an adverse impact on insulin expression, causing insulin mRNA levels to fall by 15-20%, accompanied by a drop of nearly 40% in expression of *Nkx6-1*. *Mafa*, which is believed to be negatively regulated by TXNIP (Xu et al., 2013), was unaffected.

TXNIP KD caused a fall in *Mlxipl* transcript levels in LG-cells equivalent to that achieved by ChREBP KD (figure 5.7b). This points to a complex interplay between these two proteins. TXNIP is known to promote its own expression through ChREBP in a positive feedback loop (J. Chen et al., 2014), although this mechanism is based on dephosphorylation and nuclear translocation of ChREBP rather than increased ChREBP expression. Knocking down ChREBP should enable the transcription factor FoxO1 to compete more effectively with ChREBP for DNA binding at the TXNIP promoter to repress *Txnip* expression (Kibbe et al., 2013). However, ChREBP KD unexpectedly increased *Txnip* expression in LG-cells (figure 5.7a).

Figure 5.7: Regulatory interplay between ChREBP and Txnip

qPCR analysis of the expression of **(a)** *Txnip* in INS-1 cells cultured for 48 hrs at 5 or 25 mM glucose following siRNA knockdown of ChREBP and **(b)** *Mlxipl* in INS-1 cells cultured for 48 hrs at 5 or 25 mM glucose following siRNA knockdown of TXNIP. Cells were transfected with either 25 nM non-targeting control siRNA (siNT) or 25 nM siMLXIPL or siTXNIP. n=3, with 2-3 technical replicates per experiment. *p < 0.05, **p < 0.01, ***p<0.001; 1-way ANOVA with Bonferroni's correction.

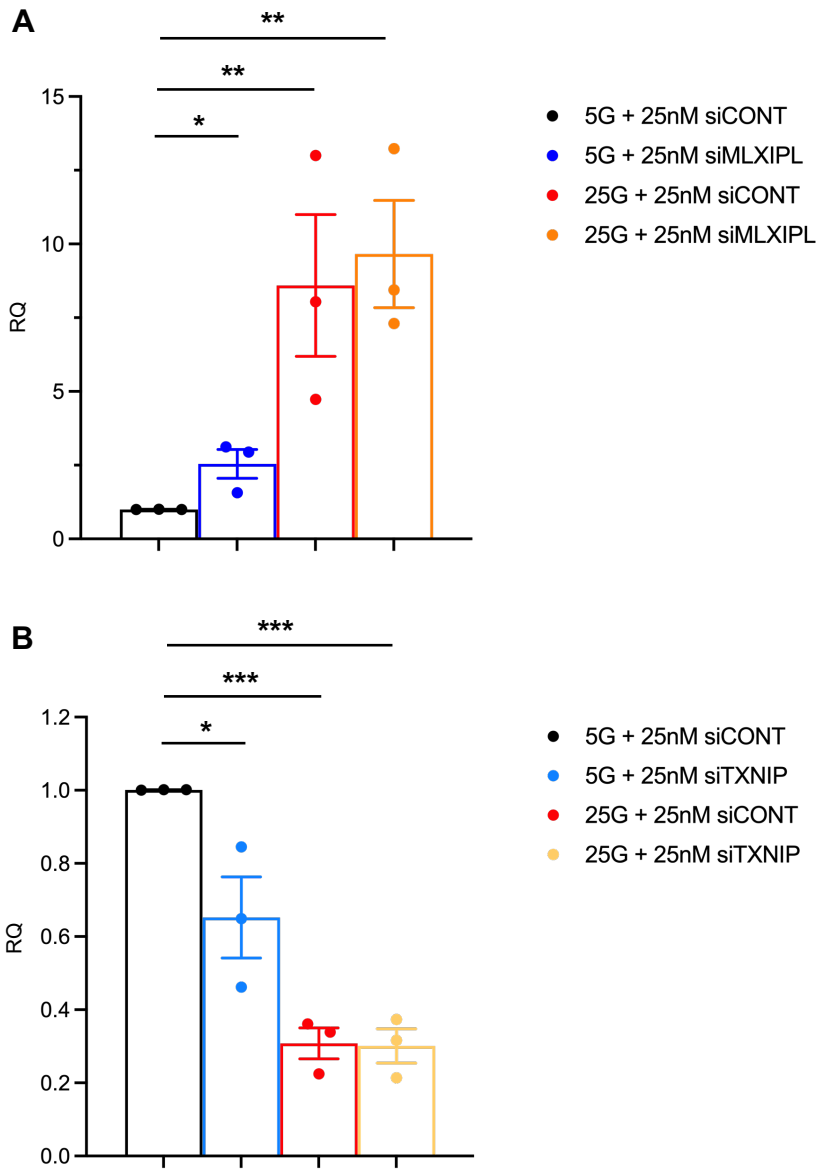

5.4.3 SHP is upregulated in hyperglycaemia by a G6P-independent mechanism

I found SHP (*Nr0b2*) to be upregulated 1.5-fold to 2-fold at the mRNA level in HG-cells (figure 5.8a). *Nr0b2* expression was increased by 25% in LG-cells cultured with KA (figure 5.8b), indicating that a metabolite upstream of GAPDH triggers induction of the gene. *Nr0b2* was not upregulated by 2-DG (figure 5.8c), indicating that a metabolite downstream of G6P is responsible for its increased expression in hyperglycaemia. Knockdown of PFKL in HG-cells potentiated the upregulation of *Nr0b2* (figure 5.8d), suggesting that F2,6BP may trigger induction of the gene. Knockdown of ALDOB appears to potentiate the upregulation of *Nr0b2* even more effectively (figure 5.8e), which might suggest a potential synergistic effect of F1,6BP and F2,6BP. However, this was only a single experiment and needs replicating. Intriguingly, *Nr0b2* expression was unaffected by 6-AN in LG-cells but was further elevated by 6-AN in HG-cells (figure 5.8f), suggesting that a pentose phosphate pathway intermediate may also be involved in augmenting levels of SHP during hyperglycaemia. Since it is upregulated in hyperglycaemic β-cells by metabolites other than G6P, SHP might account for the (small) proportion of transcriptional repression that cannot be explained by pooling of G6P and activation of associated signalling pathways.

Figure 5.8: Regulation of SHP expression by glucose metabolism

qPCR analysis of *Nr0b2* (SHP) expression in the following experiments (see figure indicated for details):

Expression at 48 hrs in LG-cells and HG-cells (data collated from figures 5.8d, 5.8e, and 5.8f)

Koningic acid (n=3; see figure 4.8)

2-deoxyglucose (n=5; see figure 4.12)

PFKL+PFKM double KD (n=2; see figure 4.10)

ALDOA+ALDOB double KD (n=1; see figure 4.11)

6-aminonicotinamide (n=4; see figure 4.14)

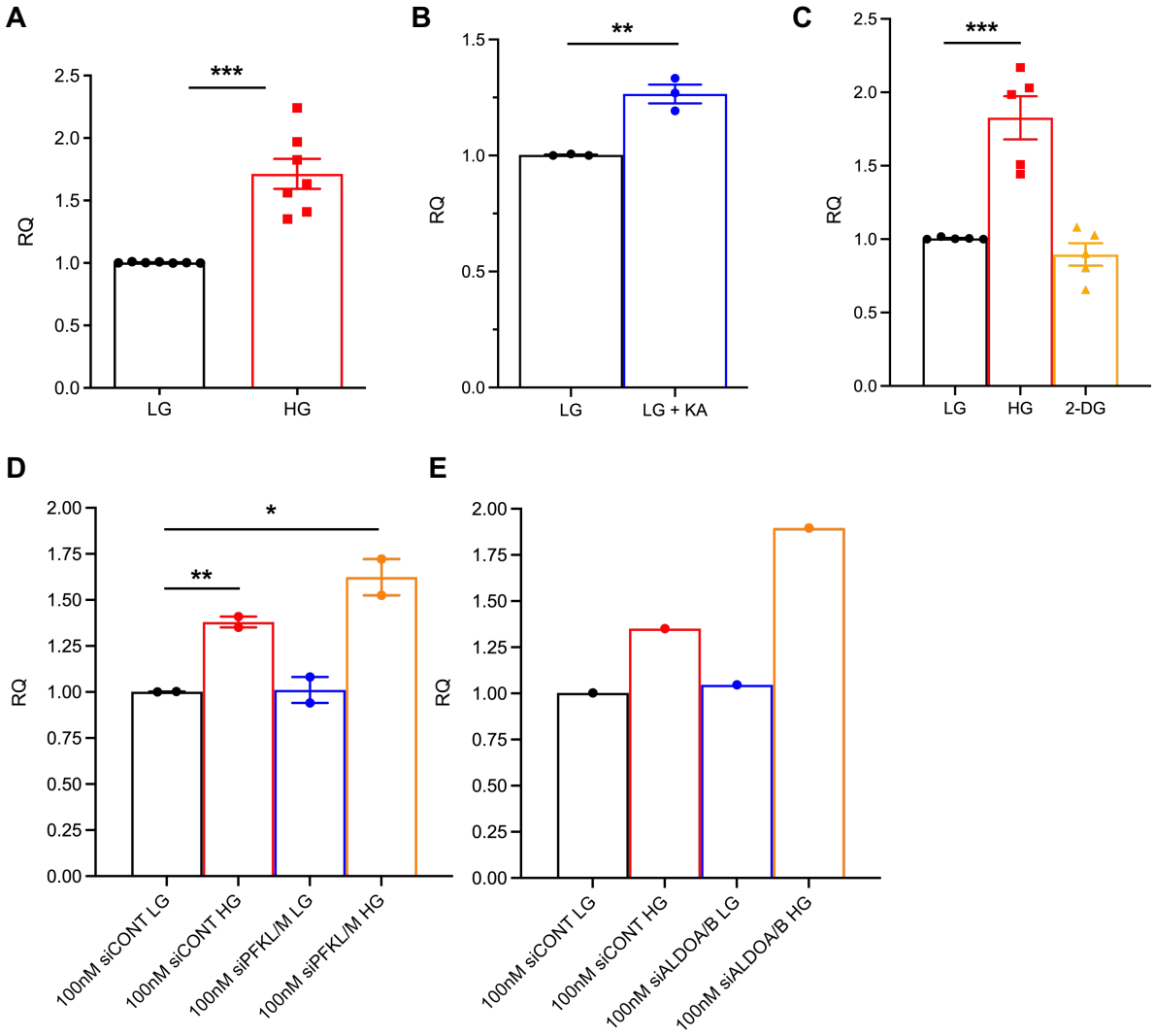

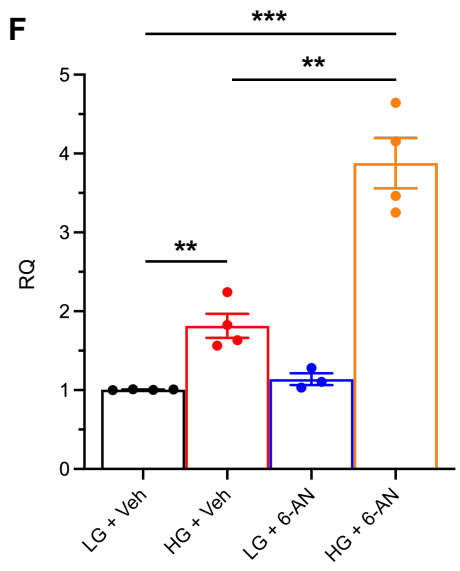

5.4.4 Inhibiting mTORC1/S6K1 signalling does not prevent the loss of insulin expression in hyperglycaemia

To inhibit mTOR signalling through p70-S6 kinase (S6K1), I used the small molecule inhibitor of S6K1, PF-4708671 (S6Ki). As well as preventing the impairment of oxidative metabolism (Haythorne et al., 2022), S6Ki prevented many of the hyperglycaemia-induced changes in metabolic gene expression (figure 5.9). The upregulation of *Pfkl* and *Eno1* was prevented by S6Ki, and upregulation of *Pfkfb3* and *Aldob* was partially prevented. S6Ki upregulated *Pfkfb2* in LG-cells but did not prevent its downregulation in HG-cells. Downregulation of TCA cycle and OXPHOS genes was not prevented by S6Ki, but upregulation of *Pdk1* appeared to be prevented, although the difference did not quite meet statistical significance ($p = 0.059$). It is interesting to note that the OXPHOS genes *Sdha*, *Ndufa4*, and *Ndufs8*, the downregulation of which in HG-cells was not prevented by S6Ki (figure 5.9b), were downregulated in cells cultured with 20 mM methyl succinate (figure 4.6b). It appears, therefore, that

expression of these genes can be regulated by both glycolytic and mitochondrial metabolites via mTORC1-independent mechanisms.

Despite these promising impacts on the expression of metabolic genes, S6Ki failed to prevent the downregulation of the insulin genes in HG-cells (figure 5.10a). Instead, S6K1 inhibition downregulated insulin gene expression in LG-cells, reducing *Ins1* expression by ~65% and *Ins2* by ~80%. Interestingly, this did not result in a change in insulin content, which was unaffected by S6Ki in both low and high glucose (Haythorne et al., 2022).

Figure 5.9: Effect of chronic S6K1 inhibition on the expression of genes involved in glycolysis and oxidative metabolism

qPCR analysis of the expression of genes involved in **(a)** glycolytic metabolism and **(b)** mitochondrial metabolism in INS-1 cells incubated with 5 or 25 mM glucose ± 10 μM PF-4708671 (S6Ki) for 48 hrs. Control samples were treated with an equivalent volume of DMSO (veh). n=3-4, with 2-3 technical replicates per experiment. *p < 0.05, **p < 0.01, ***p<0.001; 1-way ANOVA with Bonferroni's correction.

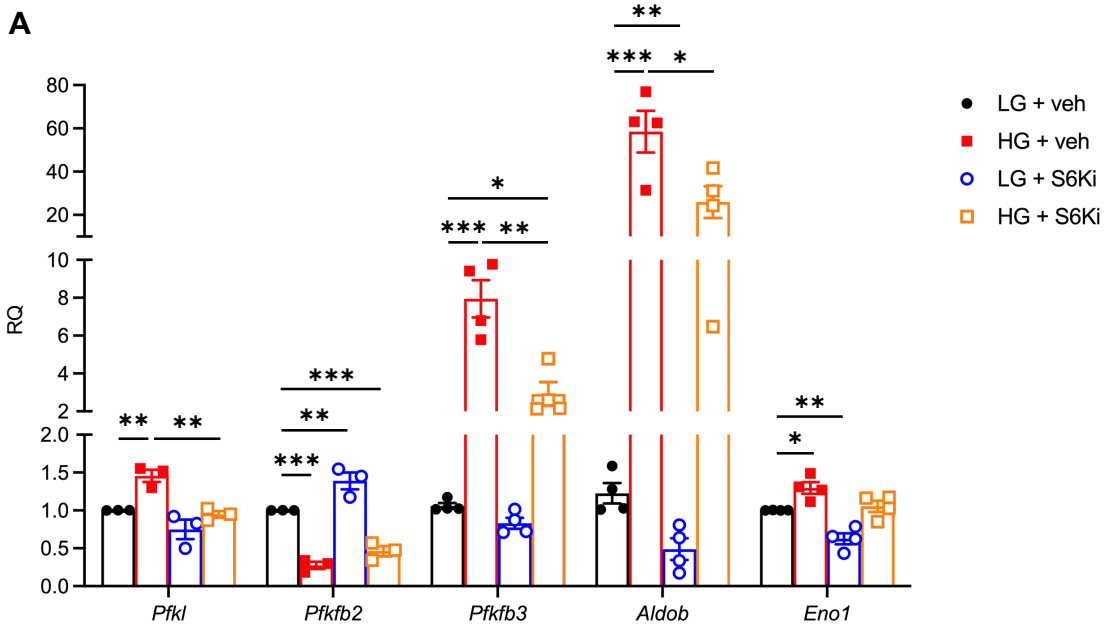

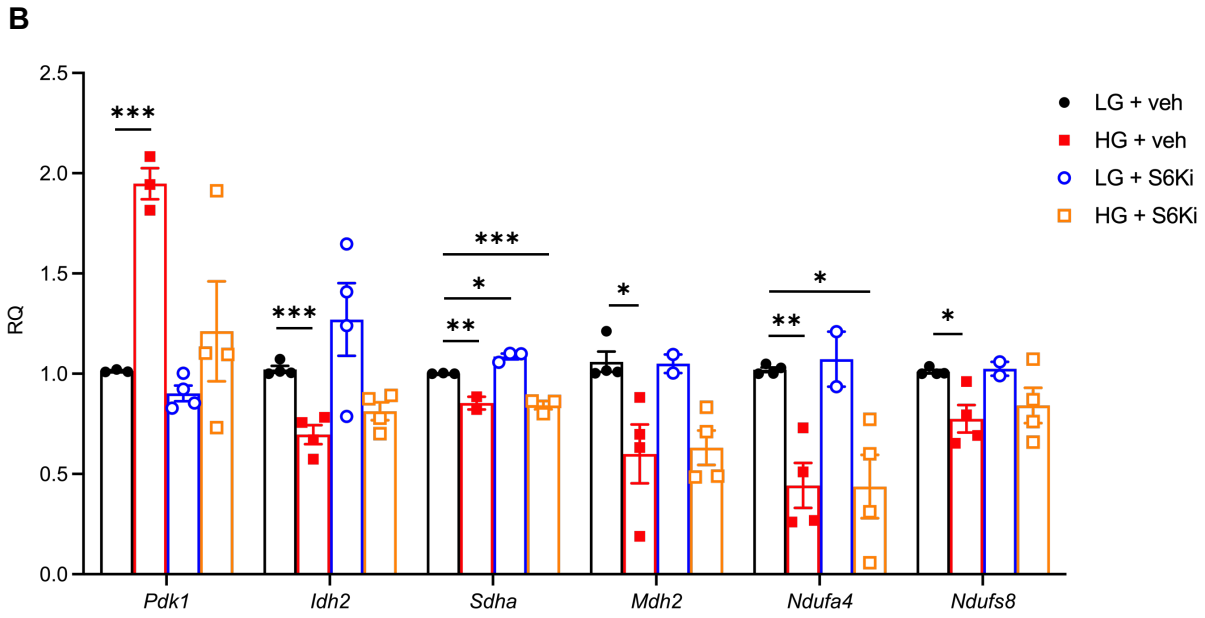

Figure 5.10: Effect of chronic S6K1 inhibition on expression of the insulin genes and *Txnip*

qPCR analysis of the expression of **(a)** the insulin genes and **(b)** *Txnip* in INS-1 cells incubated with 5 or 25 mM glucose ± 10 μM PF-4708671 (S6Ki) for 48 hrs. Control samples were treated with an equivalent volume of DMSO (veh). n=3-4, with 2-3 technical replicates per experiment. *p < 0.05, ***p<0.001; 1-way ANOVA with Bonferroni's correction.

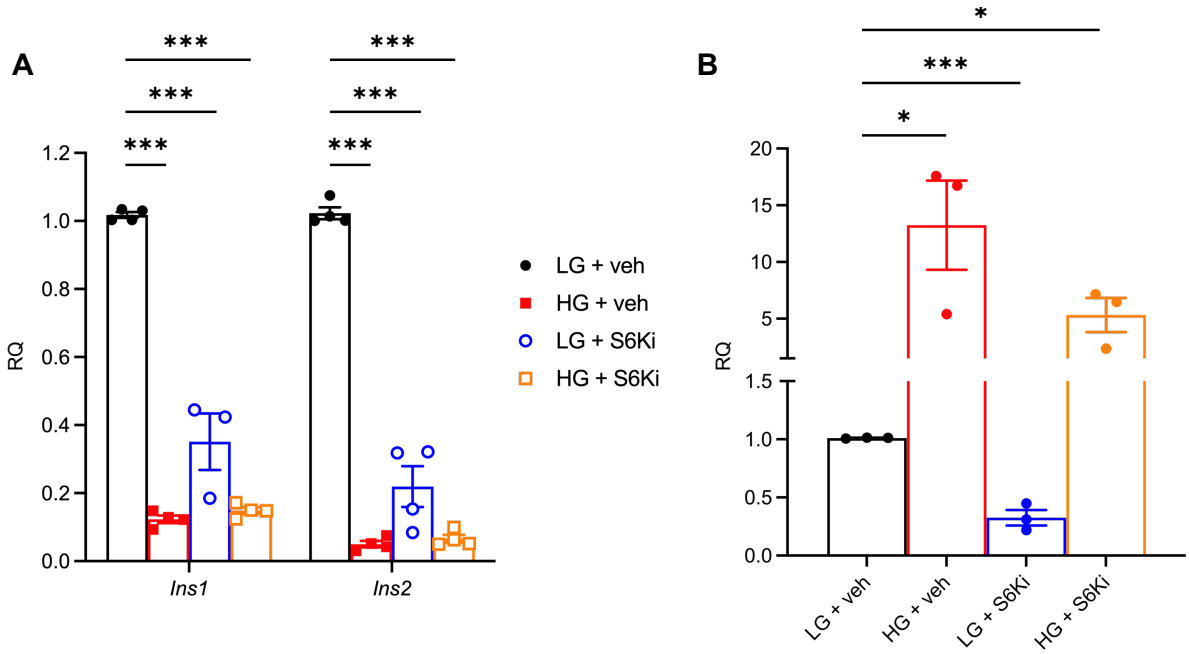

Intriguingly, mTORC1 binds to and prevents nuclear translocation of the ChREBP-MLX complex, thus reducing induction of *Txnip* (Chau et al., 2017), suggesting that mTOR signalling might regulate insulin transcription by modulating TXNIP expression. To find out whether this mechanism can explain the downregulation of insulin gene expression in euglycaemia by S6Ki, I measured expression of *Txnip* in LG-cells incubated with chronic S6Ki. *Txnip* mRNA was downregulated by ~70% in these cells, and also appeared to be downregulated to a similar extent by S6Ki in HG-cells, though this difference was not significant (figure 5.10b). This result fits with the unexpected downregulation of insulin gene expression by TXNIP KD (figure 5.6c): in each experiment, reducing *Txnip* expression was associated with a reduction in insulin mRNA levels. I plan to investigate this further by measuring expression of the β-cell identity genes in S6Ki-treated LG-cells to ascertain whether these transcription factors, particularly *Nkx6-1*, are downregulated.

5.4.5 Metformin increased insulin gene expression in euglycaemia but did not prevent loss in hyperglycaemia

To test the effect of chronic metformin treatment on insulin biosynthesis, I used a concentration of 0.5 mM. This is 10-fold to 50-fold higher than the systemic plasma concentration *in vivo* (He & Wondisford, 2015), but higher concentrations are often used *in vitro* because the drug accumulates in tissues, reaching concentrations that can (depending on the tissue) be much higher than in plasma (Wilcock & Bailey, 1994). Moreover, 0.5 mM is a concentration that has been shown to be effective in INS-1 cells for preventing glycogen accumulation (Brereton et al., 2016). In LG-cells, metformin strikingly upregulated insulin gene expression, increasing *Ins2* mRNA

levels 2.5-fold, yet paradoxically reduced *Mafa* levels by some 50% (figure 5.11a). Expression of the other β-cell identity genes in LG-cells was unaffected by metformin. In spite of this upregulation of insulin mRNA levels, metformin treatment appeared to reduce insulin content by half in LG-cells (figure 5.11b). In HG-cells, there was no effect of metformin on gene expression or insulin content. Metformin reduced *Txnip* expression in LG-cells by ~50% (figure 5.11c). This was similar to the effect of S6Ki, despite the two drugs having an opposite effect on insulin gene expression.

Figure 5.11: Effects of chronic metformin on insulin biosynthesis and *Txnip* expression

(a) qPCR analysis of the expression of the insulin genes and selected β-cell identity genes in INS-1 cells incubated with 5 or 25 mM glucose ± 0.5 mM metformin for 48 hrs. n=3, with 2 technical replicates per experiment. *p < 0.05, **p < 0.01, ***p<0.001; 1-way ANOVA with Bonferroni's correction.

(b) Total insulin content (ng/μg protein) of INS-1 cells incubated with 5 or 25 mM glucose ± 0.5 mM metformin for 48 hrs. n=1; individual values with error bars showing mean of technical replicates ± SD.

(c) qPCR analysis of the expression of *Txnip* in INS-1 cells incubated with 5 or 25 mM glucose ± 0.5 mM metformin for 48 hrs. n=2, with 2 technical replicates per experiment.

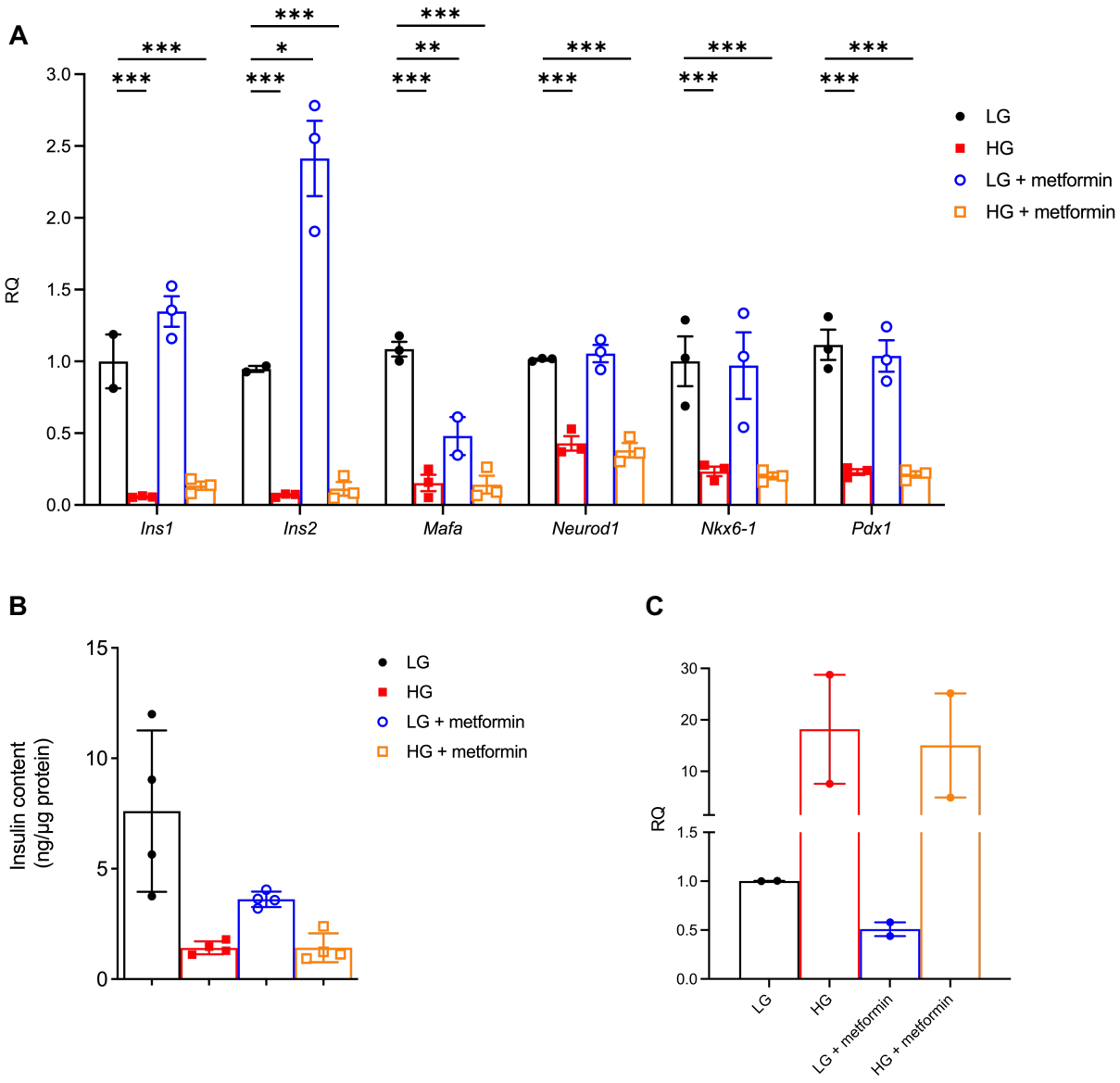
A
RQ
3.0
2.5
2.0
1.5
1.0
0.5
0.0
***
*
**
Ins1
Ins2
Mafa
Neurod1
Nkx6-1
Pdx1
LG
HG
LG + metformin
HG + metformin
B
Insulin content (ng/µg protein)
15
10
5
0
C
RQ
30
20
10
1.5
1.0
0.5
0.0
LG
HG
LG + metformin
HG + metformin

5.5 Discussion

The failure of isradipine to prevent the loss of insulin mRNA in HG-cells ruled out chronic high intracellular calcium as a cause of this loss. I did not measure the cytosolic calcium content of HG-cells, but evidence suggests that resting $[Ca^{2+}]_{in}$ is not elevated in chronic hyperglycaemia, contrary to the implicit assumption of Lawrence *et al.* (2005). Presumably the authors reasoned that the rapid increase caused by acute glucose stimulation and consequent β-cell depolarisation would persist over longer timescales. However, 4 days culture of mouse islets at 10 mM glucose did not cause elevation of resting $[Ca^{2+}]_{in}$ relative to islets cultured at 5 mM (Gilon et al., 1994). Instead, adaptations to hyperglycaemia seemingly keep $[Ca^{2+}]_{in}$ buffered at an appropriate level. In a 90% pancreatectomy rat model of mild hyperglycaemia, changes in gene expression include downregulation of several voltage-gated calcium channel subunits (*Cacna1a*, *Cacna1b*, and *Cacna1d*) and the ER calcium sensor *Stim1* and upregulation of calcium-binding proteins *S100a4* and *S100a6* (Ebrahimi et al., 2020). However, according to RNAseq, *Cacna1a* was upregulated in diabetic βV59M mice and the rest of these genes did not change (Haythorne et al., 2019). ERK1/2 activation, while calcium-dependent, does not therefore appear to be driven by high calcium. Instead, accumulation of PPP intermediates during chronic hyperglycaemia may cause ERK1/2-mediated repression of insulin promoter activity (Goehring et al., 2011). This work would be strengthened by calcium measurements or qPCR analysis of *S100a4* and *S100a6* expression, as these two genes may serve as markers of high $[Ca^{2+}]_{in}$ (Stancill et al., 2017).

The extremely rapid induction of *Txnip* at the onset of hyperglycaemia and relatively slow reversal of this upregulation following restoration of euglycaemia mirrors the rapid

downregulation and slow recovery of insulin gene expression. This comparison suggests that persistent TXNIP activity, both during and for some hours following an episode of hyperglycaemia, could contribute to a progressive decline in insulin biosynthesis. Of all the manipulations I used to probe the metabolic regulation of insulin biosynthesis, 2-DG was particularly effective at downregulating insulin gene expression (figure 4.13). 2-DG also upregulated *Txnip* robustly (figure 5.4i), probably through activation of ChREBPβ by 2-DG-6-P (Katz et al., 2022). Mannoheptulose completely prevented any hyperglycaemia-induced increase in *Txnip* expression (figure 5.4d), indicating that conversion of glucose to G6P is essential for its induction. However, the non-metabolisable sugar 3-O-methylglucose (which, unlike 2-DG, cannot be phosphorylated by glucokinase) is nevertheless able to upregulate *Txnip* even in the presence of mannoheptulose (Minn et al., 2006). 3-O-methylglucose likely acts through direct activation of ChREBP. Direct activation of ChREBP by glucose could perhaps account for the incomplete restoration of *Ins2* expression by mannoheptulose in HG-cells (figure 4.2), since the reduction in glucokinase activity is sufficient to normalise expression of most genes.

Upregulation of TXNIP is postulated to lead to downregulation of MAFA via induction of miR-204 (figure 5.1b; Xu et al., 2013). However, my data do not support this mechanism, as TXNIP KD reduced, and ChREBP KD increased, insulin gene expression in LG-cells (figures 5.5b and 5.6c). These results suggest that ChREBPβ may repress insulin gene expression through a different pathway. The interpretation of these results would be aided by determination of the expression of both isoforms of ChREBP, as chronic overexpression of ChREBPβ causes reduced expression of the insulin genes and all of the identity genes except *Neurod1* (Katz et al., 2022). Ideally, I would also determine the subcellular localisation of ChREBP in different conditions.

It is possible that, despite an overall decline in ChREBP expression in HG-cells, an elevated ratio of ChREBPβ to ChREBPα, and/or an increase in the nuclear fraction of ChREBP, is driving the loss of insulin biosynthesis in chronic hyperglycaemia. This could be through the aforementioned upregulation of TXNIP driven by ChREBPβ (Katz et al., 2022), although my data suggest that upregulation of TXNIP may merely correlate with downregulation of the insulin genes rather than being causative. Alternatively, TXNIP could be a double-edged sword, positively regulating insulin biosynthesis in euglycaemia, but repressing insulin gene expression through its ChREBPβ-mediated upregulation during chronic hyperglycaemia. This view is supported by the evidence that expression of both *Txnip* and the insulin genes is significantly lower at 0 mM and 2 mM glucose than at 5 mM glucose (figures 3.3 and 5.4a). The observation, from comparison of insulin content (figure 3.9) and *Txnip* expression (figure 5.4b) in isolated islets from IGT mice and mildly or severely hyperglycaemic mice, that the decline in insulin biosynthesis precedes the upregulation of *Txnip* suggests that, if TXNIP drives the downregulation of insulin gene expression, it is likely a secondary rather than a primary driver. To draw more solid conclusions about the roles of ChREBP and TXNIP, I would ideally achieve a high knockdown efficiency (≥ 80%) for both of these genes. An alternative strategy would be to use the novel small molecule inhibitor of TXNIP SRI-37330, which is being evaluated as a drug candidate (Thielen et al., 2020).

Whether or not TXNIP is involved in the hyperglycaemia-induced downregulation of insulin biosynthesis, it is believed to play an important role in mediating β-cell dysfunction. Apart from the mechanisms discussed here, TXNIP causes oxidative stress and promotes β-cell apoptosis by inhibiting thioredoxin (Shalev, 2014). It has been implicated in dysregulation of autophagy (W. Deng et al., 2020). Persistence of

Txnip expression following reversal of hyperglycaemia may indicate that oxidative stress also persists for some time.

In chapter 4, I concluded that G6P appears to be the most important metabolite for the downregulation of insulin biosynthesis during chronic hyperglycaemia. However, other metabolites may, to a lesser extent, also contribute to the downregulation of insulin biosynthesis. SHP, which was upregulated by high glucose but not by 2-DG (figure 5.8c), is reported to downregulate insulin gene expression through two modes of action, affecting both transcription factor expression and complex formation at the insulin promoter (figure 5.1c). Upregulation of the gene appeared to depend on a combination of glycolytic and pentose phosphate intermediates, likely including F1,6BP and/or F2,6BP.

The results of S6K1 inhibition and metformin treatment on insulin gene expression in euglycaemic INS-1 cells were curious. It was unexpected that metformin and S6Ki had opposite effects on insulin gene expression, as they have similar effects on metabolism, including suppression of glycogen storage (figures 7.7 and 7.8). It is also puzzling that changes in insulin gene expression did not correspond to changes in insulin content as has been the case in other experiments. If we suppose that metformin's mode of action is solely or largely through mTORC1, the downregulation of insulin content by metformin but not S6Ki might be reconciled by consideration of the different signalling pathways downstream of mTORC1. Insulin biosynthesis is positively regulated by the mTORC1/4E-BP2-eIF4E pathway, as 4EBP2/eIF4E promotes cap-dependent translation of the insulin-processing enzyme carboxypeptidase E, whereas S6K overactivation neutralises the enhancement of insulin processing produced by 4E-BP2/eIF4E activation (Blandino-Rosano et al.,

2017). Thus, metformin might downregulate insulin processing by inhibiting mTORC1 signalling via 4E-BP, while inhibition of only the S6K pathway by S6Ki does not affect insulin processing. The downregulation of insulin gene expression by S6Ki, however, remains unresolved, especially as PDX1 protein levels are diminished in S6K gain-of-function mice (Blandino-Rosano et al., 2017). The positive effect of metformin on insulin gene expression in LG-cells could be due to inhibition of FBPase, improving glycolytic flux and attenuating the accumulation of G6P. This mode of metformin action will be discussed in more depth in chapter 7.

In conclusion, downregulation of insulin biosynthesis in chronic hyperglycaemia is the result of the accumulation of a small number of metabolites, but the downstream signalling pathways linking metabolic impairment to the loss of insulin content are complex. It is likely that ChREBP, SHP, ERK1/2, and mTORC1 are all involved, and more work is needed to determine which pathway makes the greatest contribution.

6. siRNA screen to identify key regulators of insulin biosynthesis and secretion in human β-cell lines

6.1 Summary

1. An siRNA screen of selected genes of interest was performed to determine if they influence insulin biosynthesis and insulin secretion in two human β-cell lines (EndoC-βH1 and EndoC-βH5) in euglycaemia and in chronic hyperglycaemia.
2. The majority of genes targeted in both βH1 and βH5 cells were knocked down by at least 70%. The exceptions were *PFKL*, *TXNIP*, and *PPP1R3C*.
3. Knockdown of most genes had no clear effect on insulin gene expression, insulin secretion, or insulin content.
4. Knockdown of *TXNIP* appeared to cause a decline in insulin biosynthesis in euglycaemic βH5 cells.
5. Knockdown of *PYGL* appeared to cause a decline in insulin gene expression in βH5 cells and declines in insulin biosynthesis and secretion in both βH1 and βH5 cells. This was associated with reduced *TXNIP* expression, suggesting that glucose-6-phosphate levels were lowered due to increased glycogenesis.
6. *MLXIPL* (ChREBP) expression appeared to be reduced by Txnip KD and increased by *PYGL* KD.
7. The results of the siRNA screens suggest that glucose-6-phosphate levels affect insulin gene expression in EndoC cells, but these cells are less sensitive to glucotoxic effects of G6P than INS-1 cells.

6.2 Introduction

As part of my industrial placement at NNRCO, I followed up on my findings from INS-1 cells (described in chapter 4) regarding the metabolic regulation of insulin biosynthesis by running siRNA screens of a few selected genes of interest in EndoC cells, with insulin gene expression, GSIS, and insulin content as readouts. As described in chapter 3, EndoC cells show modest downregulation of insulin biosynthesis during chronic hyperglycaemia, but this is much less severe than seen in INS-1 cells. Due to limited time availability during the placement, I conducted the siRNA screens in parallel with the experiments described in chapter 3; I was therefore unable to apply the knowledge gained from those experiments to the design of the experiments described in this chapter.

To investigate the effects of glycolytic inhibition, and in an effort to distinguish between the effects of glucose-6-phosphate, fructose-6-phosphate, and other intermediates in upper glycolysis, I knocked down GAPDH, PFKL, FBP1, and phosphoglucose isomerase, also known as glucose-6-phosphate isomerase (GPI). All of these genes are upregulated in diabetic βV59M islets (table 4.1). I also knocked down PDK1, another enzyme that is strongly upregulated in diabetes (table 4.2) and which has been found to negatively affect GSIS in INS-1 cells by reducing flux from pyruvate into the TCA cycle (Krus et al., 2010). I knocked down TXNIP for comparison with my investigations in INS-1 cells (described in chapter 5). Finally, I knocked down PYGL, the main β-cell isoform of glycogen phosphorylase, to investigate whether glycogen metabolism can affect insulin biosynthesis and secretion. Unfortunately, I did not have

time to replicate these screens, so each figure in this chapter represents only one experiment.

6.3 Methods

Cells were cultured as described in chapter 2 (section 2.2). Cells were transfected with siRNA as described in section 2.5.2. RNA extraction and qPCR was conducted as described in section 2.6.2. Insulin secretion and content were assayed as described in sections 2.8.3 and 2.8.4. For the screen in βH5 cells, 2 plates were seeded and transfected simultaneously, one for GSIS and one for RNA samples. For insulin secretion experiments, cells were starved for 2 hours prior to the pre-stimulation incubation; during this step, RNA was extracted from the other plate.

6.4 Results

6.4.1 siRNA screen in EndoC-βH1 cells

I knocked down 8 genes in βH1 cells at the standard culture condition of 5.5 mM glucose. As a control experiment to validate the methodology, I also knocked down the insulin gene (*INS*). With 25 nM siINS, I achieved 85% knockdown efficiency (figure 6.1 and table 6.1), leading to an equivalent reduction in insulin content (figure 6.2b). As expected, *INS* knockdown severely impaired basal insulin secretion and abolished glucose-stimulated secretion (figure 6.2a).

Figure 6.1 shows the efficiency of each knockdown and its effect on insulin gene expression, and the percentage knockdown efficiency for each gene is listed in table

6.1. KD efficiencies were generally high (>70%), with the exceptions of *PFKL* (surprisingly, as this gene was knocked down by 80% at 5 mM glucose in INS-1 cells), *TXNIP* (which seems to be a difficult gene to knock down effectively whether in EndoC cells or INS-1 cells), and *PPP1R3C* (PTG), which was more highly expressed in cells transfected with siPPP1R3C than those transfected with non-targeting control siRNA. The knockdowns mostly had no effect on insulin mRNA levels, but knockdown of *PDK1* appeared to cause increased expression of *INS. INS* expression also appeared to be increased in cells transfected with siPPP1R3C. However, as stated earlier, the knockdown did not work.

Table 6.1: Knockdown efficiency (% decrease in mRNA expression relative to control) for each gene in βH1 cells

Gene	KD efficiency (%)
INS	85
GAPDH	83
PFKL	47
FBP1	77
GPI	78
PDK1	75
TXNIP	43
PPP1R3C	-21
PYGL	72

Table 6.2: Stimulation index for each combination of siRNA and chronic glucose concentration

siRNA	Glucose culture (mM)	
	5.5	**35**
siNT	1.8	1.2
siINS	1.5	1.4
siGAPDH	1.8	1.4
siGPI	1.5	1.6
siPDK1	1.5	1.4
siTXNIP	2.1	1.4
siPYGL	1.9	1.5

Figure 6.1: Effect of siRNA knockdown of selected genes on insulin gene expression in EndoC-βH1 cells

qPCR analysis of KD efficiency and *INS* mRNA expression following siRNA knockdown of *INS*, *PDK1*, *GAPDH*, *PFKL*, *FBP1*, *GPI*, *TXNIP*, *PPP1R3C*, and *PYGL* in EndoC-βH1 cells. Cells were transfected with 25 nM targeting or control siRNA and incubated at 5.5 mM glucose for 5 days. n=1; individual values plotted with error bars showing mean of technical replicates ± SD.

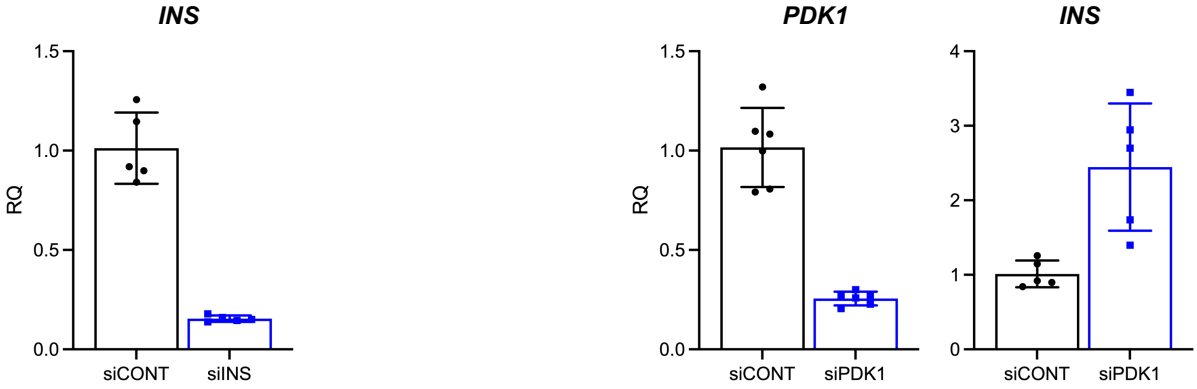

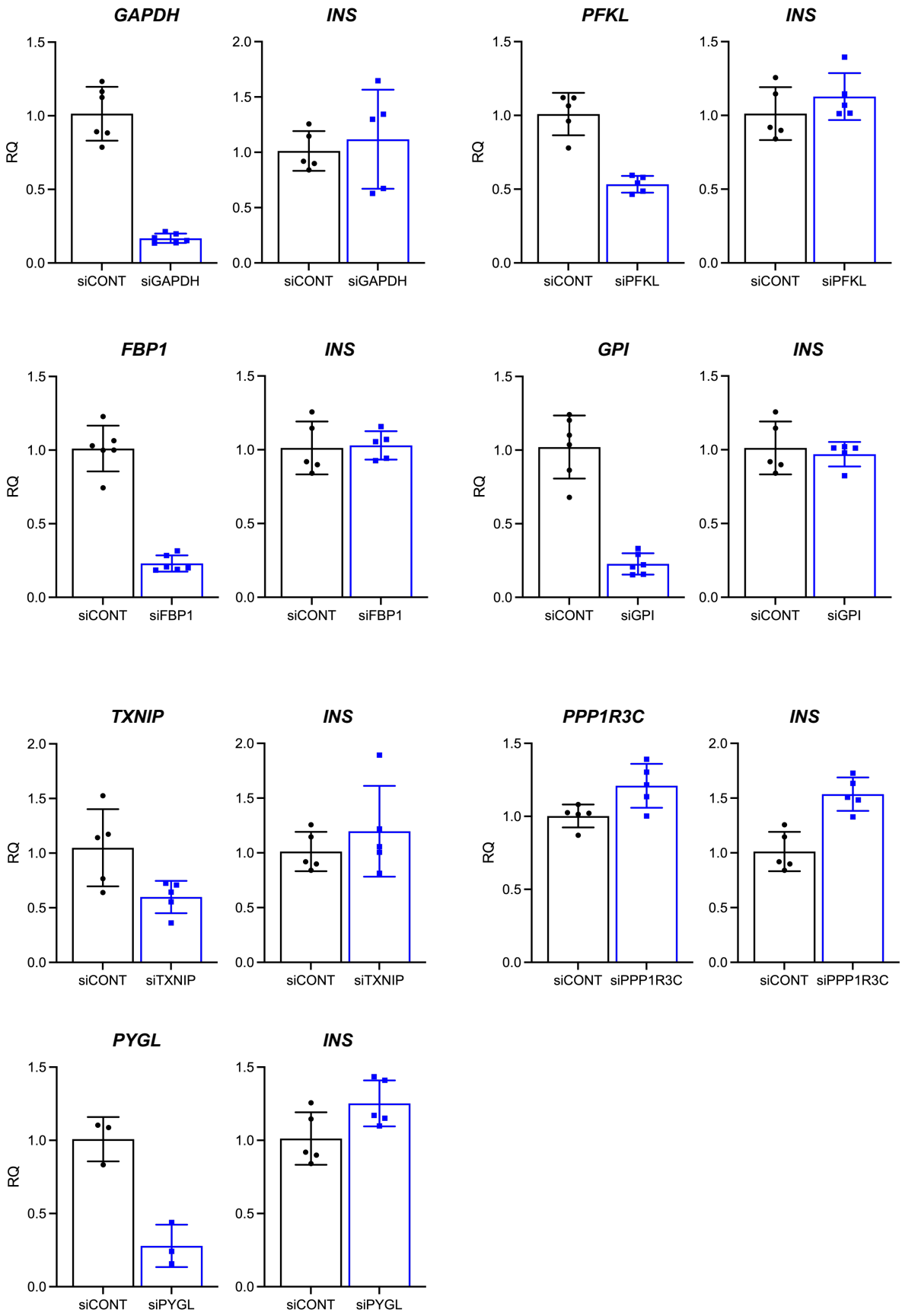
GAPDH
INS
PFKL
INS
FBP1
INS
GPI
INS
TXNIP
INS
PPP1R3C
INS
PYGL
INS
RQ
siCONT
siGAPDH
siPFKL
siFBP1
siGPI
siTXNIP
siPPP1R3C
siPYGL

Having demonstrated successful knockdowns of most genes, I then knocked down *INS*, *GAPDH*, *GPI*, *PDK1*, *TXNIP*, and *PYGL* at 5.5 mM and 35 mM glucose and measured insulin secretion and insulin content (figure 6.2). Although flawed for the reasons discussed in chapter 3, I have included stimulation index (SI) calculations (table 6.2) as SI can be considered a measure of the efficiency of stimulus-secretion coupling. On this basis, knockdown of *INS* should reduce insulin secretion in absolute terms but not substantially affect the SI, which appeared to be the case. Basal insulin secretion (at 0 mM glucose, grey) appeared to be slightly increased by chronic hyperglycaemia (culture at 35 mM glucose) and GSIS (at 20 mM glucose, orange) was decreased, resulting in a fall in the stimulation index (SI) from 1.8 to 1.2. This approximates a diabetic state.

Figure 6.2: Effect of siRNA knockdown of selected genes on insulin secretion and insulin content in EndoC-βH1 cells

(a) Basal and glucose-stimulated insulin secretion (ng/ml/hr) and **(b)** total insulin content (μg/10^6 cells) following siRNA knockdown of *INS*, *PDK1*, *GAPDH*, *GPI*, *TXNIP*, and *PYGL* in EndoC-βH1 cells. Cells were transfected with 25 nM targeting or control siRNA and incubated at 5.5 mM or 35 mM glucose for 5 days and stimulated with 0 or 20 mM glucose for 1 hr. n=1; individual values with error bars showing mean of technical replicates ± SD.

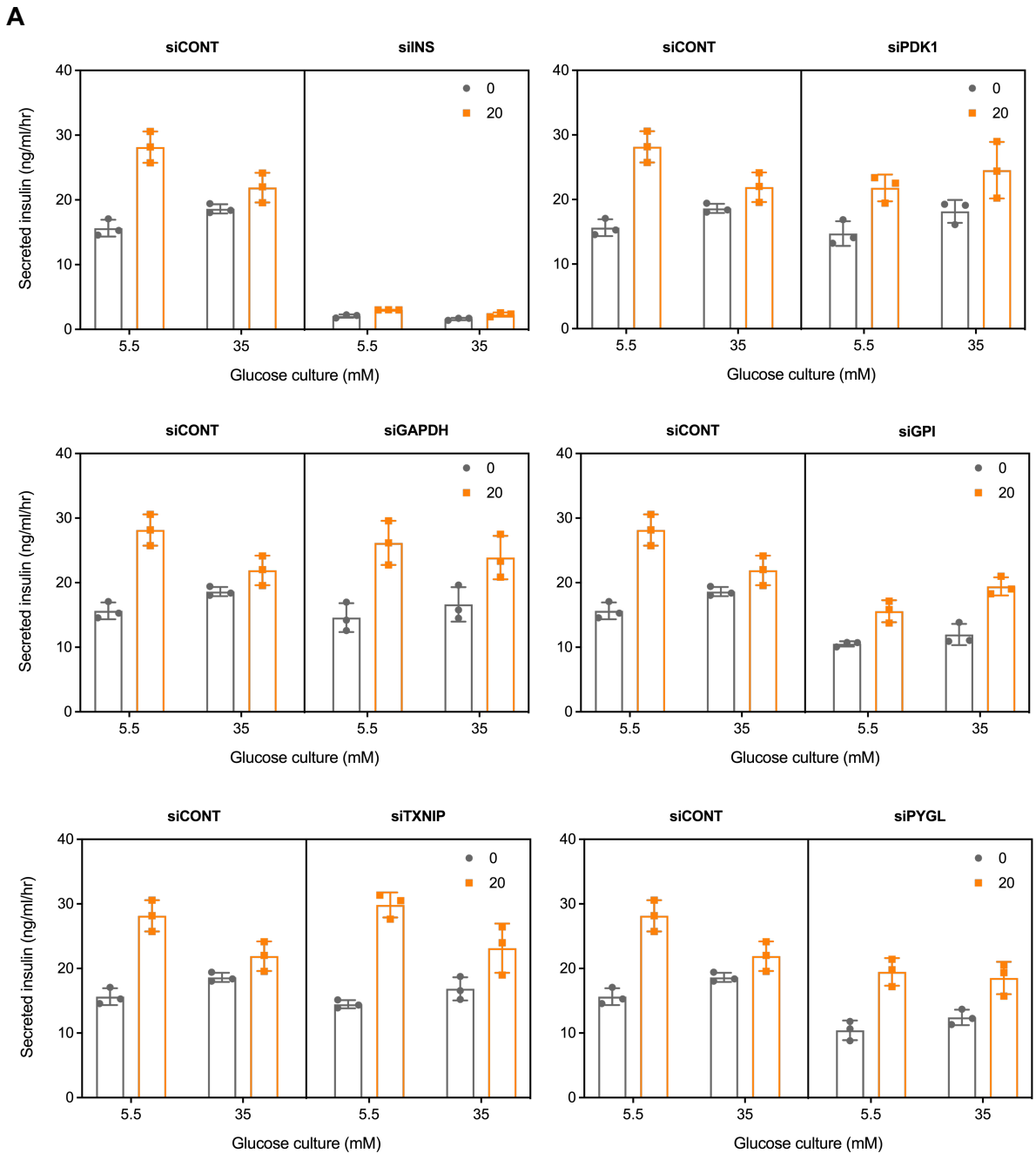
A
siCONT
siINS
siPDK1
siGAPDH
siGPI
siTXNIP
siPYGL
0
20
Secreted insulin (ng/ml/hr)
Glucose culture (mM)
5.5
35

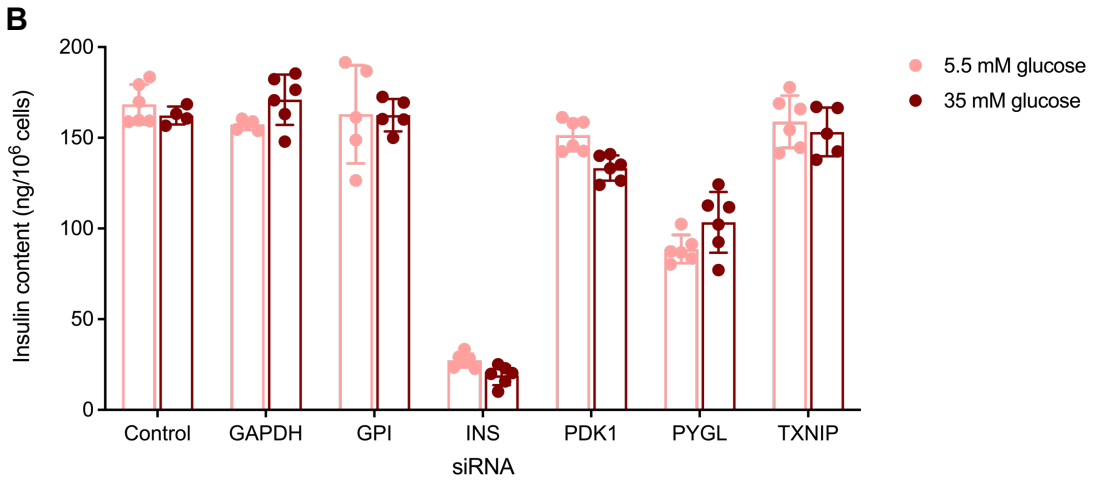
B
Insulin content (ng/10^6 cells)
5.5 mM glucose
35 mM glucose
Control
GAPDH
GPI
INS
PDK1
PYGL
TXNIP
siRNA

Knockdown of *GPI* caused both basal and stimulated insulin secretion to fall, suggesting that glycolysis was impaired, impeding stimulus-secretion coupling. However, the decline in GSIS with siGPI was negligible in cells cultured at 35 mM glucose, which might indicate that glycolysis was already impaired in these cells. In this context, it is surprising that knockdown of *GAPDH* did not impair insulin secretion. Apart from the *GPI* KD, the other knockdown that reduced both basal and stimulated insulin secretion was that of *PYGL*. Basal secretion was reduced by one third by siPYGL, which may indicate that mobilisation of stored glycogen partially sustains insulin secretion when cells are starved of glucose. The smaller reduction in stimulated secretion could be due to diversion of G6P from glycolysis towards glycogen synthesis.

Most knockdowns had no clear effect on insulin content, but *PYGL* KD appeared to reduce insulin content considerably at both 5.5 mM and at 35 mM glucose. Unfortunately, I do not have data on gene expression in βH1 cells cultured at 35 mM glucose following transfection, but *INS* expression was not decreased in cells cultured at 5.5 mM glucose following *PYGL* KD (figure 6.1).

6.4.1 siRNA screen in EndoC-βH5 cells

In βH5 cells I followed the same methodology as for βH1 cells, using 25 nM siRNA, but this time I cultured cells at three different glucose concentrations (5.5, 25, and 35 mM) for RNA extraction following transfection. In parallel, I cultured cells at 5.5 mM and 35 mM glucose following transfection for measuring insulin secretion and content. Chronic high glucose culture led to declines in insulin gene expression (figure 6.3) and insulin content (figure 6.4b). Again, I knocked down *INS*, achieving >90% knockdown

efficiency at each glucose concentration (figure 6.3 and table 6.3). This led to reductions in insulin content of nearly 40% at 5.5 mM glucose and nearly 50% at 35 mM glucose (figure 6.4b). Despite the very high KD efficiency at the mRNA level, this was a more modest reduction in insulin content than I achieved in βH1 cells, likely reflecting the much higher initial content of βH5 cells. *INS* KD reduced basal insulin secretion by 60-70% and almost completely abolished GSIS.

The knockdown efficiency for each gene is listed in table 6.3. Most genes were knocked down effectively, with KD efficiency for *PFKL* higher than in βH1 cells. The major exception was *TXNIP*, for which KD efficiency was only greater than 50% at 5.5 mM glucose and declined progressively as the glucose concentration in the culture medium increased. *TXNIP* is seemingly so strongly induced by high glucose that the capacity of the siRNA to suppress its mRNA levels is overwhelmed. Whereas *TXNIP* was potently induced by high glucose in control cells, other genes that I expected to be upregulated based on data from INS-1 cells and βV59M islets (*PDK1*, *PFKL*, and *PYGL*) were not.

Table 6.3: Knockdown efficiency (% decrease in mRNA expression relative to control) for each gene at each glucose concentration in βH5 cells

		Gene					
		INS	***PFKL***	***GPI***	***PDK1***	***TXNIP***	***PYGL***
Glucose culture (mM)	**5.5**	95	68	83	76	56	71
	25	93	56	79	79	49	77
	35	92	82	85	82	34	78

Table 6.4: Stimulation index for each combination of siRNA and chronic glucose concentration

siRNA	Glucose culture (mM)	
	5.5	**35**
siNT	3.2	6.6
siINS	2.5	2.3
siPFKL	5.1	3.3
siGPI	4.0	2.7
siPDK1	4.8	2.8
siTXNIP	4.0	2.8
siPYGL	3.6	2.8

Figure 6.3: Effect of siRNA knockdown of selected genes on insulin gene expression in EndoC-βH5 cells

qPCR analysis of KD efficiency and *INS* mRNA expression following siRNA knockdown of *INS*, *PFKL*, *GPI*, *PDK1*, *TXNIP*, and *PYGL* in EndoC-βH5 cells. Cells were transfected with 25 nM targeting or control siRNA and incubated at 5.5, 25, or 35 mM glucose for 5 days. n=1; individual values with error bars showing mean of technical replicates ± SD.

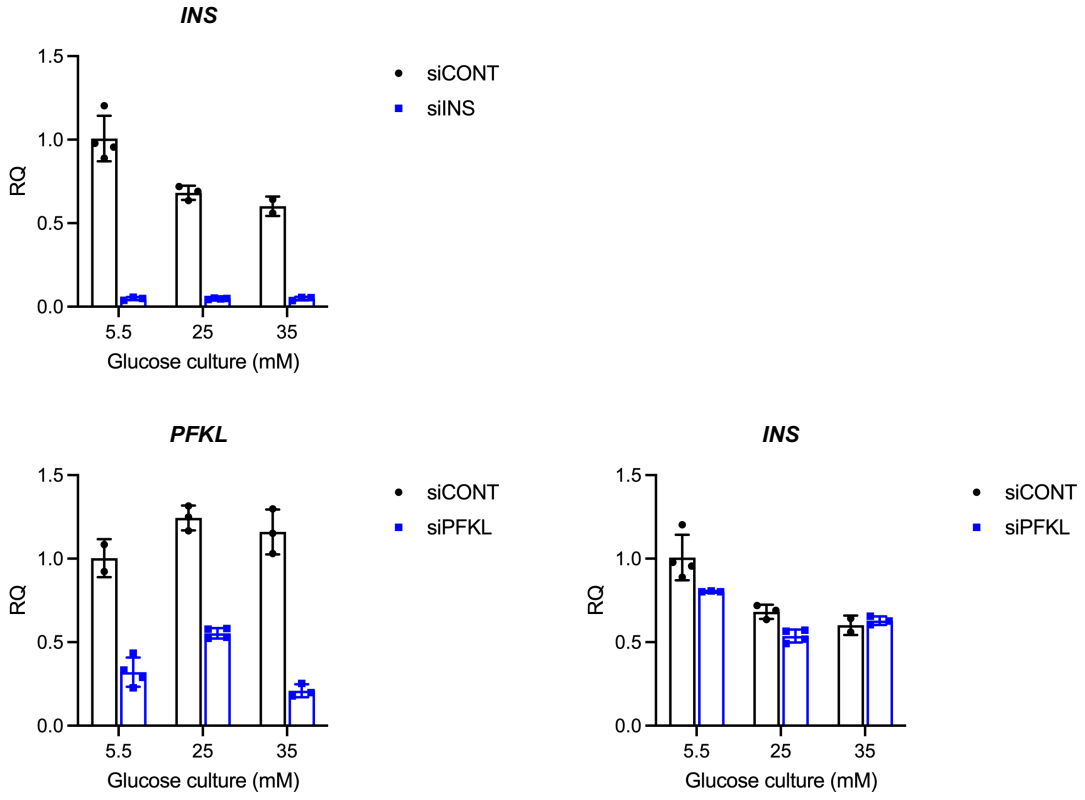

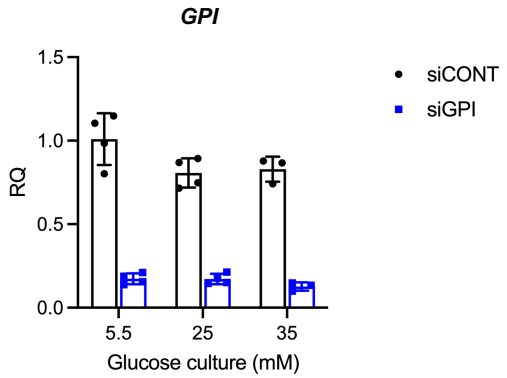
GPI
RQ
1.5
1.0
0.5
0.0
5.5
25
35
Glucose culture (mM)
siCONT
siGPI

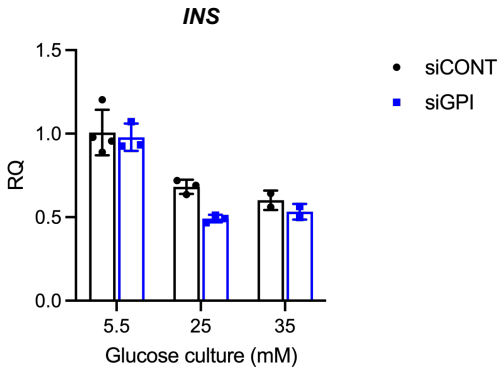
INS
RQ
1.5
1.0
0.5
0.0
5.5
25
35
Glucose culture (mM)
siCONT
siGPI

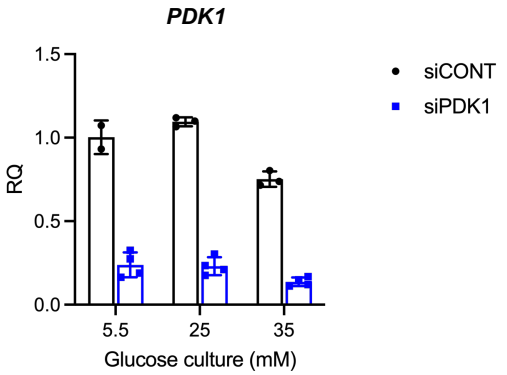
PDK1
RQ
1.5
1.0
0.5
0.0
5.5
25
35
Glucose culture (mM)
siCONT
siPDK1

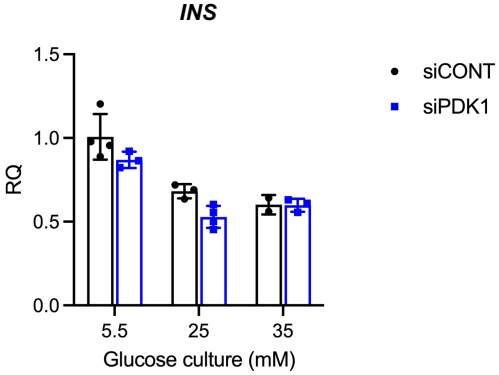
INS
RQ
1.5
1.0
0.5
0.0
5.5
25
35
Glucose culture (mM)
siCONT
siPDK1

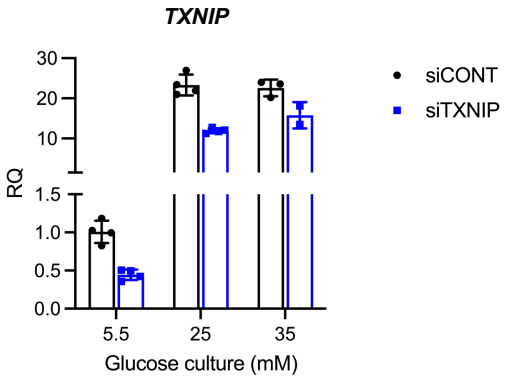
TXNIP
RQ
30
20
10
1.5
1.0
0.5
0.0
5.5
25
35
Glucose culture (mM)
siCONT
siTXNIP

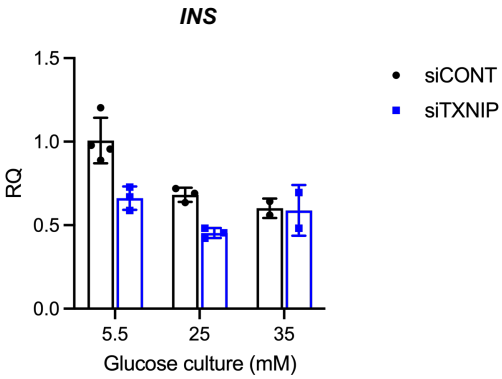
INS
RQ
1.5
1.0
0.5
0.0
5.5
25
35
Glucose culture (mM)
siCONT
siTXNIP

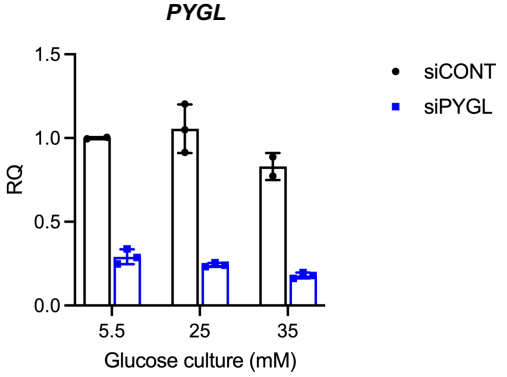
PYGL
RQ
1.5
1.0
0.5
0.0
5.5
25
35
Glucose culture (mM)
siCONT
siPYGL

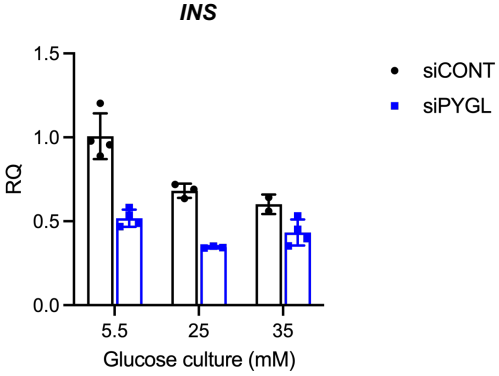
INS
RQ
1.5
1.0
0.5
0.0
5.5
25
35
Glucose culture (mM)
siCONT
siPYGL

Figure 6.4: Effect of siRNA knockdown of selected genes on insulin secretion and content in EndoC-βH5 cells

(a) Basal and glucose-stimulated insulin secretion (ng/ml/hr) and **(b)** total insulin content (μg/10^6 cells) following siRNA knockdown of *INS*, *PFKL*, *GPI*, *PDK1*, *TXNIP*, and *PYGL* in EndoC-βH5 cells. Cells were transfected with 25 nM targeting or control siRNA and incubated at 5.5 or 35 mM glucose for 5 days and stimulated with 0 or 20 mM glucose for 40 mins. n=1; individual values with error bars showing mean of technical replicates ± SD.

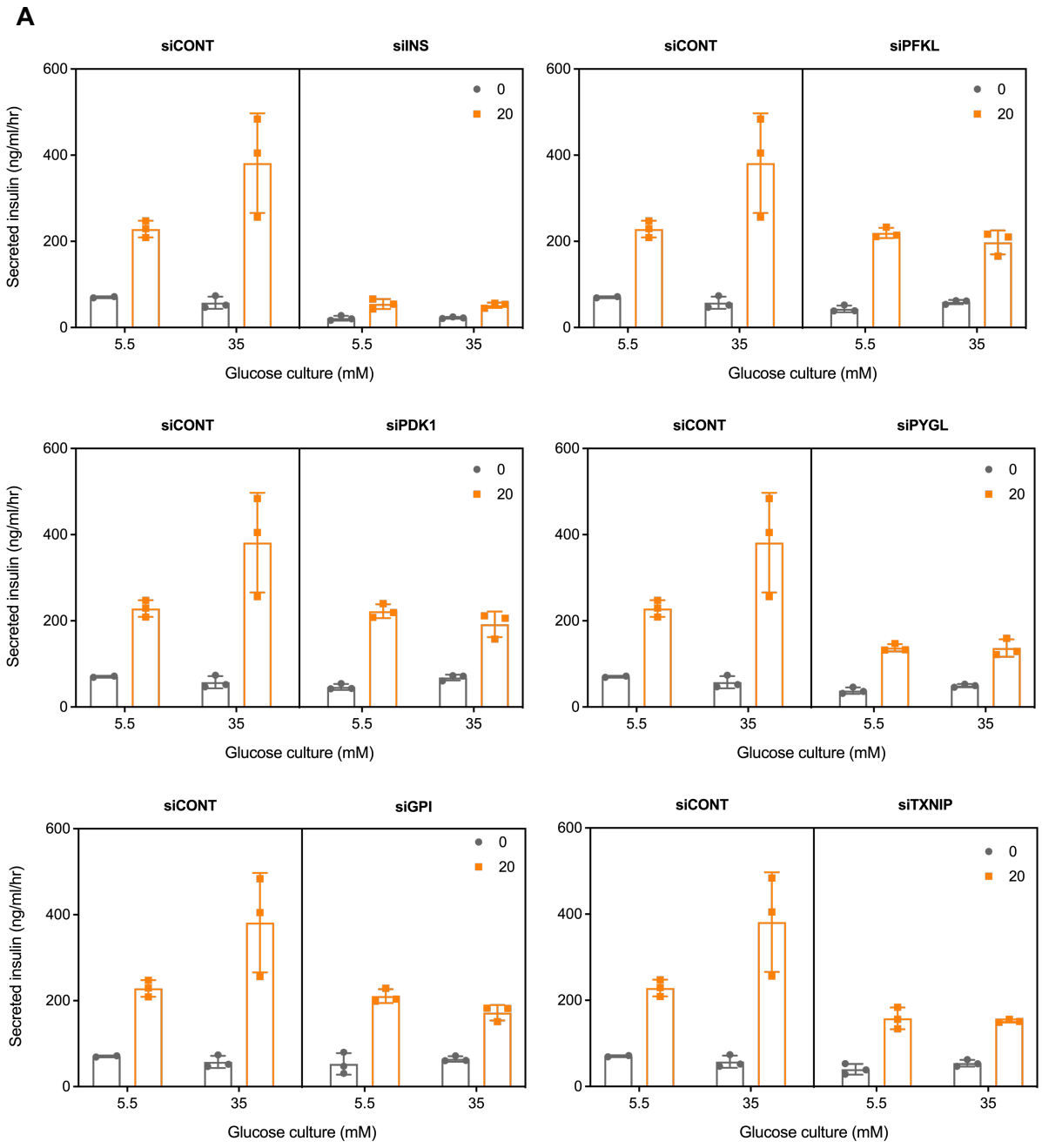

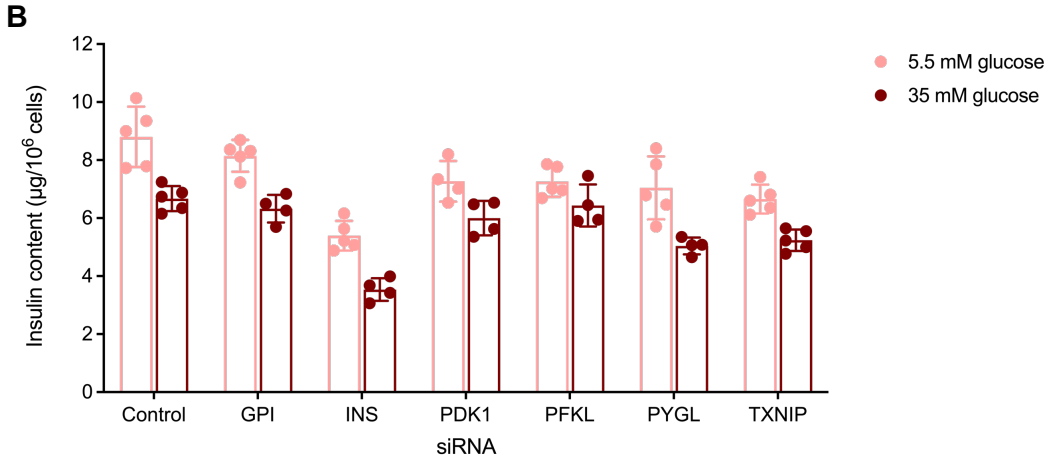

In contrast to βH1 cells, βH5 cells did not exhibit increased basal insulin secretion following chronic hyperglycaemia (figure 6.4a). This is consistent with previous experiments (figure 3.7a). Oddly, in this experiment GSIS was increased in cells cultured at 35 mM glucose relative to cells cultured at 5.5 mM glucose, causing the SI to more than double to 6.6 (table 6.4). This was not the case in previous experiments, in which GSIS appeared to be mildly impaired by chronic hyperglycaemia (figures 3.5 and 3.7), and there was no such enhancement of GSIS following any of the knockdowns, so this result can probably be dismissed as an outlier. Unfortunately, this does mean there is no reliable baseline to which I can compare any effects the knockdowns may have on insulin secretion.

The only knockdowns that appeared to have a consistent effect on insulin biosynthesis in βH5 cells were those of *TXNIP*, which unexpectedly reduced *INS* expression by one third at 5.5 mM and 25 mM glucose, and *PYGL*, which reduced *INS* expression by half at 5.5 mM and 25 mM glucose. These knockdowns also reduced insulin content by 20-25% at 5.5 mM and 35 mM glucose (figure 6.4b), and appeared to substantially impair basal insulin secretion in cells cultured at 5.5 mM glucose and GSIS in all cells (figure 6.4a).

Figure 6.5: Effect of siRNA knockdowns of TXNIP and PYGL on expression of ChREBP and MAFA in EndoC-βH5 cells

qPCR analysis of *MLXIPL* and *MAFA* mRNA expression following siRNA knockdown of *TXNIP* and *PYGL* in EndoC-βH5 cells. Cells were transfected with 25 nM targeting or control siRNA and incubated at 5.5, 25, and 35 mM glucose for 5 days. n=1; individual values with error bars showing mean of technical replicates ± SD.

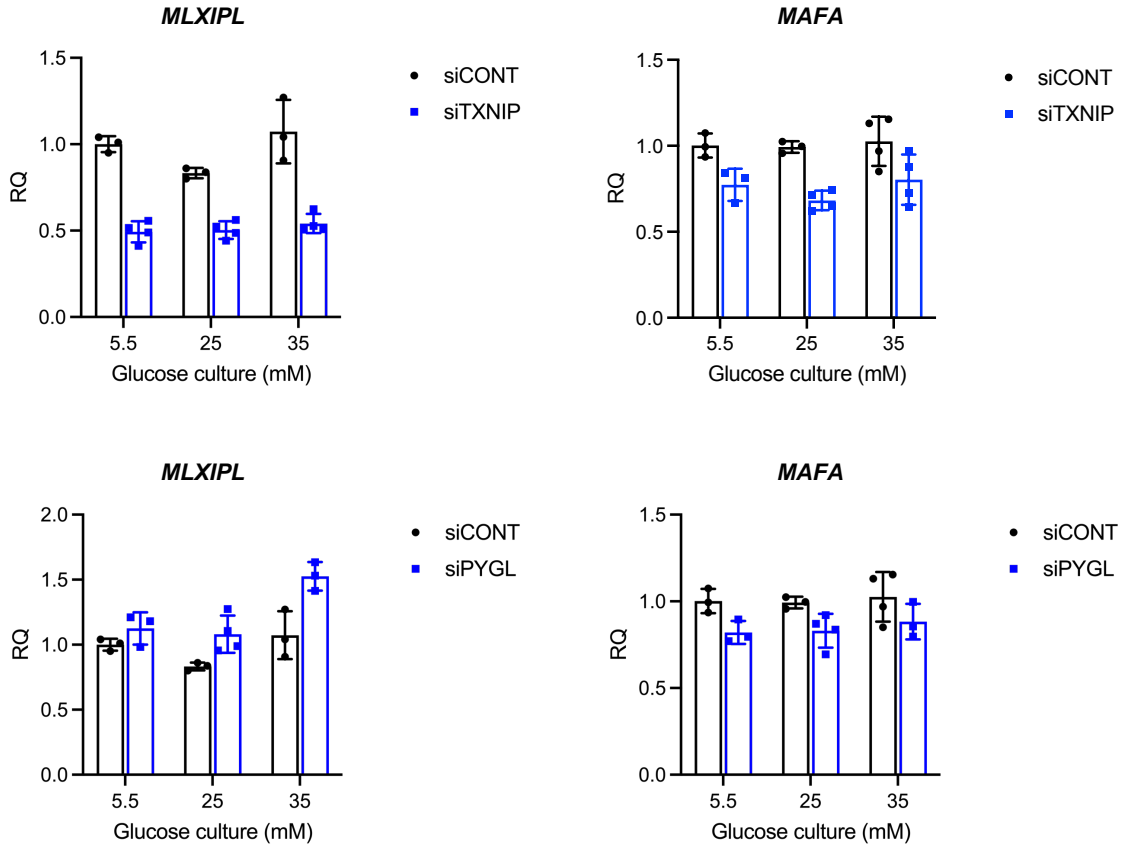

In an effort to understand how *TXNIP* and *PYGL* knockdowns affect insulin gene expression, I investigated how these knockdowns affected mRNA expression of the important glucose-responsive transcription factor ChREBP (*MLXIPL*) and the β-cell-specific transcription factor *MAFA*. *MLXIPL* expression at 5.5 mM glucose was reduced by 50% by knockdown of *TXNIP* (figure 6.5), consistent with results in INS-1 cells (figure 5.7b). Unlike in INS-1 cells, *TXNIP* KD also reduced *MLXIPL* expression at high glucose (both at 25 and 35 mM glucose). *MLXIPL* expression was apparently

enhanced by *PYGL* KD in cells cultured at high glucose. Concomitant upregulation of ChREBP and downregulation of insulin gene expression fits with results in INS-1 cells, where ChREBP knockdown increased *Ins1* and *Ins2* mRNA levels in LG-cells (figure 5.5b). *MAFA* expression appeared to be reduced by *TXNIP* KD, which may explain the decline in *INS* mRNA levels. Meanwhile, there was no clear effect of siPYGL on *MAFA* expression.

Finally, I explored how *TXNIP* expression is regulated by measuring how it was affected by knockdowns of other genes (figure 6.6). *INS* KD appeared to reduce *TXNIP* expression by some 50%, but also partially downregulated all of the other genes tested, suggesting that this may have been a general result of the loss of autocrine and/or paracrine insulin signalling rather than a specific effect. Insulin is in fact a potent repressor of TXNIP expression, according to a study in which INS-1 cells were incubated with exogenous insulin (Shaked et al., 2009), on which basis knocking down insulin would be expected to increase *TXNIP* mRNA levels. Knockdowns of *PDK1* and *GPI* appeared to slightly increase *TXNIP* expression at 5.5 mM glucose, while *PFKL* KD appeared to cause a slight decrease. The most striking effect was that of knocking down *PYGL*, which reduced *TXNIP* expression by ~65% at 5.5 mM glucose, ~50% at 25 mM glucose, and ~30% at 35 mM glucose.

Figure 6.6: Investigating the regulation of *TXNIP* mRNA expression through an siRNA screen in EndoC-βH5 cells

qPCR analysis of *TXNIP* expression following siRNA knockdown of *INS, PDK1*, *GPI*, *PFKL*, and *PYGL* in EndoC-βH5 cells. Cells were transfected with 25 nM targeting or control siRNA and incubated at 5.5, 25, and 35 mM glucose for 5 days. n=1; individual values with error bars showing mean of technical replicates ± SD.

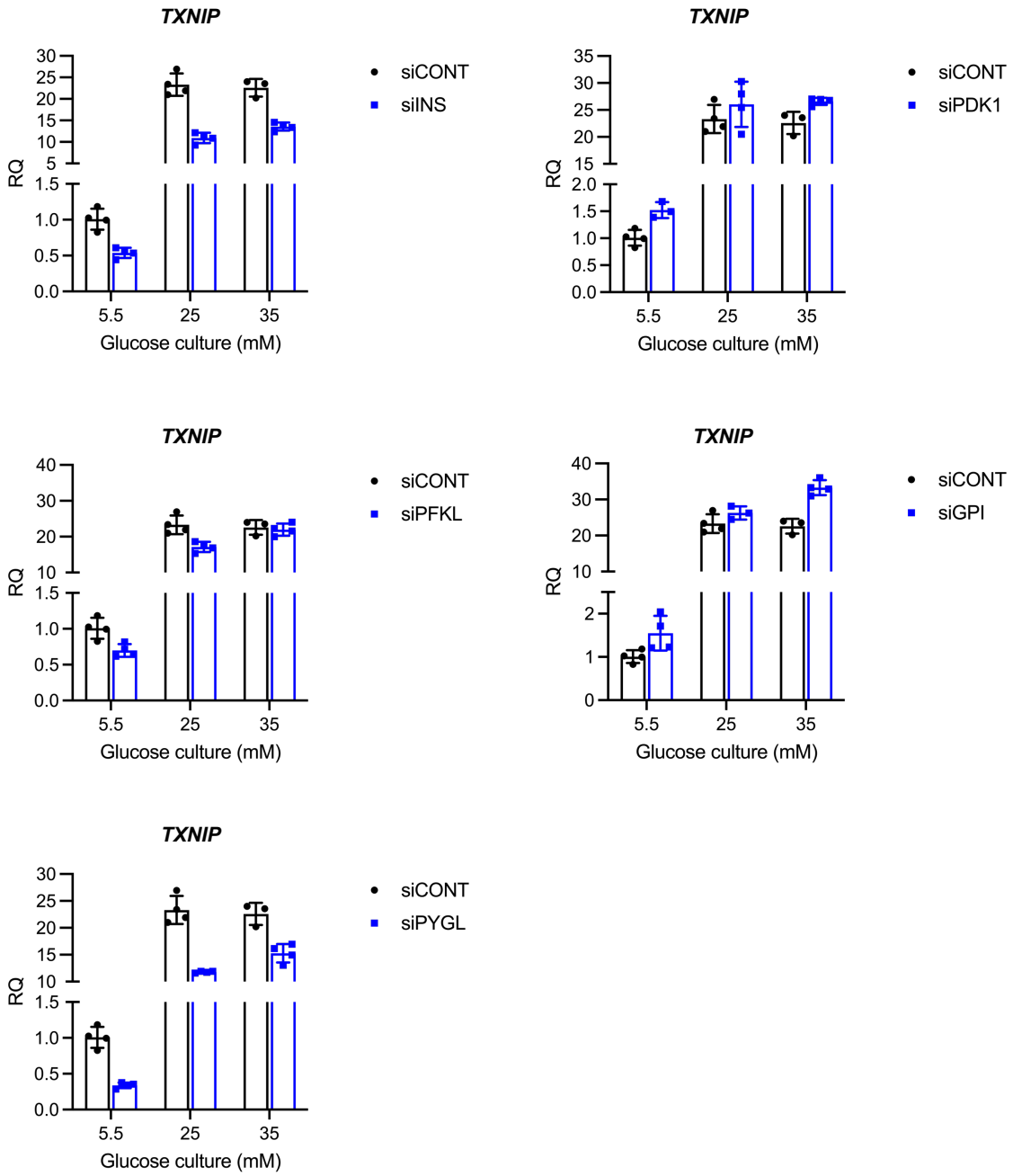

6.5 Discussion

The results of these screens must be interpreted with the caveat that they have not been replicated, but we can at least be confident that the siRNA transfection protocol was effective, as the majority of genes were knocked down by more than 70% in both cell lines. Another general observation is that, irrespective of knockdowns, the stimulation indices for GSIS were higher in βH5 cells than in βH1 cells, indicative of more robust insulin secretion in the βH5 cell line. Two targets stood out as having interesting effects on insulin biosynthesis and secretion. These were *TXNIP* in βH5 cells and *PYGL* in both cell lines.

Although I did not achieve a high knockdown efficiency, *TXNIP* KD in βH5 cells appeared to cause a decline in insulin gene expression at 5.5 mM glucose, and to some extent at 25 mM glucose. This was partially translated into changes in insulin content. The lack of effect on *INS* expression at 35 mM glucose may reflect the poorer knockdown efficacy in these conditions or could indicate that TXNIP activity starts to have deleterious effects on insulin gene expression at this level of hyperglycaemia. The effect of *TXNIP* KD seems counterintuitive considering that TXNIP is proposed to repress MAFA expression. Nevertheless, it is consistent with the result in INS-1 cells for LG-cells, in which *Txnip* KD led to a small decrease in expression of *Ins1* and *Ins2* (figure 5.6c), though not HG-cells (in which the knockdown had no effect). An interesting observation was that *TXNIP* KD led to a substantial decline in *MLXIPL* expression at each glucose concentration tested. This might indicate that the feedforward loop by which TXNIP stimulates its own transcription acts at the level of *MLXIPL* expression as well as ChREBP activity (J. Chen et al., 2014). *TXNIP* KD also

led to a smaller decline in *MAFA*, which may help to explain the downregulation of *INS*. These results are odd, however, as ChREBP is reported to negatively regulate transcription of *MAFA*, *PDX1*, and insulin, while upregulating *TXNIP* (da Silva Xavier et al., 2010). Unfortunately, I did not test whether *PDX1* expression was affected by *TXNIP* KD in EndoC cells, but there was no effect in INS-1 cells. Taken together, the evidence from INS-1 cells and βH5 cells suggests that normal levels of TXNIP expression seen in euglycaemia positively impact insulin gene expression. If TXNIP mediates glucotoxic effects on EndoC cells, these are not apparent at physiological glucose levels, or even at glucose concentrations in the upper range for uncontrolled diabetes.

Knockdown of *PYGL* was more effective at reducing target gene mRNA levels than that of *TXNIP*, and also had a more clear-cut effect on insulin biosynthesis. Although the impact of *PYGL* KD on insulin mRNA levels was not consistent between βH1 and βH5 cells, the effect on insulin content and secretion was similar in the two cell lines. Because inhibiting glycogen phosphorylase increases glycogen storage (figure 7.12; Nagy et al., 2018), the declines in *INS* expression in βH5 cells and insulin content in both cell lines following *PYGL* KD suggest that glycogen accumulation, which I would expect to be increased as a result of the knockdown, is deleterious to insulin biosynthesis. ChREBP expression was enhanced by *PYGL* KD, which might (counterintuitively) be a sign of increased glycogen accumulation leading to lower G6P levels. Although G6P activates ChREBP, it also appears to drive downregulation of *MLXIPL* mRNA levels in chronic hyperglycaemia: 24 hrs 2-DG incubation reduced *Mlxipl* expression by ~25% in INS-1 cells. The finding that *TXNIP* expression was

markedly inhibited following *PYGL* KD supports this explanation, as *Txnip* induction in INS-1 cells correlates strongly with G6P levels (Minn et al., 2006).

The impairment of basal insulin secretion by *PYGL* KD suggests that glycogen stores might be mobilised in the absence of glucose to feed into glycolysis and drive secretion. The impairment of GSIS by *PYGL* KD is less easily explained, as this should be driven by metabolism of exogenous rather than glycogen-derived glucose. Perhaps it is a result of glycogen-driven insulin secretion continuing into the start of the 20 mM glucose incubation, or it may be due to impaired insulin biosynthesis causing a shortage of insulin granules available to secrete. Typically, β-cells secrete such a small percentage of their insulin content that secretion is essentially independent of insulin biosynthesis, and even in T2D defects in insulin secretion cannot be attributed to insufficient reserves (Henquin et al., 2017), but this is not true for EndoC cells. Especially in βH1 cells, I have observed that there is often a small decline in insulin content following stimulation at 20 mM glucose relative to 0 mM glucose due to the loss of insulin to secretion; this decline becomes very apparent when GSIS is potentiated using IBMX.

To increase my confidence that glycogen phosphorylase activity affects insulin biosynthesis and secretion through control over glycogen breakdown in EndoC cells, I would need to perform a glycogen assay to determine whether *PYGL* knockdown increased glycogen storage. It is unfortunate that I failed to knock down PTG. This experiment would have offered a complementary perspective on the relationship between glycogen storage and insulin biosynthesis, since PTG KD ought to have the opposite effect on glycogen accumulation to *PYGL* KD.

In summary, it is difficult to draw firm conclusions from the set of experiments described in this chapter as the results have not been replicated. However, we can tentatively surmise from the effects of knocking down *PFKL*, *GPI*, and (most convincingly) *PYGL* that the abundance of G6P is a key regulator of transcriptional activity in EndoC cells as well as in INS-1 cells. Knocking down PFKL or PYGL should increase flux through glycolysis or into glycogen synthesis, respectively, and thus deplete G6P, while knocking down GPI should reduce glycolytic flux and thereby elevate G6P levels. The expression of the highly G6P-responsive gene *TXNIP* (which was robustly upregulated by chronic hyperglycaemia) changed accordingly in βH5 cells, with the greatest effect being from *PYGL* KD, suggesting that glycogen synthesis has a powerful G6P-withdrawing effect. Although I didn't knock down *MLXIPL* to explore this further, *TXNIP* expression appears to be controlled by ChREBP, as most other studies have found (Shalev, 2014). Further experiments to test my conclusions could include efforts to rescue the effects of different knockdowns by reintroducing the missing downstream glycolytic intermediate, providing the metabolite can be taken up by the cells[12]. This approach would help to determine whether the phenotype in question is caused by accumulation of upstream metabolites or a deficit of downstream metabolites.

If G6P does constitute a key metabolic signal, as I have suggested, why is insulin biosynthesis so resilient in EndoC cells during chronic hyperglycaemia? It appears that G6P levels don't become sufficiently high to cause downregulation of insulin gene expression unless hyperglycaemia is very severe and long-lasting in these cells. By

[12] Some metabolites, especially phosphometabolites, are not cell permeable.

culturing βH1 cells for 8 days or βH5 cells for 5 days at very high glucose concentrations (25 or 35 mM), I was able to observe some downregulation of *Ins* mRNA and/or insulin content. Thus, the sensitivity of insulin biosynthesis to G6P, and probably other glucose metabolites, appears to be shifted considerably rightwards in these cells. The diminished impact of *PYGL* KD on *TXNIP* mRNA levels at 35 mM glucose may suggest that glycogen synthesis is less able to absorb excess G6P at this level of hyperglycaemia, allowing downregulation of insulin gene expression. An important test of this hypothesis would be to measure changes in G6P abundance in chronic hyperglycaemia and following *PYGL* KD. However, even if my hypothesis is correct, we must consider whether using glucose concentrations as high as 35 mM to model glucotoxicity *in vitro* has any clinical relevance to T2D.

7. Causes and consequences of glycogen accumulation in the hyperglycaemic β-cell

7.1 Summary

1. Chronic hyperglycaemia resulted in glycogen accumulation in INS-1 cells.
2. Glucokinase inhibition by mannoheptulose prevented hyperglycaemia-induced glycogen accumulation.
3. Glycogen accumulation proceeded at a slightly faster rate than glycogen breakdown. Accumulation was roughly linear for the first 12 hrs following the onset of hyperglycaemia, but thereafter the rate was slow; stores were broken down within 24 hrs following restoration of euglycaemia.
4. GAPDH inhibition by koningic acid (KA) did not induce glycogen accumulation in LG-cells.
5. Inhibition of FBPase reduced glycogen accumulation in HG-cells by half.
6. siRNA knockdown of *ALDOB* did not affect glycogen accumulation in HG-cells or LG-cells.
7. Metformin prevented glycogen accumulation in HG-cells.
8. An inhibitor of p70-S6 kinase (S6K1) prevented glycogen accumulation in HG-cells.
9. The AMPK activators MK-8722 and AICAR potentiated glycogen accumulation in HG-cells.
10. PTG expression in βV59M mouse islets correlated with the severity of hyperglycaemia. In INS-1 cells, PTG expression peaked around 1 hour after the onset of hyperglycaemia. PTG expression was triggered by accumulation of

metabolites in upper glycolysis; experiments with 2-DG indicated that glucose-6-phosphate (G6P) contributes to PTG induction.

11. PTG expression was unaffected by metformin, reduced by S6K1 inhibition, and enhanced by MK-8722, suggesting that metformin regulates glycogen storage in an mTORC1-independent manner and that the effect of AMPK activators on glycogen accumulation is in part mediated by increased PTG expression.
12. Chronic incubation of INS-1 cells with small molecule inhibitors of glycogen phosphorylase potentiated glycogen accumulation in HG-cells but did not affect the glycogen content of LG-cells.
13. Acute glycogen phosphorylase inhibition did not affect insulin secretion from HG-cells or basal insulin secretion from LG-cells but may reduce glucose-stimulated secretion in LG-cells.
14. Chronic glycogen phosphorylase inhibition impaired autophagy in LG-cells as effectively as chronic hyperglycaemia did.

7.2 Introduction

The β-cell is unique among islet cell types in producing glycogen, although this only occurs to a significant extent in hyperglycaemia/diabetes or other pathological states (Ashcroft et al., 2017). This chapter aims to address two key questions about hyperglycaemia-induced glycogen storage. Firstly, what drives glycogen accumulation? This might involve changes in substrate availability, or in the expression or activity of enzymes involved in glycogen synthesis, particularly glycogen synthase (GYS) and phosphorylase (PYG). Secondly, does glycogen accumulation

have any deleterious effects on β-cell function? These effects could include interference with stimulus-secretion coupling or impairment of autophagy.

As with the loss of insulin biosynthesis, the first question I wished to resolve was which are the metabolic signals that drive glycogen overaccumulation in chronic hyperglycaemia. The most obvious one is an excess of G6P, as this is both the initial substrate for glycogen synthesis and a powerful allosteric stimulator of glycogen synthase activity. G6P may be elevated in chronic hyperglycaemia as a consequence of increased extracellular glucose and low flux through GAPDH (Haythorne et al., 2022). However, accumulation of F2,6BP should also be considered as a factor, as it mediates induction of *Ppp1r3c* transcription by MondoA-MLX (Petrie et al., 2013). *Ppp1r3c*, which encodes protein targeting to glycogen (PTG), is upregulated by hyperglycaemia (table 1.3), and overexpression of PTG is by itself sufficient to stimulate glycogen synthesis (Lerín et al., 2000; Mir-Coll et al., 2016).

Metabolic signals affecting the activities of the kinases and phosphatases that regulate GYS and PYG are also likely to play an important role. The balance between the metabolic master-regulators AMPK and mTOR is of particular interest, being shifted firmly in favour of mTOR signalling during chronic hyperglycaemia (Haythorne et al., 2022). GYS is subject to inhibitory phosphorylation by AMPK, so a reduction in AMPK activity would be expected to enhance GYS activity. AMPK is also able to act as a glycogen sensor owing to the carbohydrate-binding module (CBM) on its β subunit that forms specific side-chain interactions with glycogen (McBride et al., 2009; Polekhina et al., 2005), with the β2 isoform expressed in the β-cell having a particularly high affinity for glycogen. This may help AMPK target GYS for inactivating phosphorylation, but also raises the possibility that sequestration of a glycogen-bound

fraction could be a factor involved in lowering AMPK activity in chronic hyperglycaemia. Some studies have found that glycogen inhibits AMPK activity (McBride et al., 2009), while others have not (L. Chen et al., 2012; Polekhina et al., 2005). However, AMPK inhibition in diabetes appears to be largely governed by elevation of glycolytic intermediates and the resultant activation of mTORC1 (Haythorne et al., 2022). Meanwhile, mTORC1 is an important suppressor of autophagy (Ardestani et al., 2018), which could adversely affect capability for autophagic degradation of glycogen (glycophagy).

Several gluconeogenic enzymes are upregulated in diabetic β-cells (table 4.1). These include both isoforms of FBPase (FBP1 and FBP2), which catalyse the hydrolysis of F1,6BP to F6P, a rate-limiting step in gluconeogenesis. In addition, ALDOB, which is considered to be a gluconeogenesis-favouring form of aldolase (Droppelmann et al., 2015), is one of the most highly upregulated genes in islets from T2D patients (Gerst et al., 2018; Solimena et al., 2018) as well as in diabetic βV59M mouse islets (Haythorne et al., 2019). Both FBP1 and ALDOB negatively regulate insulin secretion (Gerst et al., 2018; Kebede et al., 2008; Y. Zhang et al., 2010), and pharmacological inhibition of FBPase increases glucose utilisation and GSIS (Zhang et al., 2010). This is evidence that these enzymes reduce glycolytic flux, thereby increasing substrate availability for glycogenesis. Indeed, ALDOB has been proposed to drive glycogen accumulation, likely acting in concert with FBP1, with which it forms an isoform-specific complex[13] (Droppelmann et al., 2015; Haythorne et al., 2019; Westermeier et al., 2019). This could indicate that gluconeogenesis contributes to glycogen accumulation by further elevating G6P levels, especially as glucose-6-phosphatase (G6PC2) is

[13] Fbp1 complexes with AldoB, whereas Fbp2 complexes with AldoA

downregulated in diabetes (table 4.1). However, at least in euglycaemia, the role of gluconeogenic enzymes in the β-cell is thought to be mainly to fine-tune GSIS by modulating key substrate cycles, such as the one formed by GCK and glucose-6-phosphatase (Westermeier et al., 2019), which does not necessarily imply substantial gluconeogenic flux overall. Nevertheless, simply reducing glucose utilisation may be enough to stimulate glycogen accumulation.

Aldolase plays another important role, distinct from its catalytic function in glycolysis/gluconeogenesis, in signalling cellular energy status. F1,6BP is an important indicator of glucose availability, and aldolase, having a high K_m for F1,6BP, is able to act as its sensor across the entire physiological range of F1,6BP concentrations in mouse embryonic fibroblasts (Lin & Hardie, 2018). Aldolase forms part of a macromolecular supercomplex on the lysosomal surface: this is reorganised such that AMPK is bound and phosphorylated (activated) when aldolase is not occupied by F1,6BP, and mTOR is bound and activated instead when aldolase is occupied by F1,6BP (Li et al., 2019; C. S. Zhang et al., 2017). If this mechanism operates in the same way in β-cells, the mTOR/AMPK activity ratio would thus rise in line with F1,6BP levels in hyperglycaemia. In HEK293 cells, increased GAPDH occupancy by GA3P also contributes to mTOR activation by releasing inhibition of Rheb (Lee et al., 2009), compounding the effect of F1,6BP. Accumulation of glycolytic intermediates could thus lead to reduced inhibitory phosphorylation of GYS by AMPK as well as reduced glycophagy, compounding the direct effects of G6P on glycogen metabolism.

Returning to the second key question, does glycogen accumulation have a deleterious influence on β-cell function? One of the most potentially dangerous effects of β-cell

glycogen accumulation in diabetes is fasting hypoglycaemia due to disruption of stimulus-secretion coupling by glycogenolysis. Glycogenolysis has been shown to underlie a temporary increase in glycolytic flux after reversal of hyperglycaemia, resulting in a paradoxical stimulation of insulin secretion (Malaisse et al., 1993). In this chapter, I explore whether blocking glycogenolysis using an inhibitor of PYG can prevent such ectopic insulin secretion.

Finally, autophagy was previously found to be severely impaired in diabetic βV59M islets, with the number of autophagosomes rapidly increasing after hyperglycaemia was reversed by sulfonylurea therapy (Brereton et al., 2016). Some of these autophagosomes contained glycogen granules, suggesting that autophagic breakdown of glycogen (glycophagy) was occurring. Alpha-glucosidase, which catalyses glycophagy, is downregulated at the mRNA level but upregulated at the protein level in islets from diabetic βV59M mice (Haythorne et al., 2019). Mice with a β-cell-specific knockout of *Atg7* (autophagy-related 7) exhibit impaired insulin secretion, illustrating the deleterious impact of autophagic impairment on β-cell function (Jung et al., 2008). The vacuolated appearance of their β-cells also offers indirect evidence that glycogen accumulation can occur as a result of autophagic impairment, although this could be a downstream consequence of impaired glucose tolerance (Jung et al., 2008). In this chapter, I investigate whether impaired autophagy is a consequence of glycogen overaccumulation or of other changes that occur during chronic hyperglycaemia by testing whether potentiating glycogen accumulation could exacerbate this autophagic impairment.

7.3 Materials and methods

Methods were as described in chapter 2, with the following additions.

7.3.1 Glycogen quantification

INS-1 cells were cultured at 5 mM (LG-cells) or 25 mM (HG-cells) glucose for 48 hrs as described in chapter 2. 30 mins prior to sample collection, cells were transferred to media containing 5 mM glucose. INS-1 cells were washed twice with ice-cold PBS and lysed by sonication in ultrapure water (on ice). Lysates were immediately boiled for 10 min, centrifuged at 18,000 rcf (relative centrifugal force) for 10 min at 4°C to pellet debris, and the glycogen content of the supernatant was determined colorimetrically using the Glycogen Colorimetric/Fluorometric Assay Kit (Biovision K646) as per the manufacturer's instructions. The protein concentration in the supernatant was determined by BCA assay.

7.3.2 Autophagy detection assay

Autophagic activity was quantified using an Autophagy Detection Kit (Abcam ab139484). Cells were grown in black-walled, clear-bottomed 96-well plates to a confluency of ~90% at the time of the assay. Cells were washed once with assay buffer before being incubated at 37°C for 30 mins (while protected from light) with 100 µl detection reagent comprising 0.1% green detection reagent and 0.1% nuclear stain in OptiMEM supplemented with 5% FBS (to reduce cell detachment). Cells were then washed twice with assay buffer and 100 µl assay buffer was again added. The assay was read on a CLARIOstar plate reader (BMG LABTECH) with excitation at 480 nm/emission at 530 nm for green detection reagent and excitation at 340 nm/emission at 480 nm for the nuclear stain.

7.4 Results

7.4.1 Glycogen assay optimisation and validation

I originally intended to perform immunocytochemistry to visualise glycogen stores as had been done previously (Haythorne et al., 2019), but was unable to obtain the requisite anti-glycogen antibody. I therefore selected an enzymatic method of glycogen quantification in which glycogen is hydrolysed by glucoamylase and the liberated glucose is oxidised and quantified colorimetrically. A drawback of this method is that the absorbance due to existing glucose must be subtracted from the combined absorbance produced by glycogen-derived glucose and existing glucose. HG-cells contain considerable intracellular glucose, and β-cells (even in chronic hyperglycaemia) have a relatively low glycogen content compared to liver or muscle, so the background produced by existing glucose can be very significant. I therefore optimised sample preparation to reduce this background signal by incubating cells at 5 mM glucose for 30 minutes before sample collection, and then washing cells twice with PBS before lysis. While this approach may cause a small reduction in glycogen yield, this is outweighed by the improvement in sensitivity.

The principle is illustrated by figure 7.1. Here, cells were incubated at 5 mM or 25 mM glucose for 48 hrs, followed by 30 minutes incubation at 2 mM or 20 mM glucose. Transfer of LG-cells to 20 mM glucose appeared to lead to a slightly higher glycogen content than transfer to 2 mM glucose (figure 7.1a), presumably due to glycogen synthesis and breakdown at 20 mM and 2 mM glucose, respectively. However, whereas HG-cells transferred to 2 mM glucose yielded ~3 μg glycogen/mg protein, HG-cells transferred to 20 mM glucose appeared to have a negligible glycogen

content. The latter result was due to the high glucose background (figure 7.1b) rather than a true lack of glycogen. For subsequent experiments, I used 5 mM rather than 2 mM glucose for the pre-incubation so that LG-cells did not lose any of their (already small) glycogen stores prior to assaying. Finally, I also verified that freezing samples to assay at a later date did not affect the glycogen yield. A previous study (Andersson et al., 2016) found similar levels of glycogen (<0.5 μg/mg protein) in INS-1 cells cultured at 2.8 mM glucose for 48 hrs as I did in LG-cells but around twice as much glycogen (~7 μg/mg protein) in cells cultured at 16.7 mM glucose for 48 hrs glucose as I did in HG-cells. This discrepancy may be explained in part by loss of glycogen during my low-glucose pre-incubation and washing steps and in part by differences in methodology, with the KOH/ethanol precipitation technique combined with gas chromatography/mass spectrometry used by Andersson *et al.* potentially producing a greater glycogen yield. The rate of glycogen loss in the first hour after a change from 25 mM to 5 mM glucose (figure 7.3) suggests the answer is a combination of the two factors.

Figure 7.1: Low glucose pre-extraction incubation improves glycogen detection

(a) Normalised glycogen content of INS-1 cells cultured at 5 or 25 mM glucose for 48 hrs before being transferred to 2 or 20 mM glucose (black and red symbols, respectively) for 30 mins before glycogen was extracted. n=3, with 3 technical replicates per experiment.

(b) Background glucose present in samples in (a) as inferred from OD at 570 nm of sample aliquots not treated with hydrolysis enzyme in glycogen assay.

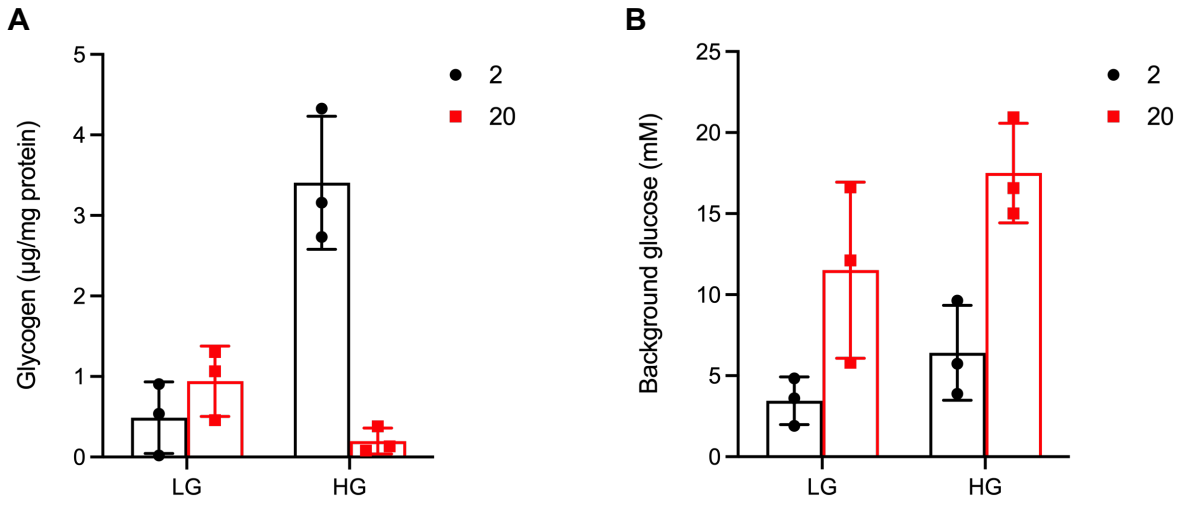

7.4.2 Mannoheptulose prevents glycogen accumulation in chronic hyperglycaemia

I next tested whether mannoheptulose could prevent glycogen storage. As mannoheptulose inhibits glucokinase, and thus the production of glucose-6-phosphate, it can be used as a control to demonstrate that the assay was truly measuring glycogen rather than glucose that had not been properly washed out of the cells. It also provides a proof of concept for the potential therapeutic use of glucokinase inhibitors in T2D (Ashcroft et al., 2023). As expected, 48 hrs incubation with 10 mM mannoheptulose successfully prevented significant glycogen accumulation in HG-

cells relative to LG-cells (figure 7.2). Thus, partial inhibition of glucokinase can protect β-cells against glycogen accumulation and any deleterious effects thereof.

Figure 7.2: Glucokinase inhibition prevents glycogen accumulation in chronic hyperglycaemia

Normalised glycogen content of INS-1 cells cultured for 48 hrs at 5 mM (LG) or 25 mM (HG) glucose ± 10 mM mannoheptulose (MANNO). n=3, with 2 technical replicates per experiment. **p < 0.01; 1-way ANOVA with Bonferroni's correction.

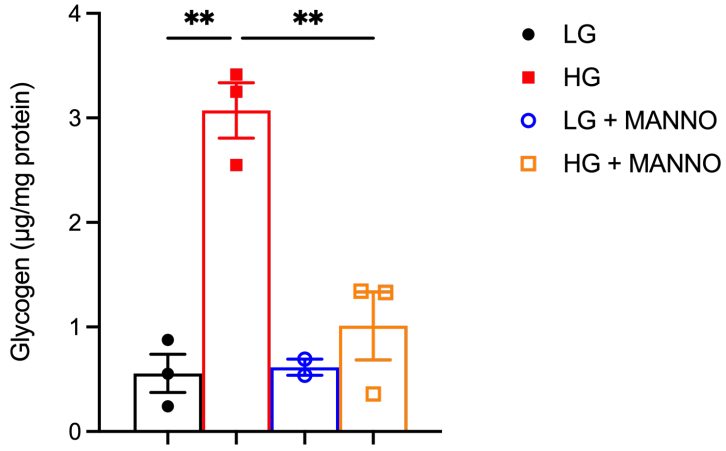

7.4.3 Temporal dynamics of glycogen accumulation and breakdown following onset and reversal of hyperglycaemia

To investigate the temporal dynamics of glycogen accumulation and breakdown following the onset and reversal of hyperglycaemia, I pre-cultured INS-1 cells at 5 mM glucose (LG) or 25 mM glucose (HG) for 48 hrs before transferring them to HG (onset) or LG (reversal) respectively for 1, 3, 6, 12, or 24 hours. It was previously concluded that glycogen accumulation proceeded at twice the rate of glycogen breakdown (the respective rates being 1 µg/mg protein/hr and 0.5 µg/mg protein/hr), suggesting that

β-cell glycogen levels may act as a metabolic memory of previous episodes of hyperglycaemia (Andersson et al., 2016). This was a striking result, so I tested whether it was reproducible, as well as extending the duration of the time course. The figure presented by Andersson *et al.* (2016) appears to show glycogen accumulation or breakdown plateauing after 6 hrs. However, the initial glycogen content of cells pre-cultured at 16.7 mM glucose for 48 hrs was significantly higher than that reached after 6 hrs incubation at 16.7 mM glucose by cells pre-cultured at 2.8 mM glucose. This suggested that, despite the curve appearing to plateau, glycogen accumulation actually continued for some time after the 6 hrs timepoint. Hence, for my time course experiment, I additionally quantified glycogen levels at 12 hrs and 24 hrs after onset or reversal of hyperglycaemia.

Figure 7.3: Time course of glycogen accumulation or breakdown for 24 hrs following the onset or reversal of hyperglycaemia

Normalised glycogen content of INS-1 cells at time points of 1, 3, 6, 12, and 24 hrs following onset or reversal of hyperglycaemia. Cells were pre-cultured at 5 or 25 mM glucose for 48 hrs before being transferred to the opposite condition (25 or 5 mM to simulate onset or reversal, respectively) at the time point 0. n=3, with 3 technical replicates per experiment.

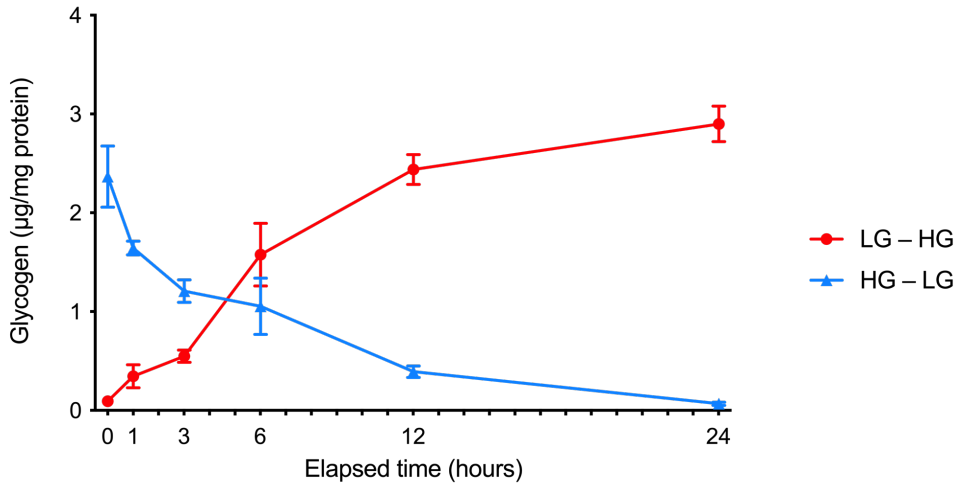

Figure 7.3 shows the change in β-cell glycogen content following the onset of hyperglycaemia (red) or restoration of euglycaemia (blue). For the sake of clarity, individual values are not plotted. Glycogen accumulation following the onset of hyperglycaemia proceeded along an S-shaped curve (a sigmoidal curve can be fitted with R^2 = 0.9883). Although the rate of accumulation in INS-1 cells slowed considerably after 12 hrs, accumulation continued throughout the 24 hrs. By contrast, glycogen breakdown following restoration of euglycaemia followed a more linear profile that was fitted better by a quadratic polynomial. Over the period between 1 hr and 12 hrs, for which both curves are roughly linear, the rate of glycogen accumulation (0.19 μg/mg protein/hr) was indeed close to twice the rate of glycogen breakdown (0.11 μg/mg protein/hr), although the absolute rates were around 20% of those reported by Andersson *et al.* (2016). The difference in rates almost disappears when the total change in glycogen content over 24 hrs is considered: the accumulation rate was 0.12 μg/mg protein/hr (2.8 μg/mg protein/day) versus a breakdown rate of 0.10 μg/mg protein/hr (2.3 μg/mg protein/day). Thus, the rate difference is timescale dependent. The implication is that, while glycogen can be cleared effectively given time, over shorter timescales glycogen accumulation is difficult to curb and may impact β-cell function.

7.4.4 Identification of metabolic factors driving glycogen accumulation in β-cells

7.4.4.1 GAPDH inhibition did not increase glycogen accumulation in LG-cells

By blocking glycolysis at GAPDH and causing the accumulation of upstream metabolites, koningic acid (KA) was able to mimic the impact of hyperglycaemia on

the expression of glycolytic enzymes in LG-cells (figure 4.9a). I therefore tested if KA could also induce excess glycogen synthesis in LG-cells. However, KA had no effect on glycogen levels (figure 7.4), perhaps because there was not enough substrate or because there was insufficient ability to generate UTP for UDP-glucose synthesis due to impaired metabolism.

Figure 7.4: Inhibition of GAPDH in LG-cells does not cause glycogen accumulation

Normalised glycogen content of INS-1 cells cultured for 48 hrs at 5 mM glucose (LG), at 25 mM glucose (HG), or at 5 mM glucose + 5 μM koningic acid (LG + KA). n=3, with 2 technical replicates per experiment. *p < 0.05; 1-way ANOVA with Bonferroni's correction.

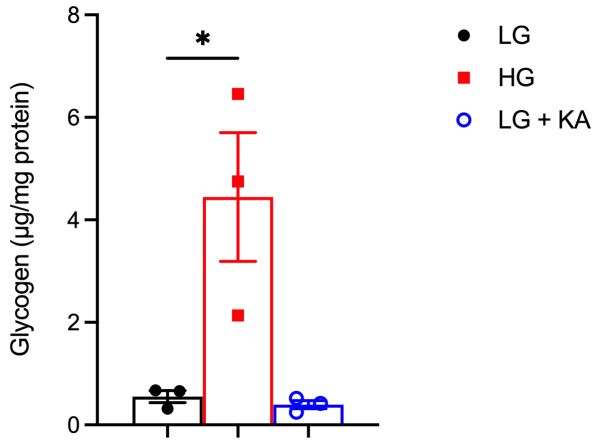

7.4.4.2 FBPase inhibition partially prevented glycogen accumulation

FBPase protein levels are significantly increased in βV59M diabetic islets: FBP1 is upregulated 9-fold and FBP2 is upregulated 6-fold (table 4.1). Moreover, FBPase activity is increased at least 4-fold (Haythorne et al., 2022). FBPase is subject to allosteric inhibition by F1,6BP, F2,6BP and AMP. To investigate whether the upregulation of FBPase in chronic hyperglycaemia contributes to the

overaccumulation of glycogen, I tested whether MB05032 (FBPi), an AMP site-targeting inhibitor of both isoforms of FBPase, could prevent glycogen accumulation. FBPi mimics the inhibitory action of AMP and enhances insulin secretion (Westermeier et al., 2019). Incubation of HG-cells with 0.5 mM FBPi restored insulin secretion to such an extent that GSIS was higher than in LG-cells (figure 7.5a) but without having any effect on insulin content (figure 7.5b). FBPase inhibition reduced glycogen accumulation by half (figure 7.5c). This indicates that FBPase activity plays an important role in driving glycogen accumulation.

Figure 7.5: Inhibition of FBPase reduces glycogen accumulation in HG-cells

(a) Basal and glucose-stimulated insulin secretion (ng/ml/µg protein) from INS-1 cells incubated with 5 or 25 mM glucose ± 0.5 mM FBPase inhibitor (FBPi) for 48 hrs. Control samples were treated with an equivalent volume of DMSO (veh). n=1; mean of technical replicates ± SD shown.

(b) Total insulin content (ng/µg protein) of INS-1 cells incubated with 5 or 25 mM glucose ± 0.5 mM FBPase inhibitor (FBPi) for 48 hrs. Control samples were treated with an equivalent volume of DMSO (veh). n=1; mean of technical replicates ± SD shown.

(c) Normalised glycogen content of INS-1 cells cultured for 48 hrs at 5 or 25 mM glucose ± 0.5 mM FBPi. Control samples were treated with an equivalent volume of DMSO (veh). n=4, with 2-3 technical replicates per experiment. *$p < 0.05$, **$p < 0.01$; 1-way ANOVA with Bonferroni's correction.

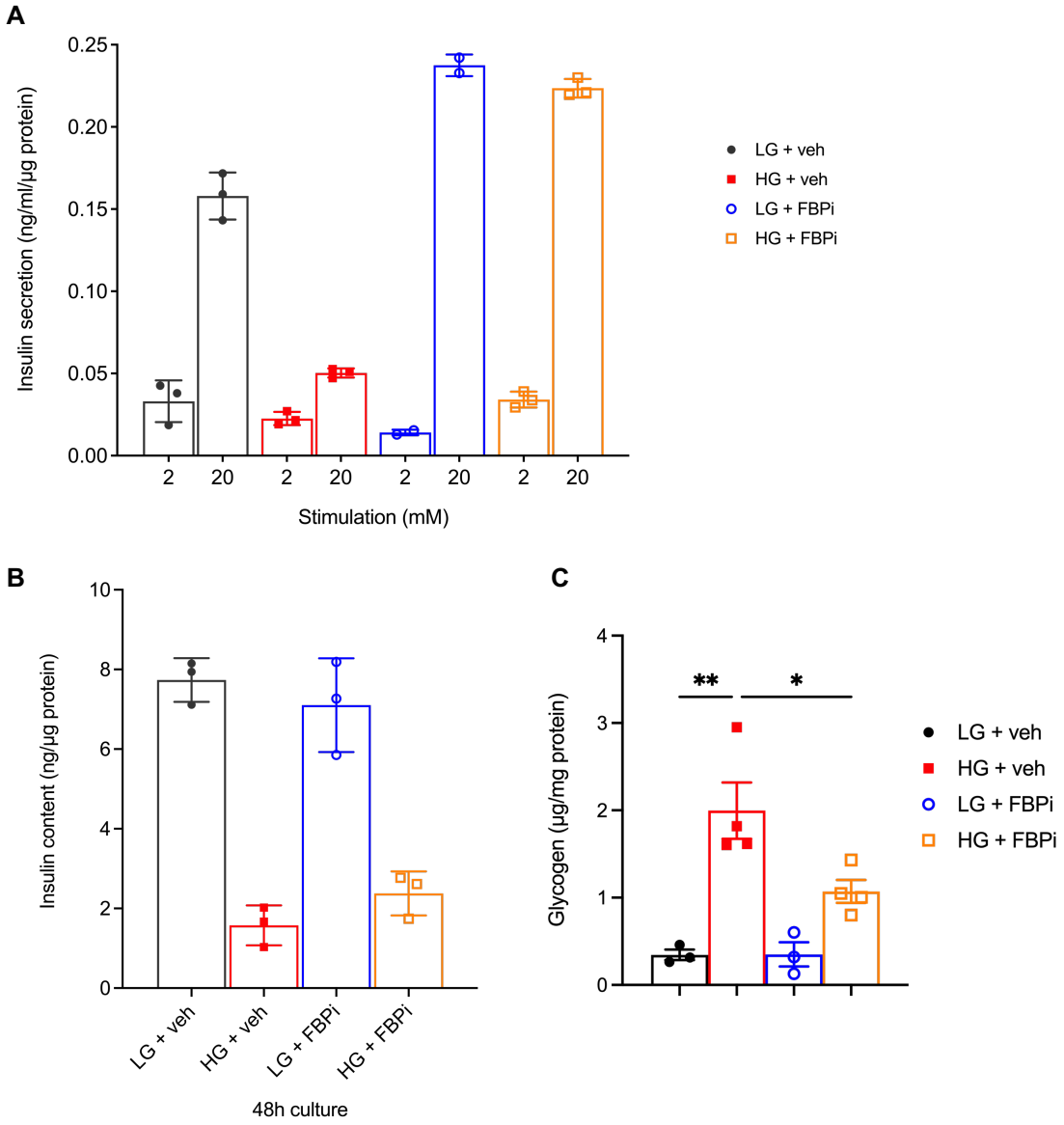

7.4.4.3 *ALDOB* knockdown did not affect glycogen accumulation

Potentially, ALDOB might stimulate glycogen accumulation both as part of a gluconeogenic complex with FBP1 and as an F1,6BP-sensing inhibitor of AMPK at the lysosome, thereby preventing inhibitory phosphorylation of GYS by AMPK. I therefore assessed the effect of *ALDOB* siRNA knockdown on glycogen levels. I anticipated that *ALDOB* KD would reduce glycogen accumulation, and even hypothesised that combining *ALDOB* KD with FBP1 inhibition might synergistically enhance glycolytic

flux and further reduce glycogen accumulation. However, despite a high knockdown efficiency (table 4.3), *ALDOB* KD had no effect on glycogen levels (figure 7.6). Nor was there any potentiation of the action of FBPi by concomitant *ALDOB* KD in a pilot experiment. This may be because the knockdown reduced *ALDOB* expression but did not bring levels in HG-cells down as low as in LG-cells (figure 4.11a). Furthermore, it may be that metabolite levels are more important determinants of glycogen accumulation, and ALDOB need not be upregulated to function effectively as their sensor.

Figure 7.6: siRNA knockdown of AldoB did not affect glycogen levels

Normalised glycogen content of INS-1 cells cultured for 48 hrs at 5 or 25 mM glucose following siRNA knockdown of AldoB. Cells were transfected with 50 nM non-targeting control siRNA (siNT) or 50 nM siALDOB. n=3, with 2 technical replicates per experiment. **p < 0.01, ***p < 0.001; 1-way ANOVA with Bonferroni's correction.

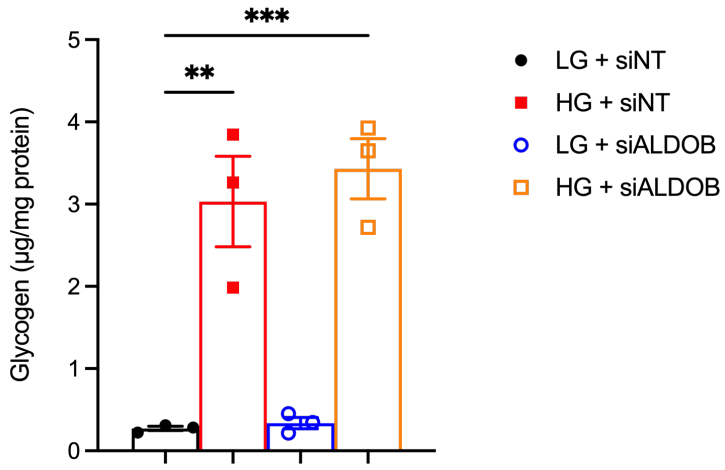

7.4.5 Investigating the relationship between β-cell glycogen and the AMPK/mTOR signalling axis

In this section, I compare how glycogen levels are affected by metformin, by inhibition of mTOR signalling through S6K1, and by direct activation of AMPK. Metformin is the most commonly prescribed drug for T2D treatment, yet its mechanism of action remains contested. Metformin activates AMPK at clinically relevant concentrations, and its glycaemia-lowering effects have generally been ascribed to AMPK activation, although it has also been suggested to inhibit mitochondrial complex I and thereby lower the ATP/AMP ratio. However, the latter mechanism requires very high metformin concentrations (~5 mM), the uncertainty around actual intracellular concentrations *in vivo* discussed in chapter 5 notwithstanding (He & Wondisford, 2015). Metformin can activate AMPK, and hence simultaneously inactivate mTOR, through the lysosomal pathway (C. S. Zhang et al., 2016). However, metformin also inhibits FBP1 at the AMP allosteric site (Hunter et al., 2018). It is argued that, when there is an excess of glucose or of gluconeogenic substrates, metformin lowers G6P levels by AMPK-independent mechanisms, most likely by allosteric activation of PFK and/or inhibition of FBPase (Agius et al., 2020). By comparing the effects of metformin, S6K1 inhibition, and direct AMPK activation on glycogen levels, I aim to shed light on the interplay of AMPK, mTOR, and PFK/FBPase in controlling glycogen storage in the β-cell.

7.4.5.1 Metformin prevents glycogen accumulation

Metformin was previously shown to prevent glycogen accumulation in β-cells, as measured by PAS staining (Brereton et al., 2016). I aimed to investigate this further using a quantitative measure of glycogen. In keeping with prior results, 0.5 mM

metformin prevented glycogen accumulation in HG-cells (figure 7.7). As discussed above, this could be due to direct effects on metabolic enzymes or due to changes in AMPK/mTOR signalling.

Figure 7.7: Metformin reduces glycogen accumulation in HG-cells

Normalised glycogen content of INS-1 cells cultured for 48 hrs at 5 or 25 mM glucose ± 0.5 mM metformin. n=4, with 2-3 technical replicates per experiment. *p < 0.05, **p < 0.01; 1-way ANOVA with Bonferroni's correction.

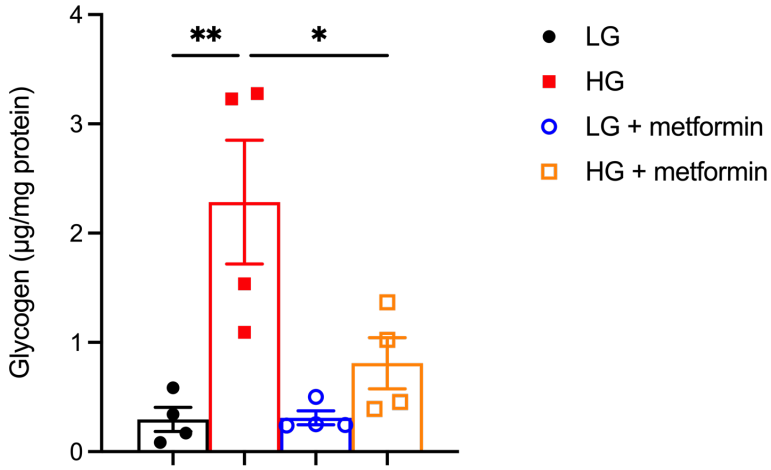

7.4.5.2 Inhibition of mTOR signalling via S6K1 prevents glycogen accumulation

To investigate whether hyperactivation of mTORC1 and downstream signalling through S6K1 drives glycogen accumulation during chronic hyperglycaemia, I used PF-4708671 (S6Ki) to inhibit S6K1. 10 µM S6Ki prevented or partially prevented most of the changes in expression of glycolytic and gluconeogenic genes in HG-cells (figure 5.9), indicating that these are mTOR-mediated. Incubation of HG-cells with S6Ki almost entirely prevented glycogen accumulation (figure 7.8), indicating that mTOR signalling is also involved in driving glycogen accumulation.

Figure 7.8: S6K1 inhibition reduces glycogen accumulation in HG-cells

Normalised glycogen content of INS-1 cells cultured for 48 hrs at 5 or 25 mM glucose ± 10 μM PF-4708671 (S6Ki). Control samples were treated with an equivalent volume of DMSO (veh). n=5, with 3 technical replicates per experiment. ***p < 0.001; 1-way ANOVA with Bonferroni's correction.

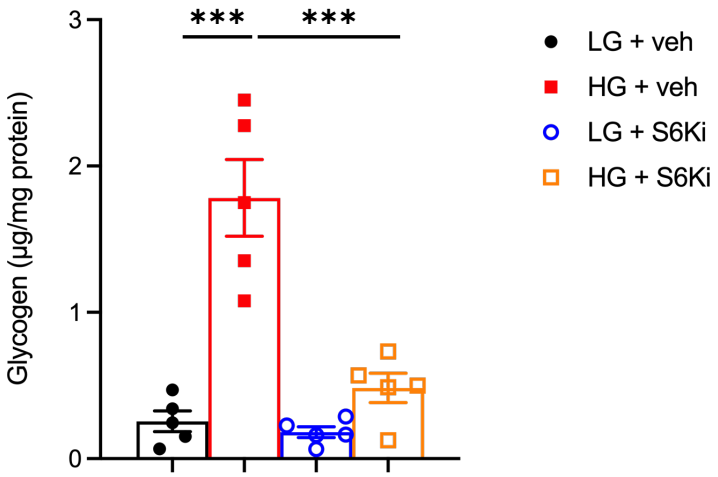

7.4.5.3 AMPK activators enhance glycogen accumulation

Whereas mTORC1 is hyperactivated, AMPK activity is very low in chronic hyperglycaemia. Having demonstrated that inhibiting mTOR signalling prevented glycogen hyperaccumulation, I next tested whether pharmacological activation of AMPK could also prevent glycogen accumulation in INS-1 cells, using the allosteric pan-AMPK activator MK-8722. Significantly, MK-8722 potently activates β2 AMPK complexes as well as β1 complexes (Myers et al., 2017). Paradoxically, chronic incubation with 0.5 μM MK-8722 led to the glycogen content of HG-cells nearly doubling (figure 7.9a). This was unexpected, since GYS is subject to inhibitory phosphorylation by AMPK. However, the team that developed MK-8722 had observed that it also promoted glycogen storage in skeletal and cardiac muscle. This was

associated with increased glucose uptake, which cannot be the case in β-cells as MK-8722 only increases glucose uptake in tissues expressing GLUT4 (Myers et al., 2017). A potential alternative explanation is that MK-8722 sterically hinders the CBM or otherwise interferes with AMPK binding to glycogen and thereby blocks inhibition of GYS and/or activation of PYG. However, MK-8722 is not a particularly bulky molecule, suggesting that a conformational change induced by binding of the drug is more likely than a steric effect.

Figure 7.9: AMPK activators paradoxically enhanced glycogen accumulation in HG-cells

(a) Normalised glycogen content of INS-1 cells cultured for 48 hrs at 5 or 25 mM glucose ± 0.5 μM MK8722. Control samples were treated with an equivalent volume of DMSO (veh). n=3, with 3 technical replicates per experiment. **p < 0.01, ***p < 0.001; 1-way ANOVA with Bonferroni's correction.

(b) Normalised glycogen content of INS-1 cells cultured for 48 hrs at 5 or 25 mM glucose ± 50 μM AICAR. n=3, with 3 technical replicates per experiment. *p < 0.05, **p < 0.01; 1-way ANOVA with Bonferroni's correction.

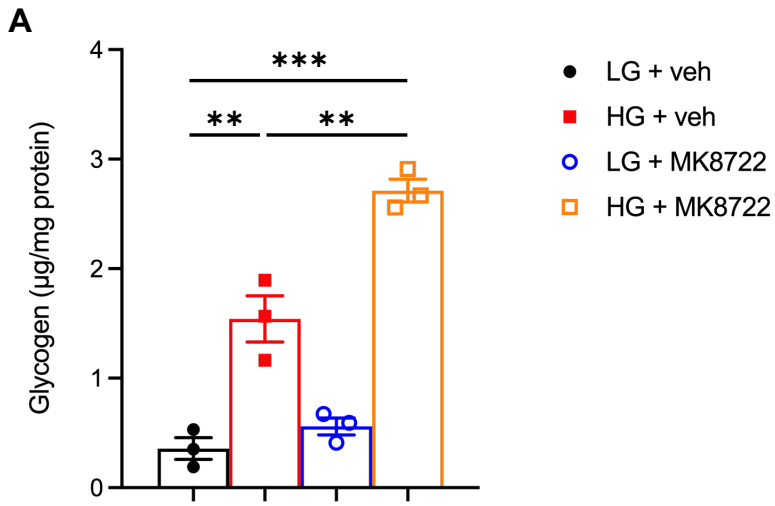

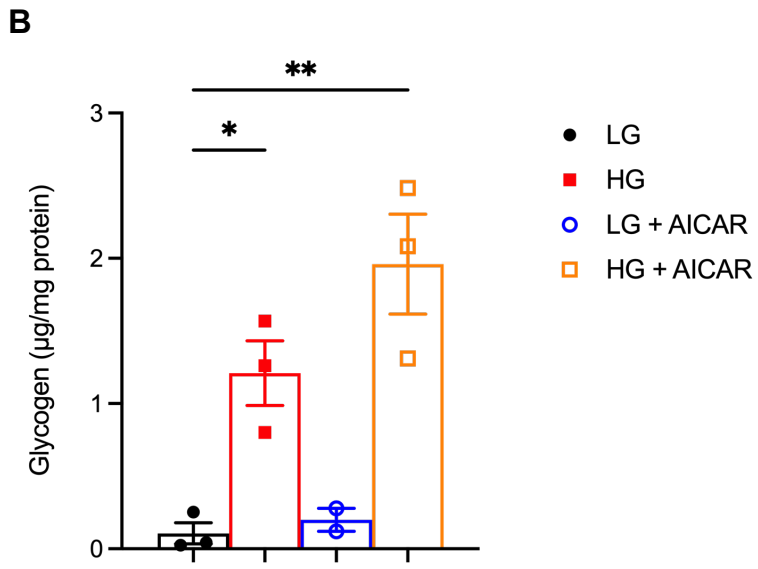

In an effort to confirm that enhancement of glycogen accumulation by MK-8722 was truly AMPK-mediated, I used 5-aminoimidazole-4-carboxamide ribonucleotide (AICAR). However, AICAR is an AMP analogue and is not a selective activator of AMPK, unlike MK-8722, which has 1000 times greater potency (Myers et al., 2017). AICAR enhanced glycogen accumulation in HG-cells similarly to MK-8722 (figure 7.9b). This result ruled out the possibility of steric effects as AMP and MK-8722 bind at distinct sites. This suggests that AMPK does in fact promote glycogen accumulation, paradoxical as it seems considering that AMPK activity is reduced while glycogen stores are increased in diabetes.

7.4.6 Investigating the regulation of PTG expression

PTG expression is strongly induced in response to hyperglycaemia and its expression is closely linked to glycogen content, which increases in response to PTG overexpression and decreases in response to PTG knockdown (Brereton et al., 2016; Greenberg et al., 2003, 2006; Mir-Coll et al., 2016). PTG-PP1 functions predominantly

as a phosphorylase phosphatase, whereas G_L-PP1 functions as the primary glycogen synthase phosphatase, at least in the liver (Green et al., 2004). Due to the sequential nature of (inactivating) PYG dephosphorylation and GYS (activating) dephosphorylation, PTG probably has regulatory primacy.

To gain a better understanding of how PTG expression is controlled in β-cells, and whether this differs from other cell types such as adipocytes and hepatocytes in which it has been more thoroughly characterised, I have collated data on how *Ppp1r3c* (PTG) mRNA levels in INS-1 cells are affected by the various inhibitors and alternative metabolic substrates detailed in chapter 4 (figure 7.10). In addition, I assessed how *Ppp1r3c* expression varies with the severity of hyperglycaemia in islets isolated from βV59M mice. As described in chapter 3, mice were injected with a range of tamoxifen doses in order to induce differing levels of glycaemia. Figure 7.10a shows a positive correlation between *Ppp1r3c* expression and glycaemia, with islets from mice with impaired glucose tolerance (IGT) appearing to show a very small increase in *Ppp1r3c* mRNA, while islets from mildly and severely hyperglycaemic mice displayed a significant induction of *Ppp1r3c*.

Figure 7.10b shows the changes in *Ppp1r3c* expression over time following the onset of hyperglycaemia (red) or restoration of euglycaemia (blue) in INS-1 cells. Strikingly, *Ppp1r3c* was upregulated >100-fold 1 hour after hyperglycaemia onset. Subsequently, *Ppp1r3c* expression progressively decreased until it stabilised (around 20-fold increased from baseline) from 24 hrs onwards. This temporal profile fits well with that of glycogen accumulation, which is rapidly initiated in response to high glucose and slows after 12 hrs (figure 7.3), supporting the designation of PTG as a key driver of

glycogen accumulation. In contrast to the insulin genes and associated transcription factors (figure 3.4a), *Ppp1r3c* mRNA levels responded quickly to hyperglycaemia reversal, falling back to 4-fold above baseline within 3 hours. Interestingly, this response was much quicker than that of *Txnip* (figure 5.4c), despite theoretically similar regulation of the two genes by the paralogous transcription factors ChREBP and MondoA. *Ppp1r3c* is thus not only very sensitive to glucose availability, but also one of the most rapidly glucose-responsive genes in the β-cell.

Figure 7.10: Investigating the metabolic regulation of *Ppp1r3c* (PTG) expression

(a) Effect of varying tamoxifen dosage in βV59M mouse islets (as described in chapter 3) on *Ppp1r3c* mRNA expression. Each data point represents one mouse: n=13 for control, n=4 for IGT, n=5 for mild, n=3 for severe. *p < 0.05; 1-way ANOVA with Bonferroni's correction.

(b) qPCR analysis of the expression of *Ppp1r3c* in INS-1 cells at time points of 1, 3, 6, 12, 24, 48 and 72 hrs following onset or reversal of hyperglycaemia. Cells were pre-cultured at 5 or 25 mM glucose for 48 hrs before being transferred to the opposite condition (25 or 5 mM to simulate onset or reversal, respectively) at the time point 0. n=2 up to 24 hrs; n=1 at 48 and 72 hrs.

(c) qPCR analysis of the expression of *Ppp1r3c* in INS-1 cells cultured for 48 hrs at 5 or 25 mM glucose ± 10 mM mannoheptulose (MANNO). n=6, with 2-3 technical replicates per experiment. ***p < 0.001; 1-way ANOVA with Bonferroni's correction.

(d) qPCR analysis of the expression of *Ppp1r3c* in INS-1 cells cultured for 48 hrs at 5 or 25 mM glucose or with 20 mM methyl pyruvate (PYR) or at 5 mM glucose with 20 mM methyl pyruvate. n=4, with 2-3 technical replicates per experiment. **p < 0.01, ***p < 0.001; 1-way ANOVA with Bonferroni's correction.

(e) qPCR analysis of the expression of *Ppp1r3c* in INS-1 cells cultured for 48 hrs at 5 or 25 mM glucose or with 20 mM methyl succinate (MMS). n=3, with 2-3 technical replicates per experiment. ***p < 0.001; 1-way ANOVA with Bonferroni's correction.

(f) qPCR analysis of the expression of *Ppp1r3c* in INS-1 cells cultured for 48 hrs at 5 or 25 mM glucose or with 20 mM leucine (LEU). n=3, with 2-3 technical replicates per experiment. *p < 0.05; 1-way ANOVA with Bonferroni's correction.

(g) qPCR analysis of the expression of *Ppp1r3c* in INS-1 cells cultured for 48 hrs at 5 mM glucose ± 5 μM koningic acid (KA). n=6, with 2-3 technical replicates per experiment. *p < 0.05; two-tailed unpaired Student's t-test.

(h) qPCR analysis of the expression of *Ppp1r3c* in INS-1 cells cultured for 48 hrs at 5 or 25 mM glucose ± 0.5 mM FBPase inhibitor (FBPi). Control samples were treated with an equivalent volume of DMSO (veh). n=3, with 3 technical replicates per experiment. **p < 0.01, ***p < 0.001; 1-way ANOVA with Bonferroni's correction.

(i) qPCR analysis of the expression of *Ppp1r3c* in INS-1 cells incubated with 5 or 25 mM glucose or with 25 mM 2-DG for 24 hrs. n=6, with 2-3 technical replicates per experiment. ***p < 0.001; 1-way ANOVA with Bonferroni's correction.

(j) qPCR analysis of the expression of *Ppp1r3c* in INS-1 cells incubated with 5 or 25 mM glucose ± 100 μM 6-AN for 48 hrs. Control samples were treated with an equivalent volume of DMSO (veh). n=3, with 2-3 technical replicates per experiment. *p < 0.05, **p < 0.01; 1-way ANOVA with Bonferroni's correction.

(k) qPCR analysis of the expression of *Ppp1r3c* in INS-1 cells incubated with 5 or 25 mM glucose ± 100 μM EBPC or tolrestat for 48 hrs. Control samples were treated with an equivalent volume of DMSO (veh). n=2, with 2-3 technical replicates per experiment.

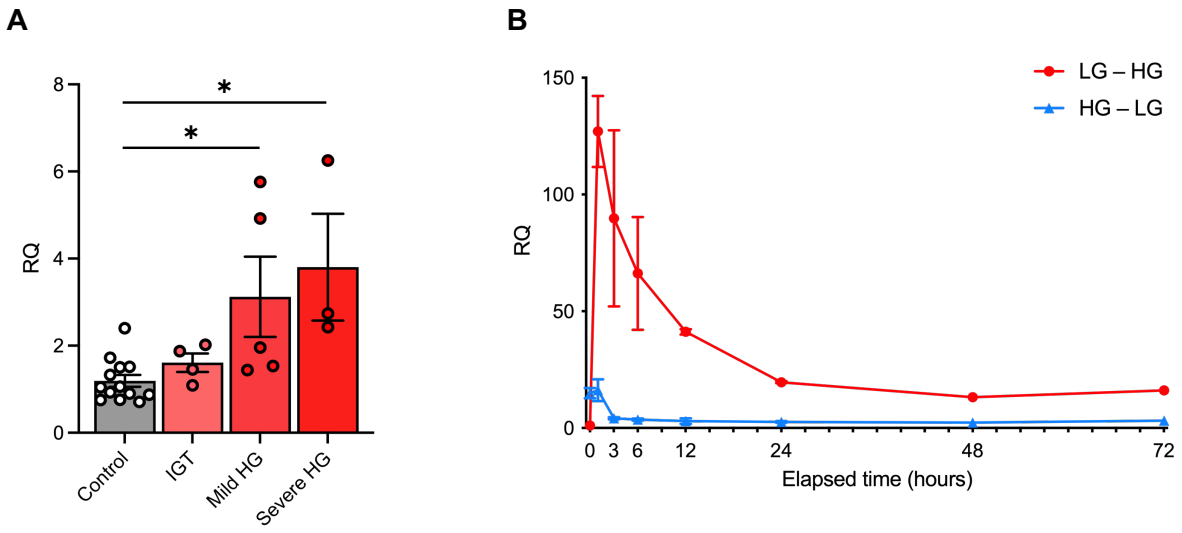

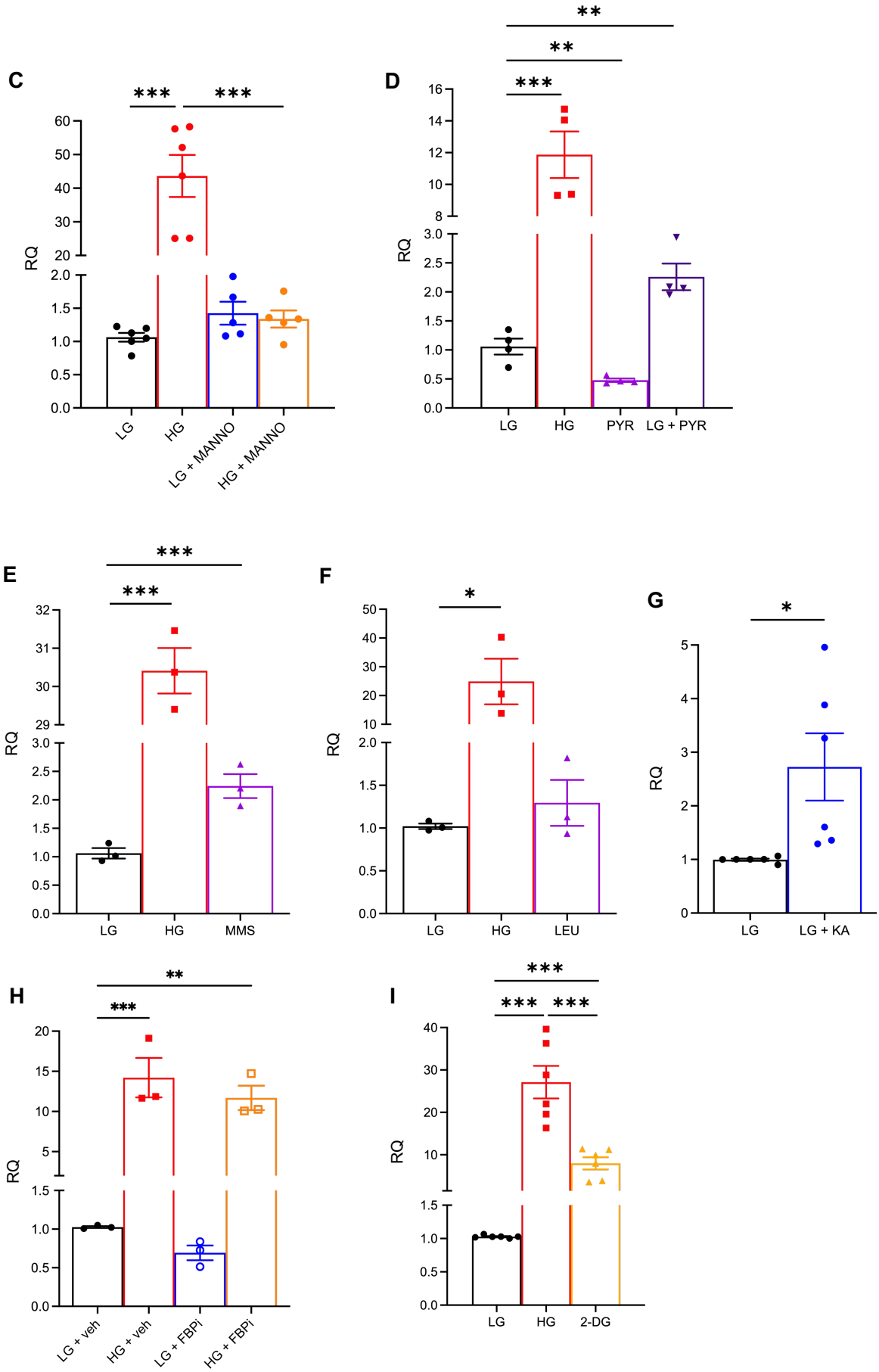
C
***
***
RQ
LG
HG
LG + MANNO
HG + MANNO
D
**
**
***
RQ
LG
HG
PYR
LG + PYR
E
***
***
RQ
LG
HG
MMS
F
*
RQ
LG
HG
LEU
G
*
RQ
LG
LG + KA
H
**
***
RQ
LG + veh
HG + veh
LG + FBPi
HG + FBPi
I
***
***
***
RQ
LG
HG
2-DG

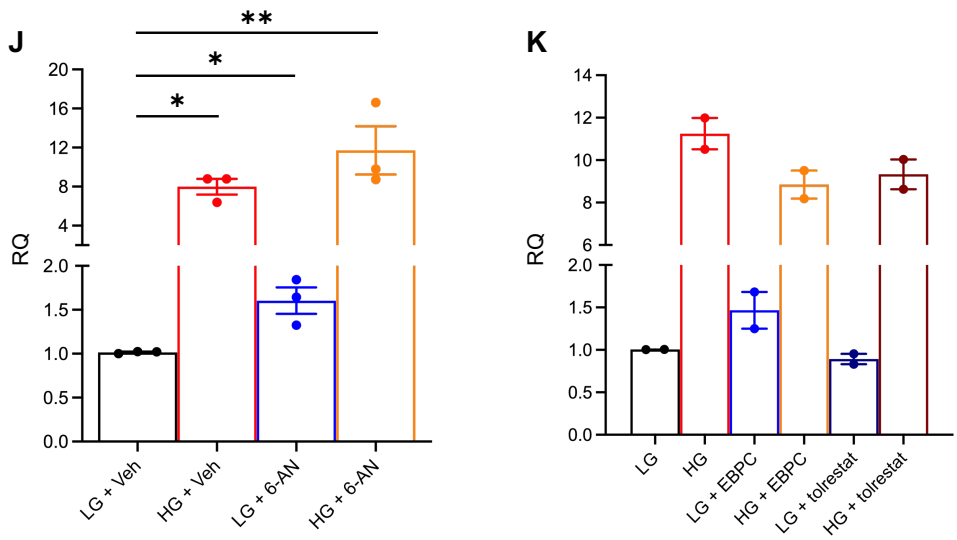

As expected, *Ppp1r3c* induction by high glucose was prevented by mannoheptulose (figure 7.10c). Neither methyl pyruvate nor leucine triggered *Ppp1r3c* upregulation (figures 7.10d and 7.10f), although surprisingly methyl succinate did so, albeit much less potently than glucose (figure 7.10e; note break in y-axis). *Ppp1r3c* was also upregulated by LG + PYR culture: as discussed previously, this is probably due to an accumulation of glycolytic intermediates caused by utilisation of the exogenous mitochondrial fuel instead of pyruvate produced by glycolysis. *Ppp1r3c* was also upregulated by KA (figure 7.10g), indicating that *Ppp1r3c* is induced by accumulation of metabolites in upper glycolysis. This is in keeping with the reported dependence of PTG induction on F2,6BP (Petrie et al., 2013). FBPi had no effect on *Ppp1r3c* expression (figure 7.10h), indicating that regulation of PTG expression is not a factor in its glycogen-lowering effect and that it may work by simply enhancing glycolytic flux without affecting steady state concentrations of intermediates. It is intriguing that *Ppp1r3c* was potently upregulated by 2-DG (figure 7.10i), as 4 hrs incubation with 10 mM 2-DG did not cause any induction of PTG in hepatocytes (Petrie et al., 2013). This indicates that PTG expression is induced by G6P in β-cells, unlike in hepatocytes.

Inhibition of the pentose phosphate pathway (figure 7.10j) or polyol pathway (figure 7.10k) slightly increased *Ppp1r3c* expression in LG-cells, likely through a small increase in the pool of G6P. Whether MondoA is the binding partner for MLX in activating *Ppp1r3c* transcription in β-cells as in hepatocytes, or whether a role for G6P also implies a role for ChREBP, remains to be determined. The similarities in the metabolic regulation of *Ppp1r3c* expression and *Txnip* expression suggests that they are probably induced by the same transcription factor, likely ChREBP.

Since I had found that modulation of AMPK and mTOR signalling affected glycogen accumulation, which was prevented by S6K1 inhibition and paradoxically increased by AMPK activation, I investigated whether *Ppp1r3c* expression was similarly affected. Although metformin and S6Ki both prevented glycogen accumulation, *Ppp1r3c* expression was unaffected by metformin (figure 7.11a) but reduced by two thirds by S6Ki (figure 7.11b; note break in y-axis). This indicates that mTORC1 hyperactivation contributes to the hyperglycaemia-induced upregulation of PTG, leading to increased glycogen storage, but metformin prevents glycogen accumulation through a different mechanism that does not involve changes in PTG expression. A possible candidate for this mechanism is FBPase inhibition. A single preliminary experiment found that the AMPK activator MK8722 increased *Ppp1r3c* expression (figure 7.11c), suggesting that AMPK may promote glycogen accumulation via induction of *Ppp1r3c*. Unfortunately, time constraints prevented replication of this result.

Figure 7.11: Investigating regulation of PTG expression by mTOR and AMPK

(a) qPCR analysis of the expression of *Ppp1r3c* (PTG) in INS-1 cells cultured for 48 hrs at 5 or 25 mM glucose ± 0.5 mM metformin. n=3, with 2 technical replicates per experiment. *p < 0.05; 1-way ANOVA with Bonferroni's correction.

(b) qPCR analysis of the expression of *Ppp1r3c* in INS-1 cells cultured for 48 hrs at 5 or 25 mM glucose ± 10 μM PF-4708671 (S6Ki). Control samples were treated with an equivalent volume of DMSO (veh). n=3, with 2 technical replicates per experiment. *p < 0.05, **p < 0.01; 1-way ANOVA with Bonferroni's correction.

(c) qPCR analysis of the expression of *Ppp1r3c* in INS-1 cells cultured for 48 hrs at 5 or 25 mM glucose ± 0.5 μM MK8722. Control samples were treated with an equivalent volume of DMSO (veh). n=1; individual values with error bars showing mean of technical replicates ± SD.

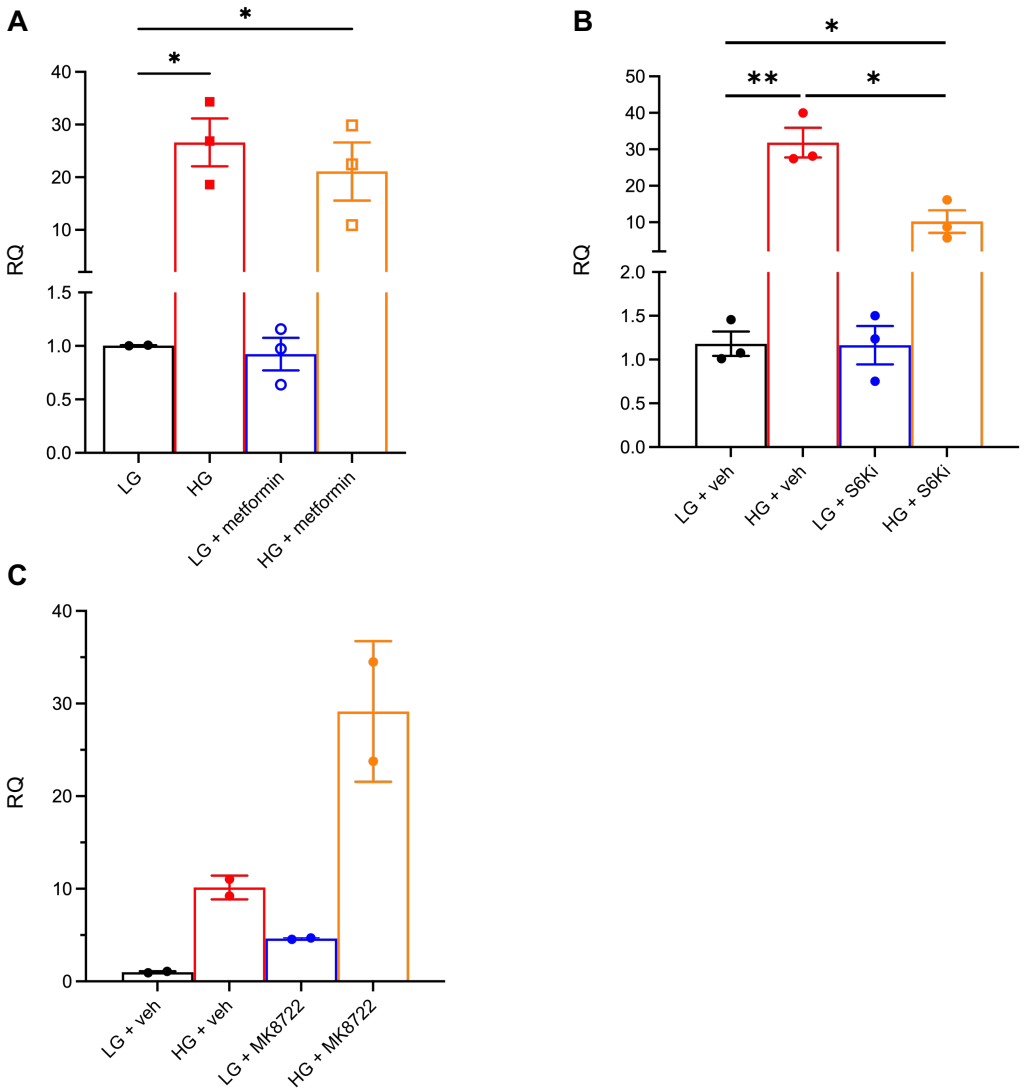

The variability in the magnitude of fold-change in *Ppp1r3c* expression in HG-cells relative to LG-cells may be due to *Ppp1r3c* expression being very low in LG-cells, with C_T values typically in the range of 34-36. Unfortunately, the lack of available specific antibodies against PTG meant that it was not possible to check the magnitude of changes at the protein level.

7.4.7 Inhibition of glycogen phosphorylase increases glycogen accumulation

To help better understand the consequences of glycogen storage, I sought to exacerbate glycogen accumulation by inhibiting glycogen phosphorylase. Initially, I trialled the inhibitor BAY U6751, which produced a small but significant increase in glycogen levels in HG-cells (figure 7.12a). I next tested CAS 648926-15-2 (henceforth referred to simply as GPi) at a range of concentrations. I found that this inhibitor, at an optimal concentration of 1 μM, produced a larger increase in glycogen levels in HG-cells (figure 7.12b). Being both more effective and more potent than BAY U6751, I used GPi for all subsequent experiments involving PYG inhibition.

Figure 7.12: Inhibition of glycogen phosphorylase enhances glycogen accumulation in chronic hyperglycaemia

Normalised glycogen content of INS-1 cells cultured for 48 hrs at 5 or 25 mM glucose ± glycogen phosphorylase inhibitors.

(a) 100 μM BAY U6751. n=3, with 3 technical replicates per experiment. *$p < 0.05$, ****$p < 10^{-4}$; 1-way ANOVA with Bonferroni's correction.

(b) 0.5, 1, or 2 μM CAS 648926-15-2 (GPi). Control samples were treated with an equivalent volume of DMSO (veh). n=2-4, with 2-3 technical replicates per

experiment. *p < 0.05, **p < 0.01, ***p < 0.001, ****p < 10^{-4}; 1-way ANOVA with Bonferroni's correction.

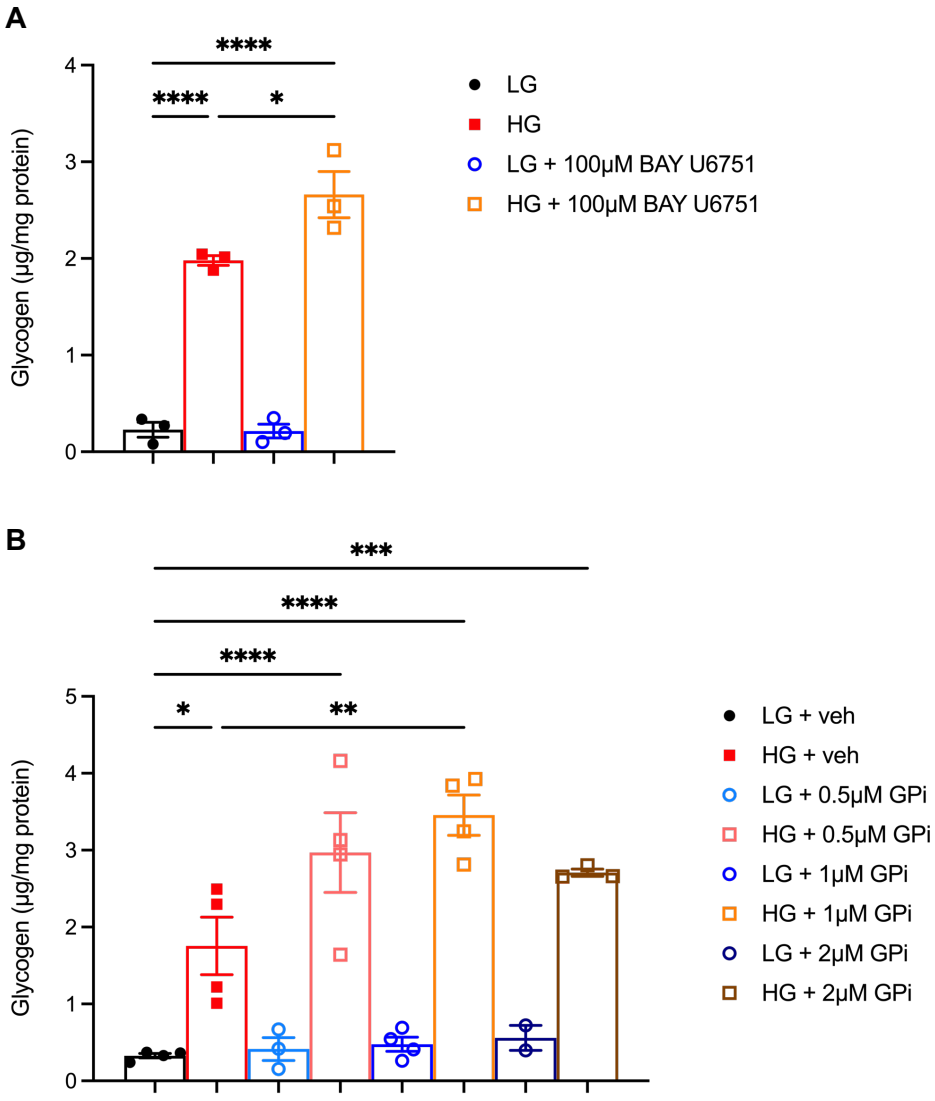

7.4.8 Impact of glycogen stores on insulin secretion

To investigate whether glycogen mobilisation could stimulate insulin secretion, and particularly if this might account for the enhanced basal insulin secretion often seen in diabetes, I pre-cultured INS-1 cells at 5 or 25 mM glucose for 48 hrs and then measured insulin secretion in the presence or absence of the PYG inhibitor. 1 µM GPi

was added to the Krebs-BSA buffer during both the pre-stimulation and stimulation incubations. If glycogen mobilisation drives basal insulin secretion in HG-cells, GPi ought to reduce insulin secretion at 2 mM glucose by blocking glycogenolysis. However, there was no apparent effect on insulin secretion from HG-cells (figure 7.13) – although this result should be interpreted with caution since secretion was already severely diminished in HG-cells. Unexpectedly, PYG inhibition appeared to cause a slight decrease in stimulated insulin secretion (at 20 mM glucose) from LG-cells. Glycogen mobilisation would not be expected at 20 mM glucose due to the high concentration of exogenous glucose available, and PYG inhibition has in fact been reported to enhance GSIS in cells cultured at similar glucose concentrations (Nagy et al., 2018). This decrease is therefore counterintuitive but could be due to activation of S6K1: other PYG inhibitors are known to cause increased phosphorylation of S6K1 (Nagy et al., 2018), while S6K1 inhibition partially prevents the loss of GSIS in HG-cells (Haythorne et al., 2022). Unfortunately, time constraints prevented me repeating this experiment and finding out whether these unexpected results can be replicated.

Figure 7.13: Effect of acute glycogen phosphorylase inhibition on GSIS

Basal and glucose-stimulated insulin secretion (ng/ml/µg protein) from INS-1 cells incubated at 5 or 25 mM glucose for 48 hrs, incubated for 1 hr at 2 mM glucose ± 1 µM GPi (CAS 648926-15-2), and stimulated for 30 mins at 2 or 20 mM glucose ± 1 µM GPi. Control samples were treated with an equivalent volume of DMSO (veh). n=1; mean of technical replicates ± SD shown.

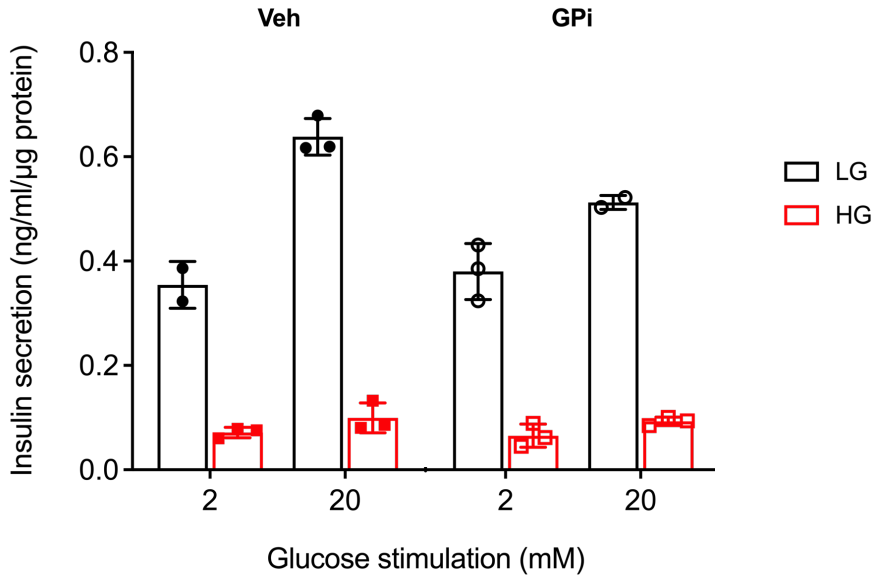

7.4.9 Investigating the relationship between β-cell glycogen and defective autophagy

To investigate whether chronic PYG inhibition could cause or exacerbate the impaired autophagy observed in chronic hyperglycaemia, I used an autophagy detection kit. When excited at 488 nm, any molecules of the pH-sensitive detection reagent that have been taken up into autophagosomes produce a green fluorescent signal; this is then normalised to the nuclear counterstain signal to control for cell number. A higher ratio of green fluorescence to nuclear signal therefore indicates higher autophagic activity. Autophagy was significantly impaired in HG-cells, with a >30% reduction relative to LG-cells (figure 7.14). Inhibition of PYG resulted in a comparable autophagic

impairment in LG-cells, but did not cause further impairment in HG-cells. Thus, PYG inhibition in LG-cells mimicked the effect of hyperglycaemia on autophagy, suggesting that a lack of glycogenolysis results in (attempted) autophagic clearance of glycogen during chronic hyperglycaemia, leading to impairment of autophagy. However, PYG inhibition did not increase the glycogen content of LG-cells (figure 7.12), perhaps due to insufficient substrate availability for glycogenesis, which argues against the GPi-induced autophagic impairment being a direct effect of glycogen accumulation. Instead, it may be a downstream effect of mTORC1 activation, as PYG inhibitors can increase S6K1 phosphorylation (Nagy et al., 2018), and mTORC1 is a well-known inhibitor of autophagy.

Figure 7.14: Chronic glycogen phosphorylase inhibition causes impaired autophagy in LG-cells

Normalised autophagic activity (ratio of autophagy signal to nuclear signal relative to LG + veh control) in INS-1 cells cultured for 48 hrs at 5 or 25 mM glucose ± 1 μM GPi. Control samples were treated with an equivalent volume of DMSO (veh). n=3, with 4-6 technical replicates per experiment. **p < 0.01; 1-way ANOVA with Bonferroni's correction.

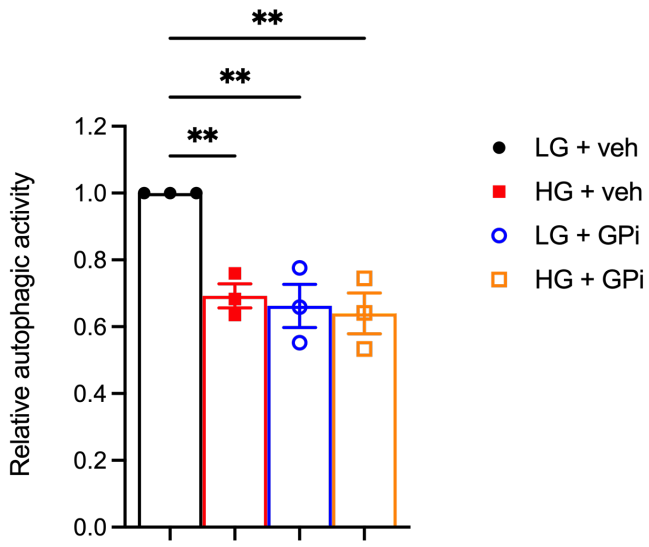

A potential extension of this experiment would be to reverse hyperglycaemia (changing the glucose concentration from 25 mM to 5 mM) for a few hours in the presence or absence of GPi to ascertain whether PYG inhibition affected the recovery of autophagic activity, since restoration of euglycaemia in diabetic βV59M mice was previously shown to induce a 2-3 fold increase in the density of autophagosomes as measured 24 hours after glibenclamide administration restored euglycaemia (Brereton et al., 2016).

7.5 Discussion

Pancreatic β-cells accumulate physiologically significant quantities of glycogen during hyperglycaemia. In INS-1 cells, this accumulation continued for at least the first 24 hours following the onset of hyperglycaemia, although the rate slowed substantially after 12 hrs (figure 7.3). A discrepancy between the rates of glycogen accumulation and breakdown was apparent, albeit less pronounced than that reported previously (Andersson et al., 2016). This supports the hypothesis that the persistent presence of glycogen can serve as a metabolic memory of hyperglycaemia and disrupt β-cell function. Native β-cells appear to have a larger storage capacity, as the ^{14}C-labelled glycogen content of isolated rat islets increased continuously throughout 72 hrs culture at 30 mM glucose, with the rate of accumulation moderately slowing after 24 hrs but there being no sign of glycogen stores reaching a maximum (Doherty & Malaisse, 2001).

Figure 7.15: Overview of the findings described in this chapter in the context of glycogen metabolism and glycolysis and the associated regulatory networks

Solid arrows indicate direct actions and reactions, while dashed arrows indicate indirect mechanisms and pathways with multiple steps. Question marks indicate putative regulatory mechanisms.

Figure created with BioRender.com

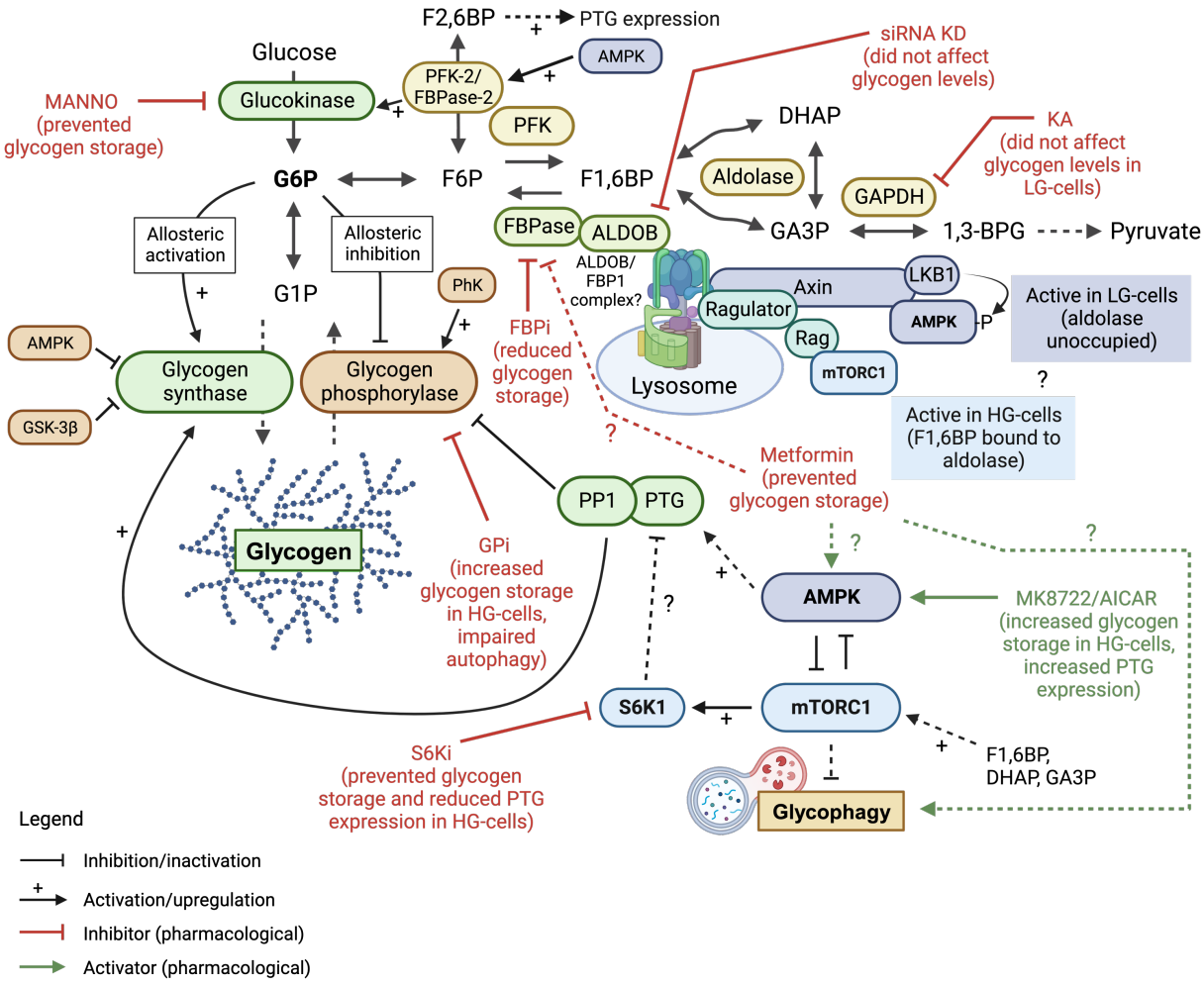

Glycogen synthesis is driven by accumulation of glycolytic intermediates, and accordingly can be blocked by mannoheptulose (figure 7.2). This appears to involve direct effects, such as hexose monophosphate supply and allostery by G6P, as well as indirect effects involving changes in gene expression, such as induction of *Ppp1r3c* (PTG), and changes in the activity of key metabolic regulators, such as mTORC1

(figure 7.15). I did not test the effect of 2-DG on glycogen accumulation, but based on previous research I would expect 2-DG to enhance glycogen accumulation (when sufficient glucose is present to serve as a substrate), since 2-DG-6P can mimic G6P in allosterically inhibiting PYG (Dringen & Hamprecht, 1993). Moreover, 2-DG caused upregulation of *Ppp1r3c* (figure 7.10i), which alone is sufficient to drive increased glycogen accumulation according to studies in which PTG was overexpressed (Greenberg et al., 2003; Lerín et al., 2000; Mir-Coll et al., 2016). Incubating INS-1 cells with 2-DG at different glucose concentrations could illuminate the extent to which signalling by G6P, including allosteric regulation of GYS and PYG, drives glycogen accumulation in β-cells.

Glycogen accumulation was partially prevented by FBPase inhibition (figure 7.5c), indicating that this enzyme plays a key role in driving glycogen synthesis, probably by increasing hexose monophosphate levels. It seems likely that metformin also prevents glycogen accumulation at least in part through disrupting FBPase, and possibly the FBP1/ALDOB complex. In keeping with this model, metformin has been shown to inhibit FBP1 in liver, resulting in suppression of both gluconeogenesis and glycogenolysis (Hunter et al., 2018). S6K1 inhibition prevented glycogen accumulation as effectively as metformin (figures 7.8 and 7.7), potentially implicating inhibition of mTOR signalling as a mode of action for metformin on glycogen metabolism. However, whereas S6Ki reduced *Ppp1r3c* expression, metformin had no effect (figure 7.11), which argues against metformin regulating glycogen in an mTORC1-dependent manner. Reports that metformin does not by itself block S6 phosphorylation in β-cells (Soliman et al., 2022) offer further evidence that the modulation of glycogen levels by metformin is not mTORC1-mediated. The surprising results of AMPK activation (figure

7.9) surely rule out an AMPK-mediated mechanism of metformin action. Only mTORC2 is known to directly upregulate glycogen synthesis – via activation of AKT and consequent inhibition of GSK-3β and activation of GYS (Liu & Sabatini, 2020). mTORC1/S6K1 signalling may rather impact glycogen levels through inhibition of glycophagy, as well as through upregulation of PTG. S6Ki may also indirectly lower G6P levels by restoring oxidative metabolism, leading to improved glycolytic flux. Metformin has been found to ameliorate the impairment of autophagy in the β-cells of *ex vivo* cultured T2D donor islets and non-diabetic islets exposed to high levels of non-esterified fatty acids (Masini et al., 2009), suggesting that metformin may restore glycophagy. Thus, through dual actions on FBPase and on the autophagic system, metformin may target glycogenesis, glycogenolysis, and glycophagy to prevent glycogen accumulation. Activity assays for key enzymes, particularly FBPase, could help confirm the mode(s) of metformin action. In summary, small molecule inhibitors targeting gluconeogenic enzymes and mTORC1 signalling can reduce or prevent glycogen accumulation in hyperglycaemia, and prevention of glycogen hyperaccumulation in β-cells may contribute to the efficacy of metformin in the treatment of T2D.

The most perplexing result in this chapter was the enhancement of glycogen accumulation by both of the AMPK activators tested (figure 7.9). However, this outcome was consistent with previous studies in other cell types (Myers et al., 2017). Despite causing modest inactivation of GYS via phosphorylation, AICAR has been found to promote glycogen accumulation in muscle by increasing allosteric activation of GYS by G6P (Hunter et al., 2011). Hunter et al. generated knock-in mice in which wild-type *Gys1* was replaced with a mutant that was G6P-insensitive but catalytically

active and regulated normally by phosphorylation. AICAR was unable to promote glycogen synthesis in these mice. The effect of G6P accumulation, leading to allosteric activation of GYS, must override the direct inhibitory effect of GYS phosphorylation. AMPK activation promotes glycogen accumulation in muscle via increased glucose uptake (through GLUT4 translocation to the cell surface). However, a different mechanism must underpin increased G6P accumulation in the GLUT2-expressing β-cell. Among the many metabolic enzymes regulated by AMPK is PFK-2/FBPase-2, which it activates by phosphorylation at Ser-461 (Arden et al., 2008; Marsin et al., 2002). One function of PFK-2/FBPase-2 is to increase glucokinase activity (Arden et al., 2008). The most likely mechanism for enhanced glycogen accumulation by AMPK activation is therefore as follows: increased PFK-2/FBPase-2 activity leads to increased glucokinase activity, leading to increased G6P accumulation, which causes feedforward stimulation of glycogenesis. In addition, an AMPK-mediated increase in F2,6BP production, which is already elevated in chronic hyperglycaemia, may further stimulate PTG expression (Petrie et al., 2013). The effect of MK8722 on *Ppp1r3c* expression (figure 7.11c) suggests that this is the case. F2,6BP also decreases the association constant between FBP1 and ALDOB (Droppelmann et al., 2015), which could have a positive feedback effect on AMPK. In future, I plan to test whether glucokinase activators induce a similar increase in glycogen synthesis. In conclusion, whilst AMPK cannot be a major driver of glycogen accumulation in diabetic β-cells due to its hypophosphorylated status, it is clear that AMPK activation is not a viable strategy to ameliorate glycogen hyperaccumulation.

I attempted to address the possibility that glycogen mobilisation in euglycaemia following an episode of hyperglycaemia can cause aberrant insulin secretion. First, I

successfully demonstrated enhancement of glycogen accumulation in HG-cells by inhibitors of glycogen phosphorylase (figure 7.12). PYG inhibitors didn't affect the glycogen content of LG-cells despite GPi impairing autophagy in these cells (figure 7.14), presumably because G6P levels were too low for inhibition of glycogenolysis or glycophagy to have an effect. Although the results of chronic PYG inhibition were promising, I failed to show an effect of acute PYG inhibition on basal insulin secretion (figure 7.13). However, this was probably due to limitations of the model and experimental design, and I have not repeated the experiment. The rate of glycogenolysis is proportional to the glycogen content and consequently decreases progressively following an initial peak when the glucose concentration is lowered (Malaisse et al., 1993), so an effect of PYG inhibition may be apparent if the pre-stimulation incubation at 2 mM glucose were eliminated. The transient nature of the glycogenolysis-driven increase in insulin observed by Malaisse *et al.* (1993) upon lowering of the glucose concentration from 16.7 to 2.8 mM, which lasted only 5 minutes, suggests this is the case. It may be possible to enhance the effect of PYG inhibition to further increase glycogen accumulation by using a glucokinase activator in combination with GPi (Hampson & Agius, 2005). In future, I would continue these investigations in HG-cultured *ex vivo* islets, which (unlike INS-1 cells) exhibit elevated basal secretion following chronic hyperglycaemia. I would pick these straight into low-glucose buffer for measurement of insulin secretion. I would also use an siRNA knockdown of PYG (*Pygb* + *Pygl*) to rule out effects on mTOR signalling and ensure any effect on insulin secretion is attributable to the reduction in PYG activity.

In conclusion, β-cells synthesise glycogen during hyperglycaemia in response to the accumulation of glycolytic intermediates upstream of GAPDH, especially G6P, that

results from flux through GAPDH being throttled. This may temporarily help to mitigate glucotoxicity by consuming excess G6P, but excess glycogen might itself impair β-cell function. When glycogen content becomes extremely high, the β-cell ultrastructure becomes severely distorted (Brereton et al., 2016), which might even physically impair functions such as insulin granule trafficking. However, the fact that FBPi, S6Ki and metformin each prevented glycogen accumulation but did not prevent downregulation of insulin gene expression or insulin content in HG-cells suggests that glycogen accumulation does not cause the hyperglycaemia-induced decline in insulin biosynthesis. Further research is needed to understand the repercussions of glycogen accumulation for β-cell function. In patients, the consequences of β-cell glycogen storage are likely more subtle, but nevertheless could be an impediment to proper blood glucose homeostasis.

8. Discussion and future directions

8.1 Summary

In chapter 3, I showed that insulin biosynthesis is impaired in mild as well as severe chronic hyperglycaemia and that insulin gene expression is slow to recover following an episode of hyperglycaemia. Insulin gene expression in INS-1 cells showed a bell-shaped relationship with the extracellular glucose concentration, peaking around 5 mM glucose, and was significantly lower even at a mild level of hyperglycaemia (8 mM glucose). The β-cell identity genes *Mafa* and *Pdx1* showed a similar relationship, whereas *Neurod1*, *Nkx6-1* and *Pax6* were downregulated at high glucose only. Insulin gene and *Mafa* expression in INS-1 cells declined rapidly at the onset of hyperglycaemia and recovered slowly when euglycaemia was restored. The β-cell identity genes also declined rapidly with hyperglycaemia onset but mostly recovered within 48 hours of reversal (except *Mafa*). Modest impairments of insulin biosynthesis were observed in EndoC-βH1 cells cultured for 8 days at 25 mM or 35 mM glucose and in EndoC-βH5 cells cultured for 5 days at 35 mM glucose. The insulin content of islets from diabetic βV59M mice appeared to decline progressively with impaired glucose tolerance, mild hyperglycaemia, and severe hyperglycaemia.

In chapter 4, I showed that the hyperglycaemia-induced downregulation of insulin biosynthesis is caused by impairment of glycolysis and is not triggered by mitochondrial metabolites. Downregulation of insulin gene expression was prevented by glucokinase inhibition by mannoheptulose, not induced (with some exceptions) by mitochondrial substrates, and was partially induced by the GAPDH inhibitor koningic

acid. Of the metabolites between glucokinase and GAPDH in glycolysis and connected pathways, G6P appears to be a particularly important, as accumulation of its analogue 2-deoxyglucose-6-phosphate reduced insulin biosynthesis nearly as much as 25 mM glucose. The results of pentose phosphate pathway inhibition by 6-aminonicotinamide suggest that accumulation of some PPP intermediates also contributes to the downregulation of insulin biosynthesis.

In chapter 5, I investigated possible pathways through which accumulation of these metabolites might reduce insulin gene expression. The L-type calcium channel blocker isradipine had no effect on insulin gene expression in HG-cells, indicating that elevated cytosolic Ca^{2+} does not cause the loss of insulin expression. S6K1 inhibition reduced insulin gene expression in LG-cells but did not affect expression in HG-cells, indicating that mTORC1 hyperactivation is not responsible for the loss of insulin expression in hyperglycaemia. I explored the regulation of TXNIP, which was strongly upregulated by G6P, and the effects of ChREBP and TXNIP on insulin gene expression by knocking down the two genes. These experiments found no evidence for the proposed downregulation of MAFA expression and insulin transcription by TXNIP, but suggested that ChREBP negatively regulates expression of the insulin and β-cell identity genes.

In chapter 6, I presented results of pilot siRNA screens in EndoC-βH1 and EndoC-βH5 cells. While I could not draw firm conclusions from this work, the results of *PYGL* knockdown suggested that glycogen storage reduces G6P levels in these cells and glycogen breakdown can stimulate insulin secretion.

In chapter 7, I explored the causes and consequences of the substantial β-cell glycogen accumulation that occurs in chronic hyperglycaemia. Glycogen accumulation was prevented (fully or partially) by glucokinase inhibition, FBPase inhibition, S6K1 inhibition, and metformin. Glycogen accumulation was increased by AMPK activation and glycogen phosphorylase inhibition. These results indicate that a combination of G6P accumulation and mTORC1 activation (as a result of accumulation of glycolytic metabolites downstream of G6P) drives glycogen accumulation. The underlying mechanisms likely include increased G6P availability, allosteric inhibition of glycogen phosphorylase and activation of glycogen synthase, induction of PTG expression, and impairment of glycophagy. Metformin may regulate glycogen levels via FBPase inhibition rather than AMPK inhibition. Whether or not glycogen accumulation is deleterious for β-cell function remains an outstanding question.

8.2 Exploring the hyperglycaemia-induced downregulation of insulin biosynthesis

In my investigations of the hyperglycaemia-induced downregulation of insulin biosynthesis, I found two observations particularly striking. The first was that mild hyperglycaemia (48 hrs culture of INS-1 cells at 8 mM glucose) caused a significant reduction in insulin mRNA levels. The second was that insulin gene expression recovered much slower after reversal of hyperglycaemia than it declined at the onset of hyperglycaemia.

Mild hyperglycaemia did not impair insulin biosynthesis only in INS-1 cells. Using different doses of tamoxifen to induce different levels of hyperglycaemia in βV59M

mice revealed an apparent reduction in insulin content in mild hyperglycaemia *in vivo* (figure 3.9). There also appeared to be a trend towards lower insulin content in islets isolated from mice displaying impaired glucose tolerance in an IPGTT despite normal resting blood glucose. I was unable to demonstrate any clear corresponding reductions in expression of the insulin genes, but I hope that forthcoming RNAseq data will provide a clearer picture of changes in the expression of the insulin genes and β-cell identity genes in mildly hyperglycaemic mice and mice with impaired glucose tolerance.

While expression of the β-cell identity genes mostly recovered to normal levels within 48 hrs following reversal of hyperglycaemia, mRNA levels of *Ins1*, *Ins2*, and *Mafa* were still not restored after 72 hrs of euglycaemia. I now plan to extend the time course experiment beyond 72 hrs, adding further timepoints at 24-hour intervals, to ascertain how much time is required for full recovery of insulin gene expression in INS-1 cells. The criticism could be made that my time course experiments are not designed in a way that would enable detection of circadian variations in gene expression. However, while many aspects of β-cell function, including insulin secretion, show circadian variation, neither insulin content nor mRNA expression of insulin or *Pdx1* do (Perelis et al., 2015).

Following my exploration of the metabolic regulation of insulin biosynthesis, I concluded that accumulation of intermediates in upper glycolysis causes the downregulation of insulin gene expression and insulin content seen in chronic hyperglycaemia. Glucose-6-phosphate (G6P) appears to be the most important of these. As G6P appears to play such a central role in signalling the status of glucose

metabolism and regulating gene expression, I would like to quantify the changes in the G6P concentration with glycaemia and with time. I expect the G6P concentration to increase with both variables. Polymorphisms in *G6PC2* and *GCK* identified in genome-wide association studies have significant (and additive) effects on insulin secretion and fasting blood glucose (Bouatia-Naji et al., 2008), testifying to the importance of flux through G6P *in vivo*, but further studies are needed to determine whether these genetic variants also affect insulin gene expression. It would also be interesting to determine whether *Txnip* expression, which is seemingly exquisitely sensitive to G6P levels, can be used as an easy-to-measure proxy for the G6P concentration.

8.2.1 A privileged role for MAFA in the regulation of insulin gene expression?

The work described in this thesis has advanced our understanding of which are the metabolic signals that trigger the downregulation of insulin biosynthesis during chronic hyperglycaemia. However, the relative importance of different downstream pathways linking changes in metabolite abundance to transcriptional regulation of the insulin gene(s) remains uncertain. In experiments in INS-1 cells, *Mafa* stood out among the β-cell identity genes as being the most strongly repressed in chronic hyperglycaemia (figure 3.3), as well as being the slowest to recover upon subsequent restoration of euglycaemia (figure 3.4a). Moreover, *MAFA* expression was also reduced by 50% or more in islets from T2D human donors (Guo et al., 2013; Marselli et al., 2020). Expression of *Mafa*, *Nkx6-1*, and *Pdx1* were all reduced according to qPCR analysis of islets (though not FACS-sorted β-cells) isolated from 4-week-diabetic βV59M mice

(Brereton et al., 2014). Isradipine had no effect on *Mafa* expression in INS-1 cells (figure 5.2), suggesting that its downregulation in diabetic βV59M mouse islets is due to chronic hyperglycaemia rather than hyperpolarisation of the β-cells. MAFA protein levels may be further reduced by proteasomal degradation induced by oxidative stress (Harmon et al., 2005). In islets isolated from *db/db* mice, a dramatic loss of MAFA (as measured by immunostaining) was observed within 4 weeks of the onset of hyperglycaemia, while a decline in NKX6-1 expression became apparent after a further 2 weeks (Guo et al., 2013). This body of evidence suggests that MAFA plays a particularly important role in driving insulin gene expression.

The striking responsiveness of *Mafa* expression to the extracellular glucose concentration appears to fit with the model where TXNIP (which is also highly glucose responsive) mediates hyperglycaemia-induced downregulation of insulin gene expression via degradation of *Mafa* mRNA (Xu et al., 2013). However, knockdown of TXNIP offered no evidence in support of this (figure 5.6c). I intend to use a small molecule inhibitor of TXNIP to investigate this further. The results of *Mlxipl* knockdown (figure 5.5b), on the other hand, suggested that ChREBP may be involved in the downregulation of *Mafa* during chronic hyperglycaemia.

If MAFA does function as a master transcription factor for insulin gene expression, it would be valuable to know why it tends to show different patterns of expression to the other β-cell identity genes. *Mafa* transcript levels appear to be particularly sensitive to concentrations of G6P and any other glycolytic metabolites upstream of GAPDH that trigger downregulation of insulin gene expression. *Mafa* was more severely downregulated than other β-cell identity genes by koningic acid (figure 4.8) and by 2-

deoxyglucose (figure 4.13b). *Pdx1* was the next most downregulated gene in those experiments. It has been proposed that *Mafa* expression is regulated by flux through the hexosamine pathway, which is increased during hyperglycaemia as the pathway is linked to glycolysis via fructose-6-phosphate (Vanderford et al., 2007). If this mechanism switches from acute activation to chronic repression of *Mafa* expression, it could account for the additional sensitivity to glycaemia displayed by *Mafa* relative to the other β-cell identity genes. Overexpression of glutamine:fructose-6-phosphate amidotransferase (the rate-limiting enzyme for the glucosamine pathway) or treatment with exogenous glucosamine led to reduced DNA binding activity of PDX1 and reduced insulin gene expression (Kaneto et al., 2001). However, *Mafa* is so far the only β-cell identity gene that has been shown to be transcriptionally regulated by hexosamine biosynthesis.

It is interesting to note that MAFA is the last identity gene to be expressed in β-cell development, downstream of PDX1 and NKX6-1 (Cerf, 2006; Matsuoka et al., 2004), as well as being the most sensitive to the deleterious impacts of chronic hyperglycaemia. Dedifferentiation was beyond the scope of my investigations, but MAFA is believed to play a critical role in maintaining a mature β-cell phenotype (Hang & Stein, 2011; Nishimura et al., 2015). Alternatively, loss of MAFA could be an early indicator of β-cell dysfunction but not as impactful as loss of NKX6-1 and PDX1 (Guo et al., 2013).

Mafa expression usually correlated well with insulin mRNA levels – especially *Ins2* mRNA, consistent with studies suggesting that MAFA controls *Ins2* expression and PDX1 controls *Ins1* expression (Docherty et al., 2005) – but there were some

exceptions. Knockdown of phosphofructokinase reduced *Mafa* expression in LG-cells by ~50% yet did not significantly alter expression of the insulin genes or any of the four other β-cell identity genes (figure 4.10b). In some cases, interpretation of results was confounded by *Mafa* expression being inconsistent between experiments. For instance, in ChREBP and TXNIP knockdown experiments (figures 5.5b and 5.6c) there was a large spread of RQ values from the three experiments. I also observed considerable inconsistency in EndoC cells. *MAFA* expression appeared to be downregulated by chronic hyperglycaemia in βH1 cells (figure 3.6), consistent with results in INS-1 cells, but upregulated 4-fold to 5-fold in βH5 cells (figure 3.8). However, in samples from the siRNA screen in βH5 cells there was no apparent effect of glycaemia on *MAFA* expression (figure 6.5).

In summary, MAFA is a crucial transcription factor for insulin gene expression in adult rodent β-cells and there appear to be unique elements in its regulation by glucose metabolism. To better understand how its expression is controlled, it would be informative to test whether or not *Mafa* is the only β-cell identity gene downregulated by hexosamine. Considering that *Ins2* is the rodent insulin gene orthologous to human *Ins*, the tight correlation between *Mafa* and *Ins2* expression in INS-1 cells might suggest that MAFA is also important in human β-cells. PDX1 is thought to have primacy in the control of human *INS* transcription (Bernardo et al., 2008), but further exploration of the importance of MAFA in human β-cells would be worthwhile.

8.3 Exploring the causes and consequences of β-cell glycogen accumulation

My investigations suggest that glycogen accumulation in hyperglycaemic β-cells is driven by a combination of excess glucose-6-phosphate, acting both as precursor (via glucose-1-phosphate) for UDP-glucose and as allosteric regulator of glycogen synthase and phosphorylase, upregulation of PTG, and overactivation of mTORC1. As discussed above with regard to the regulation of insulin biosynthesis, an important next step will be measurement of G6P levels following incubation of INS-1 cells with small molecules that increase or reduce glycogen storage. Comparing the effects of FBPi and metformin on G6P levels should be particularly interesting and may help to determine whether or not metformin prevents glycogen accumulation (in part) by acting as an FBPase inhibitor. Comparing the changes in G6P and glycogen levels over time might shed light on the capacity of glycogen metabolism to buffer G6P levels and whether this declines with longer durations of hyperglycaemia. If possible, it would be desirable to also measure flux through the G6P pool, likely using ^{13}C labelling, as this could vary without a change in the steady state G6P concentration.

Glycogen accumulation in HG-cells was prevented by S6K1 inhibition (figure 7.8), indicating that it is driven by the hyperactivation of mTORC1 that occurs during chronic hyperglycaemia. This could occur via impairment of oxidative metabolism, with increased PDK1 expression leading to reduced flux through pyruvate dehydrogenase and accumulation of glycolytic metabolites (since the lack of lactate export from β-cells limits anaerobic glycolysis). The reduction in *Ppp1r3c* expression in HG-cells incubated with S6Ki (figure 7.11b) might indicate that this is the case, and that enhancement of glycogen accumulation by mTORC1 signalling is in part mediated by increased PTG expression. Alternatively, an mTORC1-mediated decrease in autophagic activity could lead to elevated glycogen stores. These mechanisms may

work synergistically to enhance glycogen accumulation. More work is needed to understand the relationship between glycogen accumulation and impaired autophagy in chronic hyperglycaemia.

To extend my investigation of PYG inhibition and avoid inadvertently affecting glycogen levels via modulation of autophagic activity, I plan to knock down PYG in INS-1 cells. I might then knock down GYS and PTG, which ought to have the opposite effect to PYG KD, preventing or reducing glycogen accumulation. The results of *PYGL* KD in the siRNA screen in EndoC cells were intriguing, showing downregulation of *INS* and *TXNIP* expression and upregulation of *MLXIPL*, suggesting that glycogen metabolism plays a significant role in regulating G6P levels. It will be interesting to see if knocking down PYG has similar effects in INS-1 cells.

Finally, as discussed in the previous section, I am also planning to test whether glucokinase activators enhance glycogen accumulation in β-cells as they do in liver (Nakamura & Terauchi, 2015). I have shown that glucokinase inhibition by mannoheptulose prevents glycogen accumulation in HG-cells (figure 7.2), so I expect glucokinase activation to result in increased G6P production and thereby increased glycogen synthesis.

8.4 Limitations of these studies

A limitation of this study is the use of transformed, proliferative cells to study metabolism. Transformed cells have altered metabolism, and proliferation places metabolic demands that are not present in quiescent cells. Cell lines also lack the heterogeneity of native β-cells – for instance, a subpopulation that is metabolically

highly active and excitable at low glucose – that influences the co-ordination of electrical activity and insulin secretion across the islet (Benninger & Hodson, 2018; Benninger & Kravets, 2021). However, unlike some clones, INS-1 832/13 cells do display tight coupling between glycolysis and mitochondrial metabolism, comparable to true β-cells, ensuring robust GSIS (Malmgren et al., 2009).

While rodent β-cells continue to proliferate during adulthood at a rate of approximately 1%, the rate of proliferation in an adult human pancreas is very low, resting around 0.2% (Spears et al., 2021). It is not surprising, therefore, that the non-proliferative EndoC-βH5 cells tended to show a more appropriate (i.e., more similar to human islets) response to the challenge of chronic hyperglycaemia than the proliferative EndoC-βH1 cells. We might question whether culturing these cells at 35 mM glucose has any physiological relevance, but it appears that the threshold glucose concentration required to elicit a given effect (for instance, downregulation of insulin gene expression) can vary considerably between different models. Arguably, the optimal glucose concentration to use is the one that best recapitulates the response of native β-cells to the stimulus.

Another limitation of the cell line models used is that they represent pure β-cell populations, at least in theory. In reality, β-cell lines produce detectable levels of other islet hormones besides insulin (Bollheimer et al., 2005; Nakashima et al., 2009), although a native islet architecture is absent. Whilst the relative purity of cell lines enables attribution of results to β-cells alone, without substantial confounding contamination of RNA or other material by different cell types, it does mean there is no crosstalk between β-cells and other islet cell types, most pertinently the somatostatin-secreting δ-cells, as there would be in a native intra-islet environment.

The βV59M mouse model overcomes this limitation and has the advantages of permitting rapid induction and reversal of diabetes and allowing changes to be attributed to hyperglycaemia alone (as there is no dyslipidaemia). However, the β-cells in these mice are hyperpolarised, which may not be representative of β-cells in T2D. The electrical status of T2D human β-cells *in vivo* is unclear, as it takes considerable time to isolate the islets, but human islets cultured *ex vivo* for 3 days at high (16.7 mM) glucose were found to be depolarised (Oduori et al., 2020). Human islets are in some ways the gold-standard for the study of diabetic β-cells, but also have drawbacks. These include the time elapsed post-mortem before islets are isolated and cultured (if the islets are cadaveric) and complicated patient histories, which are not always fully known and are highly variable in terms of age, BMI, medications, and other variables that could affect islet function. Furthermore, islets from donors with T2D are not easily obtained.

Considering that some of the inhibitors used can be toxic to cells above a certain concentration, I should have tested their effects on cell viability in a quantitative manner, for instance with propidium iodide, rather than relying on visual inspection of cell growth and morphology.

Finally, I have relied quite heavily on gene expression data in this thesis, but mRNA levels do not necessarily correspond well to protein expression or activity. For instance, GAPDH is upregulated in chronic hyperglycaemia yet has dramatically reduced activity (Haythorne et al., 2022). My conclusions could be strengthened by proteomics data and/or immunoblotting or enzymatic activity assays for selected proteins of interest.

8.5 Does the decline in insulin biosynthesis matter?

The function of pancreatic β-cells is to synthesise and secrete insulin, so it is tempting to assume that a significant fall in insulin content is important. However, β-cells secrete such a small proportion of their insulin stores per hour – mouse β-cells release only 2-3% of their granules (30% of docked granules) in 10 minutes of stimulation with 75 mM K^+ (Olofsson et al., 2002) – that it remains possible to stimulate normal levels of secretion when cells have lost most of their insulin content. For example, the FBPase inhibitor MB05032 robustly enhanced insulin secretion in INS-1 cells without any restoration of insulin content (figure 7.5). This is not surprising. Even after a 90% reduction in insulin mRNA levels, as I observed in INS-1 cells, transcripts encoding insulin are still more abundant than any other transcript. This could be interpreted as indicating that the hyperglycaemia-induced reduction in insulin biosynthesis does not matter (unless there were a loss of insulin so severe that no granules remained to be secreted) and that only the loss of normal stimulus-secretion coupling pathways should cause concern. On the other hand, it would be odd for β-cells to maintain such a large reserve of insulin granules unless there were an advantage to doing so. In addition, given that INS-1 cells and other β-cell lines contain less insulin than native β-cells, the severity of loss of insulin in HG-cells may be great enough to limit secretory capacity in these models.

Arguably, a steep decline in insulin biosynthesis matters in the long term. Newly synthesised insulin is secreted in preference to existing stores during the late phase of insulin secretion (Jainandunsing et al., 2016; Rhodes & Halban, 1987), which could mean that a low rate of insulin biosynthesis initially manifests in a relatively subtle impairment of postprandial secretion, causing impaired glucose tolerance without

fasting hyperglycaemia. The studies of βV59M mice discussed in chapter 3 appear to support this hypothesis. The loss of β-cell insulin content might then contribute to elevated blood glucose following the progression from pre-diabetes to overt diabetes. Are these models clinically relevant? Perhaps the changes we observe in INS-1 cells and βV59M islets also occur in T2D (especially if the disease is poorly controlled) but the rate at which they occur is accelerated in our models. Islets from human T2D organ donors contain one quarter to one third less insulin than non-diabetic control islets (Cinti et al., 2016; Henquin et al., 2017; Marselli et al., 2014). This is less dramatic than the loss of insulin in our models, but still significant. The decline in insulin biosynthesis should certainly not be dismissed as a factor in reduced glucose-stimulated insulin secretion in type 2 diabetes.

8.5 Therapeutic potential of glucokinase inhibition

Because the downstream pathways regulating insulin transcription, translation, and processing are various and complex, the best strategy for preserving β-cell insulin content in T2D is surely to prevent the accumulation of metabolites that trigger downregulation of insulin biosynthesis in the first instance. One approach that could accomplish this goal is partial inhibition of glucokinase.

Glucokinase possesses sole control over the flux of glucose into glycolysis, and thus plays a critical rate-limiting role in glucose metabolism in the β-cell. Glucokinase is not subject to product inhibition, so G6P accumulation does not stem the phosphorylation of glucose. Consequently, during chronic hyperglycaemia, β-cells attempt to cope with excess glucose by various mechanisms, redirecting G6P towards alternative non-oxidative fates including glycogen synthesis, fructose synthesis via the polyol

pathway, and glycerol and lipid synthesis (Malinowski et al., 2020; Mugabo et al., 2017). However, these mechanisms are only successful up to a point. Carefully titrated inhibition of glucokinase therefore represents an attractive therapeutic approach to protect β-cells from the deleterious effects of hyperglycaemia and preserve insulin secretion and content in T2D (Ashcroft et al., 2023). This can be achieved effectively by mannoheptulose (figure 4.2; Haythorne et al., 2022), but to apply this approach clinically would require a small molecule inhibitor with a high affinity and favourable pharmacokinetics.

Glucose may exert some direct effects on β-cell gene expression independent of its metabolism. For instance, direct activation of ChREBP by glucose might explain the failure of mannoheptulose to completely prevent downregulation of *Ins2* in HG-cells (figure 4.2). However, most of the deleterious impacts of chronic hyperglycaemia appear to depend on formation of G6P from glucose, arguing that glucokinase inhibition is a sound strategy. Further evidence in support of this approach comes from a glucokinase haploinsufficiency model. Islets isolated from *Gck*$^{+/-}$ *db/db* mice had significantly higher insulin content and mRNA expression of the transcription factors *Mafa*, *Nkx6-1*, and *Pdx1* than islets from *Gck*$^{+/+}$ *db/db* mice (Omori et al., 2021). In addition to restoring normal metabolism and insulin biosynthesis and secretion, glucokinase inhibition prevented glycogen accumulation in HG-cells (figure 7.2). If glycogen accumulation is found to cause impairment of β-cell function, prevention of this would be an additional benefit.

Pharmacological activation of glucokinase, conversely, would be expected by this logic to exacerbate hyperglycaemia-induced impairment of β-cell function. Several glucokinase activators (GKAs) have been trialled for the treatment of T2D and have

produced short-term improvements in insulin release and blood glucose homeostasis, but failed after a few months (see Ashcroft et al. (2023) for review). In mice, genetic activation of glucokinase caused DNA damage and β-cell apoptosis (Tornovsky-Babeay et al., 2014). Chronic glucokinase activation appears to cause excess de novo lipogenesis in the liver as well as β-cell glucotoxicity (O'Doherty et al., 1999; Kawata et al., 2022). I am planning to investigate whether GKAs lower the glucose threshold for impairment of β-cell metabolism, as measured by changes in metabolic gene expression and glycogen storage, and downregulation of insulin biosynthesis. I will also explore whether there is any difference in these variables between cells incubated with the original generation of GKAs and cells incubated with newer GKAs, such as dorzagliatin. The latter drug has so far displayed a more sustainable hypoglycaemic effect, lasting at least 24 weeks (Nakamura et al., 2021).

8.6 Closing remarks

The work described in this thesis has provided fresh insights into the regulation of insulin gene expression and glycogen formation by chronic hyperglycaemia. Targeting these pathways with new drugs or novel combinations of existing drugs could help preserve β-cell function in T2D patients. My work has also raised many new questions, some of which I hope to address in future studies.

References

Agius, L., Ford, B. E., & Chachra, S. S. (2020). The Metformin Mechanism on Gluconeogenesis and AMPK Activation: The Metabolite Perspective. *International Journal of Molecular Sciences*, *21*(9), 3240. https://doi.org/10.3390/ijms21093240

Alan Permutt, M., & Kipnis, D. M. (1972). Insulin Biosynthesis: On The Mechanism of Glucose Stimulation. *Journal of Biological Chemistry*, *247*(4), 1194–1199. https://doi.org/10.1016/S0021-9258(19)45633-0

Andersson, L. E., Nicholas, L. M., Filipsson, K., Sun, J., Medina, A., Al-Majdoub, M., Fex, M., Mulder, H., & Spégel, P. (2016). Glycogen metabolism in the glucose-sensing and supply-driven β-cell. *FEBS Letters*, *590*(23), 4242–4251. https://doi.org/10.1002/1873-3468.12460

Anello, M., Lupi, R., Spampinato, D., Piro, S., Masini, M., Boggi, U., Del Prato, S., Rabuazzo, A. M., Purrello, F., & Marchetti, P. (2005). Functional and morphological alterations of mitochondria in pancreatic beta cells from type 2 diabetic patients. *Diabetologia*, *48*(2), 282–289. https://doi.org/10.1007/S00125-004-1627-9

Arden, C., Hampson, L. J., Huang, G. C., Shaw, J. A. M., Aldibbiat, A., Holliman, G., Manas, D., Khan, S., Lange, A. J., & Agius, L. (2008). A role for PFK-2/FBPase-2, as distinct from fructose 2,6-bisphosphate, in regulation of insulin secretion in pancreatic β-cells. *Biochemical Journal*, *411*(1), 41–51. https://doi.org/10.1042/BJ20070962

Arden, C., Tudhope, S. J., Petrie, J. L., Al-Oanzi, Z. H., Cullen, K. S., Lange, A. J., Towle, H. C., & Agius, L. (2012). Fructose 2,6-bisphosphate is essential for glucose-regulated gene transcription of glucose-6-phosphatase and other ChREBP target genes in hepatocytes. *Biochemical Journal*, *443*(1), 111–123. https://doi.org/10.1042/BJ20111280

Ardestani, A., Lupse, B., Kido, Y., Leibowitz, G., & Maedler, K. (2018). mTORC1 Signaling: A Double-Edged Sword in Diabetic β Cells. *Cell Metabolism*, *27*(2), 314–331. https://doi.org/10.1016/J.CMET.2017.11.004

Asfari, M., Janjic, D., Meda, P., Li, G., Halban, P. A., & Wollheim, C. B. (1992). Establishment of 2-mercaptoethanol-dependent differentiated insulin-secreting cell lines. *Endocrinology*, *130*(1), 167–178. https://doi.org/10.1210/ENDO.130.1.1370150

Ashcroft, F. M., Lloyd, M., & Haythorne, E. A. (2023). Glucokinase activity in diabetes: too much of a good thing? *Trends in Endocrinology and Metabolism*, *34*(2), 119–130. https://doi.org/10.1016/j.tem.2022.12.007

Ashcroft, F. M., Rohm, M., Clark, A., & Brereton, M. F. (2017). Is Type 2 Diabetes a Glycogen Storage Disease of Pancreatic β Cells? *Cell Metabolism*, *26*(1), 17–23. https://doi.org/10.1016/j.cmet.2017.05.014

Barrow, J., Hay, C. W., Ferguson, L. A., Docherty, H. M., & Docherty, K. (2006). Transcription factor cycling on the insulin promoter. *FEBS Letters*, *580*(2), 711–715. https://doi.org/10.1016/J.FEBSLET.2005.12.061

Basu, A., Dalla Man, C., Basu, R., Toffolo, G., Cobelli, C., & Rizza, R. A. (2009). Effects of type 2 diabetes on insulin secretion, insulin action, glucose effectiveness, and postprandial glucose metabolism. *Diabetes Care*, *32*(5), 866–872. https://doi.org/10.2337/dc08-1826

Benninger, R. K. P., & Hodson, D. J. (2018). New Understanding of β-Cell Heterogeneity and In Situ Islet Function. *Diabetes*, *67*(4), 537–547. https://doi.org/10.2337/DBI17-0040

Benninger, R. K. P., & Kravets, V. (2021). The physiological role of β-cell heterogeneity in pancreatic islet function. *Nature Reviews Endocrinology 2021 18:1*, *18*(1), 9–22. https://doi.org/10.1038/s41574-021-00568-0

Bernardo, A. S., Hay, C. W., & Docherty, K. (2008). Pancreatic transcription factors and their role in the birth, life and survival of the pancreatic β cell. *Molecular and*

Cellular Endocrinology, *294*(1–2), 1–9. https://doi.org/10.1016/J.MCE.2008.07.006

Blandino-Rosano, M., Barbaresso, R., Jimenez-Palomares, M., Bozadjieva, N., Werneck-de-Castro, J. P., Hatanaka, M., Mirmira, R. G., Sonenberg, N., Liu, M., Rüegg, M. A., Hall, M. N., & Bernal-Mizrachi, E. (2017). Loss of mTORC1 signalling impairs β-cell homeostasis and insulin processing. *Nature Communications*, *8*(1), 1–15. https://doi.org/10.1038/ncomms16014

Blum, B., Roose, A. N., Barrandon, O., Maehr, R., Arvanites, A. C., Davidow, L. S., Davis, J. C., Peterson, Q. P., Rubin, L. L., & Melton, D. A. (2014). Reversal of β cell de-differentiation by a small molecule inhibitor of the TGFβ pathway. *ELife*, *3*, e02809. https://doi.org/10.7554/ELIFE.02809

Bollheimer, L. C., Wrede, C. E., Rockmann, F., Ottinger, I., Schölmerich, J., & Buettner, R. (2005). Glucagon production of the rat insulinoma cell line INS-1—A quantitative comparison with primary rat pancreatic islets. *Biochemical and Biophysical Research Communications*, *330*(1), 327–332. https://doi.org/10.1016/J.BBRC.2005.01.168

Bouatia-Naji, N., Rocheleau, G., Van Lommel, L., Lemaire, K., Schuit, F., Cavalcanti-Proença, C., Marchand, M., Hartikainen, A.-L., Sovio, U., De Graeve, F., Rung, J., Vaxillaire, M., Tichet, J., Marre, M., Balkau, B., Weill, J., Elliott, P., Jarvelin, M.-R., Meyre, D., … Froguel, P. (2008). A polymorphism within the G6PC2 gene is associated with fasting plasma glucose levels. *Science (New York, N.Y.)*, *320*(5879), 1085–1088. https://doi.org/10.1126/science.1156849

Brawerman, G., Pipella, J., & Thompson, P. J. (2022). DNA damage to β cells in culture recapitulates features of senescent β cells that accumulate in type 1

diabetes. *Molecular Metabolism*, *62*, 101524. https://doi.org/10.1016/J.MOLMET.2022.101524

Brereton, M. F., Iberl, M., Shimomura, K., Zhang, Q., Adriaenssens, A. E., Proks, P., Spiliotis, I. I., Dace, W., Mattis, K. K., Ramracheya, R., Gribble, F. M., Reimann, F., Clark, A., Rorsman, P., & Ashcroft, F. M. (2014). Reversible changes in pancreatic islet structure and function produced by elevated blood glucose. *Nature Communications*, *5*, 1–11. https://doi.org/10.1038/ncomms5639

Brereton, M. F., Rohm, M., Shimomura, K., Holland, C., Tornovsky-Babeay, S., Dadon, D., Iberl, M., Chibalina, M. V., Lee, S., Glaser, B., Dor, Y., Rorsman, P., Clark, A., & Ashcroft, F. M. (2016). Hyperglycaemia induces metabolic dysfunction and glycogen accumulation in pancreatic β-cells. *Nature Communications*, *7*, 1–15. https://doi.org/10.1038/ncomms13496

Brun, T., Li, N., Jourdain, A. A., Gaudet, P., Duhamel, D., Meyer, J., Bosco, D., & Maechler, P. (2015). Diabetogenic milieus induce specific changes in mitochondrial transcriptome and differentiation of human pancreatic islets. *Human Molecular Genetics*, *24*(18), 5270–5284. https://doi.org/10.1093/HMG/DDV247

Brusco, N., Sebastiani, G., Di Giuseppe, G., Licata, G., Grieco, G. E., Fignani, D., Nigi, L., Formichi, C., Aiello, E., Auddino, S., Quero, G., Cefalo, C. M. A., Cinti, F., Mari, A., Ferraro, P. M., Pontecorvi, A., Alfieri, S., Giaccari, A., Dotta, F., & Mezza, T. (2022). Intra-islet insulin synthesis defects are associated with endoplasmic reticulum stress and loss of beta cell identity in human diabetes. *Diabetologia*, *66*(2), 354–366. https://doi.org/10.1007/S00125-022-05814-2/FIGURES/4

Bu, P., Chen, K. Y., Xiang, K., Johnson, C., Crown, S. B., Rakhilin, N., Ai, Y., Wang, L., Xi, R., Astapova, I., Han, Y., Li, J., Barth, B. B., Lu, M., Gao, Z., Mines, R., Zhang, L., Herman, M., Hsu, D., … Shen, X. (2018). Aldolase B-Mediated Fructose Metabolism Drives Metabolic Reprogramming of Colon Cancer Liver Metastasis. *Cell Metabolism*, *27*(6), 1249-1262.e4. https://doi.org/10.1016/j.cmet.2018.04.003

Butler, A. E., Janson, J., Bonner-Weir, S., Ritzel, R., Rizza, R. A., & Butler, P. C. (2003). β-Cell Deficit and Increased β-Cell Apoptosis in Humans With Type 2 Diabetes. *Diabetes*, *52*(1), 102–110. https://doi.org/10.2337/DIABETES.52.1.102

Cantley, J., Burchfield, J. G., Pearson, G. L., Schmitz-Peiffer, C., Leitges, M., & Biden, T. J. (2009). Deletion of PKC Selectively Enhances the Amplifying Pathways of Glucose-Stimulated Insulin Secretion via Increased Lipolysis in Mouse β-Cells. *Diabetes*, *58*, 1826–1834. https://doi.org/10.2337/db09-0132

Cerf, M. E. (2006). Transcription factors regulating β-cell function. *European Journal of Endocrinology*, *155*(5), 671–679. https://doi.org/10.1530/EJE.1.02277

Cha-Molstad, H., Saxena, G., Chen, J., & Shalev, A. (2009). Glucose-stimulated expression of Txnip is mediated by carbohydrate response element-binding protein, p300, and histone H4 acetylation in pancreatic beta cells. *Journal of Biological Chemistry*, *284*(25), 16898–16905. https://doi.org/10.1074/jbc.M109.010504

Chau, G. C., Im, D. U., Kang, T. M., Bae, J. M., Kim, W., Pyo, S., Moon, E. Y., & Um, S. H. (2017). mTOR controls ChREBP transcriptional activity and pancreatic β cell survival under diabetic stress. *Journal of Cell Biology*, *216*(7), 2091–2105. https://doi.org/10.1083/jcb.201701085

Chen, J., Jing, G., Xu, G., & Shalev, A. (2014). Thioredoxin-Interacting Protein Stimulates Its Own Expression via a Positive Feedback Loop. *Molecular Endocrinology*, *28*(5), 674–680. https://doi.org/10.1210/me.2014-1041

Chen, J., Saxena, G., Mungrue, I. N., Lusis, A. J., & Shalev, A. (2008). Thioredoxin-interacting protein: A critical link between glucose toxicity and β-cell apoptosis. *Diabetes*, *57*(4), 938–944. https://doi.org/10.2337/db07-0715

Chen, L., Wang, J., Zhang, Y. Y., Yan, S. F., Neumann, D., Schlattner, U., Wang, Z. X., & Wu, J. W. (2012). AMP-activated protein kinase undergoes nucleotide-dependent conformational changes. *Nature Structural & Molecular Biology 2012 19:7*, *19*(7), 716–718. https://doi.org/10.1038/nsmb.2319

Cinti, F., Bouchi, R., Kim-Muller, J. Y., Ohmura, Y., Sandoval, P. R., Masini, M., Marselli, L., Suleiman, M., Ratner, L. E., Marchetti, P., & Accili, D. (2016). Evidence of β-Cell Dedifferentiation in Human Type 2 Diabetes. *The Journal of Clinical Endocrinology & Metabolism*, *101*(3), 1044–1054. https://doi.org/10.1210/JC.2015-2860

Cuozzo, F., Nasteska, D., Jiao, Z., Smith, H. R., Bonner, C., Kerr-Conte, J., Pattou, F., Nano, R., Piemonti, L., Roberts, J., Lavery, G. G., Akerman, I., Tennant, D. A., Ludwig, C., & Hodson, D. J. (2022). High-resolution glucose fate-mapping reveals LDHB-dependent lactate production by human pancreatic β cells. *BioRxiv*, 2022.12.21.521364. https://doi.org/10.1101/2022.12.21.521364

da Silva Xavier, G., Sun, G., Qian, Q., Rutter, G. A., & Leclerc, I. (2010). ChREBP regulates Pdx-1 and other glucose-sensitive genes in pancreatic β-cells. *Biochemical and Biophysical Research Communications*, *402*(2), 252–257. https://doi.org/10.1016/J.BBRC.2010.10.010

Davis, J. C., Alves, T. C., Helman, A., Chen, J. C., Kenty, J. H., Cardone, R. L., Liu, D. R., Kibbey, R. G., & Melton, D. A. (2020). Glucose Response by Stem Cell-Derived β Cells In Vitro Is Inhibited by a Bottleneck in Glycolysis. *Cell Reports*, *31*(6). https://doi.org/10.1016/j.celrep.2020.107623

Dean, P. M. (1973). Ultrastructural morphometry of the pancreatic β-cell. *Diabetologia*, *9*(2), 115–119. https://doi.org/10.1007/BF01230690

Deng, W., Li, Y., Ren, Z., He, Q., Jia, Y., Liu, Y., Zhang, W., Gan, X., & Liu, D. (2020). Thioredoxin-interacting protein: a critical link between autophagy disorders and pancreatic β-cell dysfunction. *Endocrine*, *70*(3), 526–537. https://doi.org/10.1007/S12020-020-02471-6/FIGURES/6

Deng, Z., Kuno, A., Ojima, M., & Takahashi, S. (2022). MafB Maintains β-Cell Identity under MafA-Deficient Conditions. *Molecular and Cellular Biology*, *42*(8). https://doi.org/10.1128/MCB.00541-21

Dentin, R., Tomas-Cobos, L., Foufelle, F., Leopold, J., Girard, J., Postic, C., & Ferré, P. (2012). Glucose 6-phosphate, rather than xylulose 5-phosphate, is required for the activation of ChREBP in response to glucose in the liver. *Journal of Hepatology*, *56*(1), 199–209. https://doi.org/10.1016/J.JHEP.2011.07.019

Dhar-Chowdhury, P., Harrell, M. D., Han, S. Y., Jankowska, D., Parachuru, L., Morrissey, A., Srivastava, S., Liu, W., Malester, B., Yoshida, H., & Coetzee, W. A. (2005). The Glycolytic Enzymes, Glyceraldehyde-3-phosphate Dehydrogenase, Triose-phosphate Isomerase, and Pyruvate Kinase Are Components of the KATP Channel Macromolecular Complex and Regulate Its Function. *Journal of Biological Chemistry*, *280*(46), 38464–38470. https://doi.org/10.1074/JBC.M508744200

Docherty, H. M., Hay, C. W., Ferguson, L. A., Barrow, J., Durward, E., & Docherty, K. (2005). Relative contribution of PDX-1, MafA and E47/β2 to the regulation of the human insulin promoter. *Biochemical Journal*, *389*(3), 813–820. https://doi.org/10.1042/BJ20041891

Doherty, M., & Malaisse, W. J. (2001). Glycogen Accumulation in Rat Pancreatic Islets: In Vitro Experiments. *Endocrine*, *14*(3), 303–309.

Dringen, R., & Hamprecht, B. (1993). Inhibition by 2-Deoxyglucose and 1,5-Gluconolactone of Glycogen Mobilization in Astroglia-Rich Primary Cultures. *Journal of Neurochemistry*, *60*(4), 1498–1504. https://doi.org/10.1111/J.1471-4159.1993.TB03313.X

Droppelmann, C. A., Sáez, D. E., Asenjo, J. L., Yáñez, A. J., García-Rocha, M., Concha, I. I., Grez, M., Guinovart, J. J., & Slebe, J. C. (2015). A new level of regulation in gluconeogenesis: Metabolic state modulates the intracellular localization of aldolase B and its interaction with liver fructose-1,6-bisphosphatase. *Biochemical Journal*, *472*(2), 225–237. https://doi.org/10.1042/BJ20150269

Duran, J., Gruart, A., García-Rocha, M., Delgado-García, J. M., & Guinovart, J. J. (2014). Glycogen accumulation underlies neurodegeneration and autophagy impairment in Lafora disease. *Human Molecular Genetics*, *23*(12), 3147–3156. https://doi.org/10.1093/HMG/DDU024

Duran, J., Tevy, M. F., Garcia-Rocha, M., Calbó, J., Milán, M., & Guinovart, J. J. (2012). Deleterious effects of neuronal accumulation of glycogen in flies and mice. *EMBO Molecular Medicine*, *4*(8), 719–729. https://doi.org/10.1002/EMMM.201200241

Ebrahimi, A. G., Hollister-Lock, J., Sullivan, B. A., Tsuchida, R., Bonner-Weir, S., & Weir, G. C. (2020). Beta cell identity changes with mild hyperglycemia: Implications for function, growth, and vulnerability. *Molecular Metabolism*, *35*, 100959. https://doi.org/10.1016/J.MOLMET.2020.02.002

Fernandez, C., Fransson, U., Hallgard, E., Spégel, P., Holm, C., Krogh, M., Wårell, K., James, P., & Mulder, H. (2008). Metabolomic and proteomic analysis of a clonal insulin-producing β-cell line (INS-1 832/13). *Journal of Proteome Research*, *7*(1), 400–411. https://doi.org/10.1021/pr070547d

Flanagan, S. E., Edghill, E. L., Gloyn, A. L., Ellard, S., & Hattersley, A. T. (2006). Mutations in KCNJ11, which encodes Kir6.2, are a common cause of diabetes diagnosed in the first 6 months of life, with the phenotype determined by genotype. *Diabetologia*, *49*(6), 1190–1197. https://doi.org/10.1007/S00125-006-0246-Z

Foster, H. R., Ho, T., Potapenko, E., Sdao, S. M., Huang, S. M., Lewandowski, S. L., Vandeusen, H. R., Davidson, S. M., Cardone, R. L., Prentki, M., Kibbey, R. G., & Merrins, M. J. (2022). β-cell deletion of the PKm1 and PKm2 isoforms of pyruvate kinase in mice reveals their essential role as nutrient sensors for the KATP channel. *ELife*, *11*. https://doi.org/10.7554/ELIFE.79422

Fred, R. G., Bang-Berthelsen, C. H., Mandrup-Poulsen, T., Grunnet, L. G., & Welsh, N. (2010). High Glucose Suppresses Human Islet Insulin Biosynthesis by Inducing miR-133a Leading to Decreased Polypyrimidine Tract Binding Protein-Expression. *PLoS ONE*, *5*(5), e10843. https://doi.org/10.1371/journal.pone.0010843

Fred, R. G., & Welsh, N. (2005). Increased expression of polypyrimidine tract binding protein results in higher insulin mRNA levels. *Biochemical and Biophysical*

Research Communications, *328*(1), 38–42. https://doi.org/10.1016/j.bbrc.2004.12.147

Gerst, F., Jaghutriz, B. A., Staiger, H., Schulte, A. M., Lorza-Gil, E., Kaiser, G., Panse, M., Haug, S., Heni, M., Schütz, M., Stadion, M., Schürmann, A., Marzetta, F., Ibberson, M., Sipos, B., Fend, F., Fleming, T., Nawroth, P. P., Königsrainer, A., … Wagner, R. (2018). The Expression of Aldolase B in Islets Is Negatively Associated With Insulin Secretion in Humans. *The Journal of Clinical Endocrinology & Metabolism*, *103*(12), 4373–4383. https://doi.org/10.1210/jc.2018-00791

Gilon, P., Jonas, J. C., & Henquin, J. C. (1994). Culture duration and conditions affect the oscillations of cytoplasmic calcium concentration induced by glucose in mouse pancreatic islets. *Diabetologia*, *37*(10), 1007–1014. https://doi.org/10.1007/BF00400464

Girard, C. A., Wunderlich, F. T., Shimomura, K., Collins, S., Kaizik, S., Proks, P., Abdulkader, F., Clark, A., Ball, V., Zubcevic, L., Bentley, L., Clark, R., Church, C., Hugill, A., Galvanovskis, J., Cox, R., Rorsman, P., Brüning, J. C., & Ashcroft, F. M. (2009). Expression of an activating mutation in the gene encoding the KATP channel subunit Kir6.2 in mouse pancreatic β cells recapitulates neonatal diabetes. *The Journal of Clinical Investigation*, *119*(1), 80–90. https://doi.org/10.1172/JCI35772

Gloyn, A. L., Pearson, E. R., Antcliff, J. F., Proks, P., Bruining, G. J., Slingerland, A. S., Howard, N., Srinivasan, S., Silva, J. M. C. L., Molnes, J., Edghill, E. L., Frayling, T. M., Temple, I. K., Mackay, D., Shield, J. P. H., Sumnik, Z., van Rhijn, A., Wales, J. K. H., Clark, P., … Hattersley, A. T. (2004). Activating Mutations in the Gene Encoding the ATP-Sensitive Potassium-Channel Subunit

Kir6.2 and Permanent Neonatal Diabetes. *New England Journal of Medicine*, *350*(18), 1838–1849. https://doi.org/10.1056/NEJMOA032922/SUPPL_FILE/NEJM_GLOYN_1838SA1.PDF

Goehring, I., Sauter, N. S., Catchpole, G., Assmann, A., Shu, L., Zien, K. S., Moehlig, M., Pfeiffer, A. F. H., Oberholzer, J., Willmitzer, L., Spranger, J., & Maedler, K. (2011). Identification of an intracellular metabolic signature impairing beta cell function in the rat beta cell line INS-1E and human islets. *Diabetologia*, *54*(10), 2584–2594. https://doi.org/10.1007/S00125-011-2249-7

Göhring, I., Sharoyko, V. V, Malmgren, S., Andersson, L. E., Spégel, P., Nicholls, D. G., & Mulder, H. (2013). Chronic High Glucose and Pyruvate Levels Differentially Affect Mitochondrial Bioenergetics and Fuel-stimulated Insulin Secretion from Clonal INS-1 832/13 Cells. *Journal of Biological Chemistry,* 289(6), 3786-3798. https://doi.org/10.1074/jbc.M113.507335

Graf, R., & Klessen, C. (1981). Glycogen in pancreatic islets of steroid diabetic rats - Carbohydrate histochemical detection and localization using an immunocytochemical technique. *Histochemistry*, *73*(2), 225–232. https://doi.org/10.1007/BF00493022

Green, A. R., Aiston, S., Greenberg, C. C., Freeman, S., Poucher, S. M., Brady, M. J., & Agius, L. (2004). The glycogenic action of protein targeting to glycogen in hepatocytes involves multiple mechanisms including phosphorylase inactivation and glycogen synthase translocation. *Journal of Biological Chemistry*, *279*(45), 46474–46482. https://doi.org/10.1074/jbc.M405660200

Greenberg, C. C., Danos, A. M., & Brady, M. J. (2006). Central role for protein targeting to glycogen in the maintenance of cellular glycogen stores in 3T3-L1

adipocytes. *Molecular and Cellular Biology*, *26*(1), 334–342. https://doi.org/10.1128/MCB.26.1.334-342.2006

Greenberg, C. C., Meredith, K. N., Yan, L., & Brady, M. J. (2003). Protein targeting to glycogen overexpression results in the specific enhancement of glycogen storage in 3T3-L1 adipocytes. *Journal of Biological Chemistry*, *278*(33), 30835–30842. https://doi.org/10.1074/jbc.M303846200

Guo, S., Dai, C., Guo, M., Taylor, B., Harmon, J. S., Sander, M., Robertson, R. P., Powers, A. C., & Stein, R. (2013). Inactivation of specific β cell transcription factors in type 2 diabetes. *The Journal of Clinical Investigation*, *123*(8), 3305–3316. https://doi.org/10.1172/JCI65390

Hamada, Y., Kitoh, R., & Raskin, P. (1991). Crucial Role of Aldose Reductase Activity and Plasma Glucose Level in Sorbitol Accumulation in Erythrocytes From Diabetic Patients. *Diabetes*, *40*(10), 1233–1240. https://doi.org/10.2337/DIAB.40.10.1233

Hampson, L. J., & Agius, L. (2005). Increased Potency and Efficacy of Combined Phosphorylase Inactivation and Glucokinase Activation in Control of Hepatocyte Glycogen Metabolism. *Diabetes*, *54*(3), 617–623. https://doi.org/10.2337/DIABETES.54.3.617

Hang, Y., & Stein, R. (2011). MafA and MafB activity in pancreatic β cells. *Trends in Endocrinology and Metabolism,* 22(9), 364–373). https://doi.org/10.1016/j.tem.2011.05.003

Harmon, J. S., Stein, R., & Robertson, R. P. (2005). Oxidative stress-mediated, post-translational loss of MafA protein as a contributing mechanism to loss of insulin gene expression in glucotoxic beta cells. *Journal of Biological Chemistry*, *280*(12), 11107–11113. https://doi.org/10.1074/jbc.M410345200

Hattersley, A. T., & Ashcroft, F. M. (2005). Activating Mutations in Kir6.2 and Neonatal Diabetes: New Clinical Syndromes, New Scientific Insights, and New Therapy. *Diabetes*, *54*(9), 2503–2513. https://doi.org/10.2337/DIABETES.54.9.2503

Hay, C. W., & Docherty, K. (2006). Comparative analysis of insulin gene promoters: Implications for diabetes research. *Diabetes*, 55(12), 3201–3213. https://doi.org/10.2337/db06-0788

Haythorne, E., Lloyd, M., Walsby-Tickle, J., Tarasov, A. I., Sandbrink, J., Portillo, I., Exposito, R. T., Sachse, G., Cyranka, M., Rohm, M., Rorsman, P., McCullagh, J., & Ashcroft, F. M. (2022). Altered glycolysis triggers impaired mitochondrial metabolism and mTORC1 activation in diabetic β-cells. *Nature Communications, 13*(1), 1–19. https://doi.org/10.1038/s41467-022-34095-x

Haythorne, E., Rohm, M., van de Bunt, M., Brereton, M. F., Tarasov, A. I., Blacker, T. S., Sachse, G., Silva dos Santos, M., Terron Exposito, R., Davis, S., Baba, O., Fischer, R., Duchen, M. R., Rorsman, P., MacRae, J. I., & Ashcroft, F. M. (2019). Diabetes causes marked inhibition of mitochondrial metabolism in pancreatic β-cells. *Nature Communications*, *10*(2474), 1-17. https://doi.org/10.1038/s41467-019-10189-x

He, L., & Wondisford, F. E. (2015). Metformin action: Concentrations matter. *Cell Metabolism*, *21*(2), 159–162. https://doi.org/10.1016/j.cmet.2015.01.003

Henquin, J. C. (2000). Triggering and amplifying pathways of regulation of insulin secretion by glucose. *Diabetes*, *49*(11), 1751–1760. https://doi.org/10.2337/diabetes.49.11.1751

Henquin, J. C., Ibrahim, M. M., & Rahier, J. (2017). Insulin, glucagon and somatostatin stores in the pancreas of subjects with type-2 diabetes and their

lean and obese non-diabetic controls. *Scientific Reports 2017 7:1*, *7*(1), 1–9. https://doi.org/10.1038/s41598-017-10296-z

Herrera, P. L. (2000). Adult insulin- and glucagon-producing cells differentiate from two independent cell lineages. *Development*, *127*(11), 2317–2322. https://doi.org/10.1242/DEV.127.11.2317

Hohmeier, H. E., Mulder, H., Chen, G., Henkel-Rieger, R., Prentki, M., & Newgard, C. B. (2000). Isolation of INS-1-derived cell lines with robust ATP-sensitive K+ channel-dependent and -independent glucose-stimulated insulin secretion. *Diabetes*, *49*(3), 424–430. https://doi.org/10.2337/DIABETES.49.3.424

Hosker, J. P., Rudenski, A. S., Burnett, M. A., Matthews, D. R., & Turner, R. C. (1989). Similar reduction of first- and second-phase B-cell responses at three different glucose levels in type II diabetes and the effect of gliclazide therapy. *Metabolism*, *38*(8), 767–772. https://doi.org/10.1016/0026-0495(89)90064-4

Hou, J., Li, Z., Zhong, W., Hao, Q., Lei, L., Wang, L., Zhao, D., Xu, P., Zhou, Y., Wang, Y., & Xu, T. (2017). Temporal Transcriptomic and Proteomic Landscapes of Deteriorating Pancreatic Islets in Type 2 Diabetic Rats. *Diabetes*, *66*(8), 2188–2200. https://doi.org/10.2337/DB16-1305

Hunter, R. W., Hughey, C. C., Lantier, L., Sundelin, E. I., Peggie, M., Zeqiraj, E., Sicheri, F., Jessen, N., Wasserman, D. H., & Sakamoto, K. (2018). Metformin reduces liver glucose production by inhibition of fructose-1-6-bisphosphatase. *Nature Medicine, 24*(9), 1395–1406. https://doi.org/10.1038/s41591-018-0159-7

Hunter, R. W., Treebak, J. T., Wojtaszewski, J. F. P., & Sakamoto, K. (2011). Molecular Mechanism by Which AMP-Activated Protein Kinase Activation Promotes Glycogen Accumulation in Muscle. *Diabetes*, *60*(3), 766–774. https://doi.org/10.2337/DB10-1148

Itoh, N., & Okamoto, H. (1980). Translational control of proinsulin synthesis by glucose. *Nature*, *283*(5742), 100–102. https://doi.org/10.1038/283100a0

Jainandunsing, S., van Miert, J. N. I., Rietveld, T., Darcos Wattimena, J. L., Sijbrands, E. J. G., & de Rooij, F. W. M. (2016). A stable isotope method for in vivo assessment of human insulin synthesis and secretion. *Acta Diabetologica*, *53*(6), 935–944. https://doi.org/10.1007/S00592-016-0896-3/FIGURES/4

Jing, X., Li, D.-Q., Olofsson, C. S., Salehi, A., Surve, V. V., Caballero, J., Ivarsson, R., Lundquist, I., Pereverzev, A., Schneider, T., Rorsman, P., & Renström, E. (2005). CaV2.3 calcium channels control second-phase insulin release. *The Journal of Clinical Investigation*, *115*(1), 146–154. https://doi.org/10.1172/JCI22518

Jones, B., Bloom, S. R., Buenaventura, T., Tomas, A., & Rutter, G. A. (2018). Control of insulin secretion by GLP-1. *Peptides*, *100*, 75–84. https://doi.org/10.1016/J.PEPTIDES.2017.12.013

Jung, H. S., Chung, K. W., Kim, J. W., Kim, J., Komatsu, M., Tanaka, K., Nguyen, Y. H., Kang, T. M., Yoon, K.-H., Kim, J.-W., Jeong, Y. T., Han, M. S., Lee, M.-K., Kim, K.-W., Shin, J., & Lee, M.-S. (2008). Loss of Autophagy Diminishes Pancreatic β Cell Mass and Function with Resultant Hyperglycemia. *Cell Metabolism*, *8*(4), 318–324. https://doi.org/10.1016/J.CMET.2008.08.013

Kaneto, H., Xu, G., Song, K. H., Suzuma, K., Bonner-Weir, S., Sharma, A., & Weir, G. C. (2001). Activation of the Hexosamine Pathway Leads to Deterioration of Pancreatic β-Cell Function through the Induction of Oxidative Stress. *Journal of Biological Chemistry*, *276*(33), 31099–31104. https://doi.org/10.1074/jbc.M104115200

Karra, E., Yousseif, A., & Batterham, R. L. (2010). Mechanisms facilitating weight loss and resolution of type 2 diabetes following bariatric surgery. *Trends in Endocrinology & Metabolism*, *21*(6), 337–344. https://doi.org/10.1016/J.TEM.2010.01.006

Katz, L. S., Brill, G., Zhang, P., Kumar, A., Baumel-Alterzon, S., Honig, L. B., Gómez-Banoy, N., Karakose, E., Tanase, M., Doridot, L., Alvarsson, A., Davenport, B., Wang, P., Lambertini, L., Stanley, S. A., Homann, D., Stewart, A. F., Lo, J. C., Herman, M. A., … Scott, D. K. (2022). Maladaptive positive feedback production of ChREBPβ underlies glucotoxic β-cell failure. *Nature Communications, 13*(1), 1–19. https://doi.org/10.1038/s41467-022-32162-x

Kawata, S., Nakamura, A., Miyoshi, H., Yang, K., Shigesawa, I., Yamauchi, Y., Tsuchida, K., Omori, K., Takahashi, K., Nomoto, H., Kameda, H., Cho, K. Y., Terauchi, Y., & Atsumi, T. (2022). Glucokinase activation leads to an unsustained hypoglycaemic effect with hepatic triglyceride accumulation in *db/db* mice. *Diabetes, Obesity and Metabolism*, *24*(3), 391–401. https://doi.org/10.1111/DOM.14586

Kebede, M., Favaloro, J., Gunton, J. E., Laybutt, D. R., Shaw, M., Wong, N., Fam, B. C., Aston-Mourney, K., Rantzau, C., Zulli, A., Proietto, J., & Andrikopoulos, S. (2008). Fructose-1,6-Bisphosphatase Overexpression in Pancreatic β-Cells Results in Reduced Insulin Secretion A New Mechanism for Fat-Induced Impairment of β-Cell Function. *Diabetes*, *57*(7), 1887–1895. https://doi.org/10.2337/DB07-1326

Kibbe, C., Chen, J., Xu, G., Jing, G., & Shalev, A. (2013). FOXO1 competes with carbohydrate response element-binding protein (ChREBP) and inhibits thioredoxin-interacting protein (TXNIP) transcription in pancreatic beta cells.

Journal of Biological Chemistry, *288*(32), 23194–23202. https://doi.org/10.1074/jbc.M113.473082

Kim, W., & Egan, J. M. (2008). The Role of Incretins in Glucose Homeostasis and Diabetes Treatment. *Pharmacological Reviews*, *60*(4), 470–512. https://doi.org/10.1124/PR.108.000604

Koberstein, J. N., Stewart, M. L., Smith, C. B., Tarasov, A. I., Ashcroft, F. M., Stork, P. J. S., & Goodman, R. H. (2022). Monitoring glycolytic dynamics in single cells using a fluorescent biosensor for fructose 1,6-bisphosphate. *Proceedings of the National Academy of Sciences of the United States of America*, *119*(31), e2204407119. https://doi.org/10.1073/PNAS.2204407119/

Krus, U., Kotova, O., Spégel, P., Hallgard, E., Sharoyko, V. V., Vedin, A., Moritz, T., Sugden, M. C., Koeck, T., & Mulder, H. (2010). Pyruvate dehydrogenase kinase 1 controls mitochondrial metabolism and insulin secretion in INS-1 832/13 clonal β-cells. *Biochemical Journal*, *429*(1), 205–213. https://doi.org/10.1042/BJ20100142

Lawrence, M. C., McGlynn, K., Park, B. H., & Cobb, M. H. (2005). ERK1/2-dependent activation of transcription factors required for acute and chronic effects of glucose on the insulin gene promoter. *Journal of Biological Chemistry*, *280*(29), 26751–26759. https://doi.org/10.1074/jbc.M503158200

Lean, M. E., Leslie, W. S., Barnes, A. C., Brosnahan, N., Thom, G., McCombie, L., Peters, C., Zhyzhneuskaya, S., Al-Mrabeh, A., Hollingsworth, K. G., Rodrigues, A. M., Rehackova, L., Adamson, A. J., Sniehotta, F. F., Mathers, J. C., Ross, H. M., McIlvenna, Y., Stefanetti, R., Trenell, M., … Taylor, R. (2018). Primary care-led weight management for remission of type 2 diabetes (DiRECT): an open-

label, cluster-randomised trial. *The Lancet*, *391*(10120), 541–551. https://doi.org/10.1016/S0140-6736(17)33102-1

Lee, M. N., Ha, S. H., Kim, J., Koh, A., Lee, C. S., Kim, J. H., Jeon, H., Kim, D.-H., Suh, P.-G., & Ryu, S. H. (2009). Glycolytic Flux Signals to mTOR through Glyceraldehyde-3-Phosphate Dehydrogenase-Mediated Regulation of Rheb. *Molecular and Cellular Biology*, *29*(14), 3991–4001. https://doi.org/10.1128/mcb.00165-09

Lerín, C., Montell, E., Berman, H. K., Newgard, C. B., & Gómez-Foix, A. M. (2000). Overexpression of protein targeting to glycogen in cultured human muscle cells stimulates glycogen synthesis independent of glycogen and glucose 6-phosphate levels. *Journal of Biological Chemistry*, *275*(51), 39991–39995. https://doi.org/10.1074/jbc.M006251200

Lewandowski, S. L., Cardone, R. L., Foster, H. R., Ho, T., Potapenko, E., Poudel, C., VanDeusen, H. R., Sdao, S. M., Alves, T. C., Zhao, X., Capozzi, M. E., de Souza, A. H., Jahan, I., Thomas, C. J., Nunemaker, C. S., Davis, D. B., Campbell, J. E., Kibbey, R. G., & Merrins, M. J. (2020). Pyruvate Kinase Controls Signal Strength in the Insulin Secretory Pathway. *Cell Metabolism*, *32*(5), 736-750.e5. https://doi.org/10.1016/j.cmet.2020.10.007

Li, M., Zhang, C. S., Zong, Y., Feng, J. W., Ma, T., Hu, M., Lin, Z., Li, X., Xie, C., Wu, Y., Jiang, D., Li, Y., Zhang, C., Tian, X., Wang, W., Yang, Y., Chen, J., Cui, J., Wu, Y. Q., … Lin, S. C. (2019). Transient Receptor Potential V Channels Are Essential for Glucose Sensing by Aldolase and AMPK. *Cell Metabolism*, *30*(3), 508-524.e12. https://doi.org/10.1016/j.cmet.2019.05.018

Li, M. V., Chen, W., Harmancey, R. N., Nuotio-Antar, A. M., Imamura, M., Saha, P., Taegtmeyer, H., & Chan, L. (2010). Glucose-6-phosphate mediates activation of

the carbohydrate responsive binding protein (ChREBP). *Biochemical and Biophysical Research Communications*, *395*(3), 395–400. https://doi.org/10.1016/J.BBRC.2010.04.028

Lin, S. C., & Hardie, D. G. (2018). AMPK: Sensing Glucose as well as Cellular Energy Status. *Cell Metabolism,* 27(2), 299–313. https://doi.org/10.1016/j.cmet.2017.10.009

Liu, G. Y., & Sabatini, D. M. (2020). mTOR at the nexus of nutrition, growth, ageing and disease. *Nature Reviews Molecular Cell Biology 21*(4), 183–203. https://doi.org/10.1038/s41580-019-0199-y

Livak, K. J., & Schmittgen, T. D. (2001). Analysis of relative gene expression data using real-time quantitative PCR and the 2-ΔΔCT method. *Methods*, *25*(4), 402–408. https://doi.org/10.1006/meth.2001.1262

Lynch, C. J., & Adams, S. H. (2014). Branched-chain amino acids in metabolic signalling and insulin resistance. *Nature Reviews Endocrinology*, *10*(12), 723–736. https://doi.org/10.1038/nrendo.2014.171

Malaisse, W. J. (2016). Role of glycogen metabolism in pancreatic islet beta cell function. *Diabetologia*, *59*(11), 2489–2491. https://doi.org/10.1007/s00125-016-4092-3

Malaisse, W. J., Maggetto, C., Leclercq-Meyer, V., & Sener, A. (1993). Interference of glycogenolysis with glycolysis in pancreatic islets from glucose-infused rats. *The Journal of Clinical Investigation*, *91*(2), 432–436. https://doi.org/10.1172/JCI116219

Malaisse, W. J., Sener, A., Koser, M., Ravazzola, M., & Malaisse-Lagae, F. (1977). The stimulus-secretion coupling of glucose-induced insulin release: Insulin

release due to glycogenolysis in glucose-deprived islets. *The Biochemical Journal*, *164*(2), 447–454. https://doi.org/10.1042/bj1640447

Malinowski, R. M., Ghiasi, S. M., Mandrup-Poulsen, T., Meier, S., Lerche, M. H., Ardenkjær-Larsen, J. H., & Jensen, P. R. (2020). Pancreatic β-cells respond to fuel pressure with an early metabolic switch. *Scientific Reports 2020 10:1*, *10*(1), 1–11. https://doi.org/10.1038/s41598-020-72348-1

Malmgren, S., Nicholls, D. G., Taneera, J., Bacos, K., Koeck, T., Tamaddon, A., Wibom, R., Groop, L., Ling, C., Mulder, H., & Sharoyko, V. V. (2009). Tight Coupling between Glucose and Mitochondrial Metabolism in Clonal β-Cells Is Required for Robust Insulin Secretion. *Journal of Biological Chemistry*, *284*(47), 32395–32404. https://doi.org/10.1074/JBC.M109.026708

Marr, L., Biswas, D., Daly, L. A., Browning, C., Vial, S. C. M., Maskell, D. P., Hudson, C., Bertrand, J. A., Pollard, J., Ranson, N. A., Khatter, H., Eyers, C. E., Sakamoto, K., & Zeqiraj, E. (2022). Mechanism of glycogen synthase inactivation and interaction with glycogenin. *Nature Communications 2022 13:1*, *13*(1), 1–14. https://doi.org/10.1038/s41467-022-31109-6

Marselli, L., Piron, A., Suleiman, M., Colli, M. L., Yi, X., Khamis, A., Carrat, G. R., Rutter, G. A., Bugliani, M., Giusti, L., Ronci, M., Ibberson, M., Turatsinze, J. V., Boggi, U., De Simone, P., De Tata, V., Lopes, M., Nasteska, D., De Luca, C., … Marchetti, P. (2020). Persistent or Transient Human β Cell Dysfunction Induced by Metabolic Stress: Specific Signatures and Shared Gene Expression with Type 2 Diabetes. *Cell Reports*, *33*(9), 108466. https://doi.org/10.1016/J.CELREP.2020.108466/ATTACHMENT/7738BDCE-98B2-4056-BDC0-8E57B13A798E/MMC5.XLSX

Marselli, L., Suleiman, M., Masini, M., Campani, D., Bugliani, M., Syed, F., Martino, L., Focosi, D., Scatena, F., Olimpico, F., Filipponi, F., Masiello, P., Boggi, U., & Marchetti, P. (2014). Are we overestimating the loss of beta cells in type 2 diabetes? *Diabetologia*, *57*(2), 362–365. https://doi.org/10.1007/S00125-013-3098-3/

Marshak, S., Leibowitz, G., Bertuzzi, F., Socci, C., Kaiser, N., Gross, D. J., Cerasi, E., & Melloul, D. (1999). Impaired beta-cell functions induced by chronic exposure of cultured human pancreatic islets to high glucose. *Diabetes*, *48*(6), 1230–1236. https://doi.org/10.2337/DIABETES.48.6.1230

Marsin, A. S., Bouzin, C., Bertrand, L., & Hue, L. (2002). The stimulation of glycolysis by hypoxia in activated monocytes is mediated by AMP-activated protein kinase and inducible 6-phosphofructo-2-kinase. *Journal of Biological Chemistry*, *277*(34), 30778–30783. https://doi.org/10.1074/jbc.M205213200

Masini, M., Bugliani, M., Lupi, R., Del Guerra, S., Boggi, U., Filipponi, F., Marselli, L., Masiello, P., & Marchetti, P. (2009). Autophagy in human type 2 diabetes pancreatic beta cells. *Diabetologia*, *52*(6), 1083–1086. https://doi.org/10.1007/S00125-009-1347-2/

Matsuoka, T. A., Artner, I., Henderson, E., Means, A., Sander, M., & Stein, R. (2004). The MafA transcription factor appears to be responsible for tissue-specific expression of insulin. *Proceedings of the National Academy of Sciences of the United States of America*, *101*(9), 2930–2933. https://doi.org/10.1073/PNAS.0306233101

McBride, A., Ghilagaber, S., Nikolaev, A., & Hardie, D. G. (2009). The Glycogen-Binding Domain on the AMPK β Subunit Allows the Kinase to Act as a Glycogen

Sensor. *Cell Metabolism*, *9*(1), 23–34. https://doi.org/10.1016/J.CMET.2008.11.008

Melnik, B. C. (2012). Leucine signaling in the pathogenesis of type 2 diabetes and obesity. *World Journal of Diabetes*, *3*(3), 38. https://doi.org/10.4239/wjd.v3.i3.38

Merrins, M. J., Corkey, B. E., Kibbey, R. G., & Prentki, M. (2022). Metabolic cycles and signals for insulin secretion. *Cell Metabolism*, *34*(7), 947–968. https://doi.org/10.1016/J.CMET.2022.06.003

Minn, A. H., Couto, F. M., & Shalev, A. (2006). Metabolism-independent sugar effects on gene transcription: The role of 3-O-methylglucose. *Biochemistry*, *45*(37), 11047–11051. https://doi.org/10.1021/bi0603625

Mir-Coll, J., Duran, J., Slebe, F., García-Rocha, M., Gomis, R., Gasa, R., & Guinovart, J. J. (2016). Genetic models rule out a major role of beta cell glycogen in the control of glucose homeostasis. *Diabetologia*, *59*(5), 1012–1020. https://doi.org/10.1007/s00125-016-3871-1

Mir-Coll, J., Moede, T., Paschen, M., Neelakandhan, A., Valladolid-Acebes, I., Leibiger, B., Biernath, A., Ämmälä, C., Leibiger, I. B., Yesildag, B., & Berggren, P. O. (2021). Human Islet Microtissues as an In Vitro and an In Vivo Model System for Diabetes. *International Journal of Molecular Sciences 2021, 22*(4), 1813. https://doi.org/10.3390/IJMS22041813

Montori-Grau, M., Guitart, M., García-Martínez, C., Orozco, A., & Gómez-Foix, A. (2011). Differential pattern of glycogen accumulation after protein phosphatase 1 glycogen-targeting subunit PPP1R6 overexpression, compared to PPP1R3C and PPP1R3A, in skeletal muscle cells. *BMC Biochemistry*, *12*(1), 57. https://doi.org/10.1186/1471-2091-12-57

Mugabo, Y., Zhao, S., Lamontagne, J., Al-Mass, A., Peyot, M. L., Corkey, B. E., Joly, E., Madiraju, S. R. M., & Prentki, M. (2017). Metabolic fate of glucose and candidate signaling and excess-fuel detoxification pathways in pancreatic β-cells. *Journal of Biological Chemistry*, *292*(18), 7407–7422. https://doi.org/10.1074/jbc.M116.763060

Myers, R. W., Guan, H. P., Ehrhart, J., Petrov, A., Prahalada, S., Tozzo, E., Yang, X., Kurtz, M. M., Trujillo, M., Trotter, D. G., Feng, D., Xu, S., Eiermann, G., Holahan, M. A., Rubins, D., Conarello, S., Niu, X., Souza, S. C., Miller, C., … Sebhat, I. K. (2017). Systemic pan-AMPK activator MK-8722 improves glucose homeostasis but induces cardiac hypertrophy. *Science*, *357*(6350), 507–511. https://doi.org/10.1126/SCIENCE.AAH5582

Nagy, L., Márton, J., Vida, A., Kis, G., Bokor, É., Kun, S., Gönczi, M., Docsa, T., Tóth, A., Antal, M., Gergely, P., Csóka, B., Pacher, P., Somsák, L., & Bai, P. (2018). Glycogen phosphorylase inhibition improves beta cell function. *British Journal of Pharmacology*, *175*(2), 301–319. https://doi.org/10.1111/bph.13819

Nakamura, A., Omori, K., & Terauchi, Y. (2021). Glucokinase activation or inactivation: Which will lead to the treatment of type 2 diabetes? *Diabetes, Obesity and Metabolism*, *23*(10), 2199–2206. https://doi.org/10.1111/DOM.14459

Nakamura, A., & Terauchi, Y. (2015). Present status of clinical deployment of glucokinase activators. *Journal of Diabetes Investigation*, *6*(2), 124–132. https://doi.org/10.1111/JDI.12294

Nakashima, K., Kanda, Y., Hirokawa, Y., Kawasaki, F., Matsuki, M., & Kaku, K. (2009). MIN6 Is Not a Pure Beta Cell Line but a Mixed Cell Line with Other

Pancreatic Endocrine Hormones. *Endocrine Journal*, *56*(1), 45–53. https://doi.org/10.1507/ENDOCRJ.K08E-172

Nasteska, D., Fine, N. H. F., Ashford, F. B., Cuozzo, F., Viloria, K., Smith, G., Dahir, A., Dawson, P. W. J., Lai, Y. C., Bastidas-Ponce, A., Bakhti, M., Rutter, G. A., Fiancette, R., Nano, R., Piemonti, L., Lickert, H., Zhou, Q., Akerman, I., & Hodson, D. J. (2021). PDX1LOW MAFALOW β-cells contribute to islet function and insulin release. *Nature Communications 2021 12*(1), 1–19. https://doi.org/10.1038/s41467-020-20632-z

Nauck, M. A., & Meier, J. J. (2016). The incretin effect in healthy individuals and those with type 2 diabetes: physiology, pathophysiology, and response to therapeutic interventions. *The Lancet Diabetes & Endocrinology*, *4*(6), 525–536. https://doi.org/10.1016/S2213-8587(15)00482-9

Nishimura, W., Kondo, T., Salameh, T., El Khattabi, I., Dodge, R., Bonner-Weir, S., & Sharma, A. (2006). A switch from MafB to MafA expression accompanies differentiation to pancreatic β-cells. *Developmental Biology*, *293*(2), 526–539. https://doi.org/10.1016/J.YDBIO.2006.02.028

Nishimura, W., Takahashi, S., & Yasuda, K. (2015). MafA is critical for maintenance of the mature beta cell phenotype in mice. *Diabetologia*, *58*(3), 566–574. https://doi.org/10.1007/S00125-014-3464-9/

O'Doherty, R. M., Lehman, D. L., Télémaque-Potts, S., & Newgard, C. B. (1999). Metabolic impact of glucokinase overexpression in liver: lowering of blood glucose in fed rats is accompanied by hyperlipidemia. *Diabetes*, *48*(10), 2022–2027. https://doi.org/10.2337/DIABETES.48.10.2022

Oduori, O. S., Murao, N., Shimomura, K., Takahashi, H., Zhang, Q., Dou, H., Sakai, S., Minami, K., Chanclon, B., Guida, C., Kothegala, L., Tolö, J., Maejima, Y.,

Yokoi, N., Minami, Y., Miki, T., Rorsman, P., & Seino, S. (2020). Gs/Gq signaling switch in β cells defines incretin effectiveness in diabetes. *The Journal of Clinical Investigation*, *130*(12), 6639–6655. https://doi.org/10.1172/JCI140046

Olofsson, C. S., Göpel, S. O., Barg, S., Galvanovskis, J., Ma, X., Salehi, A., Rorsman, P., & Eliasson, L. (2002). Fast insulin secretion reflects exocytosis of docked granules in mouse pancreatic β-cells. *Pflugers Archiv European Journal of Physiology*, *444*(1–2), 43–51. https://doi.org/10.1007/S00424-002-0781-5/METRICS

Olson, L. K., Redmon, J. B., Towle, H. C., & Robertson, R. P. (1993). Chronic exposure of HIT cells to high glucose concentrations paradoxically decreases insulin gene transcription and alters binding of insulin gene regulatory protein. *Journal of Clinical Investigation*, *92*(1), 514–519. https://doi.org/10.1172/JCI116596

Omori, K., Nakamura, A., Miyoshi, H., Yamauchi, Y., Kawata, S., Takahashi, K., Kitao, N., Nomoto, H., Kameda, H., Cho, K. Y., Terauchi, Y., & Atsumi, T. (2021). Glucokinase Inactivation Paradoxically Ameliorates Glucose Intolerance by Increasing β-Cell Mass in db/db Mice. *Diabetes*, *70*(4), 917–931. https://doi.org/10.2337/DB20-0881

Osipova, E., Barsacchi, R., Brown, T., Sadanandan, K., Gaede, A. H., Monte, A., Jarrells, J., Moebius, C., Pippel, M., Altshuler, D. L., Winkler, S., Bickle, M., Baldwin, M. W., & Hiller, M. (2023). Loss of a gluconeogenic muscle enzyme contributed to adaptive metabolic traits in hummingbirds. *Science*, *379*(6628), 185–190. https://doi.org/10.1126/SCIENCE.ABN7050

Panten, U., Willenborg, M., Schumacher, K., Hamada, A., Ghaly, H., & Rustenbeck, I. (2013). Acute metabolic amplification of insulin secretion in mouse islets is

mediated by mitochondrial export of metabolites, but not by mitochondrial energy generation. *Metabolism: Clinical and Experimental*, 62(10), 1375–1386. https://doi.org/10.1016/j.metabol.2013.05.006

Park, K. G., Lee, K. M., Seo, H. Y., Suh, J. H., Kim, H. S., Wang, L., Won, K. C., Lee, H. W., Park, J. Y., Lee, K. U., Kim, J. G., Kim, B. W., Choi, H. S., & Lee, I. K. (2007). Glucotoxicity in the INS-1 rat insulinoma cell line is mediated by the orphan nuclear receptor small heterodimer partner. *Diabetes*, 56(2), 431–437. https://doi.org/10.2337/db06-0753

Perelis, M., Marcheva, B., Ramsey, K. M., Schipma, M. J., Hutchison, A. L., Taguchi, A., Peek, C. B., Hong, H., Huang, W., Omura, C., Allred, A. L., Bradfield, C. A., Dinner, A. R., Barish, G. D., & Bass, J. (2015). Pancreatic β cell enhancers regulate rhythmic transcription of genes controlling insulin secretion. *Science*, *350*(6261), aac4250. https://doi.org/10.1126/science.aac4250

Petrie, J. L., Al-Oanzi, Z. H., Arden, C., Tudhope, S. J., Mann, J., Kieswich, J., Yaqoob, M. M., Towle, H. C., & Agius, L. (2013). Glucose induces protein targeting to glycogen in hepatocytes by fructose 2,6-bisphosphate-mediated recruitment of MondoA to the promoter. *Molecular and Cellular Biology*, *33*(4), 725–738. https://doi.org/10.1128/MCB.01576-12

Pino, M. F., Ye, D. Z., Linning, K. D., Green, C. D., Wicksteed, B., Poitout, V., & Olson, L. K. (2005). Elevated Glucose Attenuates Human Insulin Gene Promoter Activity in INS-1 Pancreatic β-Cells via Reduced Nuclear Factor Binding to the A5/Core and Z Element. *Molecular Endocrinology*, *19*(5), 1343–1360. https://doi.org/10.1210/ME.2003-0493

Polekhina, G., Gupta, A., Van Denderen, B. J. W., Feil, S. C., Kemp, B. E., Stapleton, D., & Parker, M. W. (2005). Structural basis for glycogen recognition

by AMP-activated protein kinase. *Structure*, *13*(10), 1453–1462. https://doi.org/10.1016/j.str.2005.07.008

Poudel, A., Savari, O., Striegel, D. A., Periwal, V., Taxy, J., Millis, J. M., Witkowski, P., Atkinson, M. A., & Hara, M. (2015). Beta-cell destruction and preservation in childhood and adult onset type 1 diabetes. *Endocrine*, *49*(3), 693–702. https://doi.org/10.1007/S12020-015-0534-9/FIGURES/4

Poungvarin, N., Lee, J. K., Yechoor, V. K., Li, M. V., Assavapokee, T., Suksaranjit, P., Thepsongwajja, J. J., Saha, P. K., Oka, K., & Chan, L. (2012). Carbohydrate response element-binding protein (ChREBP) plays a pivotal role in beta cell glucotoxicity. *Diabetologia*, *55*(6), 1783–1796. https://doi.org/10.1007/S00125-012-2506-4/FIGURES/7

Prentki, M., Matschinsky, F. M., & Madiraju, S. R. M. (2013). Metabolic Signaling in Fuel-Induced Insulin Secretion. *Cell Metabolism*, *18*(2), 162–185. https://doi.org/10.1016/J.CMET.2013.05.018

Ravassard, P., Hazhouz, Y., Pechberty, S., Bricout-Neveu, E., Armanet, M., Czernichow, P., & Scharfmann, R. (2011). A genetically engineered human pancreatic β cell line exhibiting glucose-inducible insulin secretion. *The Journal of Clinical Investigation*, *121*(9), 3589–3597. https://doi.org/10.1172/JCI58447

Rhodes, C. J., & Halban, P. A. (1987). Newly synthesized proinsulin/insulin and stored insulin are released from pancreatic β cells predominantly via a regulated, rather than a constitutive, pathway. *Journal of Cell Biology*, *105*(1), 145–153. https://doi.org/10.1083/JCB.105.1.145

Richards, P., Rachdi, L., Oshima, M., Marchetti, P., Bugliani, M., Armanet, M., Postic, C., Guilmeau, S., & Scharfmann, R. (2018). MondoA is an essential

glucose-responsive transcription factor in human pancreatic β-cells. *Diabetes*, *67*(3), 461–472. https://doi.org/10.2337/db17-0595

Rorsman, P., & Ashcroft, F. M. (2018). Pancreatic β-cell electrical activity and insulin secretion: Of mice and men. *Physiological Reviews*, *98*(1), 117–214. https://doi.org/10.1152/physrev.00008.2017

Rorsman, P., Braun, M., & Zhang, Q. (2012). Regulation of calcium in pancreatic α- and β-cells in health and disease. *Cell Calcium*, *51*(3–4), 300–308. https://doi.org/10.1016/J.CECA.2011.11.006

Ross Laybutt, D., Sharma, A., Sgroi, D. C., Gaudet, J., Bonner-Weir, S., & Weir, G. C. (2002). Genetic regulation of metabolic pathways in β-cells disrupted by hyperglycemia. *Journal of Biological Chemistry*, *277*(13), 10912–10921. https://doi.org/10.1074/JBC.M111751200

Sae-Lee, C., Moolsuwan, K., Chan, L., & Poungvarin, N. (2016). ChREBP regulates itself and metabolic genes implicated in lipid accumulation in β-cell line. *PLoS ONE*, *11*(1), e0147411. https://doi.org/10.1371/journal.pone.0147411

Sander, M., & German, M. S. (1997). The β cell transcription factors and development of the pancreas. *Journal of Molecular Medicine 1997 75:5*, *75*(5), 327–340. https://doi.org/10.1007/S001090050118

Scharfmann, R., Didiesheim, M., Richards, P., Chandra, V., Oshima, M., & Albagli, O. (2016). Mass production of functional human pancreatic β-cells: why and how? *Diabetes, Obesity and Metabolism*, *18*, 128–136. https://doi.org/10.1111/DOM.12728

Sdao, S. M., Ho, T., Poudel, C., Foster, H. R., De Leon, E. R., Adams, M. T., Lee, J. H., Blum, B., Rane, S. G., & Merrins, M. J. (2021). CDK2 limits the highly energetic secretory program of mature β cells by restricting PEP cycle-

dependent KATP channel closure. *Cell Reports*, *34*(4), 108690. https://doi.org/10.1016/J.CELREP.2021.108690

Segerstolpe, Å., Palasantza, A., Eliasson, P., Andersson, E.-M., Andréasson, A.-C., Sun, X., Picelli, S., Sabirsh, A., Clausen, M., Bjursell, M. K., Smith, D. M., Kasper, M., Ämmälä, C., & Sandberg, R. (2016). Single-Cell Transcriptome Profiling of Human Pancreatic Islets in Health and Type 2 Diabetes. *Cell Metabolism*, *24*(4), 593–607. https://doi.org/10.1016/J.CMET.2016.08.020

Servitja, J. M., & Ferrer, J. (2004). Transcriptional networks controlling pancreatic development and beta cell function. *Diabetologia*, *47*(4), 597–613. https://doi.org/10.1007/S00125-004-1368-9/FIGURES/5

Seufert, J., Weir, G. C., & Habener, J. F. (1998). Differential expression of the insulin gene transcriptional repressor CCAAT/enhancer-binding protein beta and transactivator islet duodenum homeobox-1 in rat pancreatic beta cells during the development of diabetes mellitus. *The Journal of Clinical Investigation*, *101*(11), 2528–2539. https://doi.org/10.1172/JCI2401

Shaked, M., Ketzinel-Gilad, M., Ariav, Y., Cerasi, E., Kaiser, N., & Leibowitz, G. (2009). Insulin counteracts glucotoxic effects by suppressing thioredoxin-interacting protein production in INS-1E beta cells and in Psammomys obesus pancreatic islets. *Diabetologia*, *52*(4), 636–644. https://doi.org/10.1007/s00125-009-1274-2

Shalev, A. (2014). Minireview: Thioredoxin-Interacting Protein: Regulation and Function in the Pancreatic β-Cell. *Molecular Endocrinology*, *28*(8), 1211–1220. https://doi.org/10.1210/me.2014-1095

Shalev, A., Pise-Masison, C. A., Radonovich, M., Hoffmann, S. C., Hirshberg, B., Brady, J. N., & Harlan, D. M. (2002). Oligonucleotide Microarray Analysis of

Intact Human Pancreatic Islets: Identification of Glucose-Responsive Genes and a Highly Regulated TGFβ Signaling Pathway. *Endocrinology*, *143*(9), 3695–3698. https://doi.org/10.1210/en.2002-220564

Sharma, R. B., Landa-Galvan, H. V., & Alonso, L. C. (2021). Living Dangerously: Protective and Harmful ER Stress Responses in Pancreatic β-Cells. *Diabetes*, *70*(11), 2431–2443. https://doi.org/10.2337/DBI20-0033

Shiao, M. S., Liao, B. Y., Long, M., & Yu, H. T. (2008). Adaptive Evolution of the Insulin Two-Gene System in Mouse. *Genetics*, *178*(3), 1683–1691. https://doi.org/10.1534/GENETICS.108.087023

Singh, P., & Irwin, D. M. (2016). Contrasting Patterns in the Evolution of Vertebrate MLX Interacting Protein (MLXIP) and MLX Interacting Protein-Like (MLXIPL) Genes. *PLOS ONE*, *11*(2), e0149682. https://doi.org/10.1371/JOURNAL.PONE.0149682

Skelly, R. H., Schuppin, G. T., Ishihara, H., Oka, Y., Rhodes, C. J., & Joslin, E. P. (1996). Glucose-Regulated Translational Control of Proinsulin Biosynthesis With That of the Proinsulin Endopeptidases PG2 and PC3 in the Insulin-Producing MIN6 Cell Line. *Diabetes*, *45*(1), 37–43. https://doi.org/10.2337/DIAB.45.1.37

Soliman, G. A., Abzalimov, R. R., & He, Y. (2022). mTORC1 and mTORC2 Complexes Regulate the Untargeted Metabolomics and Amino Acid Metabolites Profile through Mitochondrial Bioenergetic Functions in Pancreatic Beta Cells. *Nutrients 2022, Vol. 14, Page 3022*, *14*(15), 3022. https://doi.org/10.3390/NU14153022

Solimena, M., Schulte, A. M., Marselli, L., Ehehalt, F., Richter, D., Kleeberg, M., Mziaut, H., Knoch, K.-P., Parnis, J., Bugliani, M., Siddiq, A., Jörns, A., Burdet, F., Liechti, R., Suleiman, M., Margerie, D., Syed, F., Distler, M., Grützmann, R.,

… Marchetti, P. (2018). Systems biology of the IMIDIA biobank from organ donors and pancreatectomised patients defines a novel transcriptomic signature of islets from individuals with type 2 diabetes. *Diabetologia*, *61*(3), 641–657. https://doi.org/10.1007/s00125-017-4500-3

Son, J., & Accili, D. (2023). Reversing pancreatic β-cell dedifferentiation in the treatment of type 2 diabetes. *Experimental & Molecular Medicine 2023 55:8*, *55*(8), 1652–1658. https://doi.org/10.1038/s12276-023-01043-8

Son, J., Du, W., Esposito, M., Shariati, K., Ding, H., Kang, Y., & Accili, D. (2023). Genetic and pharmacologic inhibition of ALDH1A3 as a treatment of β-cell failure. *Nature Communications, 14*(1), 1–14. https://doi.org/10.1038/s41467-023-36315-4

Spears, E., Serafimidis, I., Powers, A. C., & Gavalas, A. (2021). Debates in Pancreatic Beta Cell Biology: Proliferation Versus Progenitor Differentiation and Transdifferentiation in Restoring β Cell Mass. *Frontiers in Endocrinology*, *12*, 925. https://doi.org/10.3389/FENDO.2021.722250/BIBTEX

Spégel, P., Sharoyko, V. V, Goehring, I., Danielsson, A. P. H., Malmgren, S., Nagorny, C. L. F., Andersson, L. E., Koeck, T., Sharp, G. W. G., Straub, S. G., Wollheim, C. B., & Mulder, H. (2013). Time-resolved metabolomics analysis of β-cells implicates the pentose phosphate pathway in the control of insulin release. *The Biochemical Journal*, *450*(3), 595–605. https://doi.org/10.1042/BJ20121349

Stancill, J. S., Cartailler, J. P., Clayton, H. W., O'Connor, J. T., Dickerson, M. T., Dadi, P. K., Osipovich, A. B., Jacobson, D. A., & Magnuson, M. A. (2017). Chronic β-cell depolarization impairs β-cell identity by disrupting a network of

Ca2+-regulated genes. *Diabetes*, *66*(8), 2175–2187. https://doi.org/10.2337/DB16-1355/-/DC1

Steele, A. M., Shields, B. M., Wensley, K. J., Colclough, K., Ellard, S., & Hattersley, A. T. (2014). Prevalence of Vascular Complications Among Patients With Glucokinase Mutations and Prolonged, Mild Hyperglycemia. *JAMA*, *311*(3), 279–286. https://doi.org/10.1001/JAMA.2013.283980

Stride, A., Vaxillaire, M., Tuomi, T., Barbetti, F., Njølstad, P. R., Hansen, T., Costa, A., Conget, I., Pedersen, O., Søvik, O., Lorini, R., Groop, L., Froguel, P., & Hattersley, A. T. (2002). The genetic abnormality in the beta cell determines the response to an oral glucose load. *Diabetologia*, *45*(3), 427–435. https://doi.org/10.1007/S00125-001-0770-9

Sun, Y., Gao, H. Y., Fan, Z. Y., He, Y., & Yan, Y. X. (2020). Metabolomics Signatures in Type 2 Diabetes: A Systematic Review and Integrative Analysis. *The Journal of Clinical Endocrinology & Metabolism*, *105*(4), 1000–1008. https://doi.org/10.1210/CLINEM/DGZ240

Szczerbinska, I., Tessitore, A., Hansson, L. K., Agrawal, A., Lopez, A. R., Helenius, M., Malinowski, A. R., Gilboa, B., Ruby, M. A., Gupta, R., & Ämmälä, C. (2022). Large-Scale Functional Genomics Screen to Identify Modulators of Human β-Cell Insulin Secretion. *Biomedicines 2022, 10*(1), 103. https://doi.org/10.3390/BIOMEDICINES10010103

Talchai, C., Xuan, S., Lin, H. V., Sussel, L., & Accili, D. (2012). Pancreatic β cell dedifferentiation as a mechanism of diabetic β cell failure. *Cell*, *150*(6), 1223–1234. https://doi.org/10.1016/j.cell.2012.07.029

Tariq, M., De Souza, A. H., Bensellam, M., Chae, H., Jaffredo, M., Close, A.-F., Deglasse, J.-P., Santos, L. R. B., Buemi, A., Nizar, &, Mourad, I., Wojtusciszyn,

A., Raoux, M., Gilon, P., Broca, C., Jonas, J.-C., & Be, J.-C. J. J.-C. J. (2022). Prolonged culture of human pancreatic islets under glucotoxic conditions changes their acute beta cell calcium and insulin secretion glucose response curves from sigmoid to bell-shaped. *Diabetologia 2022*, 1–15. https://doi.org/10.1007/S00125-022-05842-Y

Thielen, L. A., Chen, J., Jing, G., Moukha-Chafiq, O., Xu, G., Jo, S. H., Grayson, T. B., Lu, B., Li, P., Augelli-Szafran, C. E., Suto, M. J., Kanke, M., Sethupathy, P., Kim, J. K., & Shalev, A. (2020). Identification of an Anti-diabetic, Orally Available Small Molecule that Regulates TXNIP Expression and Glucagon Action. *Cell Metabolism*, *32*(3), 353-365.e8. https://doi.org/10.1016/j.cmet.2020.07.002

Tornovsky-Babeay, S., Dadon, D., Ziv, O., Tzipilevich, E., Kadosh, T., Schyr-Ben Haroush, R., Hija, A., Stolovich-Rain, M., Furth-Lavi, J., Granot, Z., Porat, S., Philipson, L. H., Herold, K. C., Bhatti, T. R., Stanley, C., Ashcroft, F. M., In'T Veld, P., Saada, A., Magnuson, M. A., … Dor, Y. (2014). Type 2 Diabetes and Congenital Hyperinsulinism Cause DNA Double-Strand Breaks and p53 Activity in β Cells. *Cell Metabolism*, *19*(1), 109–121. https://doi.org/10.1016/J.CMET.2013.11.007

Tsonkova, V. G., Sand, F. W., Wolf, X. A., Grunnet, L. G., Kirstine Ringgaard, A., Ingvorsen, C., Winkel, L., Kalisz, M., Dalgaard, K., Bruun, C., Fels, J. J., Helgstrand, C., Hastrup, S., Öberg, F. K., Vernet, E., Sandrini, M. P. B., Shaw, A. C., Jessen, C., Grønborg, M., … Frogne, T. (2018). The EndoC-βH1 cell line is a valid model of human beta cells and applicable for screenings to identify novel drug target candidates. *Molecular Metabolism*, *8*, 144–157. https://doi.org/10.1016/J.MOLMET.2017.12.007

Van Lommel, L., Janssens, K., Quintens, R., Tsukamoto, K., Vander Mierde, D., Lemaire, K., Denef, C., Jonas, J. C., Martens, G., Pipeleers, D., & Schuit, F. C. (2006). Probe-Independent and Direct Quantification of Insulin mRNA and Growth Hormone mRNA in Enriched Cell Preparations. *Diabetes*, *55*(12), 3214–3220. https://doi.org/10.2337/DB06-0774

Vanderford, N. L., Andrali, S. S., & Özcan, S. (2007). Glucose induces MafA expression in pancreatic beta cell lines via the hexosamine biosynthetic pathway. *Journal of Biological Chemistry*, *282*(3), 1577–1584. https://doi.org/10.1074/jbc.M605064200

Vilchez, D., Ros, S., Cifuentes, D., Pujadas, L., Vallès, J., García-Fojeda, B., Criado-García, O., Fernández-Sánchez, E., Medrão-Fernández, I., Domínguez, J., García-Rocha, M., Soriano, E., Rodríguez De Córdoba, S., & Guinovart, J. J. (2007). Mechanism suppressing glycogen synthesis in neurons and its demise in progressive myoclonus epilepsy. *Nature Neuroscience*, *10*(11), 1407–1413. https://doi.org/10.1038/nn1998

Wang, G., Chiou, J., Zeng, C., Miller, M., Matta, I., Han, J. Y., Kadakia, N., Okino, M.-L., Beebe, E., Mallick, M., Camunas-Soler, J., Santos, T. dos, Dai, X.-Q., Ellis, C., Hang, Y., Kim, S. K., MacDonald, P. E., Kandeel, F. R., Preissl, S., … Sander, M. (2023). Integration of single-cell multiomic measurements across disease states with genetics identifies mechanisms of beta cell dysfunction in type 2 diabetes. *BioRxiv Preprint*, 2022.12.31.522386. https://doi.org/10.1101/2022.12.31.522386

Wang, Z., York, N. W., Nichols, C. G., & Remedi, M. S. (2014). Pancreatic β cell dedifferentiation in diabetes and redifferentiation following insulin therapy. *Cell Metabolism*, *19*(5), 872–882. https://doi.org/10.1016/j.cmet.2014.03.010

Weir, G. C., Aguayo-Mazzucato, C., & Bonner-Weir, S. (2013). β-cell dedifferentiation in diabetes is important, but what is it? *Islets*, *5*(5), 233–237. https://doi.org/10.4161/ISL.27494

Weir, G. C., & Bonner-Weir, S. (2004). Five Stages of Evolving Beta-Cell Dysfunction During Progression to Diabetes. *Diabetes*, *53*(suppl_3), S16–S21. https://doi.org/10.2337/DIABETES.53.SUPPL_3.S16

Weir, G. C., Gaglia, J., & Bonner-Weir, S. (2020). Inadequate β-cell mass is essential for the pathogenesis of type 2 diabetes. *The Lancet Diabetes & Endocrinology*. https://doi.org/10.1016/S2213-8587(20)30022-X

Welsh, M., Scherberg, N., Gilmore, R., & Steiner, D. F. (1986). Translational control of insulin biosynthesis. Evidence for regulation of elongation, initiation and signal-recognition-particle-mediated translational arrest by glucose. *Biochemical Journal*, *235*(2), 459–467. https://doi.org/10.1042/BJ2350459

Welsh, N., & Hellerström, C. (1990). In Vitro Restoration of Insulin Production in Islets from Adult Rats Treated Neonatally with Streptozotocin. *Endocrinology*, *126*(4), 1842–1848. https://doi.org/10.1210/ENDO-126-4-1842

Welsh, N., Oberg, C., & Welsh, M. (1991). GTP-binding proteins may stimulate insulin biosynthesis in rat pancreatic islets by enhancing the signal-recognition-particle-dependent translocation of the insulin mRNA poly-/mono-some complex to the endoplasmic reticulum. *Biochemical Journal*, *275*(1), 23–28. https://doi.org/10.1042/BJ2750023

Westermeier, F., Holyoak, T., Asenjo, J. L., Gatica, R., Nualart, F., Burbulis, I., & Bertinat, R. (2019). Gluconeogenic Enzymes in β-Cells: Pharmacological Targets for Improving Insulin Secretion. In *Trends in Endocrinology and*

Metabolism (Vol. 30, Issue 8, pp. 520–531). Elsevier Inc. https://doi.org/10.1016/j.tem.2019.05.004

Wiederkehr, A., & Wollheim, C. B. (2012). Mitochondrial signals drive insulin secretion in the pancreatic β-cell. *Molecular and Cellular Endocrinology*, 353 (1-2), 128–137. Elsevier. https://doi.org/10.1016/j.mce.2011.07.016

Wilcock, C., & Bailey, C. J. (1994). Accumulation of metformin by tissues of the normal and diabetic mouse. *Xenobiotica*, *24*(1), 49–57. https://doi.org/10.3109/00498259409043220

Xu, G., Chen, J., Jing, G., & Shalev, A. (2013). Thioredoxin-interacting protein regulates insulin transcription through microRNA-204. *Nature Medicine*, *19*(9), 1141–1146. https://doi.org/10.1038/nm.3287

Yaney, G. C., Schultz, V., Cunningham, B. A., Dunaway, G. A., Corkey, B. E., & Tornheim, K. (1995). Phosphofructokinase Isozymes in Pancreatic Islets and Clonal β-Cells (INS-1). *Diabetes*, *44*(11), 1285–1289. https://doi.org/10.2337/diab.44.11.1285

Zakaria, A., Berthault, C., Cosson, B., Jung, V., Guerrera, I. C., Rachdi, L., & Scharfmann, R. (2021). Glucose treatment of human pancreatic β-cells enhances translation of mRNAs involved in energetics and insulin secretion. *Journal of Biological Chemistry*, *297*(1), 100839. https://doi.org/10.1016/J.JBC.2021.100839

Zhang, C. S., Hawley, S. A., Zong, Y., Li, M., Wang, Z., Gray, A., Ma, T., Cui, J., Feng, J. W., Zhu, M., Wu, Y. Q., Li, T. Y., Ye, Z., Lin, S. Y., Yin, H., Piao, H. L., Hardie, D. G., & Lin, S. C. (2017). Fructose-1,6-bisphosphate and aldolase mediate glucose sensing by AMPK. *Nature*, *548*(7665), 112–116. https://doi.org/10.1038/nature23275

Zhang, C. S., Li, M., Ma, T., Zong, Y., Cui, J., Feng, J. W., Wu, Y. Q., Lin, S. Y., & Lin, S. C. (2016). Metformin Activates AMPK through the Lysosomal Pathway. *Cell Metabolism*, *24*(4), 521–522. https://doi.org/10.1016/j.cmet.2016.09.003

Zhang, Y., Xie, Z., Zhou, G., Zhang, H., Lu, J., & Zhang, W. J. (2010). Fructose-1,6-Bisphosphatase Regulates Glucose-Stimulated Insulin Secretion of Mouse Pancreatic β-Cells. *Endocrinology*, *151*(10), 4688–4695. https://doi.org/10.1210/en.2009-1185

Zhao, C., Wilson, M. C., Schuit, F., Halestrap, A. P., & Rutter, G. A. (2001). Expression and Distribution of Lactate/Monocarboxylate Transporter Isoforms in Pancreatic Islets and the Exocrine Pancreas. *Diabetes*, *50*(2), 361–366. https://doi.org/10.2337/DIABETES.50.2.361

Zois, C. E., & Harris, A. L. (2016). Glycogen metabolism has a key role in the cancer microenvironment and provides new targets for cancer therapy. *Journal of Molecular Medicine*, *94*(2), 137–154. https://doi.org/10.1007/s00109-015-1377-9